EPRI
Electric Power
Research Institute

Keywords:
Fiber composites
Composite materials
Polymers
Mathematical models
Diagnostics

EPRI TR-106271
Project 8007-20
Final Report
August 1995

Characterization of Mechanical and Thermal Properties of Advanced Composite Pultrusions

Prepared by
The University of Mississippi
University, Mississippi

Characterization of Mechanical and Thermal Properties of Advanced Composite Pultrusions

Pultrusion is a process in which continuous reinforcement fibers are embedded in a polymeric matrix to produce a composite material. This project improved our understanding of the pultrusion method and provides information that will place pultrusion technology on a more scientific basis.

INTEREST CATEGORIES

Applied science and technology
Exploratory research and new science
Overhead construction, O&M
Reliability

KEYWORDS

Fiber composites
Composite materials
Polymers
Mathematical models
Diagnostics

BACKGROUND The high premium for improving reliability, increasing life, and reducing the cost of transmission and distribution structures in the United States necessitates that new developments in polymer science and technology be applied to utility systems. Polymeric materials are being used or are under consideration and development for use in such electrical systems as towers, overhead and underground cables, and transmission and distribution substation and utility support equipment. Pultruded solid rectangular and square bars have potential use in many utility applications: in transformers to separate the windings and permit air circulation, as guy strain insulators, stand-off insulators, hot-line maintenance tools, booms for electrical bucket trucks, tool handles, bus bar insulator supports, fuse tubes, and lighting poles. For most of these applications, pultruded composites are believed to offer inherent technical advantages such as structural strength, improved physical properties, reduced cost, and increased life. Over the years the art of pultrusion has evolved into an automated and technologically sophisticated production process, even though much of the basic science governing the process is not well understood.

OBJECTIVE To study the effect of process variables on the static, thermal, and dynamic characteristics of pultruded polymer composite products; facilitate an understanding of the basic science governing the pultrusion process and thus aid in providing superior products for utility use.

APPROACH In work cosponsored by the National Science Foundation, the project team pultruded hybrid composites by intermingling glass and graphite fibers in a common epoxy matrix using specially designed pre-form dies. They pultruded two different hybrid sections, a sandwich flat and a shell-core round with different fiber lay up and volume combinations, and studied their static and dynamic mechanical properties. The team maintained a set of constant process conditions in manufacturing these experimental products. The mechanical properties and the failure mechanisms of these hybrids were compared with those of mono-fiber type (all-graphite/epoxy and all-glass/epoxy) pultruded composites. The team used Differential Scanning Calorimetry (DSC) as a diagnostic tool.

RESULTS A two-dimensional thermochemical heat transfer model was developed to describe the thermal manufacturing pultrusion process. The model is based on the predicted degree of cure of the pultruded product for various process pull speeds and measured center line temperature profiles. A three-dimensional

numerical model that utilizes a fixed control volume-based finite difference approach was also developed: this model predicts the axial, radial, and circumferential temperature and degree-of-cure profiles. Model predictions were found to be in close agreement with experimental results. The kinetic parameters used for the resin to predict the temperature and degree-of-cure profiles were obtained from DSC scans.

EPRI PERSPECTIVE These studies of pultruded graphite/fiberglass epoxy systems extend knowledge of the pultrusion process with thermosetting polymers. The models demonstrate agreement between predicted temperature profiles and measured temperature. The work further demonstrates the use of DSC as a characterization tool. The results provide guidance for meeting future needs for pultruded composite materials for utility applications.

PROJECT
RP8007-20
Project Manager: Dr. Bruce S. Bernstein
Power Delivery Group
Managed for Strategic Development Group
Contractor: University of Mississippi

Characterization of Mechanical and Thermal Properties of Advanced Composite Pultrusions

TR-106271
Research Project 8007-20

Final Report, August 1995

Prepared by
The University of Mississippi
University, MS 38677

Principal Investigators
James G. Vaughan
Jeffrey A. Roux
P. Raju Mantena

Prepared for
Electric Power Research Institute
3412 Hillview Avenue
Palo Alto, California 94304

National Science Foundation
4201 Wilson Boulevard
Arlington, Virginia 22230

EPRI Project Manager
Dr. Bruce S. Bernstein

Power Delivery Group
for Strategic Development Group

DISCLAIMER OF WARRANTIES AND LIMITATION OF LIABILITIES

ORGANIZATION THAT PREPARED THIS REPORT:

THE UNIVERSITY OF MISSISSIPPI

ORDERING INFORMATION

Requests for copies of this report should be directed to EPRI Distribution Center, 207 Coggins Drive, P.O. Box 23205, Pleasant Hill, CA 94523, (510) 934-4212.

ABSTRACT

This three year grant was funded as a result of the first joint National Science Foundation and Electric Power Research Institute request for proposals that were submitted in January 1991. The total award amount of $268,332 was split equally between NSF and EPRI, with the first year funding from NSF starting in August 15, 1991. Funding from EPRI took longer to initiate and became effective April 1, 1992. This report summarizes the work performed by the Composite Materials Group at the University of Mississippi to characterize the mechanical and thermal properties of pultruded advanced composite materials. Considerable progress has been made on characterizing the effects of pultrusion process variables on the structural/dynamic and thermal properties of a mono-fiber type graphite (Hercules AS4-W-12K) - epoxy (Shell EPON 9310/9360/537) composite material system. The effects of process parameters on the mechanical properties of a mono-fiber type fiberglass (PPG 2001 E-glass) - epoxy (Shell EPON 862/W) were also investigated and correlated with the degree of cure using differential scanning calorimetry (DSC) studies. Innovative developments have been made on pultruding sandwich flat and shell-core round 'hybrids' with both glass and graphite fibers in a common epoxy binder. The mechanical properties and the failure mechanisms of these hybrids were compared with those of the mono-fiber type glass/epoxy and graphite/epoxy pultruded composites. The static properties examined were flexural strength and modulus, short-beam shear strength and tensile strength. The flexural tests were conducted under three different material conditions (as-pultruded, post-cured and hot-wet) and using two different test methods (3 point and 4 point). For the dynamic (modulus and damping) studies, the impulse frequency response technique was used for exciting the flat specimens into flexural, and the round specimens into torsional, modes of vibration using appropriately designed test fixtures. The results of these tests demonstrate the potential for the cost-effective production of stiff, light and well damped composite products having a number of practical applications. A three-dimensional numerical model which utilizes a fixed control volume based finite difference approach was also developed to predict the axial, radial and circumferential temperature and degree of cure profiles, which were found to be in close agreement with experimental results. The kinetic parameters used for the resin to predict the temperature and degree of cure profiles were obtained from DSC scans. Eight graduate students (seven masters theses and one doctoral dissertation) were supported with funds from this grant. Thirteen journal articles and/or conference proceedings have been published or are in progress. This research has equipped the grantees with an improved ability to design and produce pultruded composite materials for a given end application in the electric power industry.

CONTENTS

1
INTRODUCTION

Pultrusion is a process by which continuous reinforcement fibers are embedded in a polymeric matrix to produce a composite material. Over the years the art of pultrusion has evolved into an automated and technologically sophisticated production process, even though much of the basic science governing the process is not that well understood. High modulus, light weight composite structural elements such as beams, truss components, stiffeners, etc. have been manufactured very effectively by means of this technique. The versatility of the process has enabled pultrusion to penetrate such market areas as land transportation, construction, marine, corrosion-resistant equipment, electrical, aircraft, and specialties. With rapid advances in forming technology, the pultrusion process can produce nearly any constant cross-sectional shape that can be extruded; thus, indicating significant growth potential. Cost-competitive advantages are predicted to enable pultruded composites to become traditional materials alongside steel, wood, and aluminum before the end of the 20th century.

The high premium for improving reliability, increasing life and reducing the cost of transmission and distribution networks in the United States has necessitated that new developments in polymer science and technology be applied to utility systems. As such, polymeric materials are being used, or under consideration and development for use in electrical systems such as towers, overhead and underground cables, transmission and distribution, sub-station and utility support equipment. Pultruded solid rectangular and square bars have potential use in transformers to separate the windings and permit air circulation. Utility market applications include guy strain insulators, stand-off insulators, hot-line maintenance tools, and booms for electrical bucket trucks. Other electrical applications include tool handles, bus bar insulator supports, fuse tubes, and lighting poles. For most of these applications, pultruded composites are believed to offer inherent technical advantages such as structural strength, improved physical properties, and reduced cost along with increased life when compared to the other composite manufacturing processes.

Development and optimization of pultruded composite materials is a need recognized by a broad spectrum of governmental and industrial potential users. By concentrating the research towards the effects of process

variables on the static, dynamic and thermal characteristics of pultruded polymeric composite products, innovative material systems can be realized which are necessary for industry to provide higher quality products and service to customers at the lowest possible cost. For a number of years, commercial pultruders have used continuous glass reinforcing fibers with a thermosetting resin matrix. Processing of more advanced high-performance material systems such as graphite/epoxy is relatively new and the processing details are not as well understood. High modulus fibers such as graphite are widely used in aerospace and automotive structural applications because of their exceptionally high specific modulus and strength. Unfortunately, high cost and low impact strength are two disadvantages which limit their use. Hybridization or mixing of high cost, high modulus, low impact fibers with low cost, low modulus fibers provides a possible solution to this dilemma worth exploring further. In this way it is possible to take advantage of the combined action of individual fibers, thus optimizing the properties of the composite.

With specially designed pre-form dies, hybrid composites were pultruded at the University of Mississippi by intermingling both glass and graphite fibers in a common epoxy matrix. Two different hybrid sections, a sandwich flat and a shell-core round with different fiber lay up and volume combinations, were pultruded and their static and dynamic mechanical properties studied. In order to minimize the effects of the other pultrusion process variables a set of constant process conditions was maintained in manufacturing these experimental products. The mechanical properties and the failure mechanisms of these hybrids were compared with those of mono-fiber type (all-graphite/epoxy and all-glass/epoxy) pultruded composites.

A two-dimensional thermochemical heat transfer model was developed to describe the thermal manufacturing process based on the predicted degree of cure of the pultruded product for various process pull speeds and measured center line temperature profiles. A three-dimensional numerical model which utilizes a fixed control volume based finite difference approach was also developed to predict the axial, radial and circumferential temperature and degree of cure profiles, which were found to be in close agreement with experimental results. The kinetic parameters used for the resin to predict the temperature and degree of cure profiles were obtained from DSC scans. In the following section key results of the static, dynamic and thermal research have been summarized. For more details the reader is referred to the attached copies of the publications. A list of theses and dissertation is also appended to this report (copies will be provided under a separate correspondence).

2
RESULTS

STRUCTURAL AND DYNAMIC CHARACTERIZATION:

A 25.4mm x 3.18mm thick flat graphite (Hercules AS4-W-12K) - epoxy (Shell EPON 9310/9360/537) composite material was produced under the pultrusion process conditions suggested by a fractional factorial statistical design for the five significant process variables i.e., volume percent of fiber reinforcement, process pull speed, and three die temperature settings. Scientific characterization of the effects of these process variables on the dynamic mechanical properties (elastic modulus and material damping) of the graphite/epoxy composites has been conducted. Two techniques were used to characterize the flexural and extensional dynamic properties of the test specimens. A forced-vibration 'hysteresis loop' technique was used to generate the extensional modulus and damping data at high vibratory strains in conjunction with a servo-hydraulic MTS test system. A time-domain based logarithmic decrement method was used for computing the flexural modulus and loss factor (a measure of damping) from free vibration decay tests of cantilever beam specimens of the pultruded product. Statistical regression techniques were employed to generate mathematical models relating the pultrusion process variables to the dynamic properties. Response volume techniques have been used to show the optimum process regions for the response variables which can be evaluated for the desired end application of the pultruded product (see References A1, B2, B3 and B11 for more details).

Statistical and regression analysis techniques were employed to determine the optimal process conditions and process ability for a fiberglass (PPG 2001 E-glass) - epoxy (Shell EPON 862/W) resin system (References A6 and B8). The rheological characteristics and cure kinetics of the resin were determined using DSC techniques. Samples were taken from the finished product and tested using DSC scans to determine the total

heat of reaction and its influence on the degree of cure with respect to the process parameters (References A5, B12 and B13). Innovative developments have also been made on pultruding 'hybrids' in the Composite Materials Research Laboratory at the University of Mississippi using the in-house commercial scale PULSTAR 804 pultrusion machine (only one of two at a U.S. university). The static, dynamic mechanical properties and the failure mechanisms of these hybrids were compared with mono-fiber type all-glass/epoxy and all-graphite/epoxy pultruded products. Two different hybrid sections (a 25.4mm x 3.18mm sandwich flat and a 9.5mm diameter shell-core round) with different fiber lay up and volume combinations were pultruded and their static and dynamic mechanical properties studied. The overall fiber volume fraction was maintained at 60%. In order to minimize the effects of the other pultrusion process variables a set of constant process conditions was maintained in manufacturing these experimental products.

The static properties that were examined for these pultruded hybrids include the flexural strength and modulus, short-beam shear strength, and tensile strength. The flexural tests were conducted under three different material conditions (as-pultruded, post-cured and hot-wet) and using two different test methods (3-point and 4-point loading). The sandwich hybrid flat, with glass sandwiched between graphite, was observed to have better flexural properties compared to the other flat hybrid combinations. This fiber lay up combination also exhibited better resistance to the hot-wet environment. For desirable flexural properties, an all-graphite composite may be replaced by a hybrid of graphite-glass/epoxy designed accordingly. This gives an added advantage of reducing the amount of expensive graphite fibers by replacing the same with comparatively lower priced glass fibers. The results of the tensile tests showed a remarkable improvement in the strains to failure for all hybrid sections (regardless of the type of fiber lay up combination), compared to the all-graphite composite. For both the sandwich flat and shell-core round specimens, better tensile properties were observed with graphite sandwiched between glass for all the volume fractions tested, as opposed to glass sandwiched between graphite. The isotropic glass fibers when placed on the outer layers evidently form a protective shield for the graphite core (Reference A4).

The frequency domain impulse-frequency response vibration technique was used for exciting both the mono-fiber and hybrid type flat specimens into flexural, and round specimens into torsional, modes of vibration using appropriately designed test fixtures. Results of dynamic flexural tests on the flat specimens showed that the flexural stiffness of the all-glass/epoxy pultruded specimens can be greatly improved by the addition of graphite fibers, symmetrically distributed at the outer surfaces of the composite beams. These results are in agreement with the static flexural modulus data. In addition, the damping characteristics of these hybrids showed improvement compared to the non-hybridized composites (Reference B5). Results of the torsion tests showed that for the same fiber volume fractions, all-glass/epoxy has a higher shear modulus than all-graphite/epoxy, and that hybridization of these two material systems with glass fibers placed on the outer shell results in better dynamic performance (References A3, B6 and B10).

The improved characteristics of these hybrids demonstrate the potential for designing stiff, light and well-damped composite structures having a number of practical applications. With the proper design of such hybrid systems it is also possible to obtain materials with high impact resistance, as well as, strength and stiffness.

THERMAL AND HEAT TRANSFER PROPERTIES:

A numerical model has been developed to analyze the temperature and degree of cure profiles in pultruded composites. In pultruded composites the resin plays an important role in holding the fibers together as a structural unit and also transferring and distributing the applied load to the fibers. The degree of cure of the pultruded composite is an important phenomenon in the manufacturing process since it can be related to the mechanical properties. Therefore, the degree of cure of the resin plays a crucial role in the pultrusion process. The chemical reaction of the resin determines the degree of cure as well as the exothermic energy released by the resin. In previous research a one-step reaction model has been employed for the resin system. For some resin systems, a one-step model may not produce accurate results; therefore, it was decided to pursue a multiple-independent-step reaction model that more closely follows the actual behavior of the resin.

In this research, the effect of an approximate multiple-independent-step reaction model for the thermoset epoxy resin Shell EPON 862/W was studied. The numerical model utilized a fixed control volume based finite difference approach. This technique was used to solve the coupled, non-linear, three-dimensional steady-state energy and species equations for a cylindrical geometry. The species equation(s) utilized both a one-step Arrhenius reaction rate model as well as a multiple-independent-step Arrhenius reaction rate model for the resin. The kinetics parameters of the resin for a one-step reaction model were obtained from the DSC scans and for the multi-step model a regression fit was made to obtain the kinetic parameters from the DSC scans. The numerical model was used to predict the temperature and degree of cure for the pultruded composite both inside the die and in the post-die region. These numerical results were compared with experimental measurements. The processing variables examined in this study were die-wall temperature settings, pull speed and fiber volume fraction.

The agreement between the predicted temperature profiles and the measured temperatures for all test conditions was quite good for both the one-step and two-step chemistry model. From the numerical results, it was observed that the degree of cure predicted by a one-step reaction model was significantly lower than the two-step model. Hence, when a one-step model is used for this resin system (Shell EPON 862/W), it will predict a degree of cure for the composite which will be lower than the actual degree of cure. In such situations, a two-independent-step model will definitely improve the predicted results. From this study, it has been found that the reaction model for the resin can play an important role in modeling the curing of pultruded composites. This is supported by the fact that the reaction model is what determines the degree of cure of the composite which in turn is used in selecting the processing parameters for the manufacturing process. Additionally, it has also been determined that the pull speed and the die-wall temperature settings have a strong impact on the composite degree of cure. A higher pull speed yielded a lower degree of cure and a higher die-wall temperature settings resulted in a higher degree of cure. Similarly, a pultruded composite with a lower fiber volume resulted in a higher degree of cure. This study also helped in understanding the pultrusion process of composites for a cylindrical geometry by modeling the thermal and cure profiles both

inside the die and in the post-die region. It should be noted that the two-step reaction model for the resin was an important part of this study (References A8 and B9).

3
CONCLUSIONS AND RECOMMENDATIONS

This research has provided the Composite Materials Group at the University of Mississippi a better understanding of the interacting role of the pultruded composite structure and processing. The improved characteristics of pultruded hybrids demonstrate the potential for designing stiff, light and well damped composite structures having a number of practical applications. With the proper design of such hybrid systems it is possible to obtain materials with high impact resistance, as well as, strength and stiffness. The thermal study presents a numerical model for a three-dimensional cylindrical shaped geometry comparing a one-step with a two-independent-step reaction rate model. This model can be used to predict the temperature and degree of cure profiles of pultruded composites.

Future research efforts should be directed towards exploring the full potential of pultruded hybrid composites for optimum static and dynamic mechanical properties, as well as, impact performance, which is expected to have a profound influence on large-scale infrastructure applications. Specific needs of EPRI where pultruded products have considerable potential for application (e.g. ladders, booms, electric poles, beam and truss elements in distribution towers) should be addressed. A number of hybrid composite specimens with different lay up and fiber volume combinations of glass, graphite, Kevlar^{R} and polyethylene fibers (SPECTRA^{R}) along with epoxy, polyester and vinyl ester matrices should be pultruded using the available commercial pultrusion machine. These samples should be subjected to controlled energy and velocity impacts using the available Dynatup Model 8250 drop weight impact test machine. The fracture propagation energies for these hybrids obtained in terms of the ductility index (ratio of fracture propagation to initiation energy) should be compared with the mono-fiber type all-glass/epoxy and all-graphite/epoxy pultruded composite samples. Static mechanical properties such as axial, flexural and shear stiffness/strength should

be evaluated using three and four point bending, short beam and Iosipescue shear test fixtures. The impulse-frequency response vibration technique should be used for characterizing their dynamic modulus and loss factor (a measure of damping). The feasibility of designing pultruded composite materials and structures exhibiting high impact resistance, as well as, strength and stiffness should be validated. The long term behavior of these pultruded products in terms of creep and stress relaxation and hygrothermal degradation should also be evaluated using dynamic mechanical analysis techniques.

4

LIST OF THESES AND DISSERTATION (PARTIAL FUNDING)

[A1] Murthy Kowsika, December 1993
Optimal Pultrusion Process Variables for Improving the Dynamic Flexural Modulus and Damping in Graphite/Epoxy Composite Beams, MS Thesis.

[A2] Radesh Vangipuram, May 1994
Effect of Process Variables on the Vibro-Acoustic Material Characteristics of Pultruded Glass/Epoxy Composites, MS Thesis.

[A3] Sujit S. Kumar, May 1994
Characterization of Dynamic Mechanical Properties of Pultruded Hybrid Cylindrical Composites Rods in the Torsional and Flexural Modes of Vibration, MS Thesis.

[A4] Kumar Papineni, August 1994
Study of Static Mechanical Properties of Pultruded Hybrid Graphite/Glass Epoxy Composites, MS Thesis.

[A5] Reshma Shanku, December 1994
Rheological Characterization and Cure Analysis of EPON 862/W Epoxy Used in Pultrusion, MS Thesis.

[A6] Jack McClurg, December 1994
The Effects of Pultrusion Processing Parameters on the EPON 862/W Epoxy/Fiberglass System, MS Thesis.

[A7] Chandrasekhar Nori, August 1995
Experimental and Finite Element Analysis of Pultruded Glass-Graphite/Epoxy Hybrid Composites in Axial and Flexural Modes of Vibration, MS Thesis.

[A8] Meyyappan, Valliappan, in progress (anticipated December 1995)
Thermal, Flow, and Cure Characterization of Pultruded Circular Composites, Ph.D. Dissertation

APPENDIX A

List of Publications

[B1] J. G. Vaughan, J. A. Roux, and P. R. Mantena, "Characterization of Mechanical and Thermal Properties of Advanced Composite Pultrusions," *Proceedings of the 1992 NSF Design and Manufacturing Systems Conference*, Georgia Institute of Technology, Atlanta, Georgia, January 8-10, 1141-1145, 1992.

[B2] P. R. Mantena, J. G. Vaughan, R .P. Donti, and M. V. Kowsika, "Influence of Process Variables on the Dynamic Characteristics of Pultruded Graphite-Epoxy Composites," *Vibro-Acoustic Characterization of Materials and Structures*, ASME, NCA-Vol 14, 147-154, 1992.

[B3] J. A. Roux, P. R. Mantena, and J. G. Vaughan, "Mechanical and Thermal Behavior of Pultruded Advanced Composites," *Proceedings of the 1993 NSF Design and Manufacturing Systems Conference*, Vol 1, 285-291, 1993.

[B4] J. G. Vaughan, J. A. Roux, and P. R. Mantena, "Mechanical and Thermal Behavior of Pultruded Advanced Composites," *Proceedings of the 1994 NSF Design and Manufacturing Grantees Conference*, 659-660, 1994.

[B5] P. R. Mantena, R. Vangipuram, and J. G. Vaughan, "Dynamic Flexural Properties of Pultruded Glass/Graphite Hybrid Composites," *Proceedings of the 39th International SAMPE Symposium*, 39 (1) 174-182, 1994.

[B6] S. S. Kumar and P. R. Mantena, "Characterization of Dynamic Mechanical Properties of Hybrid Cylindrical Composite Rods in the Torsional Mode of Vibration," *Proceedings of the 35th AIAA/ASME/ASCE/AHS/ASC Structures, Structural Dynamics and Materials Conference*, Hilton Head, SC, April 18-20, 1223-1232, 1994.

[B7] J. G. Vaughan, J. A. Roux, and P. R. Mantena, "Characterization of Mechanical and Thermal Properties of Advanced Composite Pultrusions," *Proceedings of the 1995 NSF Design and Manufacturing Grantees Conference*, San Diego, CA, January 1995.

[B8] J. A. McClurg and J. G. Vaughan, "The Effects of Processing Parameters on the Shell EPON 862/W Epoxy/Fiberglass System," *Proceedings of the 50th Annual Conference of the Composites Institute*, 6D:1-7, 1995.

[B9] M. Valliappan, J. A. Roux, J. G. Vaughan, "Temperature and Cure in Pultruded Composites Using a Multi-Step Reaction for Resin,"*Journal of Reinforced Plastics and Composites*(accepted)

[B10] S. Kumar and P. R. Mantena, "Dynamic and Static Torsional Characterization of Pultruded Hybrid Cylindrical Composite Rods," *Journal of Composite Materials* (accepted)

[B11] M. Kowsika and P. R. Mantena, "Optimal Pultrusion Process Conditions for Improving the Dynamic Properties of Graphite - Epoxy Composite Beams," *Materials Evaluation* (submitted)

[B12] R. Shanku, J. G. Vaughan, and J. A. Roux, "Rheological Characteristics and Cure Kinetics of EPON 862/W Epoxy Used in Pultrusion," (in preparation)

[B13] R. Shanku, J.G. Vaughan, and J.A. Roux, "Effect of Pultrusion Variables on the Cure of Shell EPON 862/W epoxy/ fiberglass System," *41st International SAMPE Conference*, Anaheim CA, (submitted)

APPENDIX B

Copies of Publications

Characterization of Mechanical and Thermal Properties of Advanced Composite Pultrusions

James G. Vaughan, Jeffrey A. Roux, and P. Raju Mantena
Department of Mechanical Engineering
The University of Mississippi

Abstract

This paper will present an overview of the research to be conducted on the characterization of the mechanical and thermal properties of pultruded composites. The research is in the initial planning stages with no experimental or analytical work yet started. Therefore this paper will highlight the plan of study and the research efforts that will be undertaken to advance the science of pultrusion processing.

Pultrusion, though a well developed processing art, is not well understood scientifically. Much basic study remains before the process of pultruding composite materials can be stated to be on a firm scientific basis. Such fundamental understanding will be required to develop high performance structural products or products that take advantage of the wide range of possible thermal conductivities of composite materials. The studies proposed will provide a first step toward understanding the pultrusion process variables as they relate to conditions of dynamic loading or to bidirectional thermal conductivity. The study will result in models to characterize the process and an improved ability to design/produce a pultruded material for a given end use.

The need to develop and optimize pultruded composite materials is recognized by a broad spectrum of governmental and industrial potential users. By focusing the research to be conducted on the effects of process variables on the thermal, dynamic, and NDE characteristics of pultruded polymeric composite products, innovative material systems can be developed which are important to the industry in their goal of providing high quality products/service to customers at the lowest possible cost.

INTRODUCTION

Pultrusion is a process by which continuous reinforcement fibers are embedded in a polymeric matrix to produce a composite material, Figure 1. Over the years the art of pultrusion has evolved into an automated and technologically sophisticated production process, even though much of the basic science governing the process is not that well understood. High-modulus, light weight composite structural elements such as beams, truss components, stiffeners, etc. have been manufactured very effectively by means of this technique. The versatility of the process has enabled pultrusion to penetrate such market areas as land transportation, construction, marine, corrosion-resistant equipment, electrical, aircraft, and specialties. With rapid advances in forming technology, pultrusion can produce nearly any constant cross-sectional shape that can be extruded; thus, indicating significant growth potential. For many advanced applications, pultruded composites offer inherent technical advantages such as structural strength, improved physical properties, and reduced cost along with increased life when compared to the other composite processes. Cost-competitive advantages will enable pultruded composites to become traditional materials along side steel, wood, and aluminum before the end of the 20th century [1].

For a number of years the pultrusion process has used continuous glass reinforcing fibers with a thermosetting resin matrix. Pultrusion of more advanced high-performance material systems such as graphite/epoxy is relatively new and the processing details are not as well understood. Work with thermoplastic is even less understood. Pultrusion, though simple in concept, is quite complex in detail due to the numerous interacting process parameters. With a series of statistically designed experiments the authors have evaluated the interdependencies of the pultrusion process parameters for a graphite/epoxy system [2]. Through the use of these experimental techniques, the pultrusion of this product was optimized for any single measurable process or quality factor, such as, composite tensile strength and/or shear strength, or for any combination of required property values, e.g., a minimum acceptable tensile strength at a minimum acceptable shear strength. For the graphite/epoxy composite material system it was concluded that the three most important operating parameters for optimization of the pultrusion process were the die platen heating

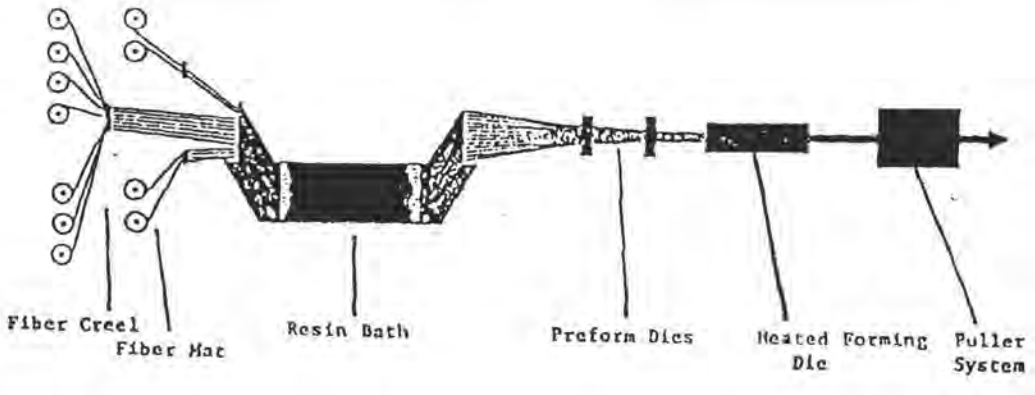

Figure 1. Illustrative schematic of the pultrusion process.

temperatures, the percent fiber content, and the pull speed. Other process parameters are likely to be more important for other resin systems. The mechanical and physical properties that were characterized as a function of these operating parameters include void content, roundness factor (for pultruded rods), tensile and compressive strengths along with torsional and short beam shear strengths.

What has not been investigated, however, is the effect of the important operating parameters (e.g. die platen heating temperatures, percent fiber content, or pull speed) on the dynamic mechanical and thermal properties of the pultruded products. With the intended end application of these pultruded components in advanced engineering structures, their performance in dynamic loading and thermal environments becomes highly critical. The present research will address the effects of these process variables on the thermal and dynamic characteristics of pultruded composite specimens for an integrated optimization of the graphite/epoxy pultrusion process. The bidirectional thermal properties will be characterized and optimized for glass and graphite reinforcements and for a combination of the two fiber systems. Vibration response measurements will also be used as a mechanistic tool in quality control operations and for non-destructive evaluation (NDE) of the structural integrity of pultruded components.

EXPERIMENTAL CHARACTERIZATION OF PULTRUSION PROCESSING

The structural/dynamic properties and the thermal properties of materials produced by the pultrusion process will be experimentally determined by use of statistical experimental design techniques. The pultrusion experiments will be conducted on a Pultrusion Technology, Inc. Pulstar 804 pultruder located at the University of Mississippi. Analysis of these carefully controlled and monitored experiments and the results of the thermal and dynamic test results will be conducted in a similar manner to that reported previously [2]. For each property value of importance, an analysis will be conducted to determine the most important process control parameters and the control volume in which these parameters must be held in order to obtain a desired product property value. The required process control volumes will be determined separately for each property value as well as in combination with other desired property values to form a useful product. From the statistical design and analysis, the optimum processing condition will be determined for producing the desired sets of structural/dynamic properties and thermal properties to be discussed below.

DIRECTIONAL THERMAL CONDUCTIVITY AND HEAT TRANSFER PROPERTIES

Understanding of the complex thermochemical processing of the pultrusion process is very important for producing a product of high/optimum mechanical properties. The quality of the manufactured pultruded composite material part will depend strongly on the thermal properties of the reinforcement fibers and resins used to manufacture the part. It is clear that the thermal conductivity in the cross-fiber and with-fiber directions will be different (bidirectional). These differences in thermal conductivity will be important for two important reasons. First the bidirectional thermal conductivity will affect the curing process which occurs in the pultrusion die. A non-uniform distribution of heat transfer could lead to non-uniform curing in the die and hence influence the mechanical properties of the pultruded part. Also the thermal conductivity of the finished part will be bidirectional. Using the finished part in a thermally sensitive application would require a clear knowledge of this bidirectional thermal behavior so that the finished part is employed in a successful design. The thermal research will investigate the experimental measurement of the bidirectional

thermal conductivity and to use this measured bidirectional thermal conductivity in a computational model to predict the heat transfer and curing behavior in the pultrusion die. Also the computational model will be used to predict the thermal properties of the finished pultrusion product. The research will investigate the situation of mixing different types of reinforcement fibers, each having a different bidirectional thermal conductivity, and how these mixtures of fibers impact curing in the pultrusion die (and hence mechanical properties) and how these mixtures impact the overall spatial distribution of thermal conductivity of the finished product. However before going into the details of the research, it is important to define the thermochemical problem and also to present the governing equations which must be solved.

Though the art of pultrusion is being mastered by experience and workmanship, the governing scientific principles have not been fully explored. A mathematical model will be developed from fundamental principles using numerical methodology to solve the mathematical model and testing the model with experimental results.

The problem considered is of a transient nature in three-dimensions. The analytical model for circular pultruded stock will deal with cylindrical coordinates. An illustrative schematic of the pultruded product is shown in Figure 2. When the resin impregnated fibers are pulled through the cylindrical die, there will be a very thin liquid region (annulus region) [3] between the die wall and the fiber-resin mass (core). The thickness of this liquid region cannot be precisely determined and so it is parameterized as the ratio of the liquid region thickness to the die diameter.

When the fiber-resin mass is pulled through the heated die, the curing of resin occurs and results in the formation of a high molecular weight material. The liquid annulus region is the first to receive heat from the die wall, but the thermal conductivity of the liquid resin is very low. Depending on the thickness of this liquid film, there will be a pronounced effect on the heat transfer. Therefore, it is necessary to solve the two momentum equations (radial and axial) to obtain the velocity profile within the annulus region. Once cured, the liquid resin becomes solid, debonds from the die wall, and then moves along with the core. The curing process is an exothermic chemical reaction and releases heat. Hence, the core temperature will reach a higher

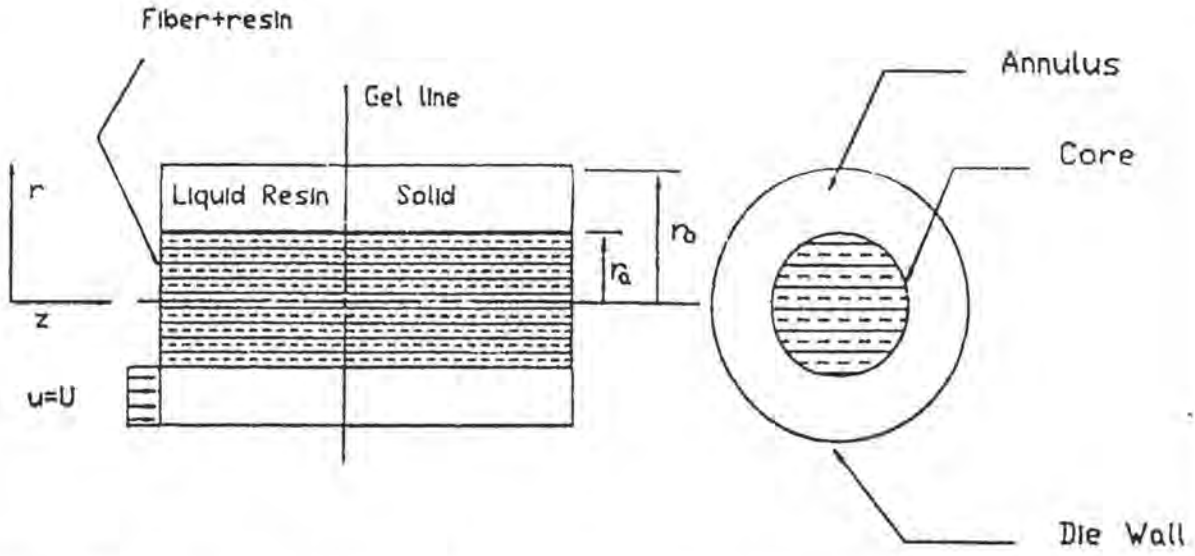

Figure 2 Physical geometry of pultrusion die and schematic of pultruded cross-section before cure (not to scale)

value than the die wall and the direction of heat transfer will become reversed, i.e. heat transfer will occur from the core to the die wall. Of course, there could be heat transfer occurring to the upstream material as well as the downstream product in the axial direction. In this research, the axial and circumferential diffusion of heat will be considered important; in earlier work [4,5,6] the circumferential and axial conduction were neglected.

A phenomenological model is used for chemical reaction. It is considered that diffusion of chemical species is negligible and the Arrhenius equation of order 'n' is incorporated. The backbone of the model is the energy equation. The reaction rate equation is coupled into the energy equation, because the cure reaction is exothermic with the heat generation term incorporated as a source term in the energy equation. Viscous terms in the energy equation are included to account for the effect of viscous dissipation. The boundary conditions required for solving the energy equation are the specified temperature at the die wall as a function of die length and specified inlet/preheat temperature at the entrance of the die. The two cross-section regions, the annulus and the core, are distinctly different. The annulus is considered to contain only resin and hence

only the bulk properties for the combined cured and uncured resin have to be considered. In the core region, the bidirectional thermal properties of combined cured resin, uncured resin and fibers have to be used in the analysis. These properties will be measured in the experimental portion of this project. The present numerical model aims at developing a mathematical model for simulating the pultrusion process as closely as possible. For a cylindrical die, with the assumption of axial symmetry and the resin flow in the gap being steady hydrodynamically, the governing equations are:

Continuity:

$$\frac{\partial v}{\partial r} + \frac{v}{r} + \frac{\partial u}{\partial z} = 0 \tag{1}$$

where v is radial velocity and u is axial velocity of the liquid resin.

Radial-momentum:

$$v\frac{\partial v}{\partial r} + u\frac{\partial v}{\partial z} = -\frac{1}{\rho}\frac{\partial p}{\partial r} + \nu\left(\frac{\partial^2 v}{\partial r^2} + \frac{1}{r}\frac{\partial v}{\partial r} - \frac{v}{r^2}\right) \tag{2}$$

where p, ρ and ν are pressure, density and kinematic viscosity of the resin respectively.

Axial-momentum:

$$v\frac{\partial u}{\partial r} + u\frac{\partial u}{\partial z} = -\frac{1}{\rho}\frac{\partial p}{\partial z} + \nu\left(\frac{\partial^2 u}{\partial r^2} + \frac{1}{r}\frac{\partial u}{\partial r}\right) \tag{3}$$

Energy :

$$\rho c\frac{\partial T}{\partial t} + \rho uc\frac{\partial T}{\partial z} + \rho vc\frac{\partial T}{\partial r} = \frac{1}{r}\frac{\partial}{\partial r}\left(k_c\frac{\partial T}{\partial r}\right) + \frac{\partial}{\partial z}\left(k_w\frac{\partial T}{\partial z}\right) + \frac{1}{r}\frac{\partial}{\partial \theta}\left(\frac{k_c}{r}\frac{\partial T}{\partial \theta}\right) + \mu\left(\frac{\partial u}{\partial r}\right)^2 + S_A \tag{4}$$

where ρ and c are the density and specific heat, and k_c and k_w are the cross-fiber and with-fiber thermal conductivities respectively; S_A is the source term due to reaction and is given by

$$S_A = C_I (\Delta H) R_A \tag{5}$$

where ΔH is the heat of reaction; C_I and R_A are defined below .

(6)

Species:

$$\frac{\partial \psi}{\partial t} + u\frac{\partial \psi}{\partial z} + v\frac{\partial \psi}{\partial r} = R_A$$

where the reaction rate term R_A is given by

$$R_A = k_o \exp(-E_k/RT)(1-\psi)^n \tag{7}$$

and the degree of cure is defined by

$$\psi = (C_I - C_A)/C_I \tag{8}$$

where C_I and C_A are the initial concentration of uncured resin and the local concentration of uncured resin at any time respectively. In equation (7), k_o is the pre-exponential constant; E_k is the activation energy, R is the universal gas constant, and n is the order of reaction.

The boundary and initial conditions for the above equations are:

$$u = U = \text{pull speed} \quad \text{at} \quad z = 0 \quad , \quad r < r_o$$

$$u = o \quad \text{at} \quad r = r_o$$

$$u = U \quad \text{at} \quad r = r_a$$

$$v = 0 \quad \text{at} \quad z = 0$$

$$v = 0 \quad \text{at} \quad r = r_o \quad , \quad r = r_a$$

$$T = T_0, \quad \psi = 0 \quad \text{at} \quad t = 0 \quad r < r_o$$

$$T = T_w \quad \text{at} \quad r = r_o$$

Equations (1)-(3) are solved numerically by a finite difference method (Patankar method [7]) to obtain the velocity profile in the annulus region. The detailed methodology of a similar problem in Cartesian coordinates can be found in the work of Anderson [8]. The energy equation and the species reaction equation are coupled and non-linear. These equations are solved simultaneously by an iterative scheme utilizing the same methodology [7] as mentioned earlier. The experimental data for the composite material will be obtained from pultrusion experiments conducted in the Composite Materials Laboratory at the University of Mississippi.

The heat transfer research will be comprised of an experimental component and a computational component. With regard to the experimental component, the proposed research will be the determination of the cross-fiber direction (k_c in equation (4)) and with-fiber direction (k_w in equation (4)) thermal conductivity measurement. The measurement of the thermal conductivity in the cross-fiber direction will be measured in compliance with the standard ASTM F 433 (C-Matic). The samples will be 2 inch in diameter and 1/8 inch thick. The thermal conductivity in the with-fiber direction will be measured in compliance with the standard ASTM E 1225. Each sample will again be 2 inch in diameter and 1/8 inch thick.

The measured thermal conductivity values for the bidirectional conductivity will be employed in the computational model. The computational model will be used to predict the temperature and degree of cure profiles within the pultrusion die. Knowledge of the degree of cure distribution within the pultrusion die is important for determining the mechanical and dynamic properties of the finished pultruded product. The

computational model will also be used to predict the thermal heat transfer characteristics of the finished product. Also, the computational model will have the capability of predicting the thermal properties of a composite material made of mixed tows of glass, graphite, and resin as long as the spatial (radial and circumferential) distribution of the glass and graphite tows is known or specified.

DETERMINATION OF STRUCTURAL/DYNAMIC PROPERTIES

Elastic modulus and internal damping of materials under vibratory loading are generally referred to as dynamic mechanical properties. Experimental data on elastic modulus and damping are often used (a) as input to design calculations, (b) as quality control parameters during manufacturing / processing, and (c) as non-destructive evaluation parameters during in-service inspection for structural integrity.

Dynamic mechanical properties may be characterized using either vibration or wave propagation experiments. This project only deals with vibration test methods, which cover the nominal frequency range 0.001 - 1000 Hz. Standard test methods, for the measurement of dynamic mechanical properties of nonreinforced plastics have been developed by ASTM [9], but these methods and commercially available dynamic mechanical analyzers based on these methods have been found to be inadequate for testing high modulus polymer composites [10]. As a result, the modulus values generated by these methods are generally too low and the damping values are too high.

The most recently developed techniques are based on the use of random or impulsive excitation of specimens to instantaneously generate the frequency response curve [11-13]. Dynamic mechanical properties are then obtained by curve fitting to the frequency response curve. For example, the frequency equation for a cantilever beam can be used to find the flexural modulus E_f, as shown in Equation (9).

$$E_f = \frac{4\ \pi^2\ L^4\ \rho\ A\ f_n^2}{\lambda_n^4\ I} \tag{9}$$

where: L = free length of beam

ρ = mass density of beam

A = cross-sectional area of beam

f_n = resonant frequency of nth mode

λ_n = eigenvalue of nth mode

I = area moment of inertia of beam about neutral axis

Similar equations can be found for other modes of vibration and boundary conditions. The storage modulus for extensional mode of vibration or the shear modulus for torsional excitation are found from

$$G' = \frac{4\,\pi^2\,L^2\,\rho\,f_n^2}{\lambda_n^2} \tag{10}$$

where, L, is the length of the specimen between grips and the rest of the parameters are as defined earlier.

The loss factor, η, a measure of damping, is found from the half power bandwidth method, Δf, according to the following equation

$$\eta = \frac{\Delta f}{f_n} \tag{11}$$

The complex flexural modulus, E_f^*, is then

$$E_f^* = E_f\,(1 + i\eta) \tag{12}$$

Similar complex module can be defined for extensional [13] and torsional vibration [14]. Frequencies can be varied by changing the dimensions of the specimen or by changing the specimen masses.

These techniques have been used to characterize a variety of composites such as graphite/epoxy [12], boron/epoxy and aramid/epoxy [13], glass/polyester [15] and polyethylene/epoxy [16]. Damping, stiffness and mode shape measurements have also been used for non-destructive evaluation of damage, degradation, flaws and defects in composites and adhesively bonded joints. For example, the technique has been used in studies of matrix cracks and delaminations in composite laminates [17-20] and debonds and porosity in adhesively bonded metal specimens [21,22]. Similar techniques have been used to study effects of moisture

and temperature on mechanical behavior of composites [23]. In all cases, defects, damage or degradation in the structure may be quantified by observing shifts of the resonant peaks to lower frequencies (i.e., reduced stiffness) and corresponding increases in the bandwidths of the peaks (i.e., increased damping). Damping is generally the more sensitive of the two parameters and can be used for non-destructive evaluation.

Although damping tests are often done at low strain levels in the linear range, higher strains can be generated by using an electromagnetic shaker to excite the specimen instead of an impulse hammer. Alternatively, the hysteresis loop technique [10,18] can be used to generate extensional damping data at high vibratory strains using a servo-hydraulically controlled structural test system. The name "hysteresis loop" comes from the fact that the plot of the sinusoidally varying load or stress versus the corresponding sinusoidally varying strain describes an elliptic loop. The modulus and the loss factor can be estimated from the dimensions of the hysteresis loop. Such parameters as frequency, mean stress and vibratory stress amplitude can be easily controlled with this technique. The flexural, extensional and torsional (for round specimens) versions of the impulse frequency-response vibration technique and the hysteresis loop technique will be used for experimental characterization of the dynamic mechanical properties of pultruded graphite/epoxy specimens. These test specimens will be fabricated (using the in-house pultrusion machine) by varying the operating parameters such as die platen heating temperatures, percent fiber content and pull speed of the pultrusion process.

The effects of hybridization, i.e., a mix of continuous glass and graphite fibers in an epoxy matrix (which will be attempted for facilitating directional thermal conductivity through the fibers) on the physical, mechanical and dynamic properties of the pultruded specimens will be investigated. Previous research has shown that such hybridization offers the potential for stiff, light, highly damped composite structures that should have numerous practical applications [16,24].

The feasibility of using the impulse frequency-response technique to quantify defects in pultruded components will be explored. In sample specimens artificially induced defects will be incorporated during the pultrusion process. For example, a mold release agent can be applied to the fibers before passing them through the epoxy bath and die platens. This would create defective pultruded specimens with poor

interfacial bonding between the fiber and matrix. The frequency and damping signatures of these defective specimens will be compared with that of "good" specimens which have been prepared by the optimized pultrusion process described earlier. The sensitivity of the impulse frequency-response technique as a viable quality control NDE tool for identifying defective pultruded components will be demonstrated.

SUMMARY

There is a lack of scientific understanding concerning the pultrusion processing of composite materials for use in dynamic or bidirectional thermal conductivity applications. The work to be conducted will provide an experimental database from which these material properties can be characterized and optimized. Models will be developed to help understand the role that processing plays in the development of dynamic and thermal properties and these models will be used to enhance these properties of the composite material, especially for use in the electric power industry.

By focusing research on the effects of process variables on the thermal and dynamic characteristics of pultruded composite products, innovative polymeric composite systems can be developed that are of importance to industry. A novel NDE technique for characterizing the structural integrity of the pultruded components will also be examined.

REFERENCES

1. Sumerak, J.E. "Understanding Pultrusion Variables for the First Time", *40th Annual Conference, Reinforced Plastics/Composites Institute*, Society of the Plastics Industry, Atlanta, Jan 1987.

2. J. G. Vaughan, R. M. Hackett, and E. C. Seal, "Optimization of the Pultrusion Process for Graphite/Epoxy," *Fiber-Tex 1988*, NASA CP-3038, 1989.

3. Walsh, S. M., and Charamchi, M., "Heat Transfer Characteristics of a Pultrusion Process", *25th National Heat Transfer Conference*, Houston, July 1988, pp. 23-28.

4. R. Gorthala, J.A. Roux, and J.G. Vaughan, "Heat Transfer Analysis for a Pultrusion Process," *Fiber-Tex 1990*, Clemson, S.C., August, 1990.

5. R. Gorthala, J.A. Roux, and J.G. Vaughan, "Impact of Pultrusion Pull Speed on Temperature and Degree of Cure Profiles Within a Composite Material," *SPI Composite Institute's 46th Annual Conference*, Washington, D.C., February 1991.

6. J.G. Vaughan, R. Gorthala, and J.A. Roux; "Characterization and Optimization of the Pultrusion of Structural Shapes," *ASCE Specialty Conference on Advanced Composites*, Los Vegas, NV, February 1991.

7. Patankar, S. V., *Numerical Heat Transfer and Fluid Flow*, Hemisphere Publishing Corp., Washington, D. C., 1980.

8. Anderson, J. D., "Numerical Investigation of Three-Dimensional, Parabolic, Developing Flow in Rectangular Solar Collector Ducts", Masters Thesis, University of Mississippi, 1986.

9. Standard Practice for Determining and Reporting Dynamic Mechanical Properties of Plastics, *ASTM Standard D 4065*, American Society for Testing and Materials, 1983.

10. Gibson, R.F., "Vibration Test Methods for Dynamic Mechanical Property Characterization", in Manual on *Experimental Methods for Mechanical Testing of Composites*, R.L. Pendleton and M.E. Tuttle, Editors, Society of Experimental Mechanics, 151-164, 1989.

11. Suarez, S.A., Gibson, R.F., and Deobald, L.R., "Random and Impulse Techniques for Measurement of Damping in Composite Materials",*Experimental Techniques*, 8(10), 19-24, 1984.

12. Suarez, S.A., and Gibson, R.F., Sun, C.T., and Chaturvedi, S.K., "The Influence of Fiber Length and Fiber Orientation on Damping and Stiffness of Polymer composites", *Experimental Mechanics*, 26 (2), 175-184, 1986.

13. Suarez, S.A., and Gibson, R.F., "Improved Impulse-Frequency Response Techniques for Measurement of Dynamic Mechanical Properties of Composite Materials", *Journal of Testing and Evaluation*, 15 (2), 114-121, 1987.

14. Mantena, P.R., Gibson, R.F., and Place, T.A., "A Torsional Impulse Frequency-Response technique for evaluating the Dynamic Mechanical Properties of Structural Materials", *Proceeding of 6th Annual ASM/ESD Advanced Composites Conference*, Detroit, Michigan, October 8-11, 1990.

15. Gibson, R.F., Yau, A., and Riegner, D.A., "Vibration Characteristics of Automotive Composite Materials", *Short Fiber Reinforced Composite Materials*, B.A. Sanders, Editor, STP, 772, ASTM, 133-150, 1982.

16. Gibson, R.F., Rao, V.S., and Mantena, P.R., "Vibration Damping Characteristics of Highly Oriented Polyethylene Fiber Reinforced Epoxy Composites," *Advanced Materials Technology*, '87, Proc. 32nd Int. SAMPE Symposium, 231-244, 1987.

17. Mantena, P.R., Place, T.A., and Gibson, R.F., "Characterization of Matrix Cracking in Composite Laminates by the Use of Damping Capacity Measurements," *Proc. of Symposium on the Role of Interfaces on Material Damping*, October 1985, Toronto, Canada, 79-94, ASM International, 1985.

18. Mantena, R., Gibson, R.F., and Place, T.A., "Damping Capacity Measurements of Degradation in Advanced Materials",*SAMPE Quarterly*, 17 (3), 20-31, 1986.

19. Lee, B.T., Sun, C.T., and Liu, D., "An Assessment of Damping Measurement in the Evaluation of Integrity of Composite Beams,"*Journal of Reinforced Plastics and Composites*, 6, 114, 1987.

20. Tracy, J.J., and Pardoen, G.C., "Effect of Delamination on the Natural Frequencies of Composite Laminates,"*Journal of Composite Materials*, 23, 1200-1215, 1989.

21. Mantena, P.R., Srivatsan, T.S., Gibson, R.F., Place, T.A., and Sudarshan, T.S., "Debond and Failure Characteristics of a Double Lap Adhesively Bonded Joint," *Journal of Adhesion Science and Technology*, 2 (3), 189-202, 1988.

22. Srivatsan, T.S., Mantena, P.R., Gibson, R.F., Place, T.A., and Sudarshan, T.S., "Electromagnetic Measurement of Damping Capacity to Detect Damage in Adhesively Bonded Material," *Materials Evaluation*, 47 (5), 564-570, 1989.

23. Gibson, R.F., Yau, A., Mende, E.W., Osborn, W.E. and Reigner, D.A., "The Influence of Environmental Conditions on the Vibration Characteristics of Chopped Fiber Reinforced Composite Materials",*Journal of Reinforced Plastics and Composites*, 1(3), 225-241, 1982.

24. Mantena, P.R., Gibson, R.F., "Dynamic Mechanical Properties of Hybrid Polyethylene/Graphite Composites," *Proceedings of the 22nd International SAMPE Technical Conference*, Boston, MA, Nov. 6-8, 1990.

Influence of Process Variables on the Dynamic Characteristics of Pultruded Graphite-Epoxy Composites

P.R. Mantena, J.G. Vaughan, R.P. Donti, and M.V. Kowsika
Department of Mechanical Engineering
University of Mississippi
University, MS 38677

ABSTRACT

In this paper the influence of pultrusion process variables on the dynamic mechanical properties (elastic modulus and internal damping) of graphite-epoxy composite materials are presented. Two techniques were used to characterize the flexural and extensional dynamic properties of the specimens that were produced under the process conditions suggested by a fractional factorial statistical design for the five significant process variables. The "hysteresis loop" technique was used to generate the extensional modulus and damping data at high vibratory strains using a servo-hydraulically controlled structural test system. A log-decrement method was used for computing the flexural modulus and loss factor (a measure of damping) from free vibration decay tests of pultruded cantilever beam specimens. Results of this study indicate that the process variables have an influence on the dynamic mechanical properties of pultruded graphite-epoxy composites and optimum process conditions for the desired end application can be evaluated.

INTRODUCTION

The pultrusion process is best suited to the production of parts of any desired length with a constant cross-section and has been used to cost-effectively manufacture products ranging from mop handles to automotive drive shafts. High-modulus, light weight composite structural elements have been manufactured very efficiently by this technique. With rapid advances in forming technology, pultrusion can produce nearly any constant cross-sectional shape; thus, indicating significant market growth potential. For most

applications, pultruded composites offer inherent technical advantages such as structural strength, improved physical properties, and reduced cost along with increased life when compared to composite materials produced by other manufacturing processes.

In the pultrusion process, resin impregnated fibers are continuously pulled through a heated die by a puller mechanism. The heat from the dies triggers the required chemical reaction in the thermoset resin. A high degree of resin cure and interfacial bonding between the fibers and matrix are obtained under the combined influence of the exothermic reaction and the pressure inside the die, especially for thin sections. The cured composite material leaves the die hot, but cools under ambient conditions before reaching the pullers. After passing through the pullers the continuous pultruded composite product is cut into desired lengths.

Although simple in concept, the quality of the pultruded product is dependent on numerous process variables through their complex interactions. The five pultrusion process variables that were considered to be significant with respect to the mechanical properties of graphite-epoxy composites and included for this study on dynamic properties were: the volume percent of fiber reinforcement, process pull speed, and the zone 1, zone 2, zone 3 die temperatures. The pull speed influences the extent of cure in the composite material thereby indirectly affecting the mechanical properties of the final product. The importance of the temperature profile on the die cannot be over-emphasized. The in-house pultrusion machine (PULSTAR 804 commercial model), used for producing the test material for the present investigation, has three die heat zones with separate heat controls for the top and bottom heating platens. The three die zone temperatures and the heat transfer conditions associated with the die establish the temperature profile. A slowly increasing temperature profile is preferred to a constant die temperature in order to raise the temperature of the material to a temperature slightly lower than the cure temperature and to provide for a small temperature gradient from the product surface to the interior. The exotherm produced by the resin chemical reaction brings the whole cross-section of the material to the curing temperature once cure has started at the outer surface region. The material temperature at exotherm point becomes greater than the die temperature. The second portion of the

die basically provides the energy to achieve a high degree of cure of the composite. The remainder of the die receives heat from the material to reduce the thermal shock to the product upon exiting the die to ambient conditions.

The above discussion is presented to indicate that the process variables affect the quality of the pultruded composite material and influence the properties of the product when placed in service. With the intended end application of the pultruded components in the form of beams, trusses, stiffeners, etc., their performance in dynamic loading environments (fatigue) becomes highly critical. Very little research has been conducted, however, to characterize the elastic modulus and internal damping of these pultruded materials under vibratory loading. This is of special interest because experimental data on elastic modulus and damping are often used as input to design calculations, as quality control parameters during manufacturing / processing, and as non-destructive evaluation parameters during in-service inspection for structural integrity.

Dynamic mechanical properties may be characterized using either vibration or wave propagation experiments. Standard test methods for the measurement of dynamic mechanical properties of non-reinforced plastics have been developed by ASTM, but these methods and commercially available dynamic mechanical analyzers based on these methods have been found to be inadequate for testing high modulus polymer composites [Gibson, 1991]. Accordingly, and due to limits in the available equipment/facilities, a forced vibration "hysteresis loop" technique and a free vibration log-decrement method have been selected to determine the extensional and flexural dynamic properties of these pultruded composites.

EXPERIMENTAL DESIGN

The five pultrusion process variables, each at two process levels or control values, suggest modeling of the variety of processing conditions through fractional factorial statistical design. The layout of the design is shown in Table 1 where -1 and +1 are coded values representing the lowest and highest levels of the five factors. These designs can provide estimates of principal factor effects and low order interactions. If the effect of one factor on the response variable is dependent on the levels of the other factors then factor

interaction is said to exist. Randomization of the trial sequence as shown in Table 1 tends to limit systematic errors.

The average of the mechanical property values for the experimental conditions shown in Table 1 were subjected to linear regression analysis using SAS software packages [Freund and Littell, 1991]. Since the present study included several independent variables, multiple regression analysis technique was employed. The number of terms in the analytical model were minimized for simplicity and ease of graphical presentation. The reduced model consists of the process variables and their interactions that estimated best the actual experimental values. The terms were arranged in a simple regression equation such as

$$y = b_0 + b_1 x + \ldots\ldots + b_{12} xy + \ldots\ldots \quad (1)$$

to estimate the response. Equation (1) consists of fit coefficients such as b_0, process variables such as x, and crossed terms (process interactions) such as xy. Regression models such as Eq. (1) can be graphically presented using response volume techniques [Vaughan, Hackett, and Seal (1988), and Vaughan (1988)]. These response volume techniques are helpful in showing the region of interest and obtaining optimum process conditions, as demonstrated later in this paper.

EXPERIMENTAL PROCEDURE AND DYNAMIC TEST METHODS

A 1"x ⅛" thick flat graphite (Hercules' AS4-W-12K) - epoxy (Shell's EPON^R 9310/9360/537) composite material was produced under carefully monitored pultrusion process conditions as suggested by the fractional factorial design of Table 1. Test specimens were cut from material pultruded from each of the 16 test conditions shown in Table 1, separated into three batches and kept under a vacuum less than 10^{-2} torr. The specimens were removed from the vacuum chamber just before dynamic testing. A minimum of three specimens (one from each batch) were tested for each set of process conditions to determine the scatter in data.

HYSTERESIS LOOP TECHNIQUE :

Viscoelastic materials such as polymer matrix composites exhibit a phase lag in the strain signal when loaded. The name "hysteresis loop" comes from the fact that the plot of the sinusoidally varying load or stress versus the corresponding sinusoidally varying strain describes an elliptic loop (as shown in the inset of Figure 1). The storage modulus and loss factor can be estimated from the dimensions of the hysteresis loop. Parameters such as frequency, mean stress and vibratory stress amplitude can be easily controlled with this technique [Mantena, Gibson, and Place (1986); Renz, Altstadt, and Ehrenstein (1988)]. This technique was used in the current research to generate the extensional modulus and damping data at high vibratory strains using a servo hydraulically controlled 22 kip MTS structural test system. The pultruded graphite-epoxy samples from each batch were subjected to a tension-tension sinusoidal cyclic loading at 4 Hz and a fatigue ratio (R) of 0.0625 (1 -16 kip) under load control. The load history was obtained from the machine's load cell.

Strain is usually monitored using strain gages for high precision. If strain level is close to ‴ 3000 μ strain, dynamic strain gages are available for about 10^5 test cycles. Reduced strain levels allow the use of the gages for test periods in excess of 10^5 test cycles. The use of standard strain gages was not feasible for the current study since the investigations also included fatigue studies of the pultruded graphite-epoxy specimens over hundreds of thousands of cycles [Donti, Vaughan and Mantena (1992)] with a maximum range of 6500 μ strain, which ruled out the use of standard strain gages. Exploration of alternatives led to a 20% extensometer (with a x10% range capability for increased precision) recommended for dynamic applications. The extensometer was connected to the test sample by springs to measure the strain in the one inch gage length region.

Loss factor is defined as the ratio of dissipated energy to the energy stored at maximum displacement. Data from the measured hysteresis loops can be converted to damping in terms of the loss factor

$$\eta = \frac{D}{2\pi U} = \frac{a}{b} \qquad (2)$$

Here η = loss factor

D = dissipated energy per cycle

U = energy stored at maximum displacement

and a and b are defined in the inset of Figure 1.

The ratio a/b gives an accurate measure of the loss factor, but when the loops are very narrow the inaccurate measurement of the dimension 'a' results in erroneous loss factor data. The pultruded graphite-epoxy specimens exhibited very narrow hysteresis loops (even at such high levels of strain), which necessitated computer based methods (developed in-house) to be adopted for determining the material damping and extensional modulus. To determine the loss factor in real-time, the two energy terms need to be measured from the loading-unloading hysteresis loop. The area of the loop bounded by the loading and unloading segments represents the dissipated energy which was determined by performing numerical integration on the data samples of load and strain obtained in real-time. The numerical method treats the area between the loading segment and x-axis of the load-strain diagram as positive and the area between the unloading segment and the x-axis as negative. Special care was taken in the computer code to ensure closure of the loop for every cycle. The algebraic addition of these two areas in energy units is the energy dissipated. A filter routine determined the maximum and minimum of each load, strain, and displacement value for any test cycle from which the energy stored at maximum displacement was computed. The ratio of energy dissipated to the energy stored gave the loss factor while the extensional modulus was determined from:

$$E = \frac{L_{max} - L_{min}}{A\,(S_{max} - S_{min})} \qquad (3)$$

where E = extensional modulus L_{max} = maximum load

L_{min} = minimum load S_{max} = maximum strain

S_{min} = minimum strain A = specimen cross-sectional area.

To plot the hysteresis loops at a later time and to verify the numerous calculations performed in real-time, 500 data samples of each of load, strain and displacement values corresponding to one complete fatigue cycle were stored at regular intervals using a high speed personal computer. Sufficient number of data samples were taken to increase the level of accuracy in the calculations. The values determined by this computer based methods were found to be in excellent agreement with those from manually measured (a/b) methods. It should be pointed out that the base data for each specimen were recorded only from stabilized hysteresis loops; stabilized loops normally developed after 500 cycles of dynamic loading.

LOG-DECREMENT METHOD :

For the flexural tests, the specimens chosen from each batch of pultruded material were clamped at one end in a vice. A cantilever span of 10 inches was found to provide good quality amplitude-time history records that were measurable with a HP 54600A digitizing oscilloscope. A small aluminum foil was attached at the free end of the graphite-epoxy specimens to facilitate the measurement of deflections with a non-contacting eddy current proximity measuring transducer (KAMAN KD-2400). The specimens were subjected to an initial disturbance (by "tweaking" the free end) and the decaying amplitude-time history obtained on the oscilloscope was digitized and stored in a computer for further processing. Due care was taken to adjust the oscilloscope settings such as time delay, trigger level and low frequency pass filter to capture a good stabilized waveform after the initial disturbance.

The damping factor, ζ, is found by fitting an exponential curve passing through the peak amplitudes of the free vibration decay curves (Figure 2) and is computed from

$$Y = X\, e^{-\zeta \omega t} \tag{4}$$

where ζ = damping factor

$\omega = 2\pi f$ = radial frequency of the waveform

t = time

and the loss factor is obtained from the relationship

$$\eta = 2\zeta \tag{5}$$

For gaining confidence on the quality of the exponential curve-fit, the loss factor was also verified from the expression for the logarithmic decrement (Figure 2)

$$\delta = \frac{1}{n} \ln \frac{X_0}{X_n} \tag{6}$$

where n = number of cycles

X_0 = initial peak amplitude of the wave form

X_n = peak amplitude after n cycles from X_0

and the relationship

$$\eta = \frac{\delta}{\pi} \tag{7}$$

The loss factors determined from both the above methods were found to be in close agreement. Also, from the decaying amplitude-time history the fundamental frequency of oscillation (in this case, the damped natural frequency) is given by

$$f = \frac{1}{T} \tag{8}$$

where f = frequency in cycles per second (Hz)

T = period of oscillation (seconds)

The storage modulus (flexural), E_f , can be found by measuring this frequency and using the

frequency equation from Beam Theory. For a cantilever beam vibrating in flexure, the frequency equation for the fundamental (first) mode is

$$f = \frac{(1.875)^2}{2\pi L^2}\sqrt{\frac{E_f I}{\rho A}} \tag{9}$$

where E_f = modulus of elasticity of the beam material

I = moment of inertia of the beam

ρ = beam mass density

A = beam cross-sectional area

L = length of the beam

From which, solving for the storage modulus,

$$E_f = \frac{4\pi^2 f^2 L^4 \rho A}{(1.875)^4 I} \tag{10}$$

RESULTS AND DISCUSSION

The average extensional modulus and loss factor values measured from the hysteresis loop technique are shown in Table 2. The regression models for the above two response variables are shown in Figures 3a, 3b, 4a and 4b in which the models are also depicted graphically using response volume techniques. Each plot shows the logical location of the optimum region in a control volume and the optimum point determined by a numerical search technique developed in-house. Two types of plots are presented to cover both ends of the spectrum of values for each response variable. The first type presents the optimum region towards the lower end and the second type presents the region towards the higher end of the spectrum of values for the response variable. It is important to mention that the origin of the control volume corresponds to the least of each of

the three variables, i.e., code value of -1. The other end of each axis corresponds to the highest code value of +1.

A high extensional modulus is one of the most appealing properties of the pultruded unidirectional graphite-epoxy composite materials. These modulus values are shown in Table 2. The actual modulus values are usually less than those by rule of mixtures, partly due to small misalignment of the fibers in the pultruded composite material from the loading direction, practical processing difficulties in achieving a perfect bond between the fibers and the resin, and experimental variations in test results. Figures 3a and 3b show the spread of the optimum regions for the worst and the best for extensional modulus. Figure 3b shows the optimum region for high extensional modulus in an area of high fiber volume and medium to high die zone 1 temperature. The location of the optimum region emphasizes the dominant influence of fiber volume on extensional modulus. High die zone 1 temperature when pull speed is high apparently contributes to thorough cure for the resin and subsequently contributes to extensional modulus. The spread of the optimum region in Fig. 3b reinforces this view. The process region that produces the lowest values of the extensional modulus can be found in an area of low fiber volume and low zone 1 die temperature (Fig. 3a). The location of this region also indicates the strong influence of fiber volume.

The extensional loss factor values determined through the computer based hysteresis loop method are also listed in Table 2. The mathematical model for the loss factor includes three dominant variables and their interactions; pull speed is kept at its highest process condition. Figure 4b shows the location of optimum region for high loss factor in an area of low to medium fiber volume and high die zone 3 temperature. The effect of fiber volume on loss factor is opposite to that of fiber volume on extensional modulus. This is in agreement with the general opinion on the effect of fiber volume on the two different properties. Figure 4a shows the optimum region for low loss factor in an area of medium to high fiber volume and low die zone 3 temperature. The presence of a strong die zone 3 temperature and its interaction with die zone 1 temperature in the regression model indicates the influence of die temperature profile on the loss factor. It is possible that thermally induced microstructural changes due to variations in fiber/resin interface bonding in zone 1 or fine

microcracks may form in the exiting pultruded material and influence the loss factor. However, caution is required in the in-depth interpretation of the optimum regions and more study is warranted.

Table 3 shows the flexural modulus and loss factor data obtained with the log-decrement technique. The regression models and the response volume plots for these two dependent response variables and the dominant process conditions are shown in Figures 5a, 5b, 6a and 6b along with their interactions. A careful observation of these plots indicates that a highly desirable combination of high flexural modulus with high loss factor can be obtained with the process conditions set at an optimum configuration of: high fiber content of 63.3 %, high pull speed of 0.0059 m/s (14 in/min), high zone 1 temperature at 449.7 K (350 F), high zone 2 temperature at 466.3 K (380 F), but a low zone 3 temperature of 455.2 K (360 F). The response plots show the non-inclusion of the fiber content (which significantly contributes to flexural modulus) for the optimum location of damping, and the insignificance of zone 2 die temperature (which influences damping) on the flexural modulus. Also, it can be noted that a high pull speed with other variables at suggested levels dropped the flexural modulus marginally while still providing high damping. These observations were used in recommending the above process conditions for obtaining optimum desirable flexural modulus and flexural loss factor.

CONCLUSIONS

Scientific characterization of the effects of pultrusion process variables on the dynamic mechanical properties of graphite-epoxy composites has been conducted. Statistical regression techniques have been employed to generate mathematical models relating the pultrusion process variables to dynamic properties of graphite-epoxy composite material. Response volume techniques have been employed to show the optimum process regions for the response variables. The results of the analysis are in reasonable agreement with the theory. Computer methods have been used to increase the accuracy in the results and offer significant time savings in this research.

ACKNOWLEDGEMENTS

The authors would like to acknowledge partial support for this work from the National Science Foundation (Grant # DDM - 9101643), NSF/Experimental Program to Stimulate Competitive Research (Grant # R - II - 089 - 02064) and the Electric Power Research Institute (Grant # 8007 - 20)

REFERENCES

Donti, R.P., Vaughan, J.G., and Mantena P.R., 1992, "Effect of Pultrusion Process Variables on Cyclic Damage of Graphite-Epoxy Composites" to be presented in the ASTM Symposium on Cyclic Deformation, Fracture, and Nondestructive Evaluation of Advanced Materials," November 16-17, Miami, Florida.

Freund, R.J., and Littell, 1991, *SAS[R] System for Regression*, 2nd ed., SAS Institute, Inc., Cary, North Carolina.

Gibson, R.F., 1989, "Vibration Test Methods for Dynamic Mechanical Property Characterization," in Manual on *Experimental Methods for Mechanical Testing of Composites*, Editors: R.L. Pendelton and M.E. Tuttle, Society of Experimental Mechanics, 151-164.

Mantena, P.R., Gibson, R.F., and Place, T.A., 1986, "Damping Capacity Measurements of Degradation in Advanced Materials,"*SAMPE Quarterly*, Vol. 17, 3.

Renz, R., Altstadt, V., and Ehrenstein, G.W., 1988, "Hysteresis Measurements for Characterizing the Dynamic Fatigue of R-SMC,"*Journal of Reinforced Plastics and Composites*, Vol. 7, 413-433.

Vaughan, James G., Hackett, R.M., and Seal, E.C., 1988, "Optimization of the Pultrusion Process for Graphite/Epoxy," *Fiber-Tex 1988*, NASA CP3038, 285-299.

Vaughan, James G., 1988, "Use of Statistical Design Experimentation to Characterize and Optimize the Pultrusion Process," *Proceedings of the 43rd Annual Conference*, The Society of the Plastics Industry, Inc., 6D:1-6.

Table 1. Fractional Factorial Design Test Pattern.

Test Plan #	Random Plan #	Test Variables 1	2	3	4	5
1	17	-1	-1	-1	-1	1
2	1	1	-1	-1	-1	-1
3	11	-1	1	-1	-1	-1
4	5	1	1	-1	-1	1
5	18	-1	-1	1	-1	-1
6	4	1	-1	1	-1	1
7	12	-1	1	1	-1	1
8	19	1	1	1	-1	-1
9	10	-1	-1	-1	1	-1
10	2	1	-1	-1	1	1
11	7	-1	1	-1	1	1
12	9	1	1	-1	1	-1
13	6	-1	-1	1	1	1
14	14	1	-1	1	1	-1
15	16	-1	1	1	1	-1
16	13	1	1	1	1	1

KEY			
		-1	+1
V1	Graphite tows (%)	103 (60.9)	107 (63.3)
V2	Pull Speed, m/s (in/min.)	0.0042 (10)	0.0059 (14)
V3	Zone 1 Temperature °K (°F)	438.6 (330)	449.7 (350)
V4	Zone 2 Temperature °K (°F)	455.2 (360)	466.3 (380)
V5	Zone 3 Temperature °K (°F)	455.2 (360)	466.3 (380)

Table 2. Properties of Pultruded Graphite-Epoxy from extensional testing (Hysteresis Loop Technique).

Test Plan #	Rule of Mixtures Modulus GPa (10^6 psi)	Actual Modulus	Loss Factor
1	141.93 (20.58)	135.68 (19.67)	0.0035
2	147.38 (21.37)	141.06 (20.45)	0.0018
3	141.93 (20.58)	134.68 (19.53)	0.0020
4	147.38 (21.37)	138.32 (20.06)	0.0027
5	141.93 (20.58)	137.19 (19.89)	0.0027
7	141.93 (20.58)	138.24 (20.05)	0.0031
8	147.38 (21.37)	140.72 (20.40)	0.0028
9	141.93 (20.58)	137.56 (19.95)	0.0024
10	147.38 (21.37)	142.55 (20.67)	0.0037
11	141.93 (20.58)	137.92 (20.00)	0.0034
12	147.38 (21.37)	138.64 (20.10)	0.0016
13	141.93 (20.58)	137.89 (19.99)	0.0032
14	147.38 (21.37)	140.21 (20.33)	0.0030
15	141.93 (20.58)	139.50 (20.23)	0.0032
16	147.38 (21.37)	142.02 (20.59)	0.0020

Table 3. Dynamic Properties of Pultruded Graphite-Epoxy (Log-Decrement Technique)

Test Plan #	Flexural Modulus GPa (10^6 psi)	Loss Factor
1	115.98 (16.82)	0.0038
2	118.53 (17.19)	0.0031
3	116.78 (16.94)	0.0024
4	117.31 (17.01)	0.0025
5	116.71 (16.93)	0.0040
7	114.41 (16.59)	0.0031
8	119.51 (17.33)	0.0033
9	113.98 (16.53)	0.0028
10	113.64 (16.48)	0.0033
11	113.45 (16.45)	0.0031
12	117.58 (17.05)	0.0041
13	113.84 (16.51)	0.0048
14	121.01 (17.55)	0.0031
15	115.28 (16.72)	0.0054
16	119.30 (17.30)	0.0046

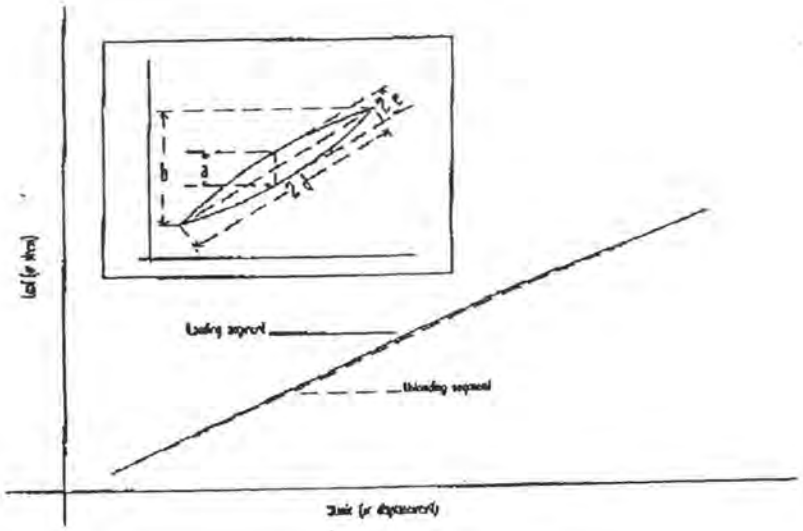

Figure 1 Typical narrow hysteresis loop from extensional tests

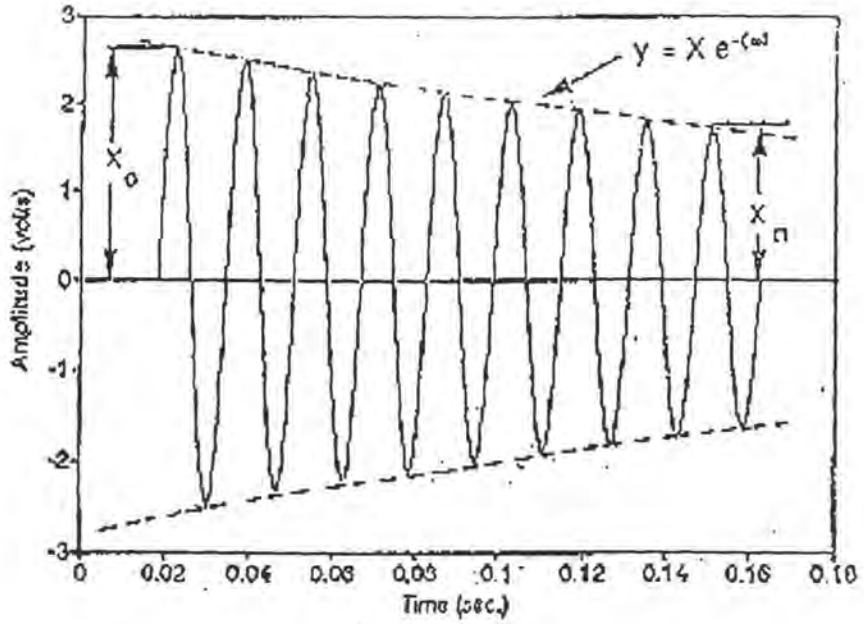

Figure 2. Amplitude-time history from free vibration decay flexural tests

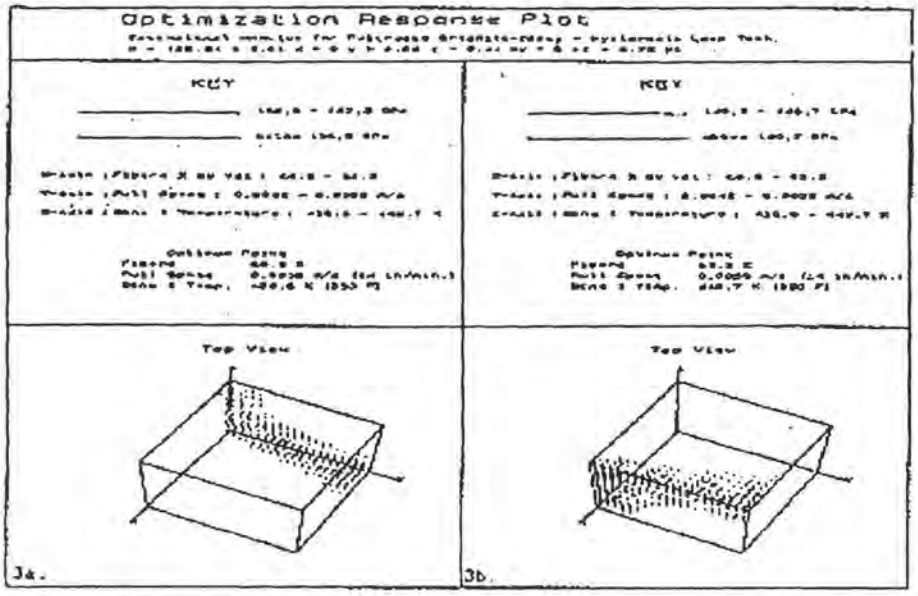

Figure 3. Extensional modulus response volume data from Hysteresis loop technique

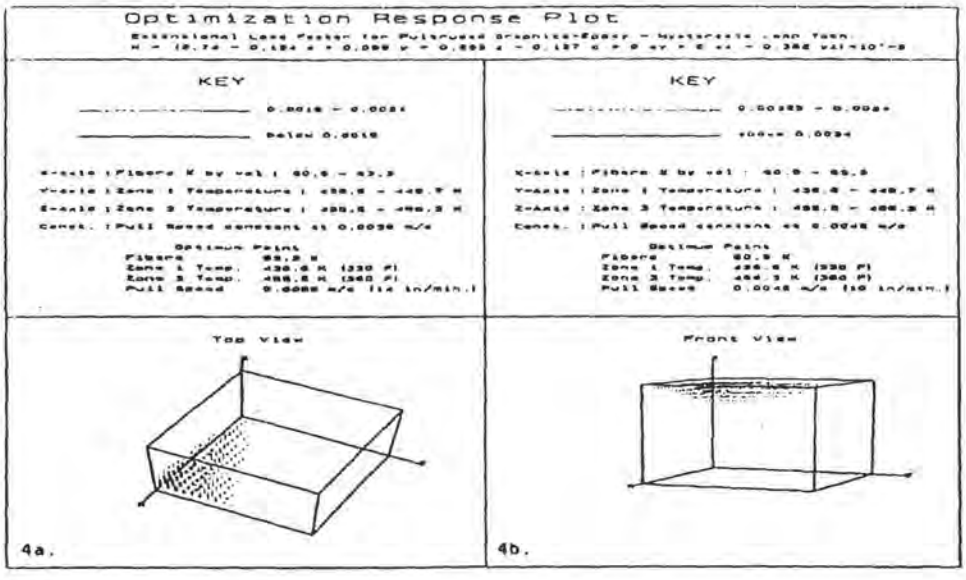

Figure 4. Extensional loss factor resonse volume data from Hysteresis loop technique

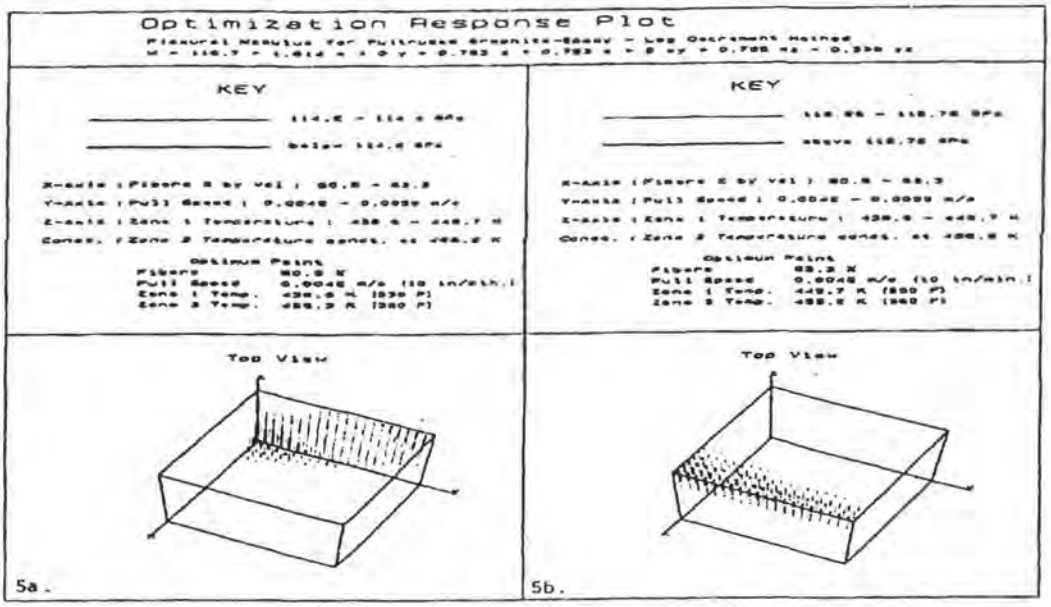

Figure 5. Flexural modulus response volume data from Log-Decrement technique

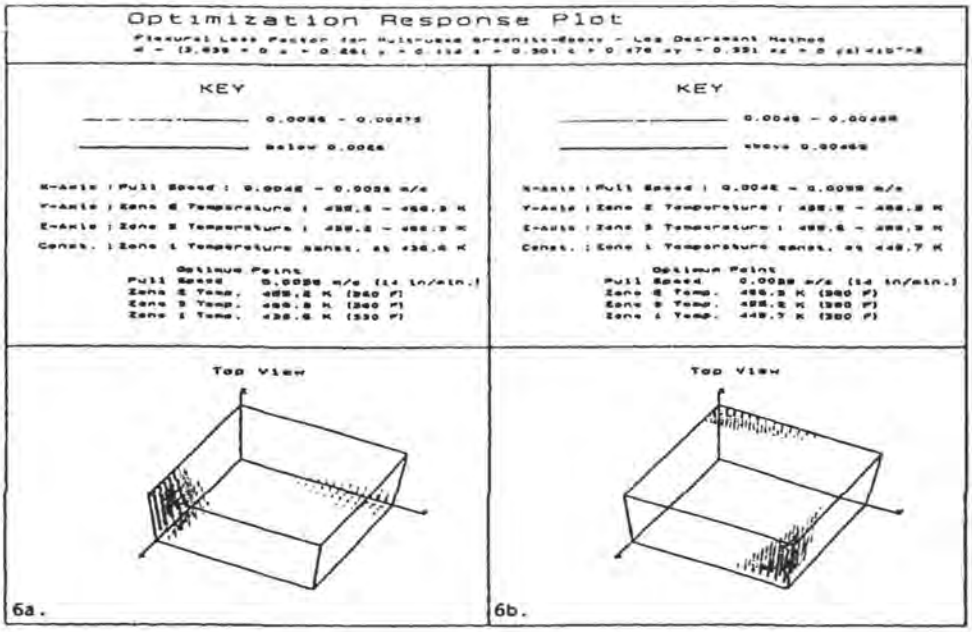

Figure 6. Flexural loss factor resonse volume data from Log-Decrement technique

Mechanical and Thermal Behavior of Pultruded Advanced Composites

Jeffrey A. Roux, P. Raju Mantena, and James G. Vaughan
Department of Mechanical Engineering
The University of Mississippi

Abstract

This research is being conducted to characterize the mechanical and thermal properties of pultruded composites. This project has been in progress for approximately one year of a three year duration. Hence this paper will highlight sample results which are subject to further refinement as the project continues.

Pultrusion is a well developed processing art, however it is not well understood scientifically. Much basic research is needed before the process of pultruding composite materials can be considered to be on a firm scientific basis. Fundamental understanding of pultrusion is required for developing high performance structural products and for developing composites with desirable thermal characteristics. This work will provide progress toward understanding the pultrusion process variables and how these variables influence the material properties, dynamic properties and thermal properties. This study is producing models to characterize the process and an improved ability to design/produce a pultruded composite material for a specific end use.

Development and optimization of pultruded composite materials is a need recognized by a broad spectrum of governmental and industrial potential users. By concentrating the research toward the effects of process variables on the thermal, dynamic, and NDE characteristics of pultruded polymeric composite products, innovative material systems can be realized which are necessary for industry to provide higher quality products and service to customers at the lowest possible cost.

INTRODUCTION

Pultrusion is a manufacturing process through which continuous reinforcement fibers are consolidated in a polymeric matrix to produce a composite material, Figure 1. The art of pultrusion has evolved into an automated and technologically sophisticated production process; however, much of the basic science governing pultrusion is not very well understood. By means of this technique light weight, high-modulus composite structural elements such as beams, truss components, stiffeners, etc. have been manufactured very effectively. Pultrusion has penetrated such market areas as land transportation, construction, marine, corrosion-resistant equipment, electrical, aircraft, and specialties. Pultrusion can produce nearly any constant cross-sectional shape that can be extruded; thus, indicating significant growth potential. For many high technology applications, pultruded composites offer inherent technical advantages such as structural strength, improved physical properties, and reduced cost along with increased life when compared to other composite manufacturing processes. Cost-competitive advantages should enable pultruded composites to become traditional materials along side steel, wood, and aluminum before the end of the 20th century [1].

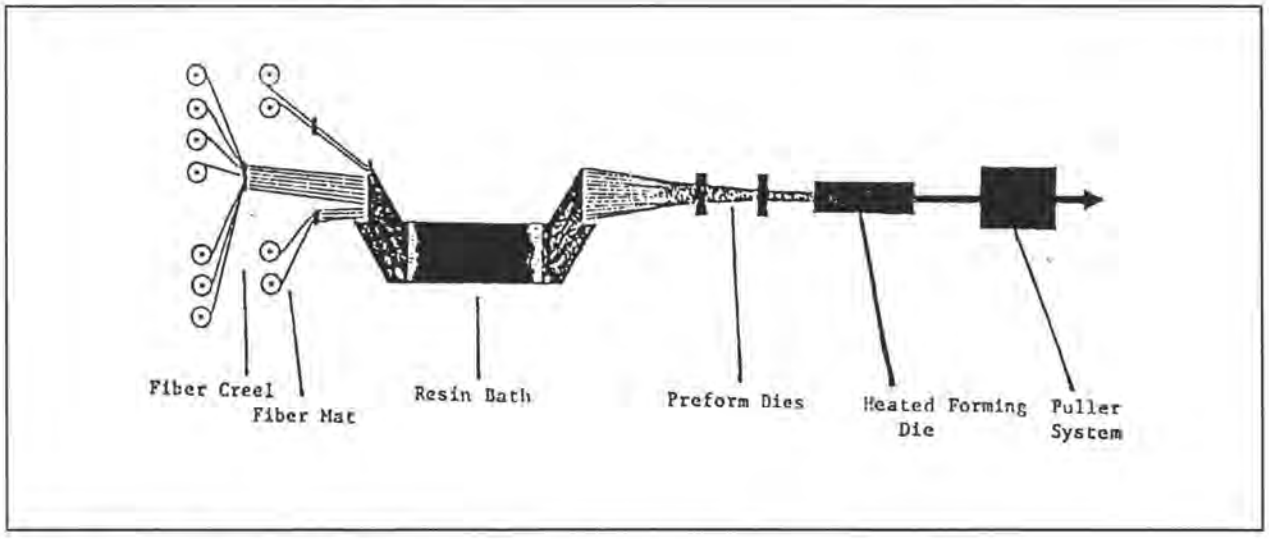

Figure 1. Illustrative schematic of the pultrusion process.

Traditionally the pultrusion process has used continuous glass reinforcing fibers with a thermosetting resin matrix. Pultrusion of high-performance material systems such as graphite/epoxy is relatively new and the processing characteristics are not as well understood. Thermoplastic composites are even less understood. Pultrusion, though simple in concept, is quite scientifically complex due to the numerous interacting process parameters. Through a sequence of statistically designed experiments the authors have evaluated the interdependencies of the pultrusion process parameters for a graphite/epoxy system [2]. Employing these experimental techniques, the pultrusion of a graphite/epoxy system was optimized for any single measurable process or quality factor, such as, composite tensile strength and/or shear strength, or for a combination of property values, e.g., a minimum acceptable tensile strength at a minimum acceptable shear strength. It was concluded that the three most important operating parameters for optimization of the pultrusion process were the die platen heating temperatures, the pull speed, and the percent fiber content. Other process parameters may be more significant for other resin systems.

Yet to be satisfactorily characterized is the effect of the dominant operating parameters (e.g., die platen heating temperatures, percent fiber content, or pull speed) on the dynamic, mechanical, and thermal properties of the pultruded products. Since these pultruded components will be applied in advanced engineering structures, their behavior in dynamic loading and thermal environments is of great importance. The present research is addressing the influence of these process variables on the thermal and dynamic characteristics of pultruded composite specimens in order to achieve an optimization of the graphite/epoxy pultrusion process. Bidirectional thermal properties will be characterized for glass and graphite reinforcements and for a combination of the two fiber systems. Vibration response measurements are being employed as a mechanistic tool in quality control operations and for non-destructive evaluation (NDE) of the structural integrity of pultruded components.

EXPERIMENTAL CHARACTERIZATION OF PULTRUSION PROCESSING

Because numerous process parameters influence the quality of the pultruded product, a systematic method is required to determine the effects of the various parameters. Since complex process interactions are known to influence the mechanical properties of the pultruded product, the experimental method used to evaluate these influences must be able to account for the interactions of the parameters as well as the individual contributions. The objective of statistical experimentation is to determine the relationship between a dependent response variable (the quantity observed or measured for a particular combination of factor levels) and the factors (the processing conditions which are controlled for the experiment). Statistical methods of experimentation provide the ability to draw conclusions that would not be possible if traditional one-factor-at-a-time methods of experimentation were used. For example, a central composite design consisting of thirty-two experiments can provide more information about the effects of five factors at five process levels than hundreds of experiments that changed one factor at a time. The 32 experiment five-factor, half-factorial central composite design used for the present study is shown in Table 1. The 32 experiments consist of 16 half-fractional factorial experiments, six center point run for repeatability, and ten axial or star points.

Central composite designs are a class of statistical experimental designs that were developed by Box and Wilson [3] in 1951. The central composite design is a 2^k factorial design augmented with repeated center points and axial points arranged around a center cube. Unlike 2^k factorial designs which do not allow quadratic terms to be estimated, central composite designs allow linear, quadratic, and interaction terms to be estimated. The central composite design model is used to fit the second-order equation

$$Y = \beta_0 + \Sigma\beta_i X_i + \Sigma\beta_{ii} X_i^2 + \Sigma\Sigma\beta_{ij} X_i X_j + \epsilon \qquad (1)$$

The magnitude of the various coefficients indicate the importance of the various process parameters. However, it should be carefully noted that the statistical models developed in such a manner should only be used to draw conclusions related to the process levels located within the experimental design region.

Table 1. Central Composite Design Matrix in Coded Form.

	Test Variables				
Test Plan #	X1	X2	X3	X4	X5
1	-1	-1	-1	-1	1
2	1	-1	-1	-1	-1
3	-1	1	-1	-1	-1
4	1	1	-1	-1	1
5	-1	-1	1	-1	-1
6	1	-1	1	-1	1
7	-1	1	1	-1	1
8	1	1	1	-1	-1
9	-1	-1	-1	1	-1
10	1	-1	-1	1	1
11	-1	1	-1	1	1
12	1	1	-1	1	-1
13	-1	-1	1	1	1
14	1	-1	1	1	-1
15	-1	1	1	1	-1
16	1	1	1	1	1
17	0	0	0	0	0
18	0	0	0	0	0
19	0	0	0	0	0
20	0	0	0	0	0
21	0	0	0	0	0
22	0	0	0	0	0
23	-2	0	0	0	0
24	0	-2	0	0	0
25	0	0	-2	0	0
26	0	0	0	-2	0
27	0	0	0	0	-2
28	2	0	0	0	0
29	0	2	0	0	0
30	0	0	2	0	0
31	0	0	0	2	0
32	0	0	0	0	2

X1:	Graphite Volume %	59.7	60.9	62.1	63.3	64.4
X2:	Pull Speed (cm/min)	20	25	30	36	41
X3:	Zone 1 Temp (°C)	160	166	171	177	182
X4:	Zone 2 Temp (°C)	177	182	188	193	199
X5:	Zone 3 Temp (°C)	177	182	188	193	199

Regression techniques are used to obtain the least-squares estimates of the β coefficients of the second-order model (Equation 1). P-values (Prob > |T|) and the magnitudes of the parameter estimates are then examined to develop a reduced set model which includes only the most significant terms from the complete model. Reduced set models simplify the interpretation of the effects of the independent variables but still accurately describe and predict the dependent variable. In addition, if a factor is involved in a significant interaction or squared term, the linear term of that factor is included in the reduced set model even if the linear term itself did not appear to be significant.

Five independent pultrusion process variables -- fiber volume, line speed, die zone 1 temperature, die zone 2 temperature, and die zone 3 temperature -- are examined in this study. The process levels are held within ranges expected for commercial pultrusion. All pultrusion experiments are conducted in the Composite Materials Laboratory at the University of Mississippi using a Pulstar 804 commercial pultruder with hydraulic, reciprocating clamp pullers. A data acquisition system connected to a personal computer is used to record set line speed, actual line speed, pull force, puller system pressure, clamp pressure, and platen temperatures throughout each experiment. A chart recorder is also used to continuously graph pull force during each experiment. This process data is being used with the statistical analyses to determine the optimum process condition(s) for producing the desired sets of structural/dynamic properties and thermal properties.

DIRECTIONAL THERMAL CONDUCTIVITY AND HEAT TRANSFER PROPERTIES

Characterizing and understanding the complex thermochemical processing of the pultrusion process is important for producing a product of high mechanical properties. Quality of the manufactured pultruded composite material part will depend on the thermal properties of the resins and reinforcement fibers used to produce the part. Clearly the thermal conductivity in the cross-fiber and with-fiber directions will be different (bidirectional). These thermal conductivity differences will be significant for two important reasons. First the bidirectional thermal conductivity will affect the curing process which occurs in the heated pultrusion die.

Non-uniform heat transfer could lead to non-uniform curing in the die and hence impact the mechanical properties of the pultruded part. Also the thermal conductivity of the finished part will be bidirectional. Using the finished part in a thermally sensitive application would require a clear knowledge of this bidirectional thermal behavior so that the finished part is successfully used in a design application. The thermal research will require the experimental measurement of the bidirectional thermal conductivity and to employ this measured bidirectional thermal conductivity in a numerical model to describe the heat transfer and curing phenomenon within the pultrusion die. Also the numerical thermal model will be used to predict the thermal properties of the finished pultrusion product. This research will study the effect of mixing different types of reinforcement fibers, each having a different bidirectional thermal conductivity, and how these fiber mixtures impact curing in the pultrusion die (and hence mechanical properties) and how these mixtures affect the overall spatial distribution of thermal conductivity of the finished product. It is important to define the thermochemical problem and also to present the governing equations which must be solved.

The heating section of the pultruder is divided into a number of control volumes. Grid points are placed within the control volumes so that there is one complete control volume surrounding each grid point. Employing conservation of energy to the non-moving portions of the die, the two-dimensional transient energy equation can be represented by

$$\rho C \frac{\partial T}{\partial t} = \frac{\partial}{\partial x}\left(k \frac{\partial T}{\partial x}\right) + \frac{\partial}{\partial y}\left(k \frac{\partial T}{\partial y}\right) + \dot{q} \qquad (2)$$

Heat conduction occurs both in the axial and the vertical directions. The first term of Equation (2) describes the rate of change of internal energy, the second term represents the heat flow due to conduction in the (axial) x-direction and, and the third term symbolizes the heat transfer due to conduction in the (vertical) y-direction. The final term corresponds to the volumetric heat generated within the control volume. In Equation (2), ρ is the density, C is the specific heat, k is the thermal conductivity, T is the temperature. The quantity $\dot{q}$ in the

non-moving sections of the pultruder is either zero or is equal to the heater power in the sections where the heaters reside. The energy equation was solved using Patankar's finite difference control volume technique [4].

The rate of cure in the composite material (moving medium) is governed by the chemical species equation based on a one-step Arrhenius reaction rate equation. The species equation is characterized by a nodal equation influenced by the nodes only in the axial direction because the composite material is being pulled in the axial direction and mass diffusion is considered to be negligible. Algebraically, the degree of cure, Ψ, is represented by $\Psi = (C_I - C_T)/ C_I$, where C_I is the initial concentration of the uncured resin and C_T is the uncured resin concentration at any given location and time. The species equation is expressed as follows

$$\frac{\partial \Psi}{\partial t} + u\frac{\partial \Psi}{\partial x} + v\frac{\partial \Psi}{\partial y} = k_0 \exp\left(-\frac{E}{RT}\right)(1-\Psi)^n \qquad (3)$$

where u is the pull speed, v is the y-component of velocity, k_0 is the pre-exponential constant, R is the universal gas constant, E is the activation energy, and n is the order of reaction in the Arrhenius expression. The right hand side of Equation (3) is the Arrhenius reaction rate expression. The species equation was converted into discretized form with the aid of the "upwind" scheme as depicted by Patankar [4].

The exothermic chemical reaction due to curing of the resin becomes the source term in the energy equation for the composite material (moving medium). The two-dimensional transient energy equation for the composite material is denoted by

$$\rho C\frac{\partial T}{\partial t} + \left(\rho u CT - k\frac{\partial T}{\partial x}\right) + \left(\rho v CT - k\frac{\partial T}{\partial y}\right) = S \qquad (4)$$

where S is the source term due to the exothermic reaction and is represented by

$$S = C_f k_0 \exp(-\frac{E}{RT})(1-\Psi)^n(\Delta H) \qquad (5)$$

In Equation (5), ΔH is defined as the heat of reaction. The energy equations (Equation (4) and Equation (5)) and the chemical species equation (Equation (3)) for the composite material are coupled and therefore must be solved simultaneously utilizing an iterative mechanism [4]. The kinetic parameters k_0, E, n and ΔH were obtained for the Shell EPON 9420/537/9470 epoxy system from experimental analysis of the resin using a differential scanning calorimeter (DSC).

The boundary and initial conditions for the above equations applicable to the composite are as follows: u = pull speed, v = 0, $T = T_{resin}$ at t = 0 and x = 0, $\Psi = 0$ at t = 0 and x = 0. At the nodes in the composite at the die exit, $\partial T/\partial x = 0$. Also, at all nodes in the non-moving parts of the heater section, T = room temperature at t = 0. The temperatures at the interface nodes between the die and the composite were assumed to be identical. The boundary nodes in the non-moving parts of the heater section in contact with the ambient room temperature experience heat transfer due to convection and radiation. In the numerical model, the power to the heaters was initially turned on to bring the temperature of the heaters to the required setting. Once the desired temperatures were reached, the power to the heaters was alternatively turned on or off to maintain the temperature settings which were equal to the actual temperatures of the heaters in the pultruder. The temperature and the degree of cure fields in the composite material are predicted by the numerical model.

In this study, graphite-epoxy composites were pultruded in the Composite Materials Laboratory at the University of Mississippi. The die cavity used in the experiments was 0.3 cm thick, 2.5 cm wide, and 91.4 cm long (1/8", 1", 36"). The materials used in the experiments were Hercules graphite AS4-12K, Shell EPON epoxy 9420, Shell EPON curing agent 9470, and Shell accelerator 537. The die wall temperatures

were monitored by means of twelve static (non-moving) thermocouples positioned within the die near the product cavity. Two other thermocouples, one in the center and the other on the surface of the composite, were pultruded through the die to measure the temperature profiles in the composite.

Figure 2 illustrates the predicted centerline temperature profiles for pull speeds of 20 cm/min, 30 cm/min, and 41 cm/min, at a fiber volume of 62.1 percent and a die temperature setting of (171-188-188)°C. It is seen that the peak temperature for the pull speed of 41 cm/min is greater than the temperatures for pull speeds of 30 cm/min, and 20 cm/min. This can be attributed to the fact that at higher pull speeds the composite does not release heat from the exothermic chemical reaction fast enough as it advances into the die. The thermal conductivity of the graphite plays a dominant role at higher pull speeds in the transfer of heat to the die. In the front portion of the die the temperatures for the slower pull speed are higher because heat is able to conduct into the composite material more readily.

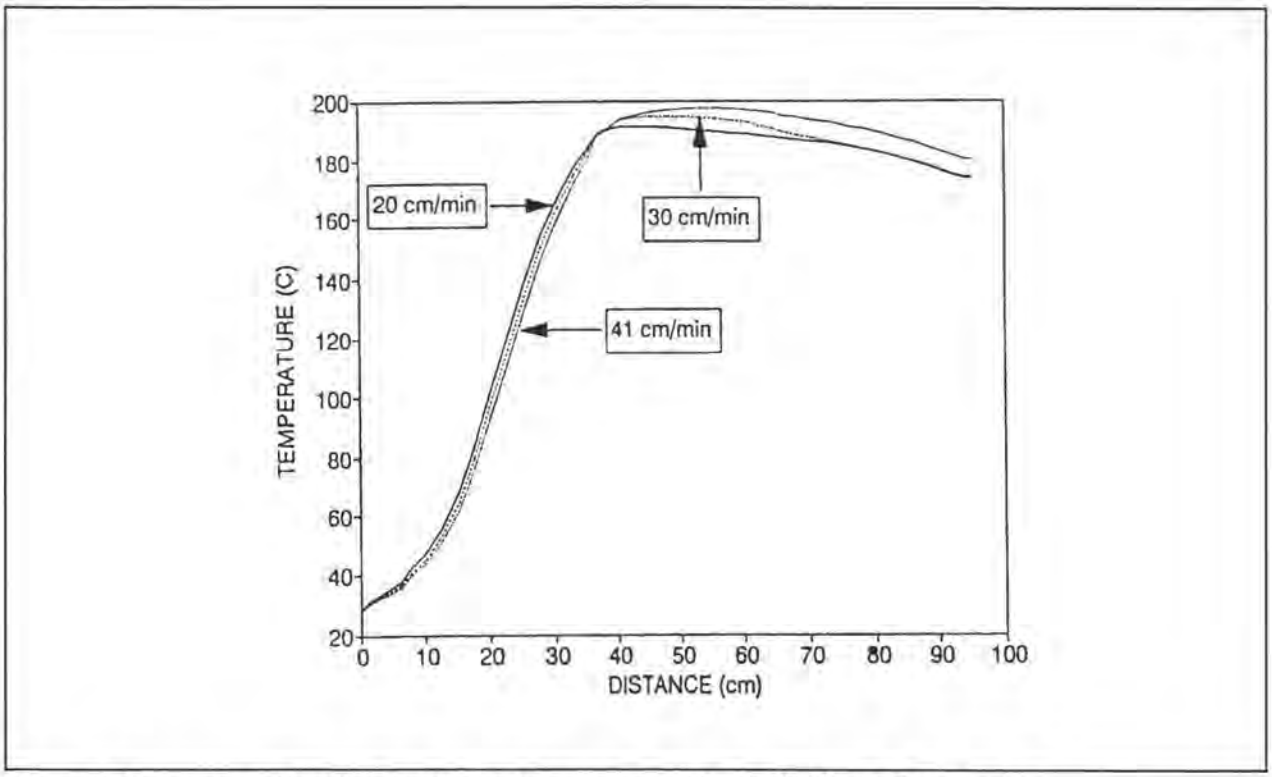

Figure 2. Comparison of predicted centerline temperature profiles for 9420 resin base graphite composites for various pull speeds, fiber volume of 62.1 percent, and a die temperature setting of (171-188-188)°C

Figure 3 illustrates the predicted degree of cure in the composite material for various pull speeds. The lower the pull speed the higher the degree of cure at the die exit. The degree of cure for pull speeds of 30 cm/min and 41 cm/min lag the cure profile for 20 cm/min due to the fact that the amount of time that the composite resides in the die decreases as the pull speed increases. The degree of cure at the die exit was 91 percent at 20 cm/min, 83 percent at 30 cm/min, and 79 percent at 41 cm/min. The measured degree of cure using a scanning differential calorimeter was 80 percent for a pull speed of 41 cm/min; the degree of cure for the other pull speeds have not been completed. Considering some of the uncertainties involved in the parameters used in the modeling, the predictions are considered to be good.

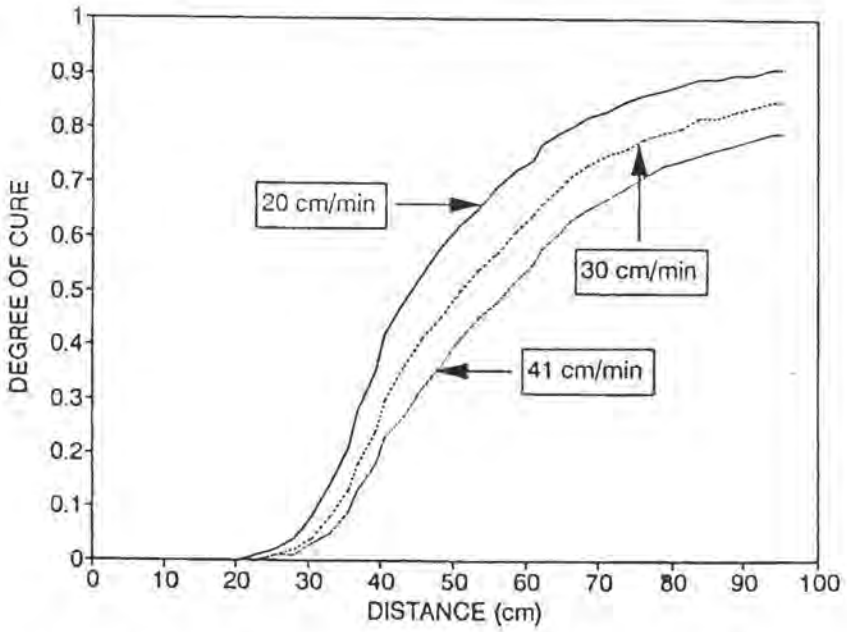

Figure 3. Comparison of predicted centerline temperature profiles for 9420 resin based graphite composites for various pull speeds, fiber volume of 62.1 percent, and a die temperature setting of (171-188-188)°C

STRUCTURAL/DYNAMIC PROPERTIES

With the intended end application of the pultruded components in the form of beams, trusses, stiffeners, etc., their performance in dynamic loading environments (fatigue) becomes highly critical. Very little research has been conducted, however, to characterize the elastic modulus and internal damping of these pultruded materials under vibratory loading. This is of special interest because experimental data on elastic

modulus and damping are often used as input to design calculations, as quality control parameters during manufacturing/processing, and as non-destructive evaluation parameters during in-service inspection for structural integrity.

Dynamic mechanical properties may be characterized using either vibration or wave propagation experiments. Standard test methods for the measurement of dynamic mechanical properties of non-reinforced plastics have been developed by ASTM, but these methods and commercially available dynamic mechanical analyzers based on these methods have been found to be inadequate for testing high modulus polymer composites [4]. For this research, a more recently developed Fast Fourier Transform technique is proposed to be used which is based on the use of impulsive excitation of the specimens to instantaneously generate the frequency response curve. The dynamic mechanical properties (modulus and damping) can be obtained rapidly by curve fitting to the frequency response curve. Variations of this impulse-frequency response technique are proposed to be used for obtaining the flexural, extensional and torsional dynamic properties of the pultruded specimens that are being characterized in this research vis a vis the pultrusion process variables (details given in Reference 6).

It may be noted that this project is a joint effort between the National Science Foundation and the Electric Power Research Institute (EPRI) and was funded as a result of the first joint NSF/EPRI initiative request for proposals that were submitted in January 1991. Due to a long delay in establishing and receiving matching funds from both agencies, the equipment for performing the dynamic mechanical property characterizing (using the impulse technique described above) could not be purchased until recently. However, initial research on characterizing the dynamic mechanical properties has proceeded using an available HP Oscilloscope, Kaman displacement measuring system and a Zenith computer system. Reported here are the results of the log-decrement method that was used for computing the flexural modulus and loss factor (a measure of damping) from the free vibration decay amplitude-time histories of pultruded graphite/epoxy specimens tested in a cantilever beam configuration. While this time-domain technique yielded reasonably good results, the method is time consuming, limited in scope and prone to errors.

Experimental Procedure for Dynamic Tests

A 2.5 cm x 0.3 cm (1"x ⅛") thick flat graphite (Hercules' AS4-W-12K) - epoxy (Shell's EPON^{R} 9310/9360/537) composite material was produced under carefully monitored pultrusion process conditions as suggested by the fractional factorial design of Table 1. Test specimens were cut from material pultruded from each of the 16 test conditions shown in Table 1, separated into three batches and kept under a vacuum less than 10^{-2} torr. The specimens were removed from the vacuum chamber just before dynamic testing. A minimum of three specimens (one from each batch) were tested for each set of process conditions to determine the scatter in data.

Log-Decrement Method:

For the flexural tests, the specimens chosen from each batch of pultruded material were clamped at one end in a vice (Figure 4). A cantilever span of 25 cm (10 inches) was found to provide good quality amplitude-time history records that were measurable with a HP 54600A digitizing oscilloscope. Aluminum foil was attached at the free end of the graphite-epoxy specimens to facilitate the measurement of deflections with a non-contacting eddy current proximity measuring transducer (KAMAN KD-2400). The specimens were subjected to an initial disturbance (by "tweaking" the free end) and the decaying amplitude-time history obtained on the oscilloscope was digitized and stored in a computer for further processing. Due care was taken to adjust the oscilloscope settings such as time delay, trigger level and low frequency pass filter to capture a good stabilized waveform after the initial disturbance.

The damping factor, ζ, is found by fitting an exponential curve passing through the peak amplitudes of the free vibration decay curves (Figure 5) and is computed from

$$y = X\, e^{-\zeta \omega t} \tag{6}$$

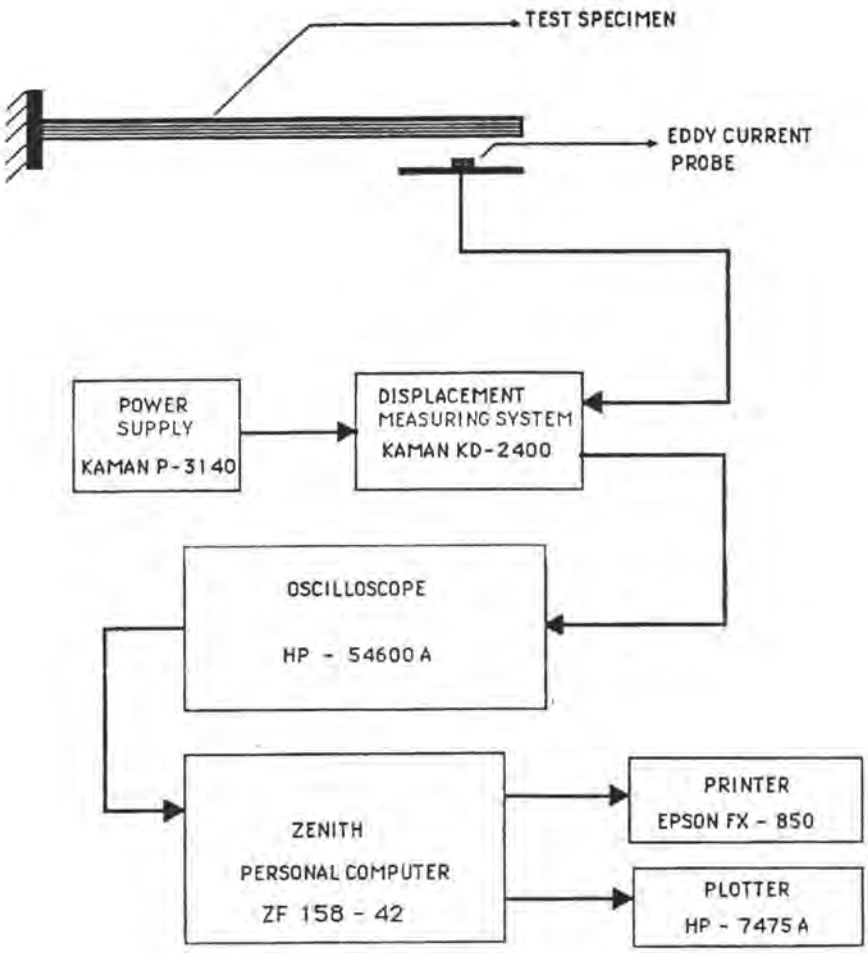

Figure 4. Experimental setup for free vibration decay flexural test.

where ζ = damping factor, $\omega = 2\pi f$ = radial frequency of the waveform, and t = time and the loss factor is obtained from the relationship

$$\eta = 2\zeta \tag{7}$$

For gaining confidence on the quality of the exponential curve-fit, the loss factor was also verified from the expression for the logarithmic decrement (Figure 5)

$$\delta = \frac{1}{n} \ln \frac{X_0}{X_n} \tag{8}$$

where n = number of cycles, X_0 = initial peak amplitude of the wave form, and X_n = peak amplitude after n cycles from X_0 and the relationship

$$\eta = \frac{\delta}{\pi} \tag{9}$$

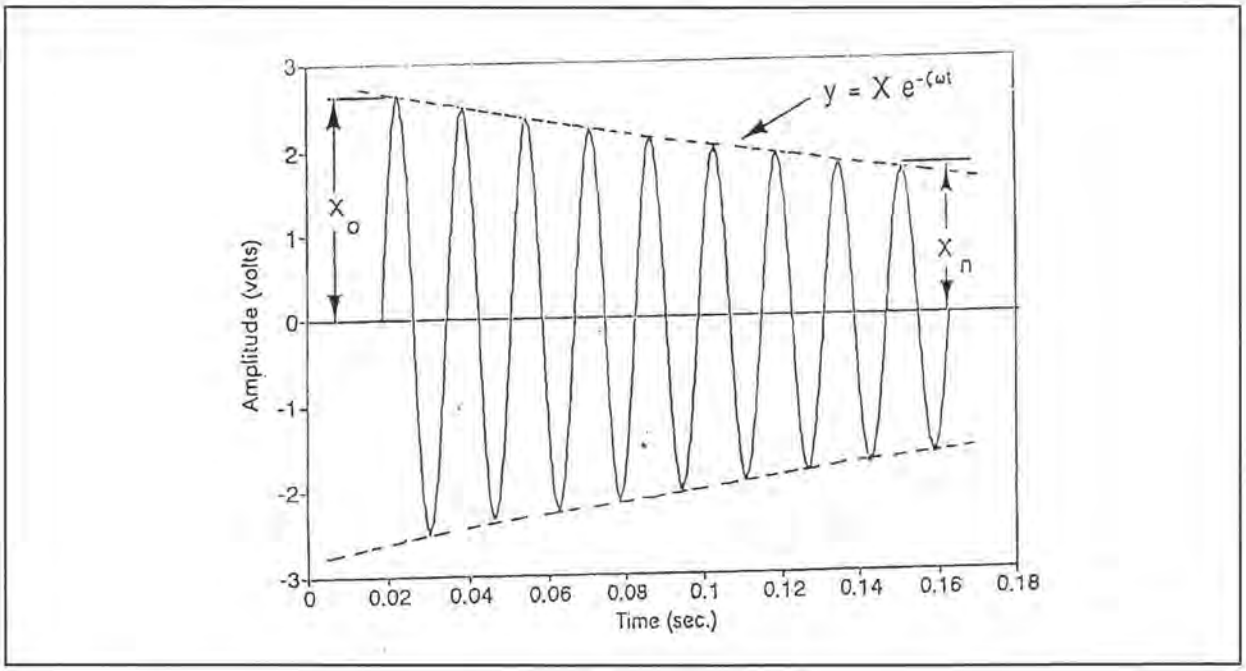

Figure 5. Amplitude-time history from free vibration decay flexural tests.

The loss factors determined from both the above methods were found to be in close agreement. Also, from the decaying amplitude-time history the fundamental frequency of oscillation (in this case, the damped natural frequency) is given by

$$f = \frac{1}{T} \tag{10}$$

where f = frequency in cycles per second (Hz), and T = period of oscillation (seconds)

The storage modulus (flexural), E_f , can be found by measuring this frequency and using the frequency equation from Beam Theory. For a cantilever beam vibrating in flexure, the frequency equation for the fundamental (first) mode is

$$f = \frac{(1.875)^2}{2\pi L^2}\frac{\sqrt{E_f I}}{\rho A} \qquad (11)$$

where E_f = modulus of elasticity of the beam material

I = moment of inertia of the beam

ρ = beam mass density

A = beam cross-sectional area

L = length of the beam

From which, solving for the storage modulus,

$$E_f = \frac{4\pi^2 f^2 L^2 \rho A}{(1.875)^4 I} \qquad (12)$$

Table 2 shows the dynamic flexural modulus and loss factor data obtained with the log-decrement technique. The regression models and the response volume plots for these two dependent response variables and the dominant process conditions are shown in Figures 6a, 6b, 7a and 7b along with their interactions. A careful observation of these plots indicates that a highly desirable combination of high flexural modulus with high loss factor can be obtained with the process conditions set at an optimum configuration of: high fiber content of 63.3 %, high pull speed of 36 cm/min (14 in/min), high zone 1 temperature at 171°C (350°F), high zone 2 temperature at 193°C (380°F), but a low zone 3 temperature of 182°C (360°F). The response plots show the non-inclusion of the fiber content (which significantly contributes to flexural modulus) for the

optimum location of damping, and the insignificance of zone 2 die temperature (which influences damping) on the flexural modulus. Also, it can be noted that a high pull speed with other variables at suggested levels dropped the flexural modulus marginally while still providing high damping. These observations were used in recommending the above process conditions for obtaining optimum desirable flexural modulus and flexural loss factor.

Table 2. Dynamic Properties of Pultruded Graphite - Epoxy (Log-Decrement Technique).

Test Plan	Flexural Modulus GPa (10^6 psi)	Loss Factor
1	115.98 (16.82)	0.0038
2	118.53 (17.19)	0.0031
3	116.78 (16.94)	0.0024
4	117.31 (17.01)	0.0025
5	116.71 (16.93)	0.0040
6	- -	-
7	114.41 (16.59)	0.0031
8	119.51 (17.33)	0.0033
9	113.98 (16.53)	0.0028
10	113.64 (16.48)	0.0033
11	113.45 (16.45)	0.0031
12	117.58 (17.05)	0.0041
13	113.84 (16.51)	0.0048
14	121.01 (17.55)	0.0031
15	115.28 (16.72)	0.0054
16	119.30 (17.30)	0.0046

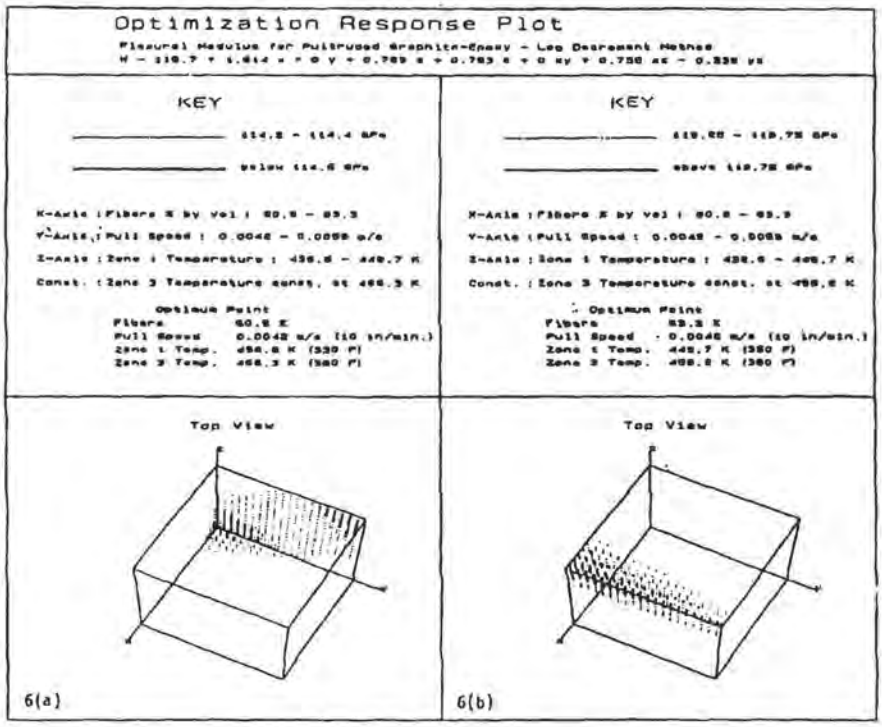

Figure 6. Flexural modulus control volume data from log-decrement technique.

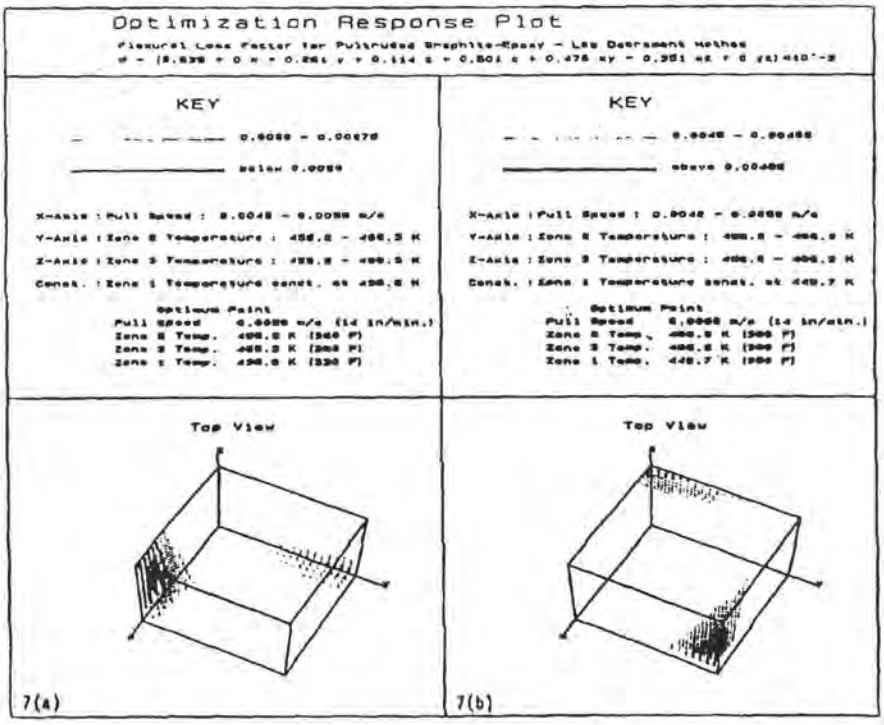

Figure 7. Flexural loss factor control volume data from log-decrement technique.

CONCLUSIONS

Scientific characterization of the effects of pultrusion process variables on the dynamic mechanical properties of graphite-epoxy composites has been conducted. Statistical regression techniques have been employed to generate mathematical models relating the pultrusion process variables to dynamic properties of graphite-epoxy composite material. Response volume techniques have been employed to show the optimum process regions for the response variables. The time domain log-decrement technique that was used yield reasonably good results. This method is, however, time consuming, limited in scope and prone to errors. The proposed frequency domain impulse technique is expected to increase the accuracy in the results and offer significant time savings in this research. Finally a thermochemical heat transfer model is being developed to describe the thermal manufacturing process for producing pultruded composite materials.

ACKNOWLEDGEMENT

The authors want to gratefully acknowledge the National Science Foundation, Division of Design and Manufacturing Systems, grant #DDM-9101643, and the Electric Power Research Institute, contract #RP 8007 20, for their support and the opportunity to present this research.

REFERENCES

1. Sumerak, J.E. "Understanding Pultrusion Variables for the First Time" *40th Annual Conference, Reinforced Plastics/Composites Institute*, Society of the Plastics Industry, Atlanta, Jan 1987.

2. J. G. Vaughan, R. M.Hackett, and E. C. Seal, "Optimization of the Pultrusion Process for Graphite/Epoxy," *Fiber-Tex 1988*, NASA CP-3038, 1989.

3. Box, G. E. P. And Wilson, K. B.,"On the Attainment of Optimal Conditions," *Journal of the Royal Statistical Society*, Series B, Vol. XIII, No. 1, 1-45 1951.

4. Patankar, S.V.,*Numerical Heat Transfer and Fluid Flow*,Hemisphere Publishing Corp. Washington D.C., 1980.

5. Gibson, R.F., "Vibration Test Methods for Dynamic Mechanical Property Characterization", in Manual on *Experimental Methods for Mechanical Testing of Composites*, R.L. Pendleton and M.E. Tuttle, Editors, Society of Experimental Mechanics, 151-164, 1989.

6. Vaughan, J.G., Roux, J.A., and P. Raju Mantena, "Characterization of Mechanical and Thermal Properties of Advanced Composite Pultrusions," *Proceedings of the 1992 NSF Design and Manufacturing Systems Conference*, Atlanta, GA, January 8-10, 1992, 1141-1145.

Mechanical and Thermal Behavior of Pultruded Advanced Composites

J.G. Vaughan, J.A. Roux, and P.R. Mantena
The University of Mississippi
University, MS 38677

Abstract

This paper presents the research of the second year in a three year effort to characterize the mechanical and thermal properties of pultruded composites. A fundamental understanding of the pultrusion process is required to develop high performance structural products and for developing composites with desirable thermal characteristics. This study is producing both experimental and analytical models to provide for such characterization and thereby providing an important ability to design/produce a pultruded composite material for a specific use. Short descriptions will be given on the advances made in understanding the effect of process variables on the mechanical and thermal behavior of pultruded composite materials.

INTRODUCTION

The development and optimization of pultruded composite materials is a need noted by a wide range of government and industrial users. Pultrusion is a cost efficient means by which high strength composite materials can be produced, yet it has been under-utilized by the advanced composites industry due to a lack of basic characterization of the process and its product. By directing the research described herein toward the basic understanding of the effects of process variables on the mechanical and thermal properties, cost/process advantages should enable pultruded composites to become competitive with traditional structural materials.

MATERIAL PROPERTY EXPERIMENTAL CHARACTERIZATION

To best understand how the numerous process variables influence the mechanical properties of pultruded composites, a series of statistically based design experiments were conducted. The major focus of this study was to determine the main effect of each major process variable on a given mechanical property.

However, not only were the direct effects of the process variables examined, but also the interaction effects among the process variables and second order non-linear variations. Included in the static mechanical property tests were flexural strength/modulus, tensile strength/modulus, compressive strength/modulus, short beam shear strength, and Iosipescue shear strength/modulus. Although not all tests have been completed, the results of the study to-date point out the major effect of the interaction terms on the mechanical property performance of pultruded composites. These interaction effects are many times more important than the variation of a single process variable such as fiber volume or pull speed and must be included in any design improvement of the pultrusion process.

Previous work by Mantena and Gibson on hybridization of 'SPECTRA' (a highly oriented polyethylene fiber manufactured by Allied Corporation) with graphite fibers has resulted in a stiff, light and highly damped composite material with numerous practical applications. These investigations were carried out on rectangular cross-section beam specimens (manufactured by the autoclave process) in the flexural and extensional modes of vibration. The concept is extended in the present research for the torsional mode of vibration of hybrid glass/graphite epoxy composite specimens with a cylindrical cross-section manufactured by the pultrusion process. Cylindrical rods were pultruded from all-graphite and all-glass fibers in an epoxy matrix and hybrids of graphite-glass/epoxy combinations. The overall fiber volume fraction was maintained constant at 60% for all the sample runs with the other pultrusion process parameters (such as pull speed and die zone temperatures) held constant. With the same resin system (Shell EPON 862) used for all the experimental runs the only process variable was the relative volume fraction of the glass and graphite fibers. The hybrids consisted of varying proportions of graphite fibers concentrated at the inner core with glass fibers as the shell (outer region) and vice-versa. The dynamic shear modulus and damping characteristics of these hybrid cylindrical specimens are being characterized using the Fast Fourier Transform based impulse-frequency response technique by subjecting the pultruded rods to a torsional mode of vibration in a specially fabricated test rig. In this type of testing, the specimen which is mounted vertically and fixed at the top is excited by using an impulse hammer with a piezoelectric force transducer in its tip. A small lathe

chuck to which two 'ears' are attached at opposite ends, is used at the bottom end to set the specimen in torsional vibration. One 'ear' is impacted with the impulse hammer and the response of the specimen is picked up and measured by a non-contacting eddy current proximity transducer located at the other 'ear'. From the Fourier transformed frequency response function displayed on the screen of the spectrum analyzer, the dynamic shear modulus is computed from the resonant frequency of the particular mode of torsional vibration and the loss factor (a measure of damping) of the rods is obtained using the half-power bandwidth relationship. The static shear modulus/strength data is also obtained from a conventional 10,000 in-lb. Tinius-Olsen torsion test machine.

ANALYTICAL MODELING

The thermochemical modeling for the Shell EPON 862 epoxy/fiberglass and graphite systems for round geometries has progressed very well. Results have shown very good agreement between the experimental thermocouple centerline measurements and the model predictions. These profiles correspond to product temperatures both inside the die and also for a two meter distance after the die exit. The post die region has been included since it is known that resin curing continues to occur in the high temperature post die region. Also, the model has been employed to predict degree of cure profiles both inside the die and in the post die regions along the centerline of the product. The predicted final degree of cures show very good qualitative agreement with differential scanning calorimeter (DSC) data, but were a little lower in value than the DSC data. This small disagreement is being investigated further.

SUMMARY

A scientific characterization of the effects of the pultrusion process variables on the static and dynamic mechanical properties of graphite/fiberglass-epoxy is underway. Statistical regression techniques have been employed to generate experimental mathematical models relating the static and dynamic properties of pultruded composites to those process variables used to produce them. In addition, a thermochemical heat

transfer model is under development to describe the thermal/chemical portion of the manufacturing process and will be most important for improving future designs for dies and heating sections of the pultruder.

ACKNOWLEDGEMENT

The authors want to gratefully acknowledge the National Science Foundation, Division of Design and Manufacturing systems, grant DDM-9101643, and the Electric Power Research Institute, contract RP 8007 20, for their support and the opportunity to present this work.

DYNAMIC FLEXURAL PROPERTIES OF PULTRUDED GLASS/GRAPHITE HYBRID COMPOSITES

P. Raju Mantena , Radesh Vangipuram and James G. Vaughan
Department of Mechanical Engineering
The University of Mississippi
University, MS

ABSTRACT

In this paper the performance of pultruded glass/graphite-epoxy hybrid composites is presented. In previous research, the dynamic mechanical properties of glass and graphite epoxy laminated composite beams have been characterized as functions of frequency and fiber volume. Based on these preliminary investigations it was concluded that hybridization of low modulus glass fibers with high modulus graphite fibers would offer the potential for a stiff, light, highly damped laminated composite structure that should have numerous practical applications. Also, the addition of glass fibers reduces the overall cost of the composite product. This previous work on laminated composites has been extended to pultruded products and the results of experimental investigations on glass/graphite hybrid composites are reported. The impulse-frequency response technique is used to study the dynamic behavior in the flexural mode of vibration of pultruded composite beams made up of different hybrid combinations of unidirectional glass and graphite fibers with epoxy as the matrix. The experimental results support our earlier conclusion that a composite material exhibiting high stiffness and damping can result by hybridizing glass and graphite fibers through the pultrusion manufacturing process.

KEYWORDS

Pultrusion, Hybrid composites, Dynamic mechanical properties

INTRODUCTION

Research on the experimental characterization of pultruded glass and graphite epoxy composite materials has been ongoing at the University of Mississippi on a industrial pultrusion machine (PULSTAR 804 commercial model) for the past few years. In this cost-effective automated manufacturing process, resin impregnated fibers are pulled through a heated die by hydraulic pullers as shown in Figure 1. The curing process is initiated inside the die where the induced pressure combined with an exothermic reaction results in a high degree of cure. The cured composite cools under ambient conditions and after passing through the pullers, is cut to the desired length. In previous research, the dynamic mechanical properties of glass and graphite epoxy pultruded composite materials were characterized using impulse-frequency response measurements. The dynamic flexural modulus of graphite/epoxy composite materials were found to be more than twice that of glass/epoxy composite materials, for the same volume fractions. Mantena and Gibson [1] reported that the hybridization of SPECTRA (a highly oriented polyethylene fiber developed by Allied Corporation) with graphite fibers resulted in a stiff, light and highly damped composite material with numerous applications. With graphite fibers exhibiting low density, high stiffness and high strength characteristics, and glass fibers which have better fracture stress, relatively lower cost but lacking stiffness, an innovative combination of these two fibers is expected to improve the load bearing characteristics of the structure [2]. 'Hybridization' of glass and graphite fibers in a single epoxy matrix could enhance the product performance by achieving a balance between the properties of all-glass and all-graphite/epoxy composites.

The pultrusion process proved to be very useful in manufacturing such glass-graphite/epoxy hybrid composites. With a limited knowledge base on pultruded hybrid composites, an attempt was made to experimentally characterize the various hybrid combinations of glass and graphite fibers in a single epoxy matrix. Since the constituent material properties and the layup sequence determine the stress distribution and

the failure modes in unidirectional composites, every effort was made during the pultrusion manufacturing process to produce the hybrid composite combinations with the fibers as symmetrically distributed about the geometric midplane as possible.

With specially designed preform plates, four different layup combinations of symmetric glass-graphite/epoxy hybrid composites were pultruded. One random combination of glass and graphite fibers in an epoxy matrix was also produced to study the effects of uneven fiber distribution on the dynamic and static behavior of the pultruded composite. To facilitate the comparison of properties of these hybrids with those of only glass and only graphite composites, some all-glass and all-graphite (60% fiber volume fraction) composites in an epoxy matrix were also pultruded for testing. The graphite fibers used were AS4W-12K, the glass fibers were fiberglass PPG 2001, #112 (E-glass) and the matrix was Shell EPON 862/W epoxy resin. The different combinations and the layup sequence of the fibers are given in Figure 2. Sample specimens cut from these long and continuous pultruded products were tested and the resonant frequency, dynamic flexural modulus, loss factor and static flexural modulus were determined, details of which are described below.

EXPERIMENTS

In the pultrusion process, at least five different process variables have been found to significantly affect the mechanical properties of the composite product. These five process variables are the fiber content, pull speed, and temperatures in the zone 1, zone 2 and zone 3 region of the heating dies [3,4]. These process variables were kept constant for all the specimens produced for this investigation. With the overall volume percentage of fibers maintained at 60%, the pull speed was 0.508 cm/s, zone 1 temperature was 193° C, Zone 2 temperature was 204° C and Zone 3 temperature was 204° C. Test specimens of length 30.48 cm, width 2.54 cm and thickness 0.32 cm were cut and used for both impulse-frequency response vibration testing and static load tests in a cantilever beam configuration

For the vibration tests, the specimen was clamped at one end in a vise as shown in Figure 3. An effective cantilever span of 25.4 cm was used for impulse-frequency response testing [1]. An impulse hammer provides the input excitation and an eddy current proximity detector is used to measure the response enabling a non-contact method of obtaining sensitive measurements of damping. A dual channel spectrum analyzer was used to measure the frequency response of the specimen. Efficient use of the digital signal processing features available in the spectrum analyzer was made to exclude the possibility of spurious data being included in the real time FFT trace [5]. The real time data is acquired and analyzed using a HP workstation and customized software developed in-house was used to calculate the dynamic mechanical properties. The dynamic flexural modulus was calculated from the resonant frequency and the eigenvalue of the particular mode. The loss factor, which is a measure of internal material damping, is obtained using the half-power bandwidth technique [6]. The all-glass and all-graphite/epoxy pultruded composites were also tested to compare the results with those of the hybrids. The entire vibration testing was performed on a pneumatic vibration isolation table to avoid any noise in the data due to spurious disturbances.

The static flexural modulus of the pultruded specimens were measured in a fixed-free cantilever beam configuration as shown in Figure 4. The deflection of the cantilever beam was measured for different loads. The loads are applied at a distance "b" and the deflection is measured at a distance "a" from the fixed end, as shown in this figure. A voltmeter and the eddy current displacement measurement probe were used to obtain the load-displacement data for the specimens. A linear fit of the load-displacement data was obtained and the slope of the line is used for calculating the static flexural modulus of the beam [7]. A typical load vs. deflection graph is shown in Figure 4. Initial calibration tests were done on a 2024 aluminum beam of identical cross-section for both the dynamic and the static tests.

RESULTS AND DISCUSSION

The results of dynamic flexural testing are shown in Table 1. Three different specimens were tested from each hybrid combination of glass and graphite fibers to determine the scatter in data. The effect of hybridization can be observed from Figures 5 and 6. Figure 5 shows the variation of dynamic flexural modulus with different layup sequence. The dynamic flexural modulus of all-glass/epoxy is about 46 GPa and that of all-graphite/epoxy is about 116 GPa. The dynamic flexural modulus of specimens with 30% of graphite fibers in the center and 30% glass fibers distributed evenly on the outer layers (CFMIX04) was found to be approximately 60 GPa. However, for the specimens with the same glass fiber content of 30% sandwiched by 30% graphite fibers on the outer layers (CFMIX06), the dynamic flexural modulus jumps to 94 GPa. Thus an increase in the flexural modulus of about 34 GPa (56%) was obtained by the appropriate use of graphite fibers at the outer surface of the composites, for identical volume fraction of glass and graphite fibers. This effect is due to the high stiffness characteristics of graphite fibers arranged further away from the geometric midplane. Since, in flexure, the strain is proportional to the distance from the midplane, a layer of highly stiff fibers nearer to the surface of the specimen greatly enhances the flexural stiffness of the composite product.

As shown in Figure 6, the all-glass/epoxy specimens (CFMIX02) exhibit higher damping compared to the all-graphite/epoxy specimens (CFMIX01). The addition of 20% graphite fibers (concentrated at the center) with 40% glass fibers (on the outside) results in an increase in loss factor (CFMIX03). This gain in damping is sacrificed, however, when the percentage of graphite fibers is increased in the center from 20 to 30% (CFMIX04), dropping to almost that of all-graphite/epoxy. On the other hand, a hybrid combination of 30% outer graphite with 30% inner glass (CFMIX06) exhibits the high damping performance of all-glass/epoxy (CFMIX02) accompanied by an increase of 34 GPa in flexural modulus when compared with the same fiber content but with reversed layup sequence (CFMIX04). Thus selective hybridization resulted in the improvement of dynamic flexural modulus compared to all-glass/epoxy and the damping characteristics show a better performance compared to all-graphite/epoxy composites.

A random mix of glass and graphite fibers in an epoxy matrix resulted in a warped product, as

anticipated. This could be due to non-symmetry of fiber layup and thermal stresses developed during manufacturing of the material. The dynamic flexural modulus of the composite with randomly distributed fibers (with 30% glass and 30% graphite fibers) was approximately 75 GPa, a value in between those of specimens CFMIX04 and CFMIX06 (with the same but symmetrically distributed glass and graphite fiber content as shown in Figure 5). The loss factor of the random mix specimen was found to be the lowest, as shown in Figure 6. No significant conclusions could be drawn from the results of this hybrid mix. This could be attributed to a lower energy loss and stiffening effect due to intertwining of glass and graphite fibers resulting in a "synergistic" effect [2].

The results of static testing of the pultruded glass-graphite hybrid composite are also given in Table 1. The static flexural modulus values are in close agreement with dynamic flexural modulus. The values of static flexural modulus for various combinations of glass-graphite layups are shown in Figure 7. A trend similar to that for dynamic flexural modulus was observed. Selective hybridization resulted in better utilization of the high stiffness characteristic of graphite fibers and the relatively higher damping nature of glass fibers. The earlier conclusion of other researchers [1,2] that the flexural characteristics of composite materials can be greatly improved by proper hybridization was demonstrated in this study.

SUMMARY

Pultruded glass-graphite/epoxy hybrid composites were characterized both dynamically and statically. The dynamic and static flexural modulus of the composites showed a remarkable variation as a function of the layup sequence. The damping characteristics of the hybrid composite materials also showed improvement compared to non-hybridized composites. The flexural stiffness of only glass composite can be greatly improved by the addition of graphite fibers, symmetrically distributed at the outer surfaces of the composite beam. Thus, a composite material with high flexural stiffness and high damping could result from hybridization. The FFT based impulse- frequency response technique provided an efficient method for the dynamic characterization of hybrid composite beams.

ACKNOWLEDGEMENTS

The authors would like to acknowledge financial support for this research from the National Science Foundation/Electric Power Research Institute (Grant # DDM - 9101643), NSF/EPSCoR, the University of Mississippi, and the State of Mississippi (Grant # OSR - 9108767)

REFERENCES

[1] P. Raju Mantena and R.F. Gibson, Proceedings of 22nd International SAMPE technical conference, MA, Nov 1990, pp. 370-382.

[2] J. Summerscales and D. Short, Composites, July 1978, pp. 157-166.

[3] J.G. Vaughan, R.M. Hackett and E.C. Seal, Fiber Tex 1988, NASA CP3038, p.p. 285-299.

[4] J.G. Vaughan, Proceedings of the 43'rd Annual Conference, SPI,Inc., 1988, 6D:1-6.

[5] D.E. Newland, Mechanical Vibration Analysis and Computation, John Wiley & Sons, Inc., New York, 1989, pp. 68-78.

[6] James L. Adcock, Hewlett Packard Journal, January 1987, pp. 33-36.

[7] J.M. Gere and S.P. Timoshenko, Mechanics of Materials, Second Edition, Brooks/Cole Engineering, Monterey, CA, 1984.

Table 1. Experimental values of dynamic flexural modulus, loss factor and static modulus for different hybrid combinations.

	Dynamic flexural modulus (GPa)			Static flexural modulus (GPa)			Flexural loss factor		
Specimen number	1	2	3	1	2	3	1	2	3
CFMIX01	116.5	117.7	117.0	114.1	113.4	112.2	0.0016	0.0014	0.0014
CFMIX02	44.8	45.8	46.1	46.6	44.7	46.5	0.0019	0.0018	0.0017
CFMIX03	51.6	53.0	51.8	54.6	54.1	51.1	0.0019	0.0021	0.0020
CFMIX04	60.0	60.4	61.9	60.3	61.6	66.2	0.0015	0.0016	0.0014
CFMIX05	102.0	100.8	102.6	98.6	96.2	100.4	0.0013	0.0015	0.0014
CFMIX06	93.1	93.5	96.0	91.3	91.1	93.2	0.0020	0.0019	0.0017
CFMIX07	71.1	77.3	78.7	76.3	74.9	78.2	0.0013	0.0012	0.0012

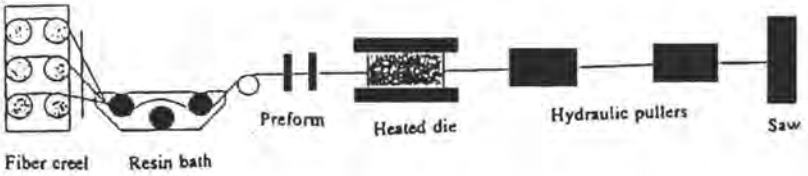

Figure 1. Schematic diagram of the pultrusion manufacturing process.

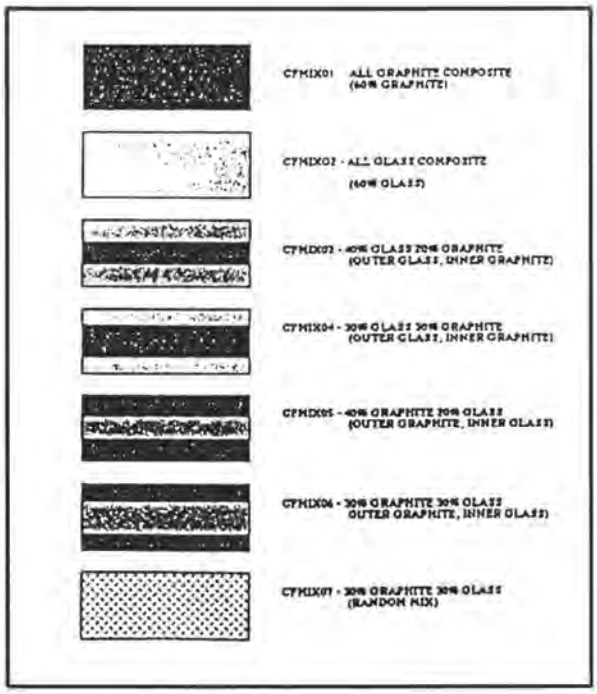

Figure 2. Cross sectional view of different combinations of glass and graphite fibers in epoxy matrix.

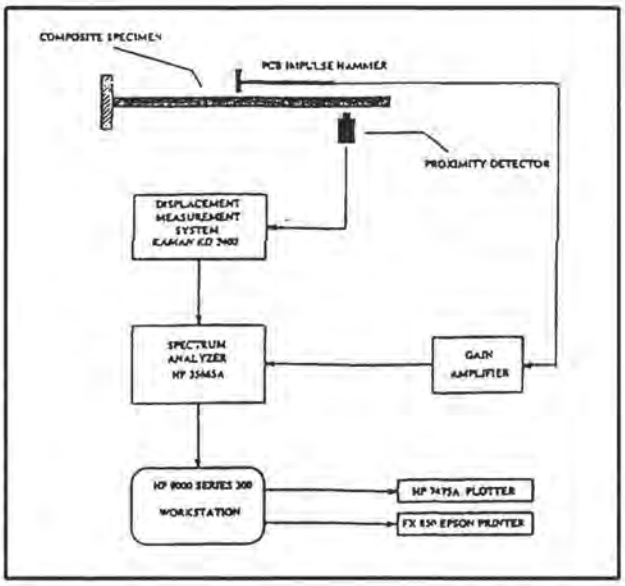

Figure 3. Schematic diagram of the impulse frequency response measurement.

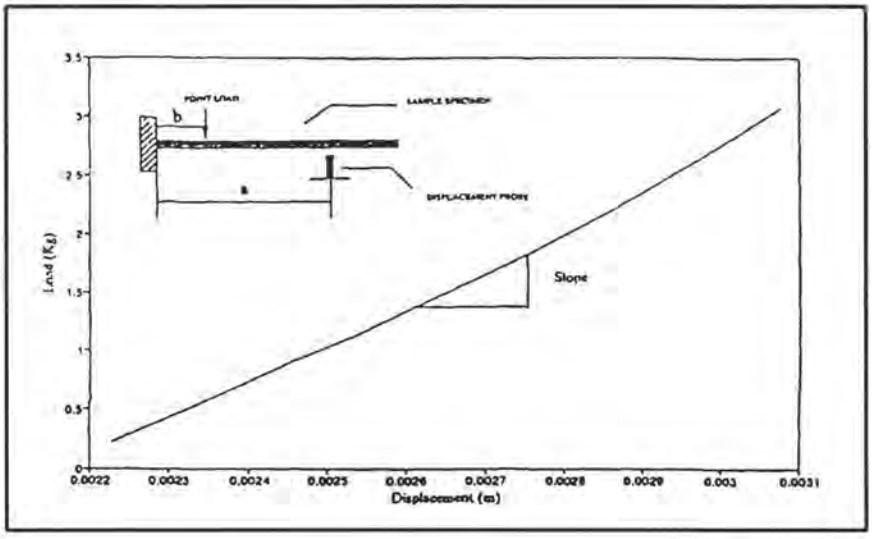

Figure 4. Experimental setup for the measurement of static modulus and a typical load deflection curve.

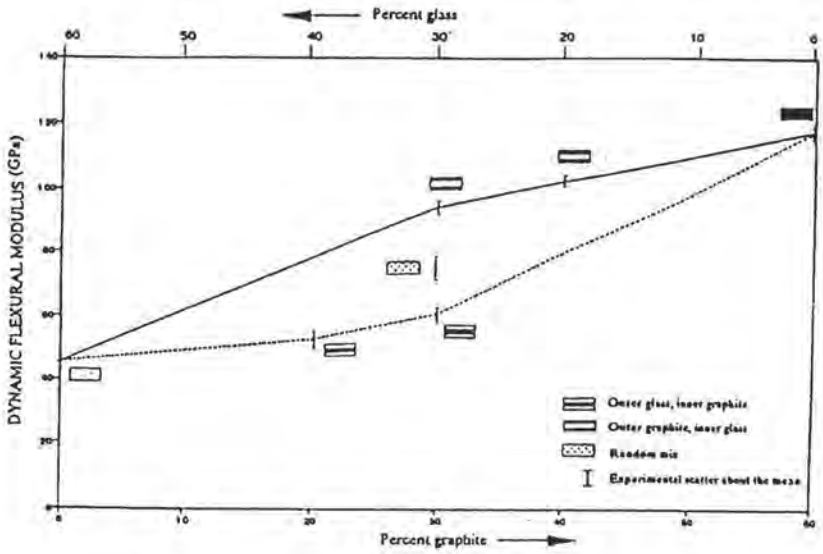

Figure 5. Variation of dynamic flexural modulus with different glass-graphite layup sequence.

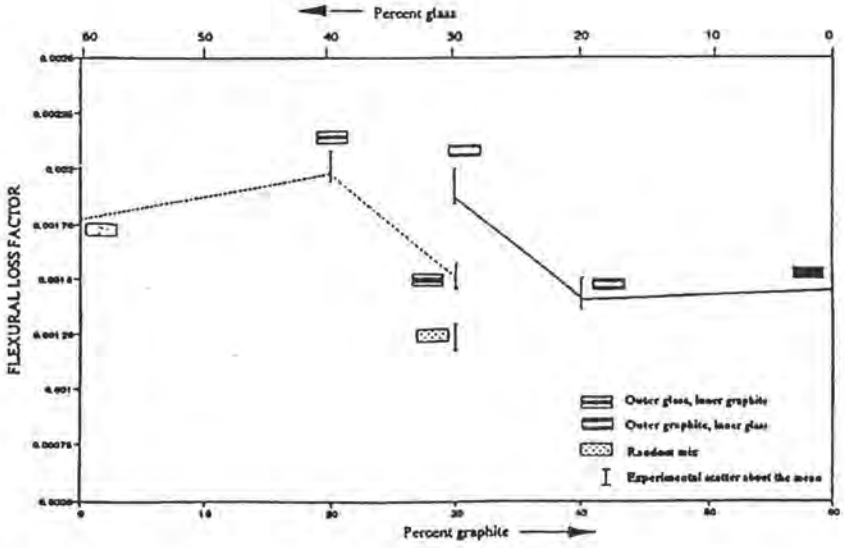

Figure 6. Variation of flexural loss factor with different glass-graphite layup sequence.

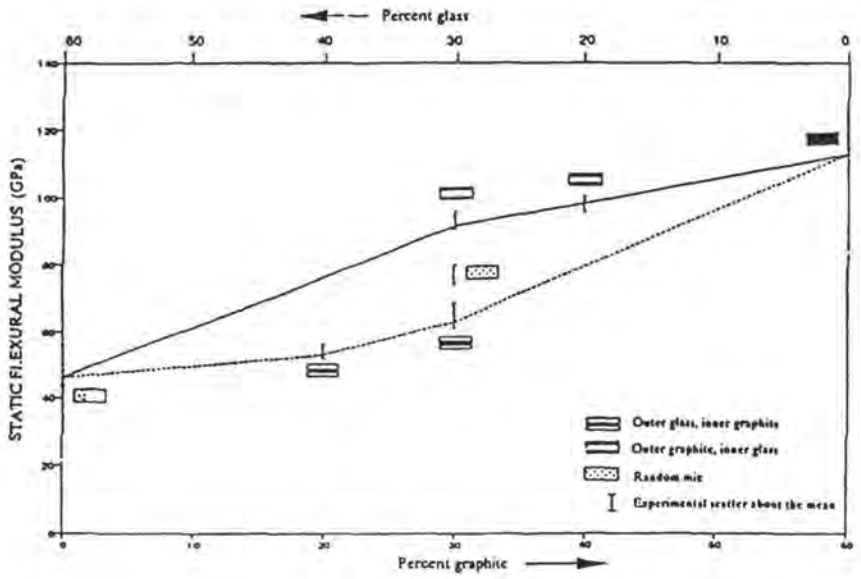

Figure 7. Variation of static flexural modulus with different glass-graphite layup sequence.

CHARACTERIZATION OF DYNAMIC MECHANICAL PROPERTIES OF PULTRUDED HYBRID CYLINDRICAL COMPOSITE RODS IN THE TORSIONAL MODE OF VIBRATION

Sujit S. Kumar* and P. Raju Mantena**
Department of Mechanical Engineering
The University of Mississippi
University, MS 38677

ABSTRACT

Hybrid composite materials show a distinct variation in mechanical properties over other composites manufactured under the same conditions by the pultrusion process. In this paper, a study is presented on the effects of hybridization on the dynamic and static behavior of cylindrical composites in the torsional mode of vibration. Previous research on flat specimens made of polyethylene and graphite fibers in an epoxy matrix resulted in a light, stiff and highly damped hybrid composite material. In the present case, the model under consideration is a pultruded cylindrical rod manufactured from glass, graphite and hybrids of glass-graphite/epoxy materials. The hybrid composite concept facilitates the possibility of tailoring materials to meet a specific need. The half-power bandwidth method is used to evaluate the dynamic torsional properties with the help of a Fast-Fourier transform based impulse-frequency response technique. The static shear modulus is obtained from a conventional low torque torsion tester. From the torque versus angle of twist data, the static shear modulus is obtained from the initial tangent modulus technique. Results show that for the same fiber volume fraction, glass/epoxy has a higher shear modulus than graphite/epoxy and that hybridization of these two material systems results in better dynamic performance with the glass fibers on the outer shell.

---

* Graduate Student ** Assistant Professor

Member AIAA Member ASME, SAMPE

NOMENCLATURE

f_n	natural frequency of vibration
G	static shear modulus of the specimen
G'	dynamic shear modulus of the specimen
I_p	polar area moment of inertia of the specimen
J	polar mass moment of inertia of end mass
L	length of the specimen (between grips)
λ_n	eigenvalue of the nth mode
ω	angular frequency of vibration
ϕ	angle of twist at the end of the specimen
ρ	mass density of the specimen
T	torque

INTRODUCTION

Hybrid composites are a combination of two or more different fiber materials in a common matrix material. Unlike conventional materials (steel, aluminum), composite materials can be tailored according to the necessity of the application. Some of the other important advantages are a high strength/weight ratio, good internal damping properties and high corrosion resistance. In this paper, characterization of dynamic mechanical properties of cylindrical hybrid composite rods made from glass and graphite fibers in an epoxy matrix, produced by the pultrusion process is carried out. The overall fiber volume fraction is maintained at 60% in all the samples and the other process parameters involved in the pultrusion process are also held constant. The same kind of resin is used in all the samples. The only variation obtained is in the relative fiber volume fractions of the different fibers.

The following combinations are tested for analysis :

1. 60% graphite and 40% epoxy
2. 60% glass and 40% epoxy
3. 48% glass, 12% graphite and 40% epoxy
4. 37% glass, 23% graphite and 40% epoxy
5. 30% glass, 30% graphite and 40% epoxy

For combinations 1 and 2, the fibers are uniformly distributed throughout the epoxy matrix. For 3,4 and 5, the following configurations are used:

1. Glass fibers concentrated on the outer shell and graphite fibers concentrated in the inner core.
2. Graphite fibers concentrated on the outer shell and glass fibers concentrated in the inner core.

Figure 1 shows the cross-sections of all the hybrid combinations.

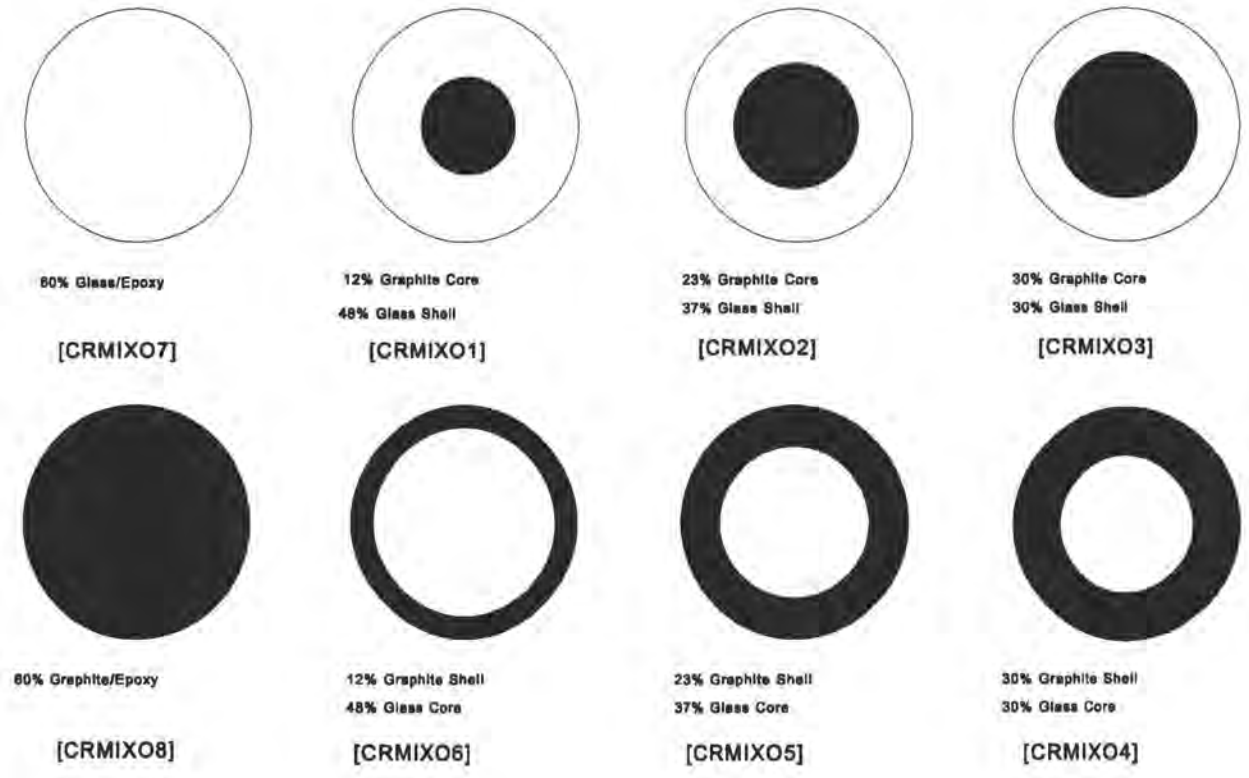

Figure 1. Cross-sections of hybrid combinations used

The glass fibers used are E-glass (PPG 2001, #112) The graphite fibers used are AS-4W-12K (Fiberite) The resin used in all the runs is Shell Epon - 862/W.

A Fast-Fourier Transform based impulse-frequency response technique is used for the dynamic testing of the composite cylindrical specimens. The frequency response is obtained on a HP 35665A spectrum analyzer and the analysis is carried out on a HP 9000 series computer. The dynamic properties are calculated from the frequency response spectrum and the half-power bandwidth relationship. The static shear modulus for the plain and hybrid specimens is obtained from a conventional (1000 N-m) Tinius-Olsen torsion tester.

PULTRUSION PROCESS

Pultrusion is an automated process used for the manufacture of continuous composite materials with constant cross-sectional profiles. The concept behind the process is simple. It involves the pulling of a nonhomogeneous compilation of materials through a resin bath and a heated die. The nonhomogeneous materials used are glass and graphite fibers and the matrix is usually a thermosetting resin. The process, though simple in concept, becomes much more complex as it is studied further[1]. Figure 2 shows a schematic of the pultrusion process. The process begins with the reinforcing fibers being pulled through a series of creels. The fibers pass through a resin bath, where they get impregnated in a formulated resin. The resin-impregnated fibers pass through a heated die that has been precision machined to the final shape of the product to be manufactured. Heat initiates an exothermic chemical reaction in the thermosetting resin matrix and after curing, the pultruded product comes out of the die. It is then cooled in ambient or forced air as it is continuously pulled by a mechanism that simultaneously clamps and pulls. The product, that emerges from the puller mechanism is cut to the desired length by an automatic cutoff saw.

Pultruded composites are known to exhibit properties such as a good surface finish, close dimensional tolerances and products of any desired length can be manufactured. Various process parameters

are involved in the manufacture of composites by the pultrusion process. The objective here was to maintain the same process parameters for all the runs and vary only the combinations of fiber volume content of the glass and graphite fibers. Plain and hybrid specimens with the same cross-sectional area and having different combinations of fiber volume content were manufactured by keeping the three die zone temperatures at 400° F (204.4° C), 380° F (193.3° C) and 380° F (193.3° C) and the pull speed at 12 inch/minute (30.48 cm/minute). A special kind of preform plate was designed to guide the fibers into the die during the manufacturing process[2]. This was done to maintain a constant circular cross-section of the fibers that go into the inner core of the hybrid.

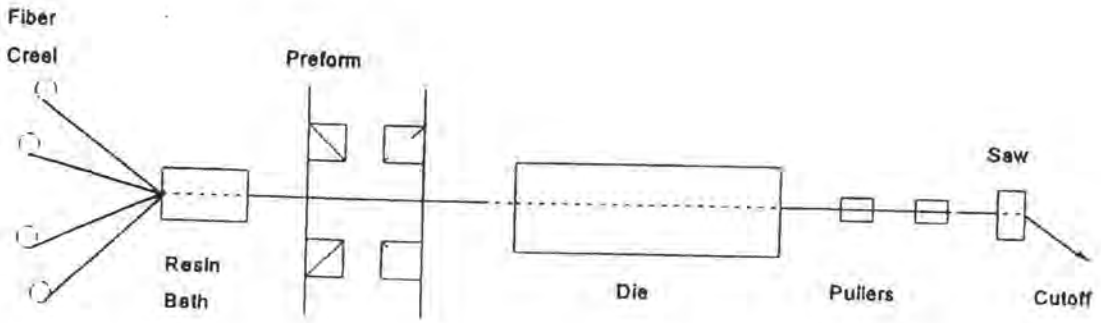

Figure 2. Schematic of the pultrusion process

DYNAMIC MECHANICAL PROPERTIES

Materials exhibit variations in properties when operated under dynamic conditions as compared to static conditions of loading. Thus, in general, design specifications based on static properties of materials need not meet the specific requirements of the operating conditions due to such property variations.

In dynamic applications, most design considerations are based on the analysis of the fundamental mode of vibration since the amplitudes in most of the cases are very high at the fundamental frequency of vibration. Efficient damping mechanisms should be incorporated in the structure to limit the amplitudes of

vibration and make the structure more stable. Composite materials exhibit good internal damping characteristics as opposed to most conventional metallic materials. Aerodynamic damping and friction between the joints ameliorate damping conditions in a structure. Utilizing the internal damping of materials would be more appropriate, however, as the structure can be designed to damp out the vibrations internally without the aid of external dampers. Composites can be manufactured according to the degree of damping required in a structure. The friction between the fibers and the matrix and a network of three-dimensional cross linked molecules formed during curing hinder the vibratory motion and assist in damping. Damping can also be enhanced by hybridization. Damping is believed to be more effective in the torsional mode of vibration [3] and thus torsional dampers are used in machinery to damp out most of the vibrations.

STATIC MECHANICAL PROPERTIES

The static properties of some materials vary from their dynamic properties. In the present case, a torsion tester is used to place the materials in a state of static shear by gripping one end of the specimen in a chuck and twisting the other end, thus imparting a torque to the specimen. When a cylindrical unidirectional composite material is subjected to torsional static loading, it tends to split along its length like a stick of wood [4]. This split extends to the full length of the specimen, and the crack simply separates the fibers on each side of an approximately hemispherical section. Also, it is the matrix that governs the torsional properties of a material and it is the matrix that transmits shear in a composite material. The relationship between the applied torque and the angle of twist gives the static shear modulus of the specimen.

EXPERIMENTAL TECHNIQUE

The torsional dynamic measurements were conducted with the help of a specially designed test fixture and the Fast-Fourier Transform based impulse-frequency response technique on pultruded rods subjected to the torsional mode of vibration [5]. In this type of testing, the specimen which is mounted vertically and fixed at the top (in an L-plate) is excited by using an impulse hammer with a piezo-electric

force transducer in its tip. A small lathe chuck to which two "ears" are attached at opposite ends (Figure 3), is used at the bottom end to set the specimen in torsional vibration. One "ear" is impacted with the impulse hammer and the response of the specimen is picked up and measured by a non-contacting eddy current proximity transducer located at the other "ear". From the Fourier transformed frequency response function displayed on the screen of the spectrum analyzer, the dynamic shear modulus is computed from the resonant frequency of the particular mode of torsional vibration and loss factor (a measure of damping) of the rods is obtained using the half-power bandwidth relationship.

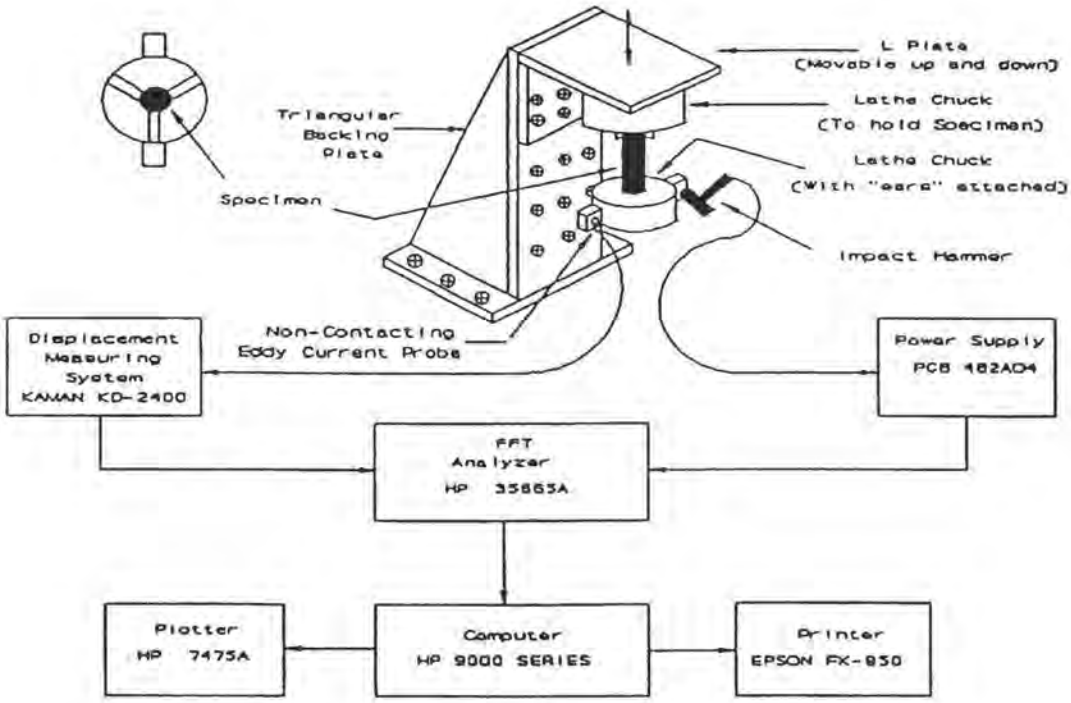

Figure 3. Experimental Setup for torsional vibration testing.

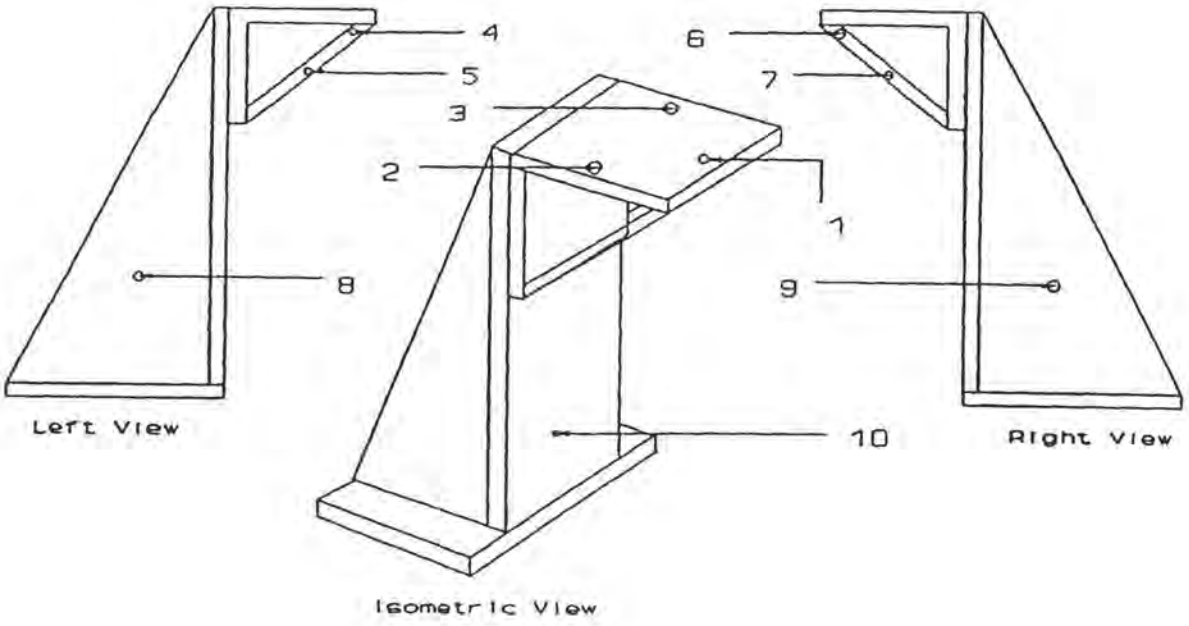

Figure 4. Fixture discretized at points of maximum displacement.

The following equations[5] are used for the analysis

$$\cot \lambda_n = \frac{J \lambda_n}{\rho I_p L} \tag{1}$$

Where the corresponding frequency is

$$f_n = \left(\frac{\lambda_n}{2\pi L}\right) * \sqrt{\left(\frac{G'}{\rho}\right)} \tag{2}$$

The shear loss factor was calculated by the half power bandwidth relationship and is given by ,

$$\eta_G = \frac{\Delta f}{f_n} \tag{3}$$

Using the values of frequency obtained from the response function on the analyzer, the mode number, density and polar mass moment of inertia of the attached mass, Equations (1) and (2) can be solved for the dynamic shear modulus G'.

POLAR MASS MOMENT OF INERTIA OF THE END MASS

The polar mass moment of inertia of the mass attached to the end of the specimen is an important parameter in the determination of the dynamic properties of the specimens. The mass attached to the end of the specimen as shown in Figure 3, is used to set the specimen into torsional excitation. The geometry of the mass is complex as there are projections attached to the body of the mass (a modified lathe chuck) and thus it was difficult to determine the exact radius of the mass to obtain its polar mass moment of inertia theoretically.

The polar mass moment of inertia was obtained experimentally by subjecting a material of known shear modulus into torsional vibration in the setup and obtaining its resonant frequency. From the experimentally determined value of the resonant frequency and other known parameters, Equation (1) was used to work back to the value of the polar mass moment of inertia. The following equation obtained from Equation (1) was used for the calculations.

$$J = \frac{G' I_p}{\omega c} \cot \frac{\omega L}{c} \qquad (4)$$

where

$$I_p = \frac{\pi r^4}{2} \quad , \quad c = \sqrt{\left(\frac{G}{\rho}\right)}$$

RESONANT FREQUENCY OF THE TEST FIXTURE

There is a strong tendency for the energy imparted to the specimen to get dissipated into the test structure. Thus, the damping values obtained may be due to the contribution of the specimen and that of the structure, and the structural frequencies of the fixture may interfere with the frequencies of the specimen. The resonant frequencies of the fixture holding the specimen (Figure 3) were analyzed by discretizing the structure at different points of probable maximum displacement as shown in Figure 4. An accelerometer was

mounted at each of these selected ten spots and the structure was impacted. As shown in Figures 5 and 6, the resonant frequencies of the structure are way beyond the range of the specimen's torsional resonant frequency. This was confirmed by making the structure more stiff and then obtaining its resonant frequency. The structure was made stiffer by moving the L-plate down. As a result of this, structural peaks moved to the right as shown in Figures 7 and 8. There was no shift in the torsional and bending frequencies of interest as shown in Figures 9a and 9b. Thus, it was concluded that the structural frequencies would not interfere with the torsional frequency of the specimens being characterized.

STATIC TORSIONAL TESTING

The static shear modulus of the cylindrical specimens was obtained from a conventional (1000 N-m) Tinius-Olsen torsion tester[4] using the standard ASTM E 111-82 testing procedure[6]. The torsion tester consists of two rigid chucks in which the specimen was held during loading. One of the chucks is fixed and the other rotates relative to the first, thus imparting a torque to the rod with one end fixed and the other end free to rotate.

The static shear modulus, G, was calculated from the torque versus angle of twist curve obtained from the torsion tester. The torsion tester was interfaced to a computer and the data from the tester was directly recorded on the computer. A program written in QuickBasic and loaded on to the computer served the purpose of data acquisition and analysis from the torsion tester. This gave greater accuracy and higher confidence in the results obtained. From the initial slope of the torque / displacement curve, as shown in Figure 10, the shear modulus was obtained according to the following equations[4]

$$\frac{T}{\phi} = \frac{G\, I_p}{L} \qquad (6)$$

Thus,

$$G = \left(\frac{T}{\phi}\right) \frac{L}{I_p} \qquad (7)$$

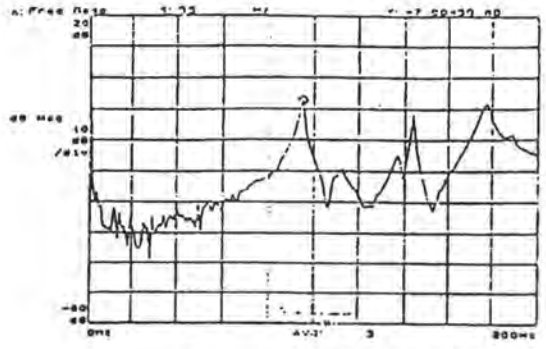

Figure 5. Resonant frequency of the test fixture (95 Hz)

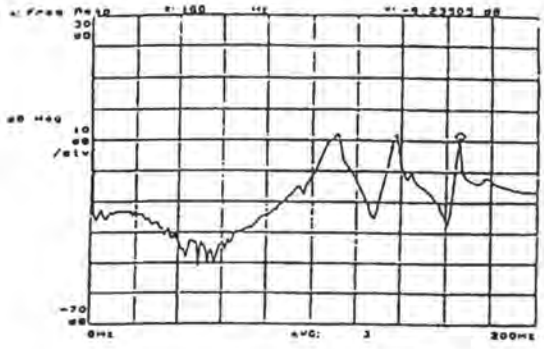

Figure 6. Resonant frequency of the test fixture (166 Hz)

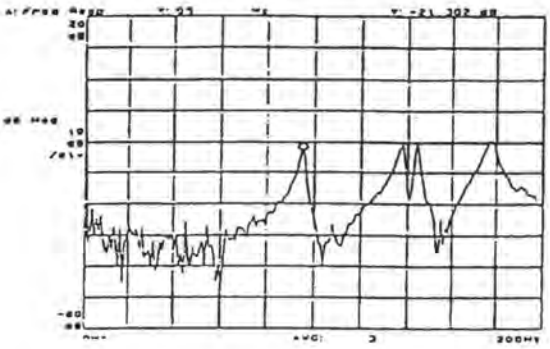

Figure 7. L-plate at the extreme top (Resonant frequency = 95 Hz)

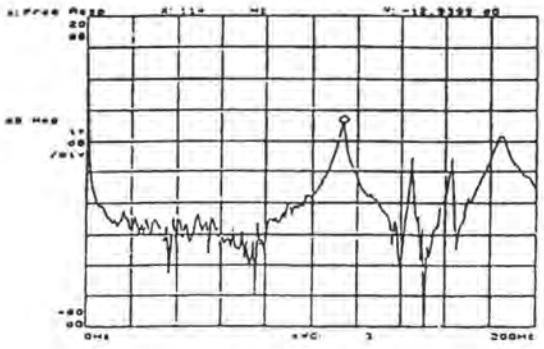

Figure 8. L-plate at 20 cm from top (Resonant frequency = 114 Hz)

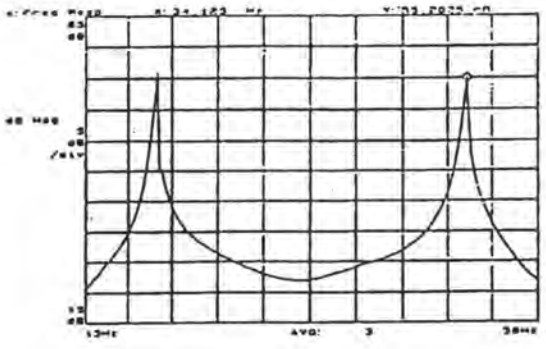

Figure 9a. Bending and torsional peaks with L-plate at extreme top

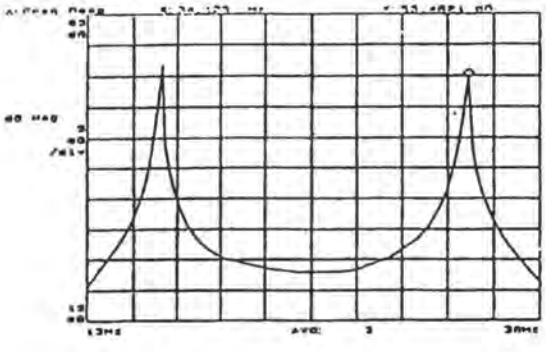

Figure 9b. Bending and torsional peaks with L-plate at 20 cm from top (showing no shift in the frequency)

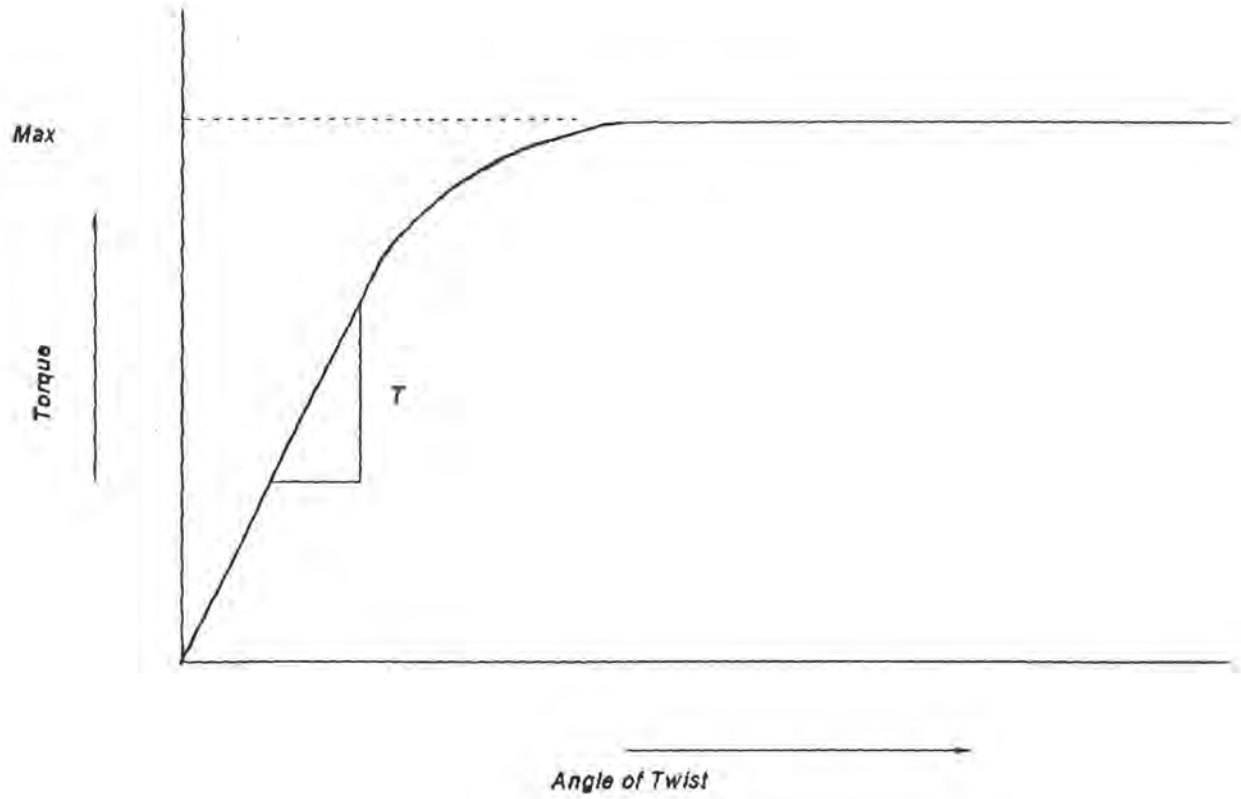

Figure 10. Torque v/s deflection for a composite specimen

RESULTS AND DISCUSSION

The specimens from all the runs were tested in torsion under both dynamic and static conditions of loading, as explained in the section on Experimental Technique.

Composite materials show a distinct change in mechanical properties with changes in their constituent materials. Samples manufactured with the same combinations of fiber volume fractions and other process variables showed an enormous amount of variation in properties with just the change in the position of fibers with respect to the neutral axis.

All the samples were loaded in the torsional setup for lengths of four inch (10.16 cm) and five inch (12.7 cm) and with two different polar mass moments of inertia of the end masses. This change in boundary conditions was imposed to obtain a variation in the frequency range. These values of the length were found out to be optimum for the setup used. A three inch sample length was too short and rigid to set into torsional vibration and a six inch sample length was too long for the type of setup used and also, the bending mode was more dominant for this length. Thus the optimum lengths were found out to be four and five inches, and consistent data was obtained for these lengths.

A comparison of the dynamic shear properties of all the combinations is shown in Figures 11 and 12. Figure 11 shows the variation of the dynamic shear modulus for all the combinations. As shown in the figure, 60% glass/epoxy has a higher shear modulus than 60% graphite/epoxy. There is a difference of about 2 GPa between the shear modulii of the two composites. This can be due to the fact that glass fibers in addition to being purely isotropic, have a higher shear modulus when compared to graphite fibers. With the change in fiber position, the modulus changes accordingly. Since glass is stiffer than graphite in shear, its position on the outer core results in a higher modulus then when it is in the inner core. This is because, in a state of torsion, the shear stresses are maximum at the surface of the specimen. This is clearly shown by the two separate curves in Figure 11. The curve showing the higher modulus represents glass on the outer shell and graphite in the inner core. Also, the modulus decreases slightly but steadily with the addition of graphite to glass and is minimum for 60% graphite/epoxy among all the combinations.

Figure 12 shows the variation in the shear loss factor for all the hybrid combinations. The contribution towards the loss factor can result from a number of factors such as the internal bonding between the fibers and the matrix, the boundary conditions of the test specimen under consideration, from the geometry of the specimen, from the resolution of the spectrum analyzer and from aerodynamic conditions. In the present case, best efforts were made to keep all the other parameters constant and vary only the material in the cylindrical structure (in this case, the cylindrical rod itself can act as a structure) and the lowest values obtained from the various experiments were chosen for the sake of comparison. The damping values

obtained in this case need not be a result of pure internal damping in the material but a comparison can be made by treating almost all the external parameters constant. In addition, among all the samples tested, the values of damping were chosen from that set which showed the lowest damping. The values of damping for five inches length of the specimen and with the heavier mass attached at the end showed the lowest damping values in almost all the cases. This could be because of the decrease in damping with the increase of mass and length of the specimen. Hence these damping values were chosen for the sake of comparison. Figure 12 shows such a comparison for the shear loss factor of all the combinations. Considering the scatter in the data, it appears that there is not a significant variation in the damping properties between all the combinations but among all the combinations, 60% glass/epoxy shows the highest damping.

Figure 13 shows the dynamic properties of all glass/epoxy and all graphite/epoxy combinations over a range of frequencies. The variation in frequencies is obtained by the change in boundary conditions of the test specimen. It is clear from Figure 13 that glass/epoxy has a higher dynamic shear modulus than graphite/epoxy for the same fiber volume fraction as discussed earlier. The damping in graphite/epoxy is better than that of glass/epoxy at a lower frequency. The change in frequency is not very large in this case and as seen in the figure, the value of dynamic shear modulus does not change significantly as a function of frequency. But the damping values change and at a certain frequency, glass/epoxy shows higher damping than graphite /epoxy. This can be due to the relative change in the mass of the structure comprising of the specimen and the end mass.

The effects of fiber position and frequency on the dynamic shear modulus and shear loss factor are shown in Figures 14 and 15 over a range of frequencies. Of all the combinations, the hybrid of 30% graphite on the outer shell and 30% glass in the inner core has the lowest shear modulus. This is expected as there is a maximum amount of graphite present in the hybrid and it is present on the outer shell. Both of these factors contribute to the weakening of the hybrid in shear. The shear modulus value increases steadily as more glass fibers are added to the hybrid. This should be expected due to the higher values of shear modulus of glass/epoxy. Figure 15 shows the effects of fiber position on the shear loss factor of the hybrid specimens.

As shown in Figure 15, there is not much of a difference in the loss factor values between the different combinations. This can be due to the fact that a lot of external factors, which as identified earlier, might be influencing the damping values in the material.

The torsional static properties were determined for all the tests from a standard low torque torsion tester. Close agreement between the static and dynamic shear properties was obtained. Figure 16 shows the static shear modulus for all the runs along with the experimental scatter. The variation is almost the same as seen in the dynamic case.

A comparison plot of dynamic and static shear modulii is shown in Figure 17. Figure 17 is an overlay of Figures 11 and 16. It is clear from the figure that there is a close agreement between the static and dynamic values of the shear modulus and that the difference is almost a constant for all the combinations. The percent difference between the two values was 3-6 % which could be attributed to the frequency dependent behavior of the polymeric matrix in these specimens.

CONCLUSIONS

Dynamic and static mechanical properties of hybrids of glass/epoxy and graphite/epoxy cylindrical composites have been characterized in the torsional mode of vibration and under a state of pure torsion. It was determined that for the same fiber volume fraction, glass/epoxy has a higher shear modulus than graphite/epoxy. Also, it was determined that hybridization of these two materials leads to a refinement in respective properties. The hybrid of 12% graphite and 48% glass, with glass on the outer shell and graphite in the inner core, was determined to have better properties over plain glass/epoxy and plain graphite/epoxy.

ACKNOWLEDGEMENTS

Financial support for this research was provided by the National Science Foundation/Electric Power Research Institute (Grant # DDM-9101643) NSF/EPSCOR, the University of Mississippi, and the State of Mississippi (Grant # OSR-9108767).

REFERENCES

1. Jeffrey D. Martin and Joseph E. Sumarek, "Pultrusion", Pultrusion Technology Inc., Engineered Materials Handbook, Engineering Plastics ASM International, Vol. 2, 1987, pp. 389-398.

2. Kumar Papineni, "MS Thesis" (in progress), Mechanical Engineering Department, University of Mississippi, 1994.

3. R. Mantena, T. S. Srivatsan, R. F. Gibson, T. A. Place and T. S. Sudershan, "Damping Capacity Measurements to Detect Damage in Adhesively Bonded Joints", Materials Evaluation, Vol. 47, Number 5, May 1989, pp. 564-570.

4. Outwater, J. W, "The Torsional Failure and Fracture Energy in Shear of a Pultruded Rod", Test Methods for Design Allowables of Fibrous Composites : 2nd Volume, ASTM STP 1003, C. C. Chamis, Ed., American Society of Testing Materials, Philadelphia, 1989, pp. 224-230.

5. P. Raju Mantena, R. F. Gibson and T. Alan Place, "A Torsional Impulse-Frequency Response Technique for Evaluating the Dynamic Mechanical Properties of Structural Materials", Proceedings of the Sixth Annual ASM/ESD Advanced Composites Conference Detroit, MI, October 8-11, 1990, pp. 477-485.

6. "Standard Test Method for Young's Modulus, Tangent Modulus and Chord Modulus", ASTM E 111 - 82.

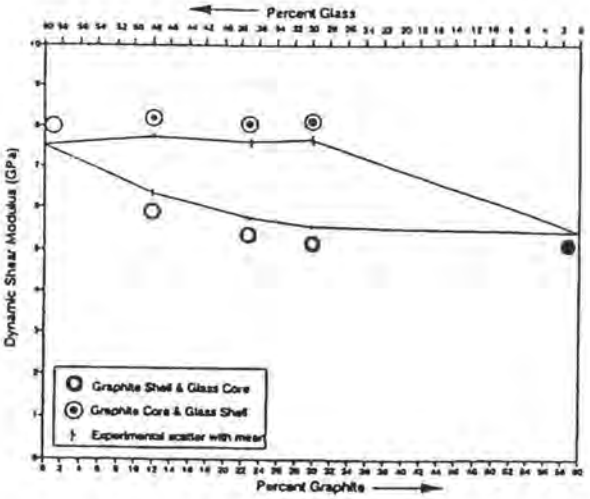

Figure 11. Variation of dynamic shear modulus for all the hybrid combinations

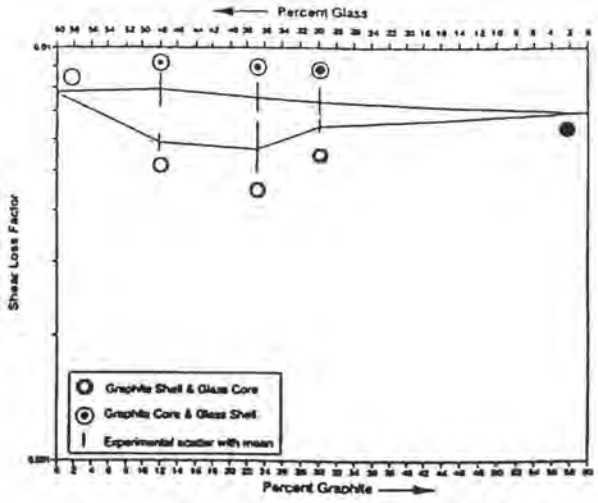

Figure 12. Variation of shear loss factor for all the hybrid combinations

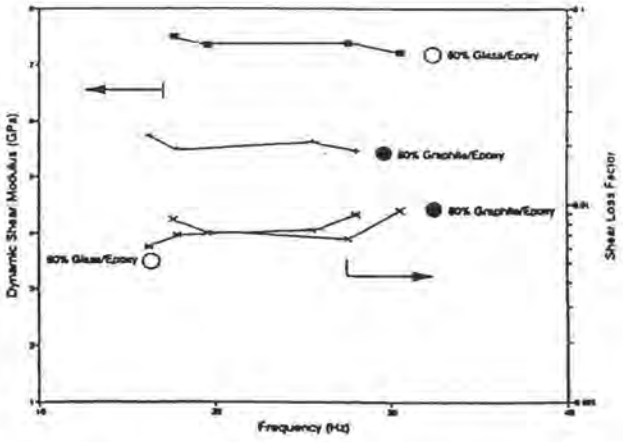

Figure 13. Comparison of dynamic shear properties of 60% glass/epoxy and 60% graphite/epoxy (average values for three specimens)

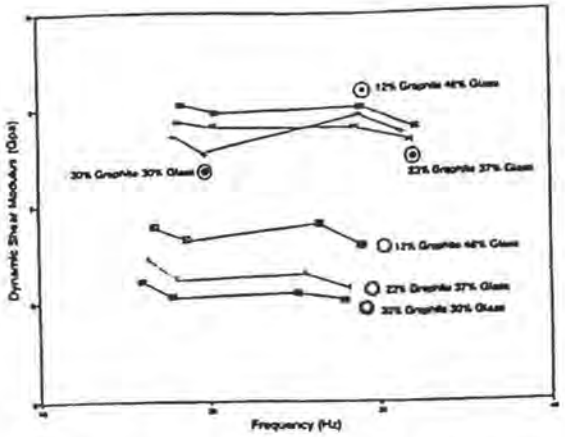

Figure 14. Effect of fiber position and frequency on the dynamic shear modulus (average values for three specimens)

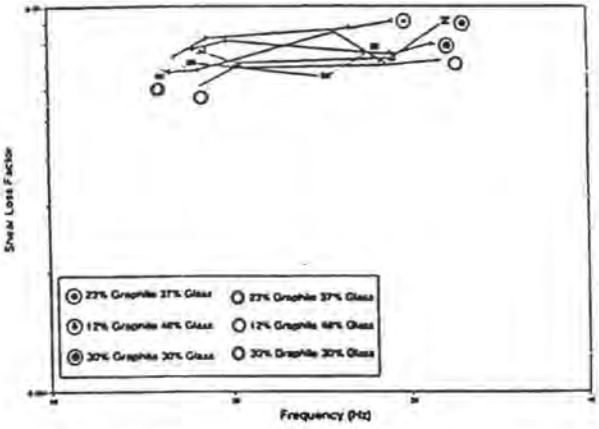

Figure 15. Effect of fiber position and frequency on shear loss factor (average values for three specimens)

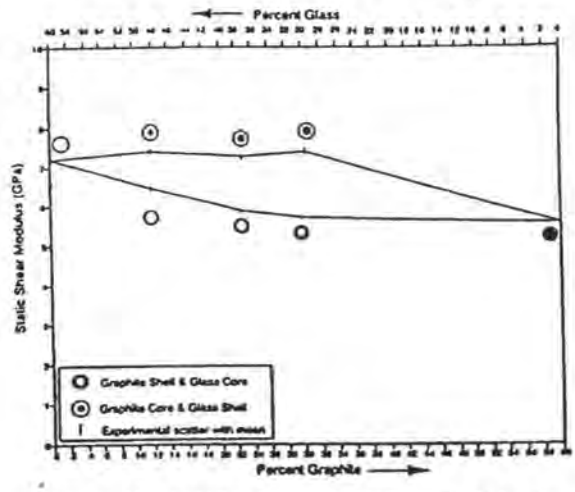

Figure 16. Variation of static shear modulus for all the hybrid combinations

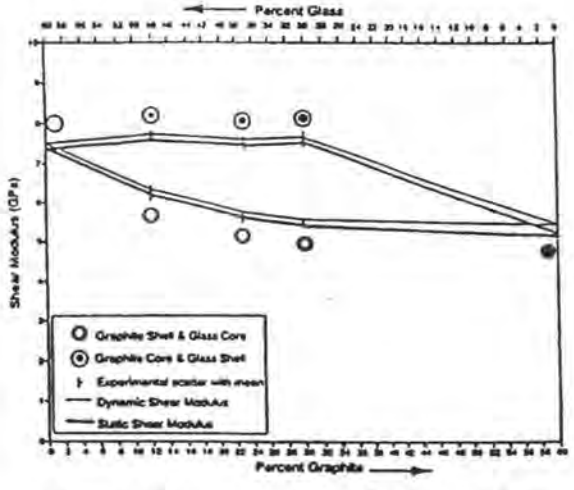

Figure 17. Comparison of dynamic and static shear modulii for all the hybrid combinations

CHARACTERIZATION OF MECHANICAL AND THERMAL PROPERTIES OF ADVANCED COMPOSITE PULTRUSIONS

James G. Vaughan , Jeffrey A . Roux, P. Raju Mantena
Department of Mechanical Engineering
The University of Mississippi
University, MS 38655

ABSTRACT

This paper presents an overview of the research conducted on the characterization of mechanical and thermal properties of pultruded composites. The pultrusion process is one of the most cost-effective continuous manufacturing techniques. In the third year of this research program, the feasibility of manufacturing hybrids (both glass and graphite fibers in an epoxy matrix) by the pultrusion process was examined, and their static, dynamic and fracture behavior was compared with mono-fiber type (glass-epoxy and graphite-epoxy) pultruded composites. The graphite fiber volume exhibited a predominant role in varying the mechanical properties through hybridization, for both axial and flexural loading. The glass fibers were more effective for torsional loading and in functioning as protective shields. These studies showed that hybrids can be pultruded with different fiber volume and layup combinations, depending on the specific application requirements. Numerical results for axial, radial and circumferential direction temperature and degree of cure profiles stress the importance of post-die analysis, where the curing is expected to increase by as much as 5% for high pull speeds.

INTRODUCTION

The need to develop and optimize pultruded composite materials is recognized by a broad spectrum of governmental and industrial potential users. For many advanced applications, pultruded composites offer inherent technical advantages such as structural strength, improved physical properties and reduced cost along with increased life, when compared to the other composite manufacturing processes. Cost-competitive

advantages will enable pultruded composites to become traditional materials along side steel, wood and aluminum before the end of the 20th century. By focusing the research on the effects of the process variables on the thermal, static and dynamic characteristics of pultruded polymeric composite products, innovative material systems can be developed. These new material systems will be important to industry in their goal of providing high quality products/service to customers at the lowest possible cost.

For a number of years, commercial pultruders have used continuous glass reinforcing fibers with a thermosetting resin matrix. Processing of more advanced high-performance material systems such as graphite-epoxy is relatively new and the processing details are not as well understood. In the past two years of this project considerable progress has been made on characterizing the effects of pultrusion process variables on the structural/dynamic and thermal properties of a mono-fiber type, graphite (Hercules AS4-W-12K) - epoxy (Shell EPON 9310/9360/537), composite material system (reported in the 1993 and 1994 NSF Design and Manufacturing Systems Grantees Conference Proceedings). Innovative developments have been made in the third year of this project on pultruding 'hybrids', i.e., both glass and graphite fibers in a common epoxy binder; resulting in a stiff, light and highly damped composite product with numerous practical applications. The advantages of hybridization are summarized in this paper.

SRUCTURAL/DYNAMIC PROPERTIES OF HYBRIDS

Hybrid composites can be manufactured by different manufacturing techniques, pultrusion being one of the most cost-effective. For this research, different types of hybrid sections were designed using graphite and glass fibers with epoxy as the binder matrix. Two different hybrid sections, a sandwich flat and a shell-core round, with different fiber layup and volume combinations were pultruded, and their static and dynamic mechanical properties were studied. These experimental sections were pultruded using various sets of special pre-form and post-die plates to tailor and control the fiber layup orientations. In order to minimize the effects of the other pultrusion process variables, a set of constant process conditions were maintained in manufacturing these experimental products. The mechanical properties and the failure mechanisms of these

hybrids were compared with those of mono-fiber type, graphite-epoxy and glass-epoxy, pultruded composites. The static properties examined were flexural strength and modulus, short-beam shear strength, and tensile strength. The flexural tests were conducted under three different material conditions (as-pultruded, post-cured and hot-wet) and using two different test methods (3-point and 4-point loading). For the dynamic (modulus and damping) studies, the impulse-frequency response technique was used for exciting the flat specimens into flexural and the round specimens into torsional modes of vibration using appropriately designed test fixtures.

The sandwich hybrid flat, with glass sandwiched between graphite, was observed to have better flexural properties compared to the other flat hybrid combinations. This fiber layup combination also exhibited better resistance to the hot-wet environment. For desirable flexural properties, an all-graphite composite may be replaced by a hybrid of graphite-glass/epoxy designed accordingly. This gives an added advantage of reducing the amount of expensive graphite fibers by replacing the same with comparatively lower priced glass fibers. The results of the tensile tests showed a remarkable improvement in the strains to failure for all hybrid sections (regardless of the type of fiber layup combination), compared to the all-graphite composite. For both the sandwich flat and shell-core round specimens, better tensile properties were observed with graphite sandwiched between glass for all the volume fractions tested, as opposed to glass sandwiched between graphite. The isotropic glass fibers when placed on the outer layers evidently form a protective shield for the graphite core.

The results of dynamic flexural tests on the flat specimens showed that the flexural stiffness of the all-glass/epoxy pultruded specimens can be greatly improved by the addition of graphite fibers, symmetrically distributed at the outer surfaces of the composite beams. This is in agreement with the static flexural modulus data. In addition, the damping characteristics of these hybrids showed improvement compared to the non-hybridized composites, demonstrating the potential for designing a stiff, light, and highly damped composite structure that should have numerous practical applications. Results of the torsion tests show that for the same fiber volume fractions, glass/epoxy has a higher shear modulus than graphite/epoxy, and hybridization

of these two material systems with the glass fibers placed on the outer shell results in better dynamic performance.

THERMAL MODELING

Many models have been proposed by researchers, but none considered a three-dimensional model which recognises the importance of post-die curing. In this research the importance of post-die analysis was stressed, where the curing is expected to increase by as much as 5% for high pull speeds. A numerical model has been developed to analyze the die and post-die temperature and degree of cure profiles in pultruded composites. The model, which utilizes a fixed control volume based finite difference approach, was used to solve the coupled non-linear three-dimensional steady state energy and species equations, for a cylindrical coordinate system. The species equation utilizes a one-step or multiple-step Arrehenius reaction rate equation for the epoxy resin system. The kinetic parameters used for the resin to predict the temperature and degree of cure profiles were obtained from differential scanning calorimeter (DSC) scans.

The post-die curing is important since the composite temperature is quite high and curing continues for some time even after the composite exits the die. The processing conditions examined in this study were the die-wall temperature settings, pull speed and fiber volume fractions, along with axial heat conduction considered to be present. Numerical results for axial, radial and circumferential temperature and degree of cure profiles were compared and found to be in close agreement with experimental results.

ACKNOWLEDGEMENT

The authors gratefully acknowledge the National Science Foundation, Division of Design and Manufacturing Systems, grant DDM-9101643; and the Electric Power Research Institute, contract RP 8007 20, for their support and the opportunity to present this work.

THE EFFECTS OF PROCESSING PARAMETERS ON THE SHELL EPON 862/W EPOXY/FIBERGLASS SYSTEM

Jack A. McClurg and James G. Vaughan
Department of Mechanical Engineering
University of Mississippi
University, MS 38677

Abstract

The objective of this study was to determine the optimal pultrusion processing parameters and processability for the EPON 862/W epoxy/fiberglass system. The five processing parameters that were taken into consideration were the fiber volume, pull speed, die zone 1 temperature, die zone 2 temperature, and die zone 3 temperature. A five factor, half-factorial, central composite experimental design using 32 experiments was used to establish the parameter settings under which the composite material was to be produced. Upon completion of the production of the composite material, test specimens were prepared and tested for flexural strength, using both three-point and four-point loading methods, and short-beam shear strength. The flexural specimens were tested in three conditions, as-pultruded which involved no post-processing, post-cured which was cured for two hours at 350°F after production, and hot-wet which included submersion in water at 200°F for two weeks prior to testing. Once the testing was completed, regression analysis was performed on the data to determine the optimal processing parameters for the composite system. Response surface techniques were used to determine the maximum mechanical properties that can be expected for this system.

INTRODUCTION

Of the many methods in use today for the production of composite materials, one of the more cost-effective methods is pultrusion. Pultrusion consists of pulling continuous fiber reinforcement through a resin bath to coat the fibers with resin, through a set of preform plates to form the product geometry and strip excess resin, through a heated die to initiate the curing of the resin, and through a cut-off saw to achieve the desired length of the composite product. Pultrusion is widely used in the industry; however, the factors

involved with the optimization of the pultrusion process are complicated. The optimization of the pultrusion process has been addressed in many papers [1-4]. Vaughan et al. [5] stated that some of the most important pultrusion processing parameters to be considered for optimization of a thermosetting epoxy resin composite are the fiber volume, pull speed, and the die zone temperatures. Because of the numerous process variables and variable interactions involved, it is important that an experimental test plan be developed to aid in process optimization and in exploring the effects of the processing parameters on the mechanical properties of the pultruded composite material. An appropriate experimental design can provide the necessary information needed for the optimization and analysis using the fewest number of test runs and keeping the cost down.

The Shell EPON 862/W/537 resin system (EPON® Resin 862/EPI-CURE® W Curing Agent/EPI-CURE Curing Agent Accelerator 537) was used for this study. The EPON 862 resin system is intended for use in applications similar to those of the Shell EPON 828 and Shell EPON 826 resin systems. However, both the EPON 826 and 828 systems possess a relatively high resin viscosity [6, 7] with associated processing difficulties. The EPON 862 resin system was developed primarily as a low viscosity resin system alternative to the currently used 828 and 826 systems.

EXPERIMENTAL PROCEDURE

The current study involves the optimization of a pultruded unidirectional epoxy/fiberglass composite material. Shell EPON 862/W/537 was used as the matrix material and was mixed according to the formulation recommended by the manufacturer [8]. PPG Hybon 2001 E-glass was used as the reinforcement. The pultrusion experiments were conducted in the University of Mississippi Composite Materials Laboratory using a Pultrusion Technology Pulstar 804 pultruder. Pultrusion process data was recorded every five seconds using a PC-based data acquisition unit. This data consisted of the static die wall temperatures, pull speed, pull load, clamp pressure, and system pressure. Occasionally thermocouples were passed through the die to acquire the temperature profile of the composite material as it was being pulled through the die.

For these profiles, one thermocouple was placed at the surface and a second in the center of the composite material. A plot of a typical thermocouple profile can be seen in Figure 1.

For the optimization experiments, a statistical experimental design was implemented. A central composite design (CCD) was used to determine the appropriate number of runs and parameter settings that were needed to acquire the necessary data. It was determined that a five factor, half-factorial design was appropriate for this experiment and that a total of 32 experiments (runs) were required to gather the data

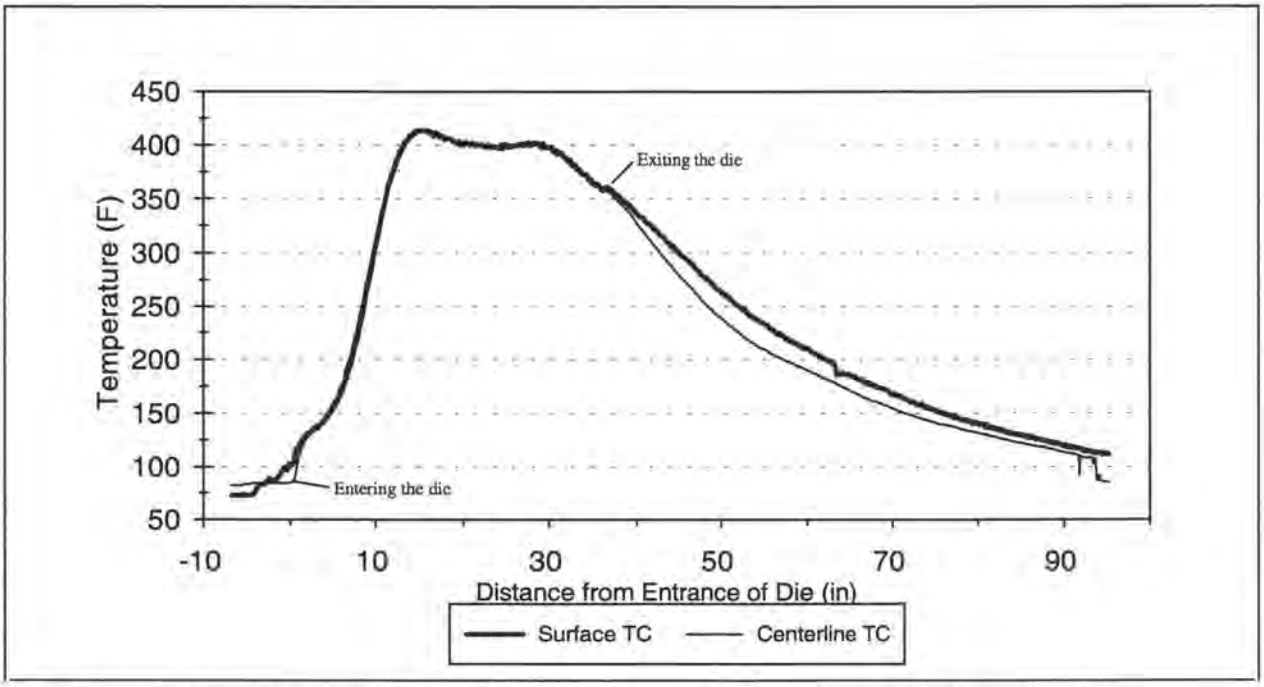

Figure 1 Temperature profile vs. Die wall Position using surface and centerline thermocouples.

needed. This design was used to establish the relationship between the dependent variables such as flexural strength, flexural modulus, short-beam shear strength and the independent variables of fiber volume, pull speed, and three die zone temperatures. Regression analysis was then used to evaluate the influences of the independent variables on the dependent variable.

In order to evaluate the interactions between the independent variables, a second-order statistical model was used. A second order model takes into account linear terms, squared terms, and interaction terms. The linear terms are simply the process variables themselves. The squared terms are the square of the linear terms and provide for non-linear effects. The interaction terms are the products of each of the combinations of process variables, e.g. the interaction that might occur when the pull speed is increased but the die

temperature is also raised to account for the shorter time at temperature. Response surface methodology was also utilized to explore the influences of the process parameters and their squared and interaction terms on the measured mechanical properties. This procedure can help determine which parameter settings should be used to produce the composite material with the best possible mechanical properties.

Coded variables for the process parameters were used in the CCD test matrix to eliminate units of measurement from the equations. The coded variables are usually represented in terms of α, 1, 0, -1, and $-\alpha$, where the numeric value for α is used to establish the ratability of the design; for these tests α=2. By utilizing the ratability of the CCD, the response can be predicted with equal variance regardless of the direction from the center of the design space [9]. The half-factorial central composite design used for this study along with the coded variables are given in Table 1. The parameters specified in the central composite design were used to produce the composite material for the 32 individual runs.

The material produced had a uniform cross-sectional area of 1/8 inch by 1 inch. Upon completion of the production process of the composite material, sample specimens were prepared for mechanical testing. Mechanical testing procedures consisted of three-point and four-point bending and short-beam shear testing. Both the three-point and four-point methods were used to test specimens that were subjected to three different processing conditions - as-pultruded, post-cured, and hot-wet. The short-beam shear test was only used for the as-pultruded specimens. The as-pultruded condition involved no post-processing after pultrusion, the post-cured product was cured for two hours at 350°F after production, and the hot-wet samples were submerged in water at 200°F for two weeks prior to testing and were tested while still hot and wet.

Three-point flex tests were conducted according to ASTM D 790 [10] using a 16:1 span-to-depth ratio.

Table 1. Testplan for experiments.

Randomized Test Plan Number	*Test Plan Number*	*Test Variables*				
		X1	*X2*	*X3*	*X4*	*X5*
16	1	-1	-1	-1	-1	1
1	2	1	-1	-1	-1	-1
11	3	-1	1	-1	-1	-1
17	4	1	1	-1	-1	1
5	5	-1	-1	1	-1	-1
10	6	1	-1	1	-1	1
12	7	-1	1	1	-1	1
18	8	1	1	1	-1	-1
8	9	-1	-1	-1	1	-1
2	10	1	1	-1	1	1
7	11	-1	1	-1	1	1
9	12	1	1		1	-1
6	13	-1	-1	1	1	1
14	14	1	-1	1	1	-1
15	15	-1	1	1	1	-1
13	16	1	1	1	1	1
3	17	0	0	0	0	0
4	18	0	0	0	0	0
19	19	0	0	0	0	0
22	20	0	0	0	0	0
20	21	0	0	0	0	0
30	22	0	0	0	0	0
24	23	-2	0	0	0	0
27	24	0	-2	0	0	0
23	25	0	0	-2	0	0
31	26	0	0	0	-2	0
29	27	0	0	0	0	-2
21	28	2	0	0	0	0
26	29	0	2	0	0	0
28	30	0	0	2	0	0
25	31	0	0	0	2	0
32	32	0	0	0	0	2

	-2	-1	0	1	2
X1: Glass ends	30	31	32	33	34
Fiber vol. (%)	63.9	66	68.2	70.3	72.4
X2: Pull speed (in/min)	8	10	12	14	16
X3: Zone 1 temp (F)	360	370	380	390	400
X4: Zone 2 temp (F)	380	390	400	410	420
X5: Zone 3 temp (F)	380	390	400	410	420

The test specimen dimensions were 3 inches long by 1 inch wide by 1/8 inch thick. The support span was 2

inches and the crosshead motion was set at 0.05 in/min. The three-point loading configuration can be seen in Figure 2. The flexural strength, peak load, modulus of elasticity, and the manner in which the specimen broke were all recorded. The flexural strength was calculated using

$$S = 3PL / 2bd^2 \quad (1)$$

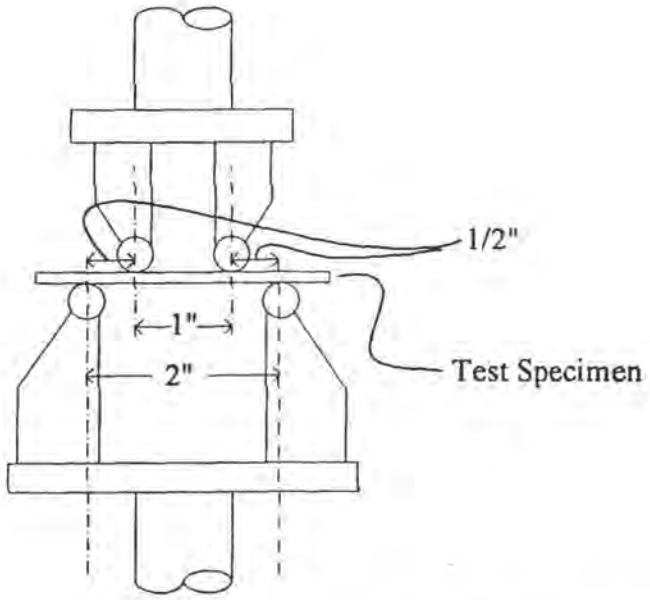

Specimen Length = 3" Specimen Thickness = 1/8" Specimen Width = 1"

Figure 2. Four-point bending diagram.

where S is the stress in the outer fiber throughout the load span, P is the load at a given point on the load deflection curve, L is the support span, b is the width of the tested beam, and d is the depth of the tested beam. The modulus of elasticity was calculated for the three-point method using

$$E_B = L^3m / 4bd^3 \quad (2)$$

where E_B is the modulus of elasticity in bending, m is the slope of the tangent to the initial straight-line

portion of the load-deflection curve, b is the width of the tested specimen, d is the depth of the tested beam, and L is the support span.

Four-point bending methods were also utilized in this study. These were conducted in accordance to the ASTM D 790 specifications [10] using a 16:1 span-to-depth with loading at 1/4 points. The specimen dimensions for the four-point procedures are the same as those used for the three-point loading. The support span for this test was set at 2 inches. However, instead of point loading such as the three-point method, the four-point method consisted of a load span of 1 inch. The crosshead motion was 0.05 in/min. The test set-up for four-point bending can be seen in Figure 3. The flexural strength for the four-point bending procedure was calculated from

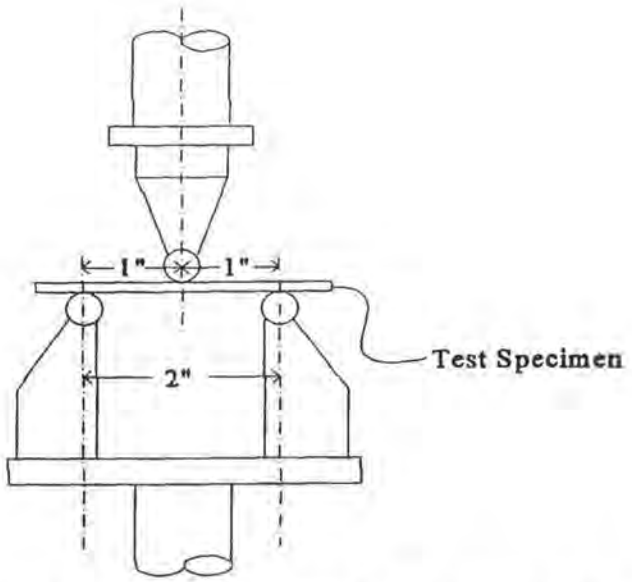

Specimen Length = 3" Specimen Thickness = 1/8" Specimen Width = 1'

Figure 3. Three-point bending diagram.

$$S = 3PL / 4bd^2 \tag{3}$$

where all parameters are the same as those in three-point loading. A displacement gage mounted to the testing apparatus was used to determine specimen deflection to calculate the tangent modulus of elasticity. The modulus was calculated using

$$E_B = 0.17L^3m / bd^3 \tag{4}$$

where E_B is the modulus of elasticity in bending, m is the slope of the tangent to the initial straight-line portion of the load-deflection curve, b is the width of the tested specimen, d is the depth of the tested beam, and L is the support span.

Interlaminar short-beam shear tests were conducted according to ASTM D 2344 [11]. The test configuration for this procedure looks very similar to a small three-point test set-up. As specified in the standards for glass reinforced composites, the specimen dimensions were 0.875 inches in length by 0.25 inches in width by 0.125 inches in depth. A span of 0.625 inches was specified as well as a crosshead rate of 0.05 in/min. A schematic of the testing apparatus may be seen in Figure 4. The interlaminar short-beam shear strength was calculated using

$$S_H = 0.75P_B / bd \tag{5}$$

where S_H is the shear strength, P_B is the breaking load, b is the width of the tested specimen, and d is the depth of the tested specimen.

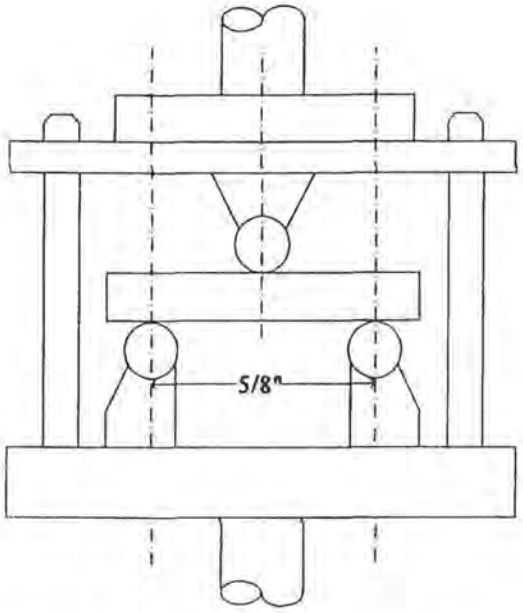

Specimen Length = 7/8" Specimen Thickness = 1/8" Specimen Width = 1/4"

Figure 4. Short-beam shear configuration.

In addition to the above ASTM tests, a non-standard short-beam shear test was performed. This test was simply a repeat of the short-beam shear test; however, the fiber orientation of the test specimen was changed. In the short-beam shear test, the fiber orientation runs parallel to the major orientational axis of the test specimen. For this non-standard test (called here the transverse short-beam shear test) the fibers were oriented transverse to the major axis of the test specimen. This was done with hopes of being able to correlate the degree of cure to the strength of the resin instead of the resin and fiber composite. A diagram of the fiber orientations for these tests can be seen in Figure 5.

Regression analysis was carried out on the measured mechanical property data. The regression analysis was used in conjunction with response surface techniques to determine the effects of the pultrusion processing parameters on the mechanical properties of the pultruded product and to determine the optimal processing parameters for the EPON 862 resin system.

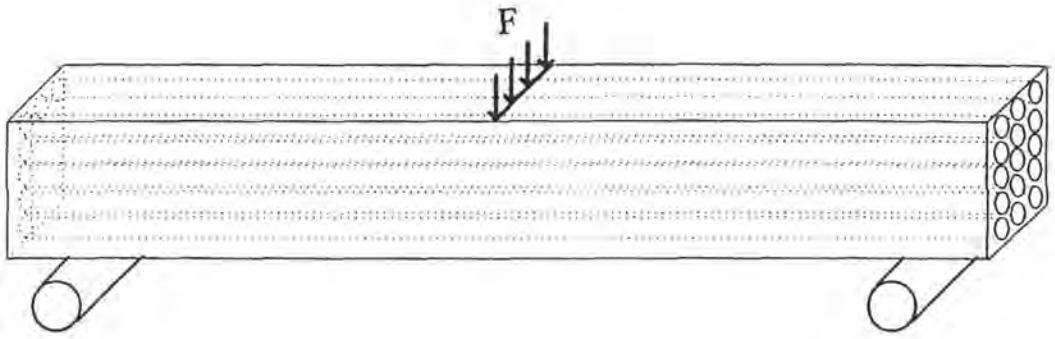

Typical short-beam shear specimen with fibers oriented along major axis.

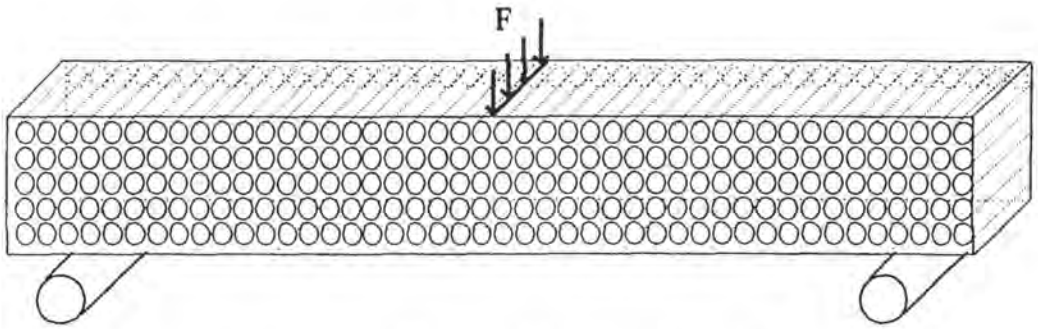

Short-beam shear specimen with fibers oriented transverse to the main axis.

Figure 5. Fiber orientation of short-beam shear specimens.

RESULTS

The measured flexural strength was very dependent upon the test method used. As seen in Figures 6, 7, and 8, there was a significant difference in the flexural strength of the composite material depending on the test method. Part of the difference in the strengths may be attributed to the method of loading the test samples; however, it is unclear if all of the differences can be attributed to the difference in loading technique.

Figures 9 and 10 indicate the effects of the post-processing on the composite material. As can be seen for both the three-point and four-point bending data, post-curing increases the flexural strength. However, the increase in flexural strength due to post-curing is fairly insignificant. These figures

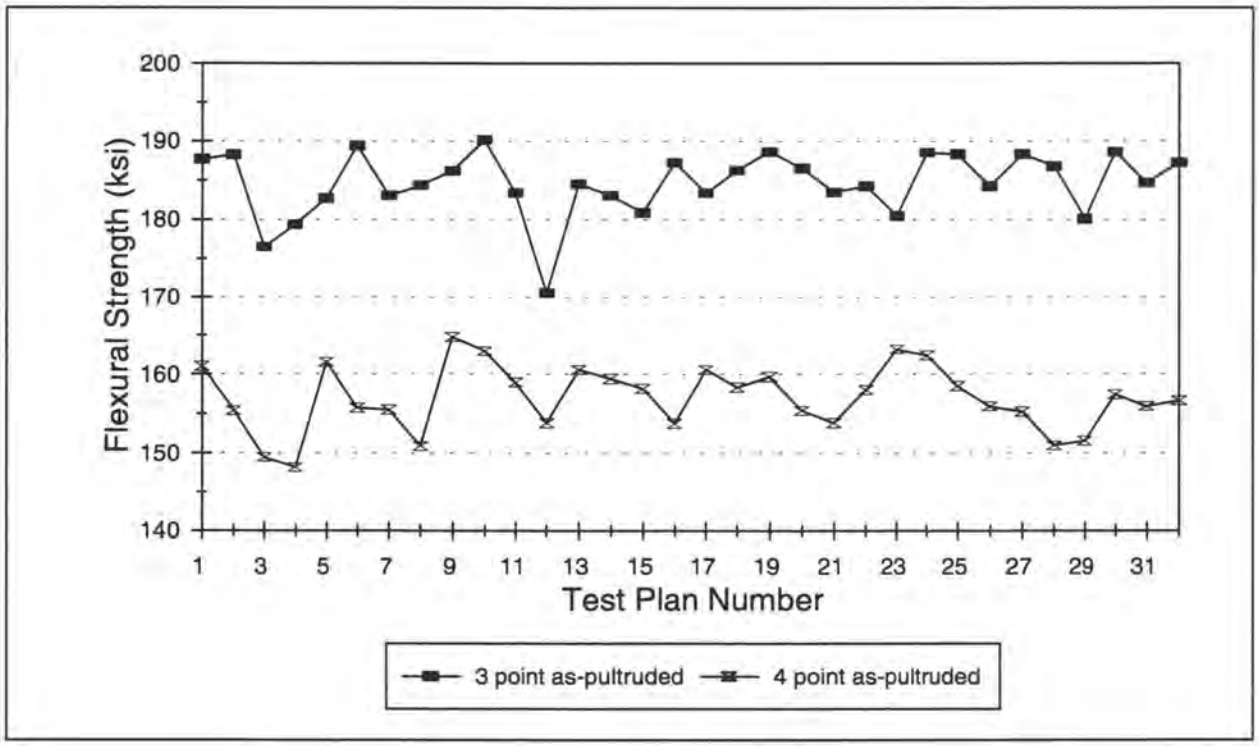

Figure 6. Three point vs. four point as-pultruded flexural strengths.

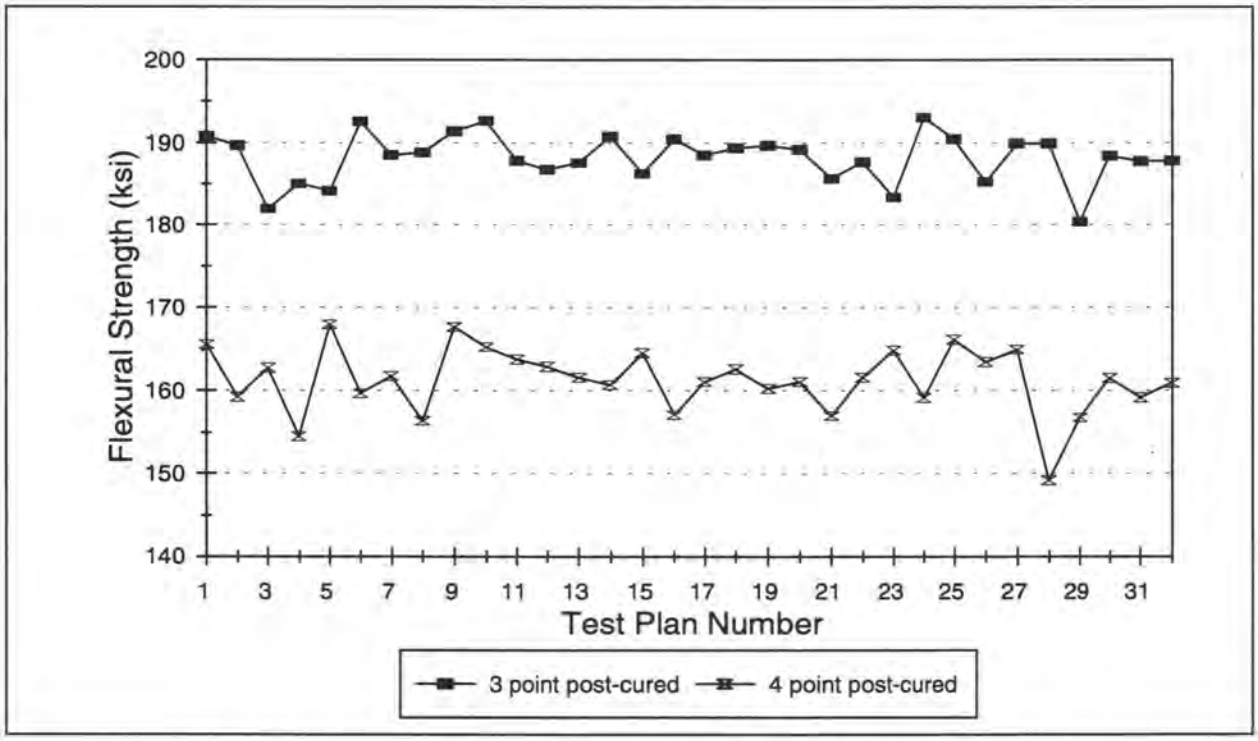

Figure 7. Three point vs. four point as-post-cured flexural strengths.

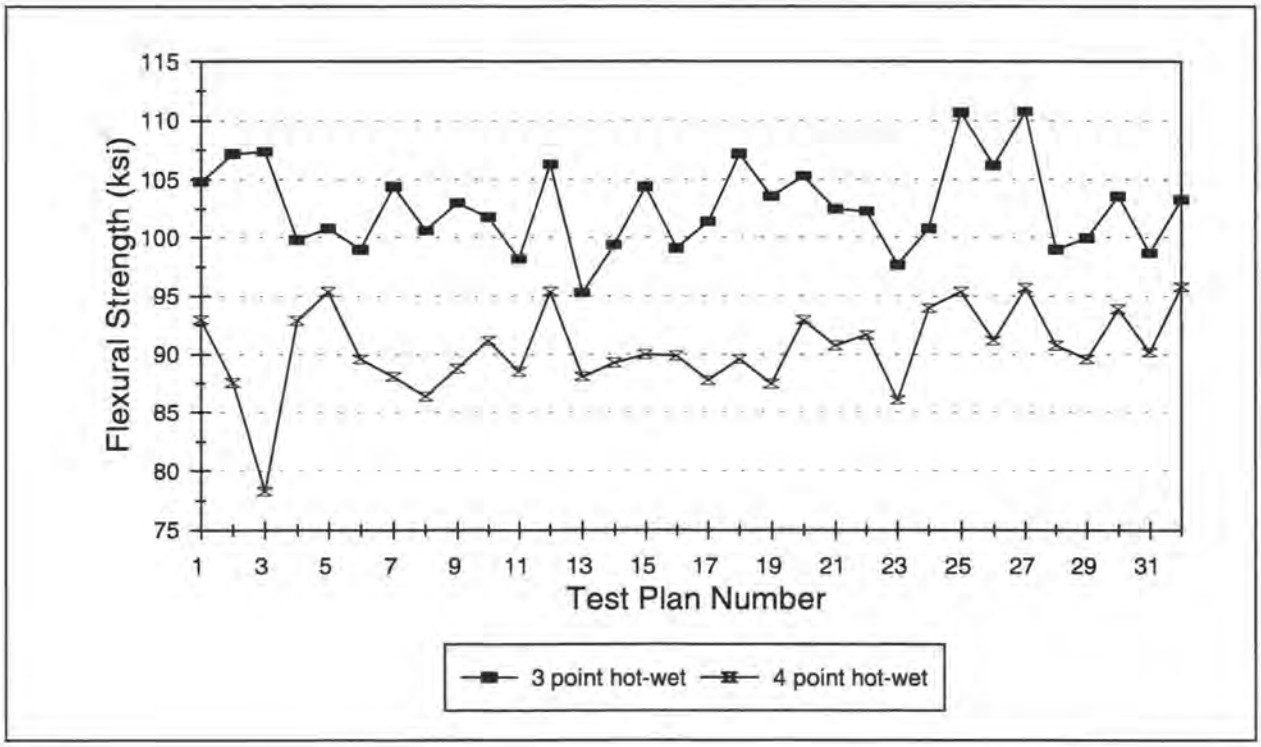

Figure 8. Three point vs. four point hot-wet flexural strengths.

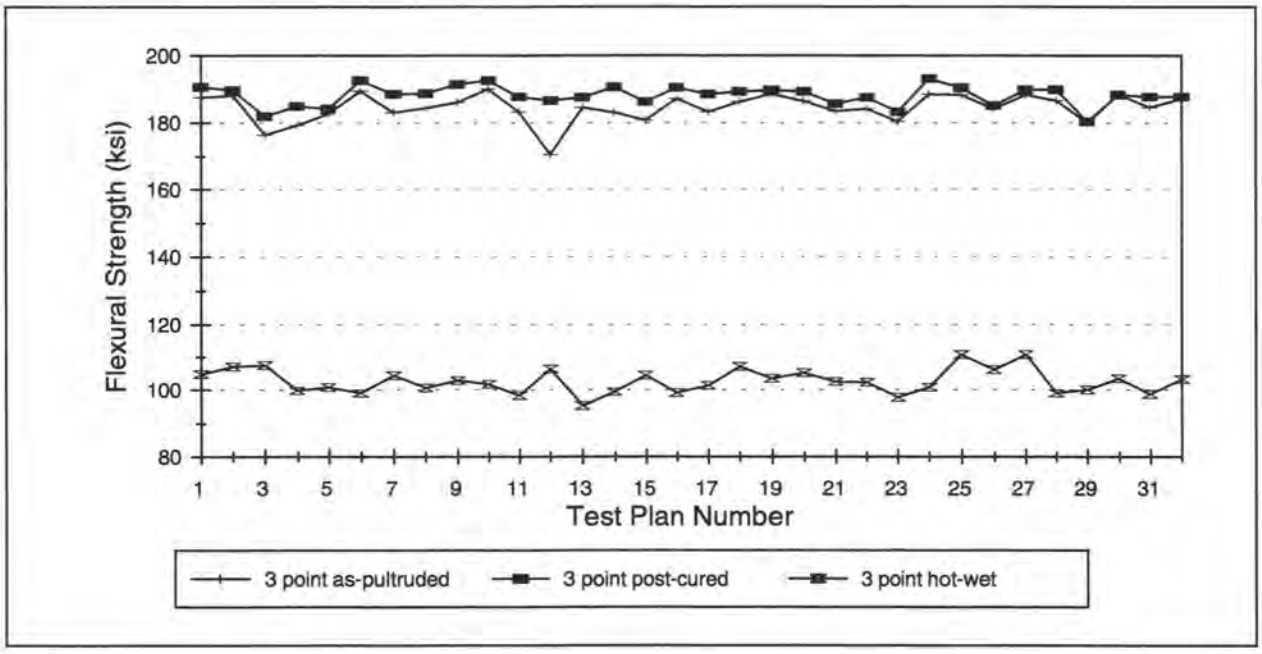

Figure 9. Three-point flexural strength data for the as-pultruded, post-cured, and hot-wet conditions.

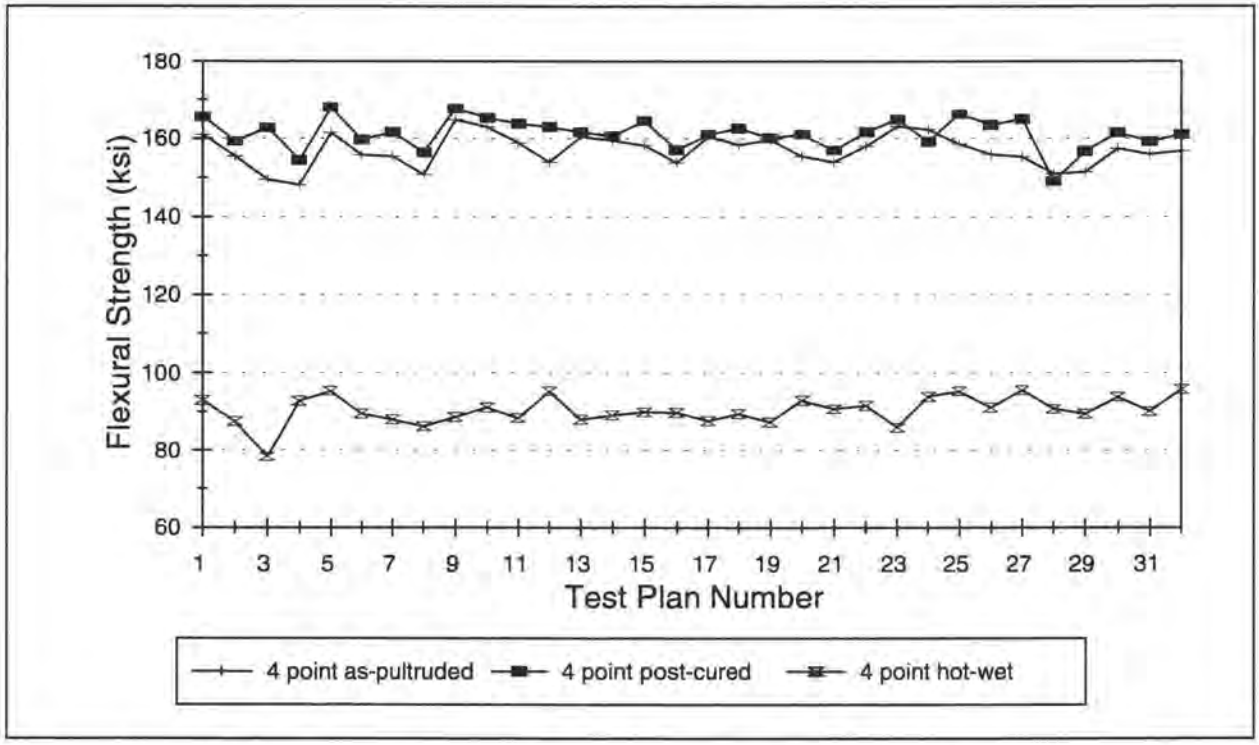

Figure 10. Four-point flexural strength data for the as-pultruded, post-cured, and hot-wet conditions.

also indicate that significant decrease in the flexural strength (approximately 45%) occurs due to the hot-wet post-processing that was performed on the samples. This decrease is typical of glass reinforced composites. The data indicate that the as-pultruded EPON 862/fiberglass composite material requires little post-processing to achieve near maximum mechanical properties; however, one must be careful about the environment in which the composite will be used since serious degradation of mechanical properties can occur in certain conditions such as the hot-wet condition.

The data that was acquired through the mechanical testing procedures was used to create statistical models that could be used to predict the mechanical properties of the composite using the input process variables. The models were used to estimate the linear, interaction, and quadratic effects of the input variables of pull speed, fiber volume, and three die zone temperatures on the dependent variables of flexural strength, short-beam shear strength, and modulus. Models for the flexural strength and modulus were developed from the mechanical testing data for both the three-point bending and four-point bending methods in the as-pultruded, post-cured, and hot-wet conditions. Two models were also developed for the short-beam

shear data. The first model was used to predict the interlaminar shear strength of the composite material according to the standard ASTM 2344 test method. The second model was constructed from the transverse short-beam shear data where the fiber orientation of the composite provided no strengthening.

Initially a full set model was developed in which all the regression coefficients were used. From this full set model, the regression coefficients were analyzed and reduced set models were developed which included only the most significant regression coefficients. The relative contributions of the regression coefficients, within a 95 percent t-test confidence level, were examined to formulate the reduced set models for each data set.

The reduced set model, in coded form, that describes the three-point flexural strength for the pultruded composite material in the as-pultruded condition is

$$Y = 184.638 + 1.145*X13 - 2.653*X2 + 2.393*X23 + 1.06*X45 + 1.28*X5 \quad (6)$$

where the factors and levels correspond to those given in Table 1. The adjusted R^2, which indicates how much of the variance in the actual data can be explained by the mathematical model, for the full set model was 0.545 or around 54.5% of the variance. By utilizing the reduced set model, the adjusted R^2 was equal to 0.435. A comparison of the regression model predictions and experimental data can be seen in Figure 11. In Figure 11, the scatter in the experimental test data is represented by the high-low vertical bar. The average of the measured test data is indicated by the small tic-mark on the high-low bar. The flexural strength predicted by the numerical model (equation 6) is shown as the dark solid line. Using the reduced set model, the process parameters predicted to produce the highest three-point flexural strength were determined to be a fiber volume of 70.3% (33 ends), a pull speed of 8 in/min, a first die zone temperature of 360° F a second die

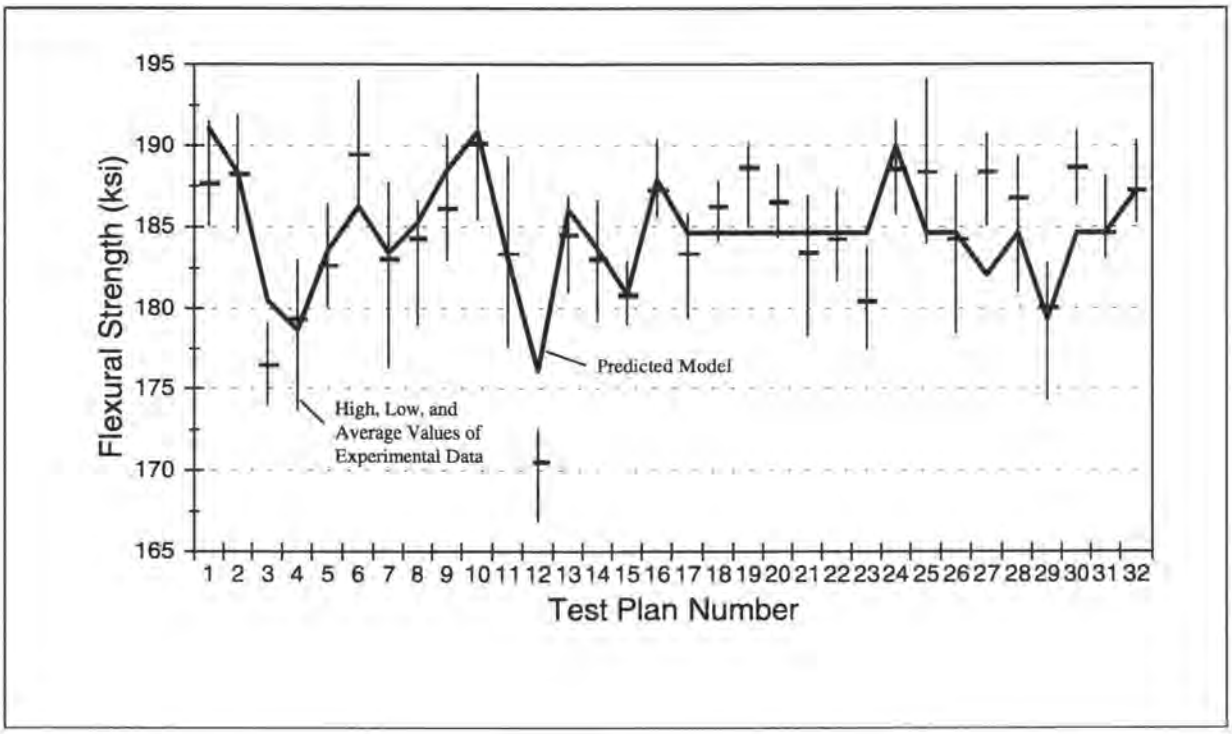

Figure 11. Three point flexural strength and model prediction for the as-pultruded condition.

zone temperature of 420°F, and a third die zone temperature of 420°F. The most influential processing parameters for the three-point as-pultruded flexural strength are the pull speed (X2), the die zone 3 temperature (X5), and the interaction between the pull speed and the die zone 1 temperature (X23).

A reduced set model for the determination of the four-point post-cured flexural modulus for the composite material is

$$Y = 9.450 + 0.069*X1 - 0.165*X2 + 0.088*X24 + 0.093*X33 - 0.120*X34 + 0.086*X45 \quad (7)$$

where the factors and levels correspond to those given in Table 1. The adjusted R^2 for the reduced set model is 0.590. The optimal processing parameters for this model were determined to be a fiber volume of 72.4% (34 ends), a pull speed of 8 in/min, a first die zone temperature at 400°F, a second die zone temperature of 380°F, and a third die zone temperature of 380°F. Equation 7 indicates that the linear term of pull speed (X2) once again has a fairly high negative influence on the reduced set model. The interaction between the first

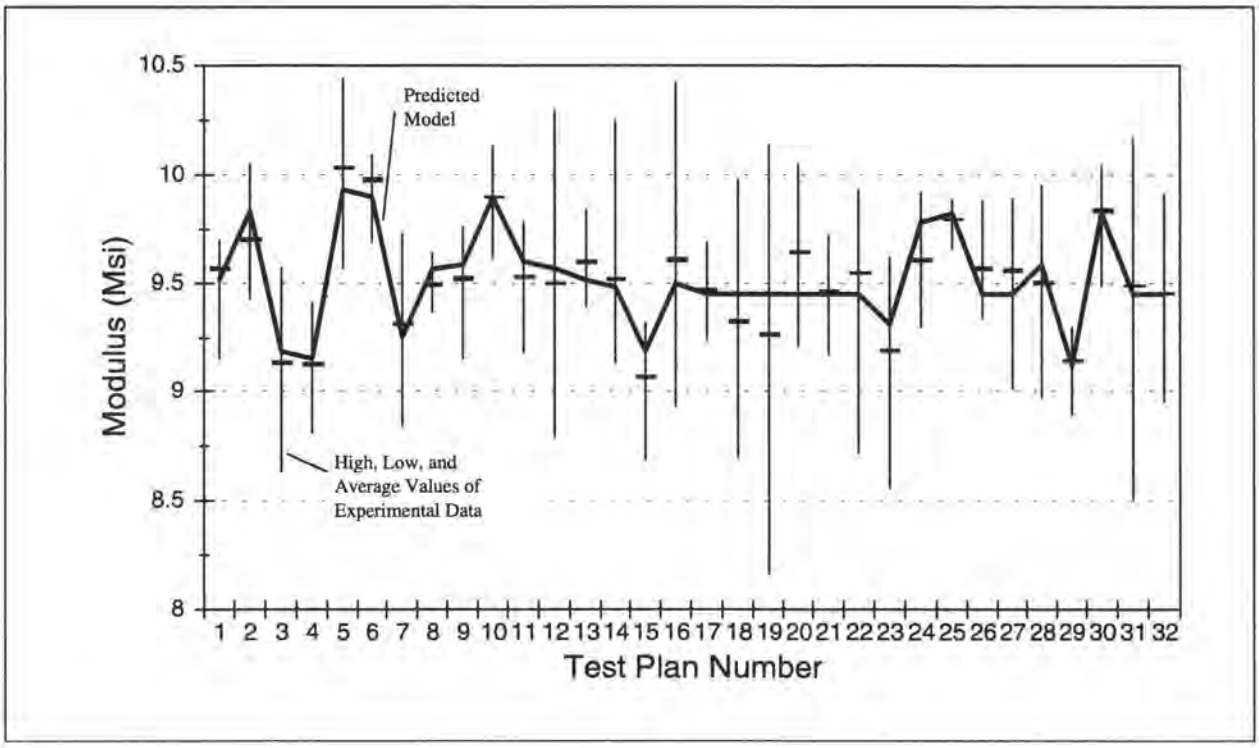

Figure 12. Four point modulus and model prediction for the post-cured condition.

and second die zone temperatures (X34) was also shown to have a fairly significant negative effect in the reduced set model. Figure 12 compares the prediction of the reduced set model with the measured experimental data.

The reduced set model equation for the short-beam interlaminar shear strength is

$$Y = 10.201 - 0.063*X14 - 0.070*X15 - 0.140*X2 + 0.065*X23 + 0.093*X4 + 0.032*X45 + 0.072*X5 \quad (8)$$

where the factors and levels again correspond to those given in Table 1. The adjusted R^2 for the reduced set model is 0.625. The optimal processing parameters for this model were determined to be a fiber volume of 63.9% (30 ends), a pull speed of 8 in/min, the first die zone temperature set at 360°F, the second die zone temperature set at 420°F, and the third die zone temperature set at 420°F. The most influential factors in the reduced set model are the pull speed (X2) and the second die zone temperature (X4). A plot of the regression

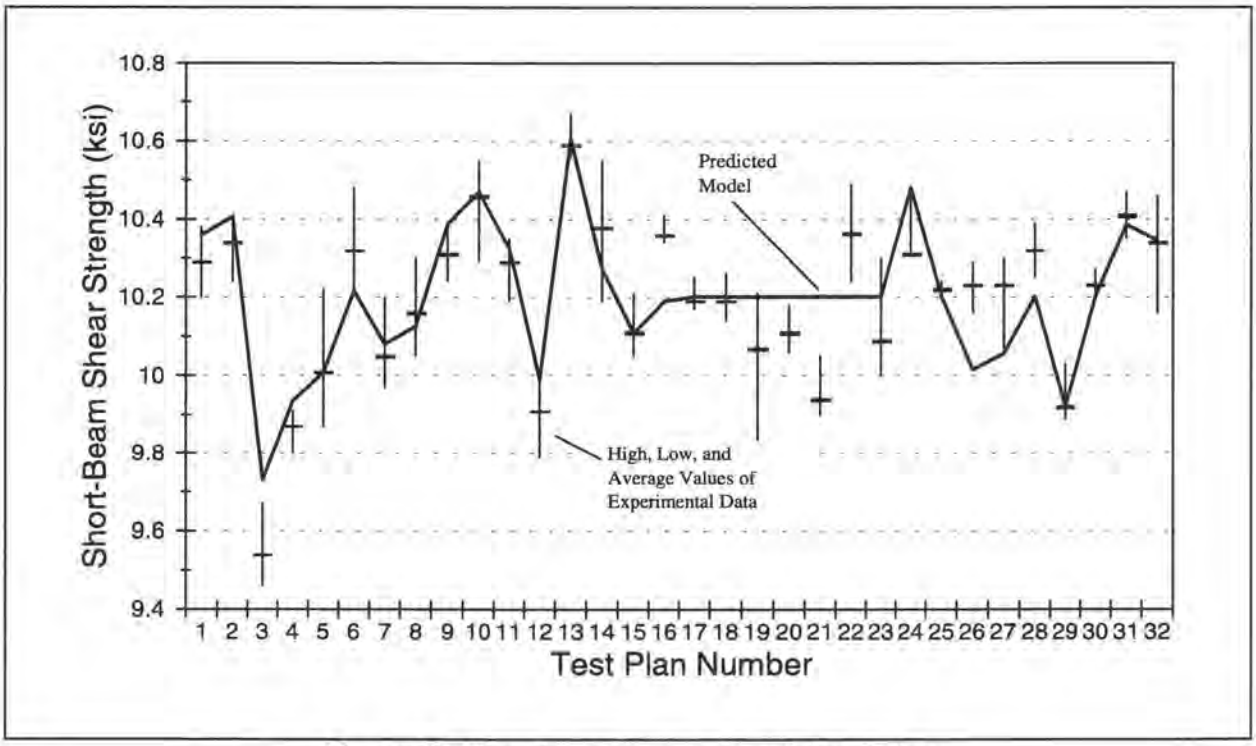

Figure 13. Short-beam shear and model prediction.

model and the measured experimental data can be seen in Figure 13.

Similar analysis procedures were used to develop reduced set pultrusion process models for the remaining mechanical property measurements. In all, six models describing the flexural strength, six models for the flexural modulus, and two models for the short-beam shear properties (the short-beam shear and the transverse short-beam shear) were determined. These reduced set models were used to view the influence of the process variables and variable interactions on the measured mechanical properties as well as to determine the maximum value of the mechanical properties that can be expected for the EPON 862/glass pultruded composite material. The optimal process parameters for the design space (all process variables ranging from -2 to +2 in coded terms) as well as for the simple experimental space (only those process conditions listed in Table 1) can be seen in Table 2. The model information presented in Table 2 can be understood using similar arguments as those used for models presented in equations 6, 7, and 8.

The reduced set models given in equations 6, 7, and 8 demonstrate that numerous pultrusion process variables and variable interactions affect the properties of the composite. It is also evident that the most

Table 2. Optimal parameters for the design space for the experimental test design.

Optimal parameters for all possible combinations within the design space

	X1	X2	X3	X4	X5	Predicted Value	Units
3 point as-pultruded flex	-2	-2	-2	2	2	211	ksi
3 point post-cured flex	-2	-2	-2	2	-2	211	ksi
3 point hot-wet flex	0.63	-0.69	-2	0.33	-2	120	ksi
4 point as-pultruded flex	-2	-2	-2	2	1.79	178	ksi
4 point post-cured flex	-2	-2	-2	-2	-2	179	ksi
4 point hot-wet flex	-0.24	-2	-2	-2	2	109	ksi
3 point as-pultruded modulus	2	-2	0.18	-2	0.51	8.1	Msi
3 point post-cured modulus	2	-2	2	0.48	0.19	8	Msi
3 point hot-wet modulus	2	0	2	2	0.96	9	Msi
4 point as-pultruded modulus	2	-2	-2	2	0.58	10.3	Msi
4 point post-cured modulus	2	-2	2	-2	-2	11.5	Msi
4 point hot-wet modulus	2	-2	2	-0.62	-0.68	8.6	Msi
short-beam shear	-2	-2	-2	2	2	11.7	ksi
transverse short-beam shear	2	-1.26	2	-2	0	1.8	ksi

Optimal parameters within the 32 experiment test plan

	X1	X2	X3	X4	X5	Predicted Value	Units
3 point as-pultruded flex	-1	-1	-1	-1	1	191	ksi
3 point post-cured flex	1	-1	-1	1	1	194	ksi
3 point hot-wet flex	0	0	0	0	-2	110	ksi
4 point as-pultruded flex	-1	-1	-1	1	-1	165	ksi
4 point post-cured flex	-1	-1	1	1	-1	169	ksi
4 point hot-wet flex	-1	-1	-1	-1	1	96	ksi
3 point as-pultruded modulus	1	-1	1	-1	1	7.6	Msi
3 point post-cured modulus	1	-1	1	-1	1	7.6	Msi
3 point hot-wet modulus	1	1	1	1	1	8.3	Msi
4 point as-pultruded modulus	1	-1	-1	1	1	9.9	Msi
4 point post-cured modulus	-1	-1	1	-1	-1	9.9	Msi
4 point hot-wet modulus	-1	-1	-1	-1	1	8.2	Msi
short-beam shear	-1	-1	1	1	1	10.6	ksi
transverse short-beam shear	0	0	2	0	0	1.7	ksi

significant combinations of variables and variable interactions vary for each mechanical property considered and that optimal processing conditions will vary for each mechanical property. However, a comparison of the models does reveal some similarities. For example, the positive regression coefficients of interactions involving pull speed and die zone temperature show that an increase in pull speed should be offset by an increase in the die zone temperature to achieve proper curing of the resin and better mechanical properties. It is important to note that a pultrusion process variable may be part of a number of model terms, and that the effect of all of these terms must be considered to determine the effect a particular process parameter level will have on the overall mechanical property response. For example, in the three-point flexural strength model (Equation 6), the linear term of pull speed (X2) has a negative coefficient but the interaction term of pull speed and die zone 1 temperature (X23) has a positive coefficient. To fully understand the effect a change in pull speed will have on the three-point flexural strength, both of these model terms must be examined.

CONCLUSIONS

Statistical analysis has been used to develop process models describing the effects of pultrusion process variables on the mechanical properties of EPON 862/W fiberglass composites. The data indicate that the optimal processing parameters depend directly upon the desired mechanical property and that different mechanical properties require different optimal process settings. The mechanical property data indicate that the EPON 862/W resin system requires no further post processing to achieve near maximum flexural strength when processed under appropriate conditions as specified by the statistical experimental model presented here.

ACKNOWLEDGEMENTS

The authors gratefully acknowledge the National Science Foundation, Division of Design and Manufacturing Systems, grant DDM-9101643; the Electric Power Research Institute, contract RP 8007 20; and the Shell Development Company for their support.

REFERENCES

1. Sumerak, J. E. and Martin, J. D., "Pultrusion Process Variables and Their Effect Upon Manufacturing Capability," 39th Annual Conference, Reinforced Plastics/Composites Institute, The Society of the Plastics Industry, Inc., January, 1984, pp 1B:1-7.

2. Sumerak, J. E., "Understanding Pultrusion Process Variables for the First Time," 40th Annual Conference, Reinforced Plastics/Composites Institute, The Society of the Plastics Industry, Inc. January 28 - February 1, 1985, pp 2B:1-8.

3. Sumerak, J. E. and Taymourian, K., "A Case Study of Pultrusion Speed Optimization of a Non-Uniform Wall Thickness Profile Using Process Exotherm Measurements," 46th Annual Conference, Composites Institute, The Society of the Plastics Industry, February 18-21, 1991, pp 13C:1-6.

4. Smith, C. and Taylor, J., "An Introduction to Taguchi Techniques Applied to Pultrusion Resins and Processing," 47th Annual Conference, Composites Institute, The Society of the Plastics Industry, February 3-6, 1992, pp 2D:1-5.

5. Vaughan, James G., Ravi Gorthala, and Jeffrey A. Roux. "Characterization and Optimization of the Pultrusion Process for Structural Shapes," *Advanced Composite Materials in Civil Engineering Structures*, 1991, pp. 12-23.

6. "EPON Resin 826," Shell Chemical Company SC:235-82.826, Jan 1992.

7. "EPON Resin 828," Shell Chemical Company SC:235-91.828, Jan 1992.

8. "EPON Resin 862/EPI-CURE W Curing Agent," Shell Chemical Company SC:1183-94. Feb 1994.

9. Schmidt, Steven R. and Robert G. Launsby. *Understanding Industrial Designed Experiments*, 3rd edition, Air Academy Press, Colorado Springs, Colorado, 1991, pp. 3.1-3.31.

10. "Standard Test Methods for Flexural Properties of Unreinforced and Reinforced Plastics and Electrical Insulating Materials D 790 - 86," *ASTM Standards.*

11. "Standard Test Method for Interlaminar Shear Strength of Parallel Fiber Composites by Short-Beam Method D 2344 - 84," *ASTM Standards.*

TEMPERATURE AND CURE IN PULTRUDED COMPOSITES USING MULTI-STEP REACTION MODEL FOR RESIN

Meyyappan Valliappan, Jeffrey A. Roux*, James G. Vaughan
Department of Mechanical Engineering
University of Mississippi
University, MS 38677, U.S.A

ABSTRACT

A numerical model has been developed to analyze the temperature and degree of cure profiles in pultruded composites. In pultruded composites the resin plays an important role in holding the fibers together in a structural unit and also transferring and distributing the applied load to the fibers. The degree of cure of the pultruded composite is an important phenomenon in the manufacturing process since it can be related to the mechanical properties. Therefore, the degree of cure of the resin plays a crucial role in the pultrusion process. The chemical reaction of the resin determines the degree of cure as well as the exothermic energy released by the resin. A one-step reaction model has been employed for the resin system in most of the previous research. For some resin systems, a one-step model may not produce good results; therefore, it was decided to pursue a multiple-independent-step reaction model that more closely follows the actual behavior of the resin. In this research, the effect of an approximate multiple-independent-step reaction model for the thermoset epoxy resin SHELL EPON 862/W was studied. The numerical model utilized a fixed control volume based finite difference approach [1]. This technique was used to solve the coupled, non-linear, three-dimensional steady-state energy and species equations for a cylindrical geometry. The species equation(s) utilized both a one-step Arrhenius reaction rate model as well as a multiple-independent-step Arrhenius reaction rate model for the resin. The kinetics parameters of the resin for a one-step reaction model were obtained from the differential scanning calorimeter (DSC) scans and for the multi-step model a regression fit was made to obtain the kinetic parameters from the DSC scans. The numerical model was used to predict the

*Author to whom the correspondence should be addressed

temperature and degree of cure for the pultruded composite both inside the die and in the post-die region. These numerical results were compared with experimental measurements. The processing variables examined in this study were die-wall temperature settings, pull speed and fiber volume fraction.

NOMENCLATURE

c ..... Bulk specific heat, J/kg-K

c_f ..... Fiber specific heat, J/kg-K

c_r ..... Resin specific heat, J/kg-K

C_I ..... Initial concentration of uncured resin, kg/m^3

C_A ..... Local concentration of uncured resin, kg/m^3

E_A ..... Activation energy, kJ/mol

ϵ ..... Emissivity

F ..... Radiation view factor

h ..... Convective heat transfer coefficient, W/m^2-K

k ..... Bulk thermal conductivity, W/m-K

k_f ..... Fiber thermalconductivity, W/m-K

k_r ..... Resin thermal conductivity, W/m-K

K_o ..... Pre-exponential constant, 1/s

L ..... Length of the pultrusion die, m

L_1 ..... Length of the calculation domain, m

n ..... Order of chemical reaction

q_{r1} ..... Radioactive heat transfer between the rear face of the pultruder and composite

q_{r2} ..... Radioactive heat loss from the composite to the environment

r_o ..... Radius of the composite stock, m

R ..... Universal gas constant, kJ/mol-K

R_A ..... Arrhenius reaction rate, 1/s

S ..... Heat source per unit volume, W/m^3

T ..... Temperature, K

T_B ..... Resin bath temperature, K

T_b ..... Temperature of the rear face of the pultruder heating section, K

T_w ..... Wall temperature, K

T_∞ ..... Ambient air temperature, K

u_z ..... Velocity in the axial direction, m/s

U ..... Pull speed, m/s

V_f ..... Fiber volume fraction

m_f ..... Fiber mass fraction

V_r ..... Resin volume fraction, (1-V_f)

m_r ..... Resin mass fraction

ρ ..... Bulk density, kg/m^3

ρ_f ..... Fiber density, kg/m^3

ρ_r ..... Resin density,kg/m^3

ΔH ..... Heat of reaction of the resin, kJ/kg

ψ ..... Degree of cure

σ ..... Stefan-Boltzmann's constant

INTRODUCTION

Composites are frequently used in many areas due to their various advantages. Composite materials have a high strength to weight ratio, excellent corrosion resistance, high damping characteristics and high fatigue strength [2]. These excellent mechanical properties translate into advantages for the composites and hence can be employed in many applications. These applications ranges from automotive, aerospace, marine, architectural structures to consumer products such as tennis rackets. In addition to its superior properties, it is relatively easy to fabricate them. There are several available techniques to manufacture composite materials. Among them, pultrusion is one of the most cost-effective methods for mass production of composite materials for a constant cross section. A wide variety of constant cross sections with desired lengths can be easily manufactured using this process.

Pultrusion is the process of pulling resin impregnated continuous fibers or mat through a pre-heated die to form a continuous composite of desired length. Cross-sectional shape of the die cavity determines the shape of the composite. The fibrous strands from spools are passed through a resin bath which wets the fibers thoroughly and uniformly. The fiber-resin mass is then passed through a set of preform plates whose function is to contour the fiber-resin mass to the approximate desired shape which is then passed through the pre-heated die. Inside the die, the heat from die-wall initiates the curing of the resin. The resin undergoes an exothermic chemical reaction as it cures. There are many variables which control the degree of cure of a pultruded composite. One important variable among them is the die-wall temperature profile and overall temperature level. The other key variables which are studied in this model include the fiber volume and the pull speed.

For a given set of processing parameters, the degree of cure of the resin (which is also called the degree of cure of the composite) depends on the chemical kinetic parameters of the resin. This indicates that the kinetic parameters must be used properly so that the numerical model can accurately predict the actual behavior of the resin. The resin used here is a thermoset epoxy Shell EPON 862/W resin system. The resin was tested in the DSC (TA Model 2910) and the energy release rate versus time curves were obtained. A

representative DSC scan is shown in Fig. 1 and shows that there is more than one lobe in the chemical reaction. The multiple lobes imply that a one-step Arrhenius reaction rate model for the resin may not reproduce the real characteristics of the exothermic reaction of the resin in the heat transfer model. This suggests that a multiple-independent-step chemistry model could improve the modeling of the exothermic reaction of the resin. Based on this reasoning, a multiple-independent-step reaction model was formulated.

The development of a realistic mathematical model is very important to simulate the ongoing process and optimize the operating parameters that produces a composite of high quality. Also, a chemical reaction model that approximates the actual behavior of the resin is important to produce accurate results from the numerical model. This model could eliminate the large amount of time and cost involved in the trial and error type of experiments needed to produce a composite of required quality. The development of this numerical model is also important in order to conduct a complete investigation of the process variables and their effects which can then be used in designing an efficient experimental test plan.

PREVIOUS RESEARCH

There have been efforts by various researchers to characterize the pultrusion process using numerical models of different approaches including finite element and finite difference techniques. Price [3] was the first to develop a mathematical model for the pultrusion process. He presented a simple one-dimensional heat transfer model coupled with chemical reaction kinetics. Walsh et al. [4] developed a two-dimensional finite difference model to predict the temperature and cure characteristics, but no experimental results were presented. Batch et al. [5] used a finite element model to analyze the temperature, pressure and pulling force distributions inside a pultrusion die. The heat transfer model studied was for a steady-state two-dimensional circular geometry and assumed negligible axial heat conduction. Han et al. [6] presented a finite difference model for a two-dimensional cylindrical shape composite; no experimental results were presented to support the numerical model. Aylward et al. [7] presented a finite element model for heat transfer and curing analysis in pultrusion. They used a Lagrangian formulation for a transient one-dimensional case; no experimental

tests were performed for comparison. Viola et al. [8] has examined the pultrusion process using a one-dimensional finite difference simulation assuming that axial heat conduction was negligible. Gorthala et al. [9,10] modeled a two-dimensional cylindrical shaped composite inside the die and compared the results with very limited experimental DSC degree of cure data. A comparison of temperature and cure characteristics of flat two-dimensional composite stock was presented by Chachad et al. [11]; they used a one-step Arrhenius reaction model for the resin system. All researchers except [6] used a one-step nth order Arrhenius reaction model. Han [6] used an empirical model for the resin system. There has been no multiple-independent-step reaction model developed and employed in a 3-D model. This could be attributed due to the fact that previous resin systems could be modeled adequately with a one-step model. However, for the resin system used in this research a multiple step reaction approach is essential.

The present work is more elaborate than the existing models by providing a comprehensive "three-dimensional model" to predict the temperature and degree of cure profiles of composite using a multiple-independent-step chemical reaction model. From model predictions it has been found that in all cases the multiple-independent-step reaction model predicts a more accurate degree of cure of the composite when compared to one-step reaction model. The other difference with the present work is the inclusion of axial heat conduction in the composite and modeling of composite in the post-die region which were neglected by most of the researchers discussed above. The post-die region is important because the composite is at a high temperature as it exits the die and curing continues for some distance (time) after the composite leaves the die. The axial heat conduction is important when a composite of large cross-sectional area is pultruded. Additionally, the numerical results are validated by experimental measurements. Radial, circumferential and axial temperature and degree of cure profiles are calculated from the numerical model. The kinetic parameters for the reaction model of the thermoset epoxy resin were taken from DSC scans obtained in the Composite Materials Laboratory at The University of Mississippi.

STATEMENT OF PROBLEM

The present work focuses on developing a comprehensive numerical model to simulate the thermal and cure characteristics of circular pultruded composites using a multiple-independent-step chemical reaction for the resin. An Eulerian type control volume based finite difference technique devised by Patankar [1] was used to solve the coupled, non-linear governing equations to predict the temperature and degree of cure profiles in the composite. There are two non-linear governing equations for the one-step reaction rate model; the three-dimensional, steady-state energy equation and the steady-state species equation. For the two-independent-step reaction rate model there are three non-linear governing equations; the three-dimensional, steady-state energy equation and two steady-state species equations.

A schematic of the pultrusion process is shown in Fig. 2. There are three heater zones along the pultrusion die which heat the die and composite for the University of Mississippi PTI Pulstar 804 Pultruder. The heaters are electrical resistance type and were power controlled to maintain pre-defined temperature zone settings of 188-199-199, 193-204-204 or 199-210-210 C for this research. The fiber-resin mass enters the die at the resin bath ambient temperature and proceeds along the length of die during which it becomes heated. During this process an exothermic chemical reaction is initiated thereby releasing heat. This release of heat consequently raises the temperature of the composite. This reaction produces a measurable exothermic temperature increase which peaks above the die wall-temperature. The magnitude of the temperature exotherm, which is the difference between the temperature at the die-wall composite interface and the temperature at the center of the composite, is a function of the processing parameters and on the chemical kinetic parameters of the resin. After the resin releases the chemical energy, the composite starts losing heat to the die-wall through conduction as it proceeds along the die and through convection and radiation to the surrounding ambient environment upon exiting the die.

A typical energy release curve of the resin system taken from the DSC scans is shown in Fig. 1. The curve exhibits more than one lobe indicating that a one-step Arrhenius reaction model may not be a reasonable model for the resin system (Shell EPON 862/W) used in the experiments. From investigations it

has been found that the heat release curve which was predicted by the kinetic parameters obtained via a one-step Arrhenius model from the DSC scans does not follow the actual heat release curve of the resin. This can be easily observed from Fig. 3. The kinetic parameters for the one-step model were calculated using Borchard and Daniels Kinetic Analysis Software available on the DSC. The software analyzes the DSC scan based on the assumption that the reaction is a one-step Arrhenius reaction model. One-step means a single step chemical process occurs in going from reactants to products. Due to the lack of fit, a multiple-independent-step reaction model was proposed for the resin. The model was based on a graphical technique rather than basing it on its chemical components. The main reason for this is the presence of many individual chemical components and reactants in the epoxy resin which are unknown and proprietary. Hence, a graphical procedure was adopted. This is similar to most of the earlier research, where researchers formulated the reaction model based on the energy release curve rather than trying to model it chemically due to these same complications (unknowns and proprietary).

The die used for the experiments and analysis had a circular cross section of 0.95 cm (3/8 inch) diameter. The length of the pultrusion die was 91.4 cm (36 inches). For the post-die analysis, the distance along the length of the composite outside the die was taken to be 137 cm (54 inches). A total of 14 experimental test conditions were analyzed in this study; the processing conditions for the experimental cases are listed in Table 1. Experimental measurements were performed to obtain the temperature of the composite as it traverses through and beyond the die cavity. This was achieved by inserting a thermocouple of very small cross-section between the fibers and then pulling the thermocouple through the die. Temperature data were recorded as the thermocouple traveled through the die and also outside the die for a pre-determined distance beyond the die exit. A 28 gage fiberglass covered J-type thermocouple wire was used in the experimental test cases. Two thermocouples were used for each of the fourteen test cases listed in Table 1, one to record the temperature along the die-wall and the other to record the temperature near the center of the composite. Though care was taken to locate the thermocouple at the center of the composite, in certain cases the thermocouple missed the center of the composite. In such cases, the radial location (r/r_o) of the

thermocouple was determined by cutting into the pultruded composite and locating the radial position of the thermocouple. For those cases where the thermocouples were off the centerline, the temperature profiles were predicted for that specific radial location using the numerical model.

ANALYSIS

The governing equations used for modeling the pultrusion process are the three-dimensional, cylindrical coordinate system based steady-state energy and species equations. The steady-state energy equation is described by [12]

$$\rho c u_z \frac{\partial T}{\partial z} - \frac{1}{r}\frac{\partial}{\partial r}\left(r k_c \frac{\partial T}{\partial r}\right) - \frac{1}{r}\frac{\partial}{\partial \theta}\left(\frac{k_c}{r}\frac{\partial T}{\partial \theta}\right) - \frac{\partial}{\partial z}\left(k_l \frac{\partial T}{\partial z}\right) = S \qquad \textbf{(1)}$$

In Eq. (1), conduction in all three directions is modeled along with one-dimensional convection; z is the axial direction, r represents the radial direction and θ represents the circumferential direction. The coordinate system for the control volume is shown in Fig. 4. The symbols ρ, c and k represent the bulk density, bulk specific heat and bulk thermal conductivity of the composite, respectively. The subscripts c and l for the bulk thermal conductivity represents the property in the cross-fiber direction and in the direction along the fiber of the composite, respectively. Bulk properties are calculated using the volume fraction and mass fraction techniques described below. The velocity of the composite in the axial direction is denoted by u_z (pull speed). The velocity in the radial and circumferential directions were assumed to be zero. The term S is the heat source which is attributed to the exothermic reaction of the resin. For the one-step reaction it is given by

$$S = R_A \Delta H C_1 \qquad \textbf{(2a)}$$

and for the two-step reaction it is given by

$$S = \sum_{i=1}^{2} R_{A_i} \Delta H_i C_i \qquad \textbf{(2b)}$$

where R_A is the chemical reaction rate, ΔH is the heat of reaction per unit mass of uncured resin and C_I is the initial concentration of uncured resin. The subscript corresponds to the respective reaction step of the resin.

The fiber reinforcements used in the composite were Hercules AS4-12K graphite fibers and PPG 2001 fiberglass fibers. The matrix used was the thermoset epoxy resin SHELL EPON 862/W as mentioned earlier.

The bulk density of the composite is calculated using the volume fraction technique and is given by

$$\rho = \rho_r V_r + \rho_f V_f$$

where V_f is the volume fraction of fiber in the composite and V_r (= 1-V_f) is the volume fraction of resin in the composite. The bulk specific heat is calculated by the mass fraction technique which is described by

$$c = m_r c_r + m_f c_f$$

where m_f is the mass fraction of fiber in the composite, m_r (= 1-m_f) is the mass fraction of resin in the composite, c_r is the specific heat of the resin, and c_f is the specific heat of the fiber. The mass fraction, m_f, is obtained by

$$m_f = \frac{\rho_f V_f}{\rho_f V_f + \rho_r V_r} \qquad (3)$$

The bulk thermal conductivity of composite in the cross-fiber and axial direction are obtained by using the mass fraction technique as defined below

$$k_{c,l} = \frac{1}{\frac{m_f}{k_{f(c,l)}} + \frac{m_r}{k_r}} \qquad (4)$$

The subscripts c and l for k_f represent the thermal conductivity of the fiber in the cross-fiber direction and axial direction, k_r represents the thermal conductivity of the resin. Properties of the fiberglass, graphite and epoxy resin used in the model are listed in Table 2.

Discretization of the energy equation is achieved by the use of the power-law scheme as recommended for a convection-conduction formulation [2]. The steady-state species equations are given by

$$u_z \frac{\partial \psi_i}{\partial z} = R_{A_i} \tag{5}$$

where R_{Ai} is the Arrhenius reaction rate expressed by

$$R_{A_i} = K_{o_i} \exp\left(\frac{-E_{A_i}}{RT}\right)(1-\psi_i)^{n_i} \tag{6}$$

where i = 1 for the one-step reaction rate model and i = 1, 2, .., N for the multiple-independent-step Arrhenius reaction rate model. The species equation was discretized using the upwind scheme. In Eq. (6), K_{oi} is the pre-exponential constant, E_{Ai} is the activation energy, R is the universal gas constant and n_i is the order of reaction in the Arrhenius reaction equation. For the multiple-independent-step reaction, the kinetics parameters K_{oi}, E_{Ai}, n_i were obtained by performing regression analysis on the individual curves from a Gaussian curve fit which is discussed in detail in the following section.

The degree of cure is represented by the symbolψ, and for the one-step reaction it is defined as

$$\psi = \frac{C_I - C_A}{C_I} \tag{7}$$

and for the multiple-independent-step reaction it is defined as

$$\psi = \frac{\sum_{i=1}^{N} \psi_i \Delta H_i}{\sum_{i=1}^{N} \Delta H_i} \tag{8}$$

where C_I and C_A are the initial concentration of uncured resin and the local concentration of uncured resin at any location respectively. The overall degree of cure of the resin for the multiple-independent-step reaction model is the ratio of summation of the product of individual degrees of cure with the corresponding heat of

reaction of the step to the summation of the heats of reaction of the steps as shown in Eq. (8).

In formulating this multiple-independent-step reaction model, the number of steps in the reaction of the resin was chosen. For the resin system under consideration, two-independent-steps were considered to be present in the exothermic reaction of the resin, since there were two lobes in the energy release curve from DSC scan. Curves using a Gaussian function are fit to the energy release curve of the resin from the DSC using PEAKFIT software. The software works on the principle that the summation of the two individual curves at any given time-location will approximately equal the original curve from the DSC scan. Gaussian function curves were found to be the most suitable fit for the energy release curve. The two individual curves labeled Gaussian A and Gaussian B and the DSC data are shown in Fig. 5.

A three-independent-step reaction rate model for the resin system was also used in this study. The results produced by the three-independent-step model were approximately the same as the results predicted by the two-independent-step model. Hence, it was decided to use a two-step model which is more efficient in simulation.

For the two-step reaction rate model (N = 2 in Eq. (8)) there are two individual Gaussian curves as shown in Fig. 5. The heat of reaction of the resin is the summation of the areas under these two curves. The heat of reaction for the first step in the two-step model is the area under the curve labeled Gaussian A in Fig. 5. The area under the curve Gaussian A is obtained by integrating the curve between its two extreme limits. The heat of reaction for the second step in the two-step model is the area under the curve labeled Gaussian B in Fig. 5. Similarly, the area under the curve Gaussian B is obtained by integrating the curve between its two extreme limits. Another point to be noted here is that the summation of the heats of reaction for the first and second step in the two-step model will approximately equal the heat of reaction of the epoxy resin given by the DSC scan. This is important since the two-step model should release the same amount of exothermic heat energy as the heat energy that is actually released by the resin.

The chemical kinetic parameters for the first step in the two-independent-step reaction model were obtained by determining the values of K_{oi}, E_{Ai}, and n_i which made the best fit between the Gaussian A and the Arrhenius reaction rate equation as defined in Eq. (6); the same procedure was followed for the curve Gaussian B. Hence, two sets of kinetic parameters were obtained for the two-independent-step reaction rate model, one for the first step represented by the curve Gaussian A and then next for the second step represented by the curve Gaussian B. The kinetic parameters for both the one-step as well as the two-step reaction model for the epoxy resin system are listed in Table 3. The comparisons of the two-independent-step Arrhenius reaction model fit to the resin, the one-step reaction rate model from DSC parameters, and the experimental DSC data are shown in Fig. 6. Clearly the two-step reaction rate model is a better approximation to the actual experimental DSC data when compared to the one-step reaction rate model. The heat release curve predicted by the two-step model follows very closely the experimental DSC data.

The physical domain was discretized into 10x8x196 nodes for a total of 15680 nodes. At any given axial distance, the cross-section was discretized into 10 radial nodes (r-direction) and 8 circumferential nodes (θ-direction). Inside the die, the axial length of 91.4 cm was discretized into 146 axial nodes. In the post-die region, the axial length of 137 cm was divided into fifty nodes. Inside the pultrusion die, the temperatures at the composite die-wall interface obtained from the thermocouple data were used as boundary condition information.

The boundary conditions used for solving Eqs. (1) and (5) are:

1) Velocity in the axial direction is equal to pull speed

$$u_z(r,\theta,z)=U$$

2) Degree of cure at the entrance (z=0) is zero

$$\psi(r,\theta,0)=0$$

For the multiple-independent-step model

$$\psi_i(r,\theta,0)=0 \quad i = 1, 2$$

3) Temperature at the composite-die wall interface T is given by the thermocouple data

$T(r_o,\theta,z)=T_w(z)$ for any θ at a given z location; r_o is the radius of the composite stock. This boundary condition is used for both theθ and the z variables.

This boundary condition is used for circumferential nodes inside the die. In the post die region, this boundary condition is replaced by the energy balance equation that is described below, Eq. (10).

4) Energy balance for the control volume at the center of the physical domain.

For this problem, it is same as

$$\frac{\partial T}{\partial r}\Big|_{r=o} \quad 0 \tag{9}$$

5) $\partial T/\partial z = 0$ at $z = L_1$

This boundary condition is typical of numerical methods and is applied in order to separate the calculation domain from the rest of the universe.

6) $T(r,\theta,0) = T_B$, where T_B is the resin bath temperature

7) $\partial T(r_o,\theta,z)/\partial\theta = 0$

This boundary condition is used only for this paper to simulate the thermocouple data. However, the model can handle cases where the fiber distribution will be random but specified and therefore this boundary condition will not be applicable. Therefore for this study, a 3-D model is used to simulate the 2-D solution experimental situation.

In the post-die region, heat loss from the surface of the composite to the environment occurs through convection and radiation. This heat loss is modeled in developing a boundary condition for the nodes on the surface of the composite as mentioned in boundary condition no. 3. Energy conservation is applied in formulating the expression for the composite surface boundary nodes. Here a zero thickness control volume in the radial direction (r-direction) was used. This eliminates the effect of conduction from the neighboring circumferential (θ-direction) and axial (z-direction) nodes. Applying conservation of energy, the following

equation was formulated as the boundary condition to compute the temperature at the surface of the composite,

$$-k\frac{dT}{dr}\Big|_{r=r_o} + q_{r1} = h(T_{r=r_o} - T_\infty) + q_{r2} \tag{10}$$

The parameter q_{r1} is the radiate heat flux from the rear face of the heating section of the pultruder reaching the surface of composite in the post-die region and is described by

$$q_{r1} \quad F(\sigma T_b^4(1\ (1\ \epsilon)F)\ \epsilon\sigma T_{r=r_o}^4) \tag{11}$$

where F is the radiation view factor.

The parameter q_{r2} is the radiate heat flux from the surface of the composite to the ambient conditions in the post-die region and is given by

$$q_{r2} \quad \epsilon\sigma(T_{r=r_o}^4\ T_\infty^4) \tag{12}$$

These two components (Eqs. (11) and (12)) constitute the radiate heat transfer. For the second component, q_{r2}, a radiation view factor of unity was assumed since the area of the surrounding environment is very large when compared to the surface area of the composite. For the first component, q_{r1}, a radiation view factor was calculated from Holman [13] based on the geometry of the pultruder and the shape of the composite exiting the die. The view factor is a function of the angle between the heating section of pultruder and the composite, which in turn is a function of the distance between them. This view factor, F, is given by

$$F = \frac{H^2W(z-L)}{\pi(H^2 + (z-L)^2)^2} \quad ; \quad z \geq L \tag{13}$$

where H, W are the height and width of the rear portion of the pultruder facing the composite. This radiation

view factor was used in conjunction with an estimated Emissivity of 0.75 for the graphite/epoxy and 0.65 for the fiberglass/epoxy composite to compute the net Radioactive heat loss from the composite.

From Holman [13], the criteria for the free convection to dominate, $Gr/Re^2 > 10$, is satisfied. Here Gr and Re represents the Grashof and Reynolds numbers. Therefore, free convection dominates the forced convection for the cases studied here. The averaged convective heat transfer coefficient was calculated from the equation provided in Holman [13] for free convection from horizontal cylinders. That equation is given as

$$Nu_d = 0.36 + \frac{0.518(Gr_d Pr)^{1/4}}{\left(1+\left(\frac{0.559}{Pr}\right)^{\frac{9}{16}}\right)^{\frac{4}{9}}} \qquad \textbf{(14)}$$

The Grashof and Prandtl numbers were evaluated at the film temperature which is the arithmetic average of the ambient air temperature and the temperature at the surface of the composite. These dimensionless numbers were calculated at every node located on the surface of the composite, due to the fact that the temperature difference between the composite surface and the ambient air is different at every axial location. The dynamic viscosity, density and thermal conductivity of air were considered to be temperature dependent and they were interpolated among the available properties of air from Holman [13].

The governing equations were discretized and a system of equations were formed. Then, they were solved simultaneously using the Tri-Diagonal Matrix Algorithm (TDMA) technique as described in [2]. This iterative technique was repeated until it met the convergence criteria for both temperature and degree of cure. This technique is relatively simple to use when compared to other standard techniques. Separate convergence criterion were used for both the temperature and the degree of cure. A convergence criteria of 0.001 K was used for temperature and a value of 0.0001 was used for degree of cure. The program took approximately 100-150 iterations to satisfy the convergence criteria; the number of iterations varied in that range depending on the processing case (see Table 1) that was being simulated.

The temperature profile for the near-centerline location taken from the thermocouple data was used to compare with the predictions from the numerical model. The degree of cure of the pultruded composites for each of the processing conditions was determined experimentally. This was done by testing five samples from each test case (see Table 1) in the DSC and then averaging the five values obtained. The degree of cure was determined from the DSC scans by the following procedure: A sample of approximately 8-12 mg in weight was cut from the pultruded product and the amount of resin present in the sample was calculated. This sample was then scanned in the DSC at a scan rate of 20 C/min. The amount of heat released by the uncured resin present in the composite was then averaged among the five samples to determine the experimental degree of cure of the composite for that test case (each of the 14 cases in Table 1). These experimental degrees of cure were compared with the predicted values (see Table 4).

RESULTS

The processing variables studied in this numerical model are pull speed, fiber volume and the die-wall temperature settings. Seven test cases were generated each for graphite/epoxy and fiberglass/epoxy composites. The test conditions for the fourteen cases are listed in Table 1.

The measured die-wall (composite-die interface) temperature and the predicted near-centerline temperature (at the r/r_o location of 0.65) for the nominal test conditions (case 2 of Table 1) are presented in Fig. 7. The factor r/r_o is the ratio of the radial location of the thermocouple from the center of the composite stock to the radius of the composite stock. It can be seen from the figure that the predicted centerline temperature profile initially lags the die-wall temperature profile. The temperature near the center of the composite is equal to the resin bath temperature when it enters the pultruder. As mentioned earlier, the resin bath temperature is approximately equivalent to the ambient temperature, and the die-wall is maintained at the preset temperature level. Since the thermal conductivity of the composite is not high enough to rapidly conduct heat from the die wall, this lag between the temperature near the center and at the outside surface of the composite exists. Once the resin in the composite reaches the reaction initiation temperature, it starts

reacting thereby releasing heat which raises the temperature of the composite. This can be seen from the figure at approximately 0.5 m from the entrance. This causes the near-centerline temperature to peak above the die-wall temperature. As the composite continues to travel through the die, the reaction continues which causes the near-centerline temperature to remain higher than the die-wall temperature. This is also evident from an axial distance of 0.5 m onwards in the figure.

The composite after exiting the die, being at a higher temperature than the environment (air at ambient temperature), starts to lose heat to the environment. As the composite continues to advance in the post-die region, the temperature begins to decrease thereby losing less heat. After some distance beyond the die exit, the temperature of the composite is reduced such that the reaction of the resin essentially subsides. This can be evidenced from the degree of cure of the composite in the post-die region becoming almost constant in Fig. 8; thus, it is not necessary to model the domain from that location (approximately 2 m) onwards.

Verification of results from the numerical model with the experimental temperature measurements for test case 10 of Table 1 is shown in Fig. 9. The verification is shown for the regions both inside the die and the post-die. It is clear that the agreement between the temperature profile predicted by the model at a given radial location (r/r_b) and the profile from the experimental data is very good.

Figure 9 illustrates a comparison of the near-centerline temperature profiles predicted by the one-step and two-step chemistry models for a graphite/epoxy composite (case 3 of Table 1). Figure 10 presents a comparison of the near-centerline temperature profiles predicted by the one-step and two-step models for a fiberglass/epoxy composite (case 10 of Table 1). Figures 9 and 10 show the impact of the resin two-step reaction model on the near-centerline composite temperature. This figure shows that there is not much difference between the centerline temperatures predicted by the one-step model and the two-step model for the resin in most of the region inside the pultrusion die except for a small region where the exothermic reaction dominates. For the region where there exists a difference between the near-centerline temperatures predicted by the two different chemistry models, the following reason could be attributed. The energy release

versus time curve from the one-step model is compared with the curve predicted by the kinetic parameters from the two-step reaction rate model in Fig. 6. It should be noted that this curve not only represents the heat release but also the reaction rate of the resin. The profile predicted by the one-step parameters follows the DSC experimental data very closely until the location C after which it tends to deviate away from the DSC data. In other words, the energy release predicted by the one-step model decreases rapidly from the location C onwards. Whereas the DSC data remain almost the same until the location D and then it begins to drop down. From this argument, it can be seen that the area under the DSC data curve up to location D is higher than that of the curve predicted by one-step model. Therefore for a given die temperature setting, the one-step reaction model yields a different distribution of heat release during the exothermic reaction when compared to the DSC resin data. This results in the temperature profile predicted by the two-step model peaking above the profile predicted by the one-step model.

Figure 11 presents a comparison of degree of cure profiles predicted by the two different reaction models for a graphite/epoxy composite (case 3 of Table 1). Figure 12 presents a comparison of degree of cure profiles predicted by the two different models for a fiberglass/epoxy composite (case 10 of Table 1). Figures 11 and 12 illustrate representative degree of cure profiles predicted by the one-step and two-step models. It is evident that the degree of cure profiles predicted by the one-step initially leads the two-step model. This can be correlated to the early lead in the temperature profiles (Figs. 9 and 10) predicted by the one-step model as well as the earlier heat release in Fig. 6. Since the one-step model starts releasing heat early, both the temperature profile and the degree of cure profile leads the profiles predicted by the two-step model. As the reaction of the resin proceeds, the two-step model better follows the resin behavior (Fig. 6) in releasing more exothermic energy. Thereby the temperature profile as well as the degree of cure profiles peak above the profiles predicted by the one-step model.

Another disadvantage with the reaction rate predicted by the one-step model is that the reaction continues for a longer time. Actually, the resin completes the reaction earlier as shown by the DSC data in Fig. 6. In this way, the one-step model needs more time to complete the reaction. Hence for this type of resin

system, a numerical model with a one-step reaction rate model will not produce results as accurate as the two-step model.

Table 4 shows a comparison of the predicted degree of cure at the pultruder exit and at the post-die location (≈ 2 m beyond the die exit) with the experimental degree of cure. Cases 1 through 7 list the degrees of cure for graphite/epoxy composites and cases 8 through 14 list the degrees of cure for fiberglass/epoxy composites. For case 1, it can be seen that the degree of cure predicted by the one-step model at the post-die location is about 78% and the cure predicted by the two-step model is about 90%. The experimental degree of cure was measured to be 94% in the DSC. Similarly for other cases, the degree of cure predicted by the two-step model at the post-die location is significantly higher than the cure predicted by the one-step model. It can also be observed that in most of the cases, the degree of cure predicted by the two-step model is in better agreement with the experimentally measured degree of cure of the pultruded composite.

Another point to be noted is that the degree of cure at the post-die location is higher than the degree of cure at the die-exit. For case 2, the composite cures by another 2% in the post-die region. For case 3, the composite cures an additional 3% in the post-die region which is a significant amount of cure taking place only 2 m outside the die. Hence, modeling the post-die region is an important part in the analysis of pultrusion process. The two-independent-step degree of cure results are slightly lower than the DSC degree of cure measurements. Part of this difference can be attributed to the reason that the samples were not measured in the DSC for several months and hence some long term on-the-shelf curing may have occurred.

From Table 4, the degree of cure for case 1 is higher than the cure for case 2 which in turn is higher than the cure for case 3. Hence the degree of cure of the pultruded composites decreases as the speed at which it is pulled increases. Similarly from the degrees of cure for cases 4, 2, and 5, which represents cases with increasing fiber volume fractions, the degree of cure decreases as the volume fraction of the fiber in the composite increases; this is because the higher fiber volume means less resin mass and hence less heat is released to help cure the composite. From the degrees of cure for cases 6, 2, and 7, which represent cases with increasing die-wall temperature settings, the degree of cure increases as the die-wall temperature setting increases. The same trend hold true for the fiberglass/epoxy composites with cases numbered 8 through 14.

CONCLUSIONS

This study presents a numerical model for a three-dimensional cylindrical shaped geometry comparing a one-step with a two-independent-step reaction rate model. This model was used to predict the temperature and degree of cure profiles which were then compared with the experimental data.

The agreement between the predicted temperature profiles and the measured temperatures for all test conditions is quite good for both the one-step and two-step chemistry model. From the numerical results, it can be observed that the degree of cure predicted by a one-step reaction model is significantly lower than the two-step model. Hence, when a one-step model is used for this resin system (Shell EPON 862/W), it will predict a degree of cure of the composite which will be lower than the actual degree of cure. In those situations, a two-independent-step model will definitely improve the predicted results. Therefore, from this study, it has been found that the reaction model for the resin can play an important role in modeling the curing of pultruded composites. This is supported by the fact that the reaction model is what determines the degree of cure of the composite which in turn is used in selecting the processing parameters for the manufacturing process.

Additionally, it has also been determined that the pull speed and the die-wall temperature settings have a strong impact on the composite degree of cure. A higher pull speed yielded a lower degree of cure and a higher die-wall temperature settings resulted in a higher degree of cure. Similarly, a pultruded composite with a lower fiber volume resulted in a higher degree of cure. This study also helps in understanding the pultrusion process of composites for a cylindrical geometry by modeling the thermal and cure profiles both inside the die and in the post-die region. It should be noted that the two-step reaction model for the resin is an important part of this study.

ACKNOWLEDGEMENT

This research is based upon the work supported by the National Science Foundation (NSF) under grant NSF DDM-9101643 and Electric Power Research Institute (EPRI) under grant RP-8007-20. The authors are also thankful to Shell Development Company and the University of Mississippi. The authors appreciate this assistance.

REFERENCES

1. Gibson, R.F.,*Principles of Composite Material Mechanics,* McGraw-Hill Inc., New York, 1994.
2. Patankar, S.V.,*Numerical Heat Transfer and Fluid Flow,* McGraw-Hill, New York, 1980.
3. Price, H.L., "Curing and Flow of Thermosetting Resins for Composite Material Pultrusion", Ph.D. Thesis, Old Dominion University, Virginia, 1979.
4. Walsh, S.M. and Charmchi, M., "Heat Transfer Characteristics of a Pultrusion Process", *ASME 25th National Heat Transfer Conference,* Houston, TX, July 1988, pp.23-28.
5. Batch, G. and Macosko, C., "A Computer Analysis of Temperature and Pressure Distributions in a Pultrusion Die", *Proceedings of SPI Composite Institute's 42nd Annual Conference*, 1987, The Society of the Plastics Industry, pp.12-B:1-7.
6. Han, C.D., Lee, D.S. and Chin, H.B., "Development of a Mathematical Model for the Pultrusion Process", *Polymer Engineering and Science,* Vol. 26, No. 6, 1985, pp. 393-404.
7. Aylward, L., Douglas, C. and Roylance, D., "A Transient Finite Element Model for Pultrusion Processing", *Polymer Process Engineering,* Vol.3, 1985, pp. 247-261.
8. Viola, G. and Amsterdam, K., "Numerical Optimization of Pultrusion Line Operating Parameters", *35th International SAMPE Symposium,* 1990, pp.1968-1981.

9. Gorthala, R., Roux, J.A. and Vaughan, J.G., "Comparison of Graphite/Epoxy with Fiberglass/Epoxy: A Heat Transfer Analysis", *Proceedings of SPI Composite Institute's 47th Annual Conference*, 1992, The Society of the Plastics Industry, 2-A. pp.1-9.

10. Gorthala, R., Roux, J.A. and Vaughan, J.G., "Resin Flow, Cure and Heat Transfer Analysis for Pultrusion Process",*Journal of Composite Materials*, Vol. 28, No. 6, 1994, pp.486-506.

11. Chachad, Y.R., Golestanian, H., Valliappan, M., Roux, J.A. and Vaughan, J.G., "Temperature and Cure Characterization of Pultruded Composites and Kinetic Analysis of Epoxy Resin Systems Using a Differential Scanning Calorimeter", *38th International SAMPE symposium*, Vol. 38, 1993, pp.1275-1290.

12. Kays, W.M. and Crawford, M.E., *Convective Heat and Mass Transfer*, McGraw-Hill, New York, 1980.

13. Holman, J.P.,*Heat Transfer*, McGraw-Hill, New York, 1989.

14. Mijovic, J. and Wijaya, J., *Effects of Graphite Fiber and Epoxy Matrix Physical Properties on the Temperature Profile Inside Their Composite During Cure*, SAMPE Journal, Vol. 25, No. 2, March 1989, pp. 35-39.

BIOGRAPHY OF AUTHORS

Meyyappan Valliappan

Mr. Valliappan received his B.E. (1989) in Mechanical Engineering from Anna University, Madras, India and M.S. (1991) in Mechanical Engineering from the University of Mississippi. He is currently working towards a Ph.D. in Mechanical Engineering with emphasis in heat transfer and composite materials. Presently, he is working on the numerical modeling of thermal and cure characteristics of composite materials in the pultrusion process. He has been working in finite difference and finite element analysis areas for the last five years. His areas of research includes thermal, stress, and vibration analysis.

Jeffrey A. Roux

Dr. Roux received his B. S. degree in Mechanical Engineering in 1967, and both the M. S. (1968) and Ph.D. (1970) from University of Tennessee. He has worked in industry for 10 years (2 with Northrop, Inc. and 8 with Sverdup, Inc.) and has taught at the University of Mississippi for the past 14 years in the Mechanical Engineering Department. His 24 years of research experience are all in the thermophysics and the heat transfer area. Dr. Roux's works have ranged from aerodynamic heating, thin film optics, radioactive heat transfer in fibrous insulation, solar energy to thermochemical analysis of composite materials.

James G. Vaughan

Dr. Vaughan received his B. S. degree in Electrical Engineering in 1971, and his M. S. and Ph.D. in Materials Science and Metallurgical Engineering (1974, 1976), all from Vanderbilt University. He worked with Bendix Corporation for 2 years before joining the University of Mississippi in 1980. Dr. Vaughan now serves as professor of Mechanical Engineering and Associate Dean of the School of Engineering at the University of Mississippi. He has worked extensively with pultrusion over the past eight years and has developed a pultrusion laboratory at the university where he conducts various experimental and analytical studies of the pultrusion process.

Table 1. Test Conditions for Shell EPON 862/W Resin System

Case No.	Pull Speed cm/min	Fiber Volume %	Temperature Profile °C	Fiber
1	20	62.2	193-204-204	Graphite
2	30	62.2	193-204-204	Graphite
3	41	62.2	193-204-204	Graphite
4	30	59.6	193-204-204	Graphite
5	30	64.9	193-204-204	Graphite
6	30	62.2	188-199-199	Graphite
7	30	62.2	199-210-210	Graphite
8	20	67.5	193-204-204	Fiberglass
9	30	67.5	193-204-204	Fiberglass
10	41	67.5	193-204-204	Fiberglass
11	30	62.7	193-204-204	Fiberglass
12	30	72.3	193-204-204	Fiberglass
13	30	67.5	188-199-199	Fiberglass
14	30	67.5	199-210-210	Fiberglass

Table 2. Properties of Fiber Reinforcements and Epoxy Resin

Material	Graphite	Fiberglass	Epoxy resin
Density, Kg/m^3	1790[a]	2560[a]	1260[b]
Specific heat, J/Kg^oK	712	670	1255
Thermal conductivity, W/m^oK	$k_{f(c)} = 11.6$ $k_{f(l)} = 66.0$	$k_{f(c)} = 1.04$ $k_{f(l)} = 11.40$	0.21

[a]Ref. [14]; [b]Ref. [14]

Table 3. Kinetic Parameters of Shell EPON 862/W Epoxy Resin

Parameters	**Symbol**	**One-Step**	**Two-Step**	
			First Step	**Second Step**
Pre-exponential constant	K_o	53.93E09 1/s	16.23E06 1/s	15.30E06 1/s
Activation Energy	E_A	101.7E03 J/mol	64.40E03 J/mol	84.54E03 J/mol
Heat of Reaction	ΔH	342.5E03 J/Kg	202.3E03 J/Kg	140.2E03 J/Kg
Order of Reaction	n	4.78	1.343	1.357

Table 4. Comparison of Predicted Degree of Cure and Experimental Degree of Cure at Die Exit and Post Die Locations.

Case No.	**Predicted Cure For One-Step**		**Predicted Cure For Two-Step**		**Experimental Cure**
	Die Exit	**Post Die**	**Die exit**	**Post Die**	
1	0.78	0.78	0.89	0.90	0.94
2	0.75	0.76	0.83	0.85	0.92
3	0.72	0.73	0.78	0.81	0.92
4	0.76	0.77	0.85	0.87	0.91
5	0.75	0.75	0.83	0.85	0.93
6	0.73	0.74	0.80	0.82	0.90
7	0.76	0.77	0.86	0.88	0.93
8	0.78	0.78	0.89	0.90	0.93
9	0.76	0.77	0.85	0.87	0.91
10	0.75	0.76	0.82	0.85	0.89
11	0.77	0.77	0.87	0.88	0.91
12	0.76	0.77	0.85	0.87	0.94
13	0.74	0.75	0.82	0.84	0.89
14	0.78	0.78	0.88	0.90	0.92

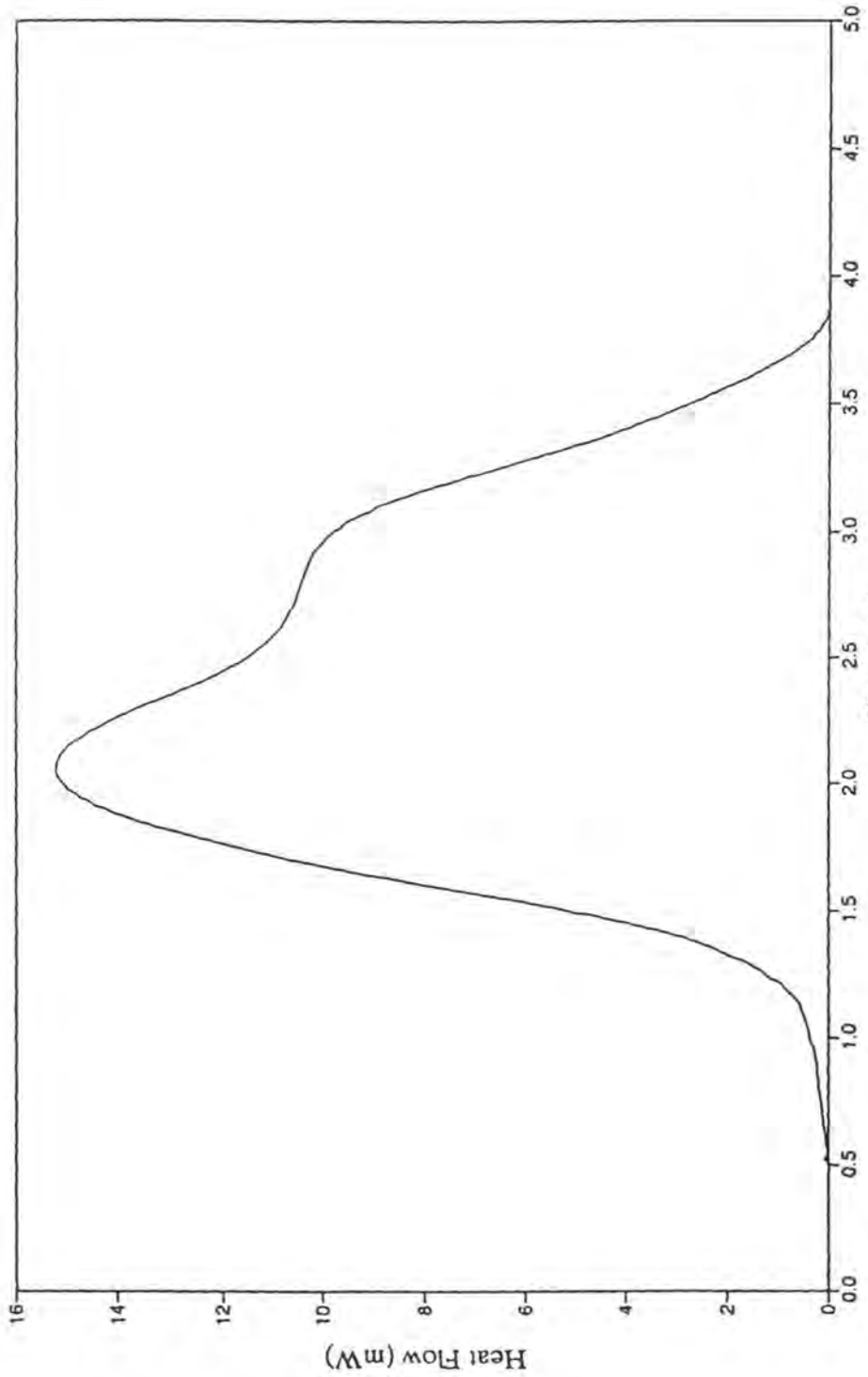

Fig. 1 A representative DSC scan showing the exothermic heat release as a function of time.

B9-27

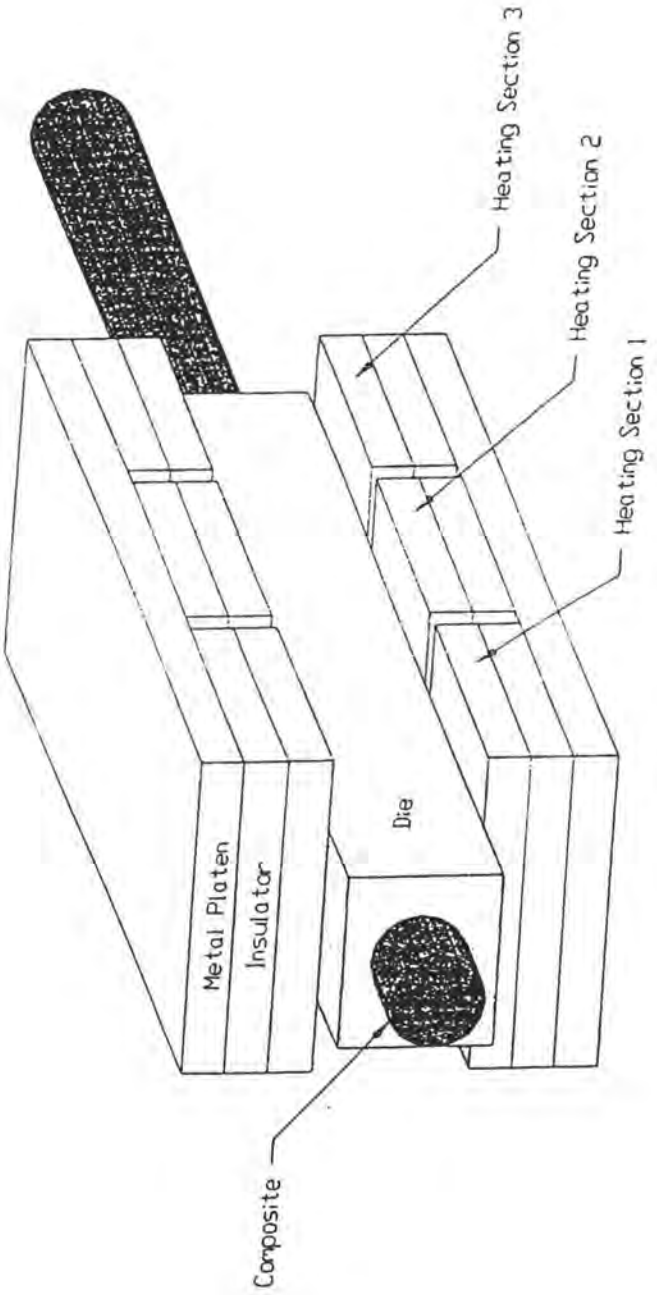

Fig. 2 Schematic of the pultrusion process.

B9-28

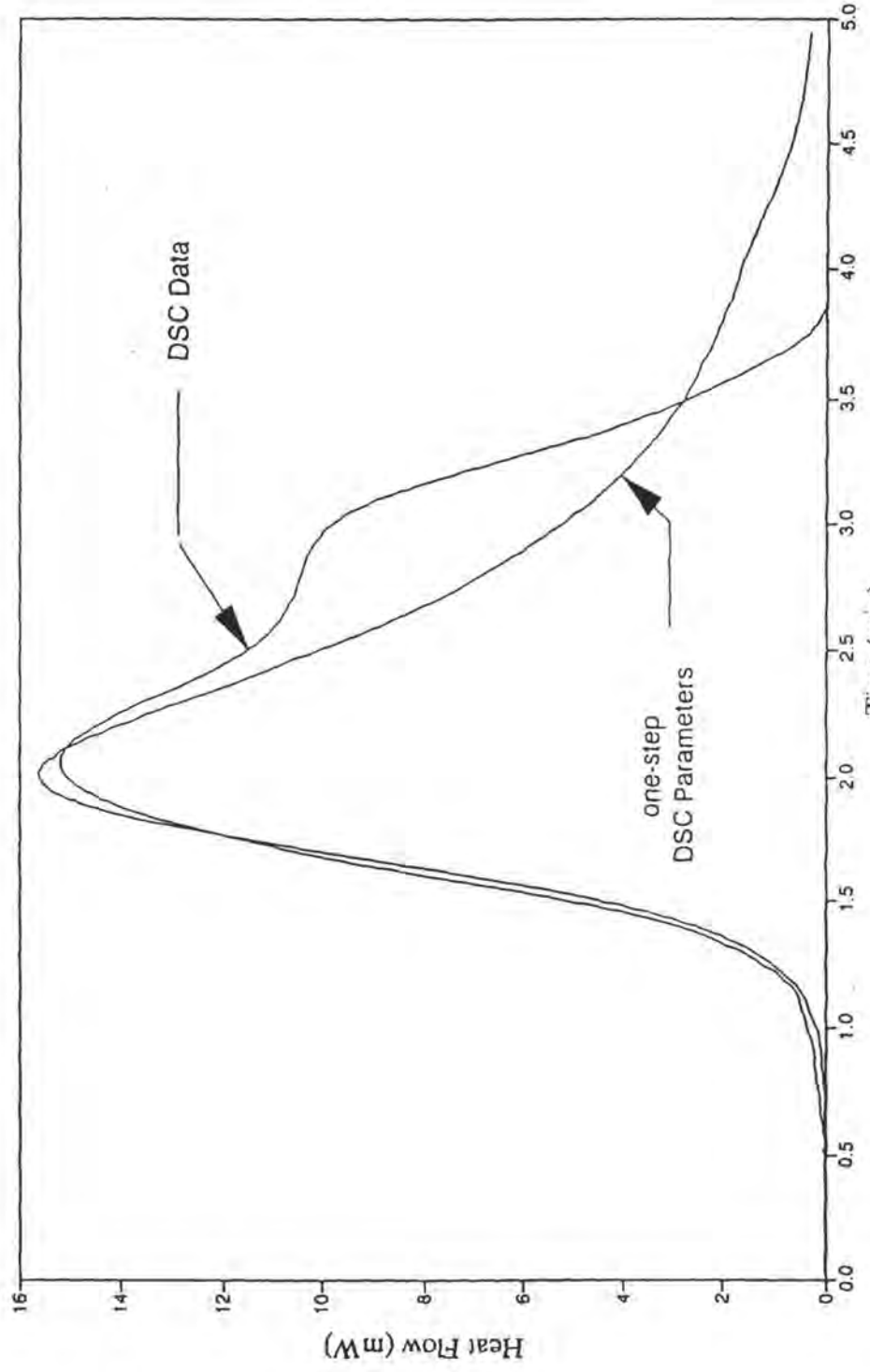

Fig. 3 Comparison of the heat release curve predicted by the one-step DSC parameters with the DSC experimental data.

B9-29

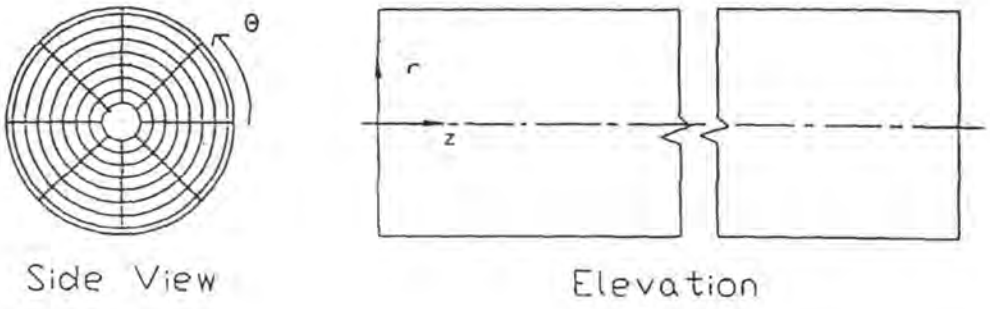

4a. Coordinate system

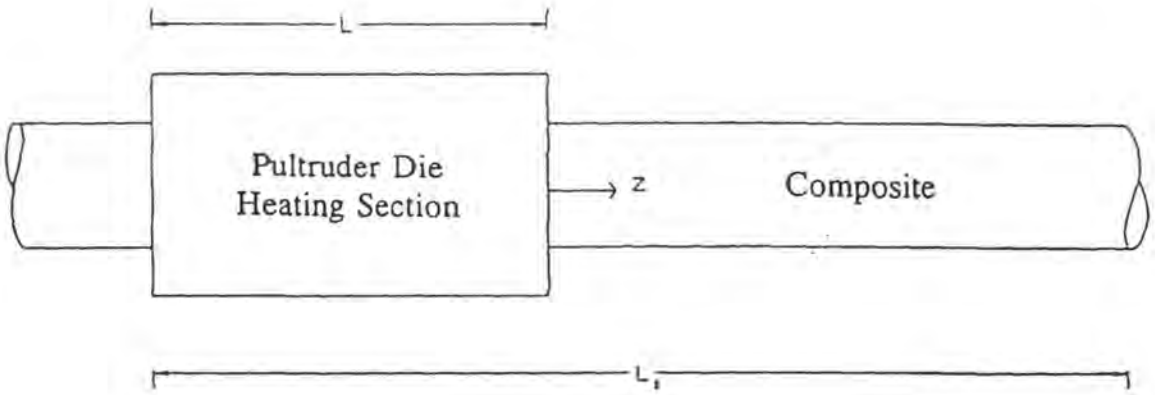

4b. Post-die geometry

Fig. 4 Schematic of the calculation domain.

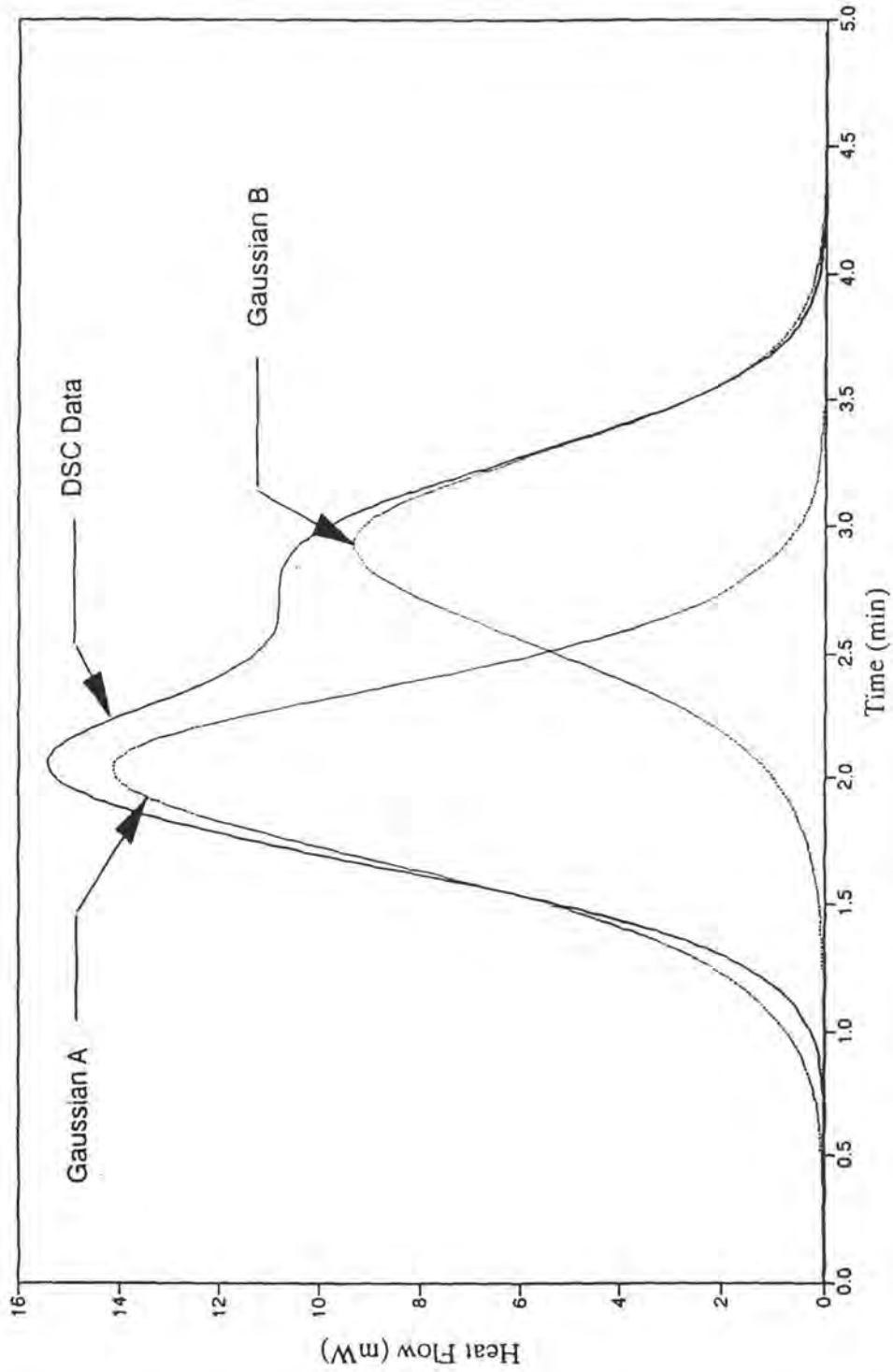

Fig. 5 Two-step Gaussian curve fit to the DSC experimental data.

B9-31

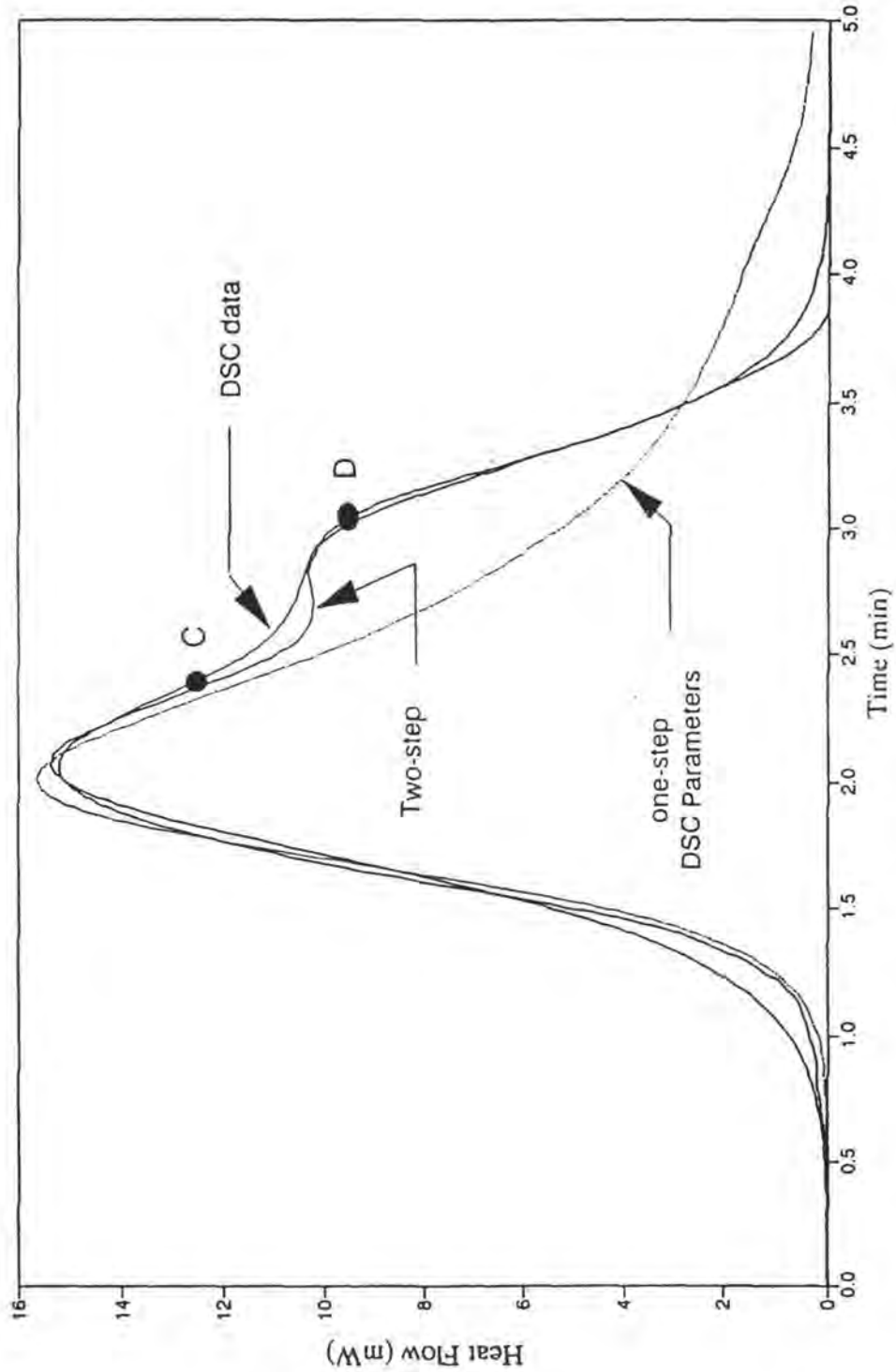

Fig. 6 Comparison of the heat release predicted by the one-step DSC parameters and the two-step reaction rate model with the DSC experimental data.

B9-32

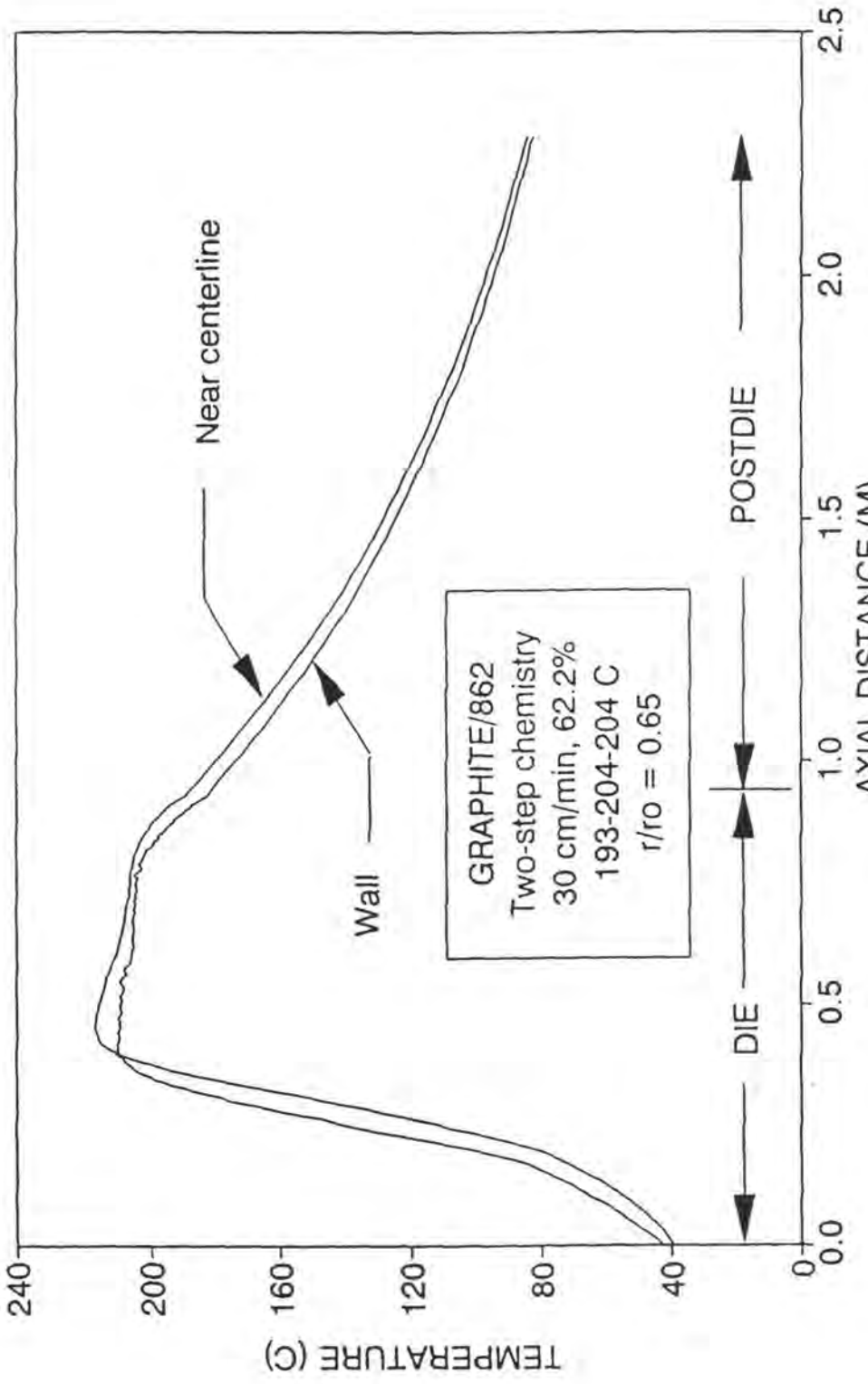

Fig. 7 Comparison of the measured die-wall temperature with the predicted near-centerline temperature showing the effect of exotherm for case 2 of Table 1.

B9-33

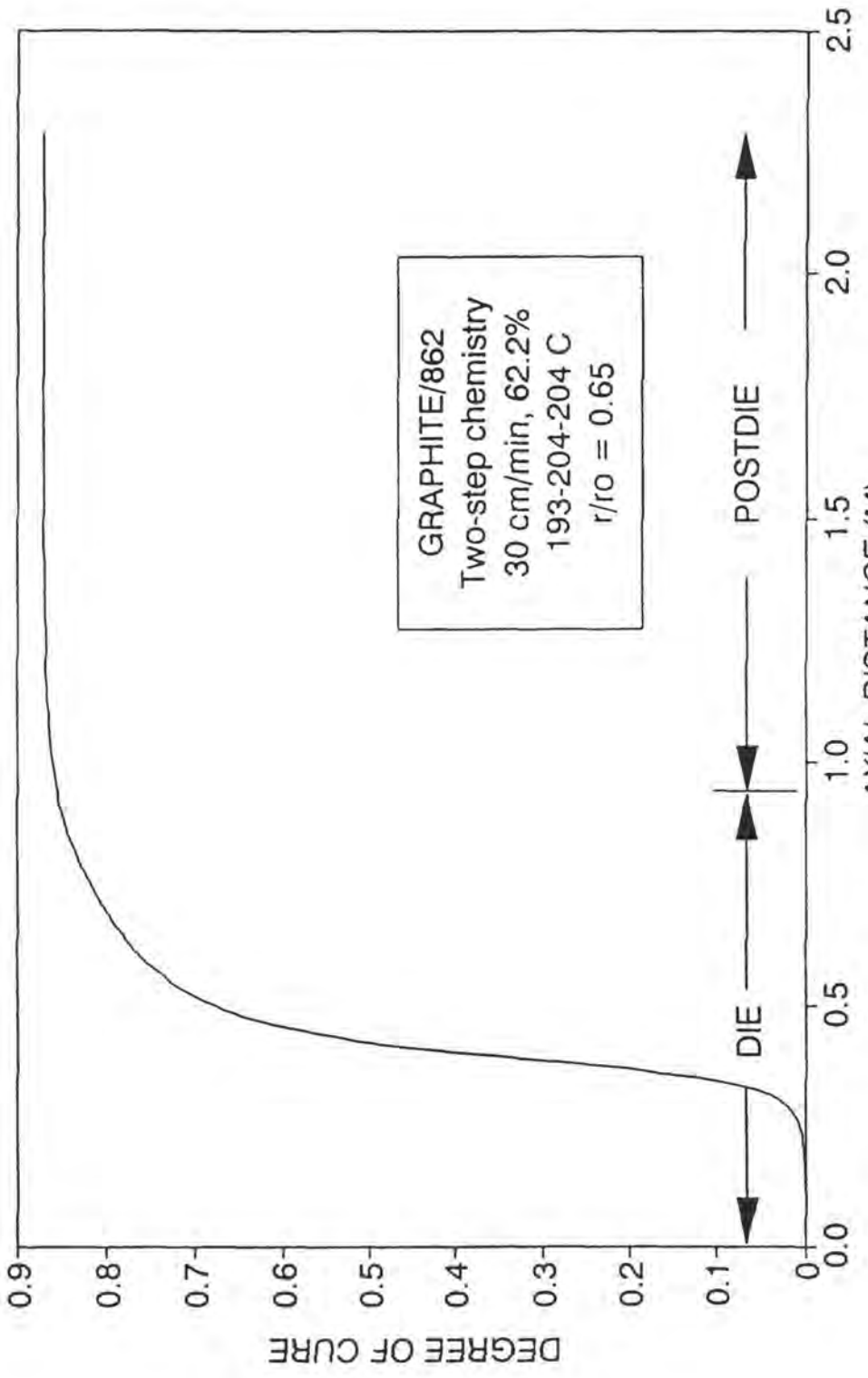

Fig. 8 Degree of cure as a function of axial distance for case 2 of Table 1.

B9-34

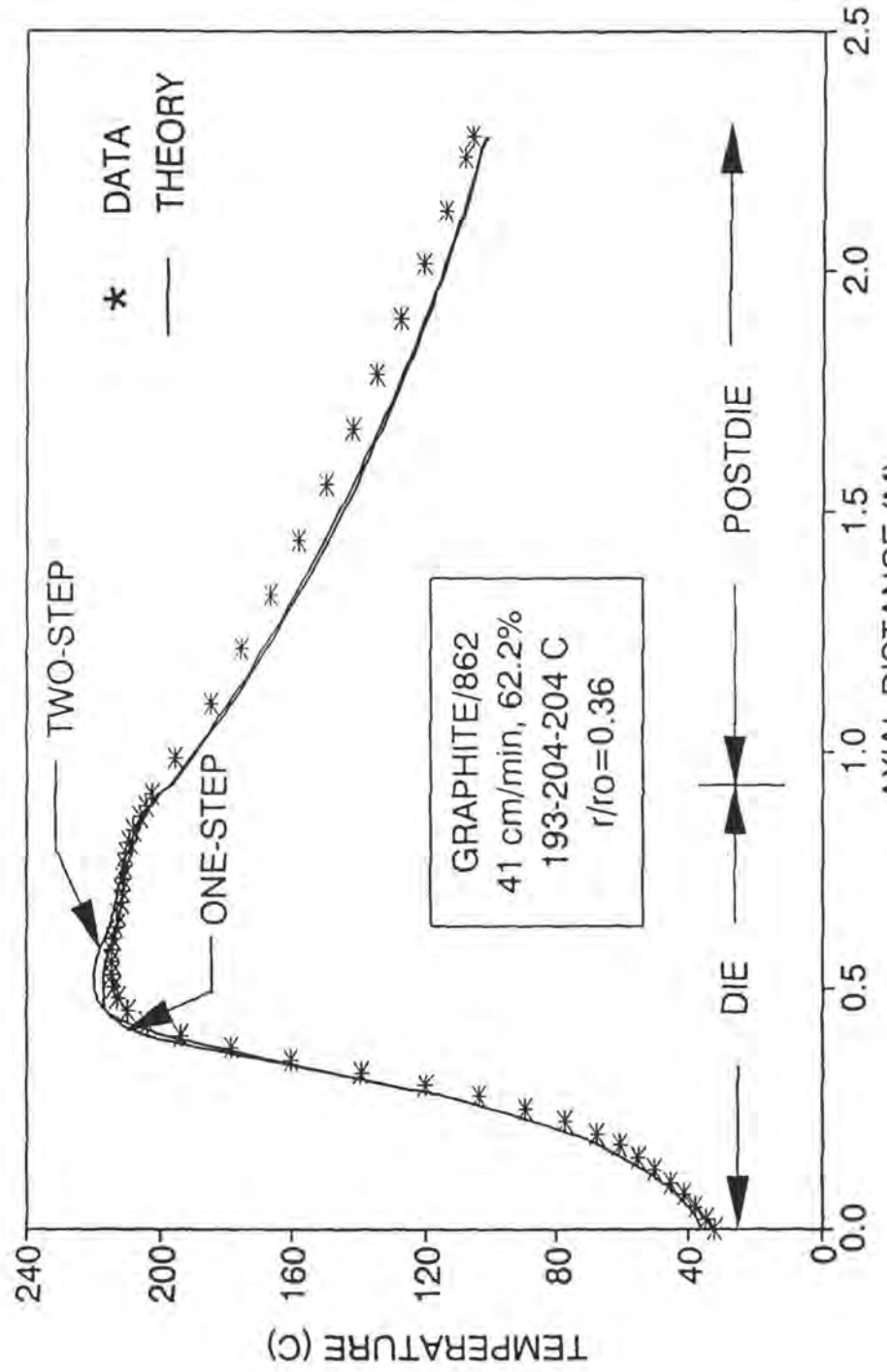

Fig. 9 Comparison of temperature profile predicted by the one-step and two-step reaction rate model with the experimental data for case 3 of Table 1.

B9-35

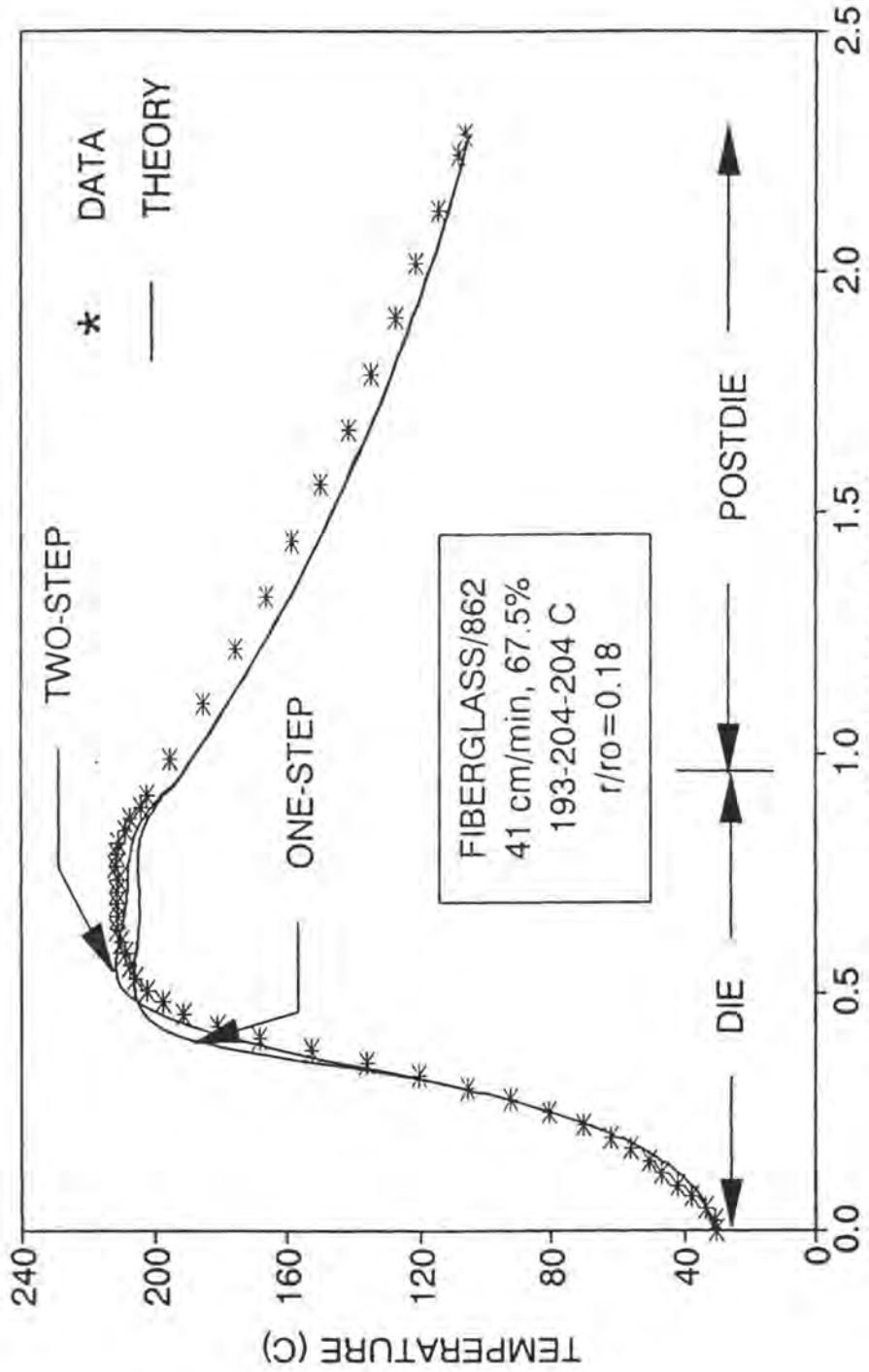

Fig. 10 Comparison of temperature profile predicted by the one-step and two-step reaction rate model with the experimental data for case 10 of Table 1.

B9-36

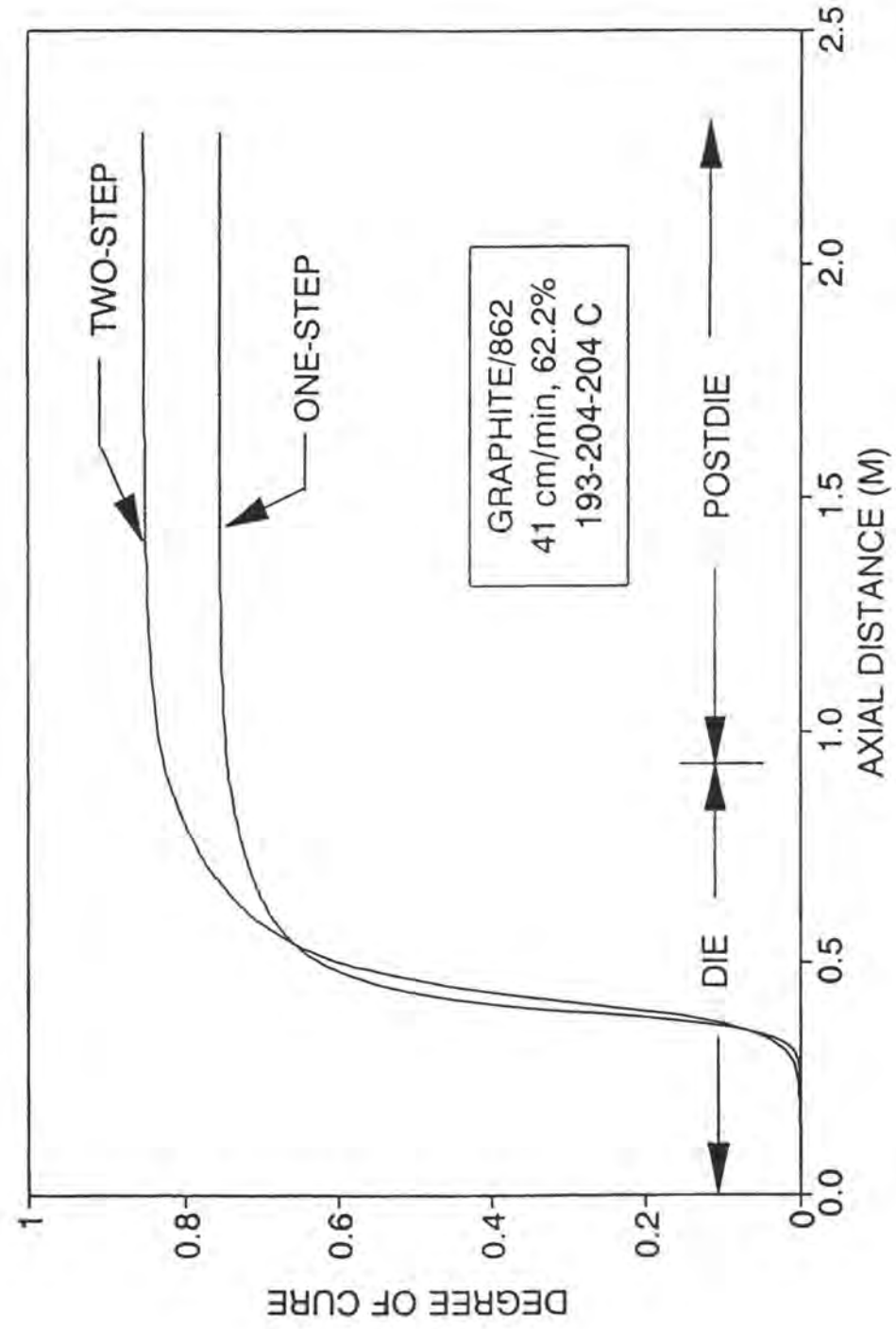

Fig. 11 Comparison of degree of cure profile predicted by the one-step and two-step reaction rate model for case 3 of Table 1.

B9-37

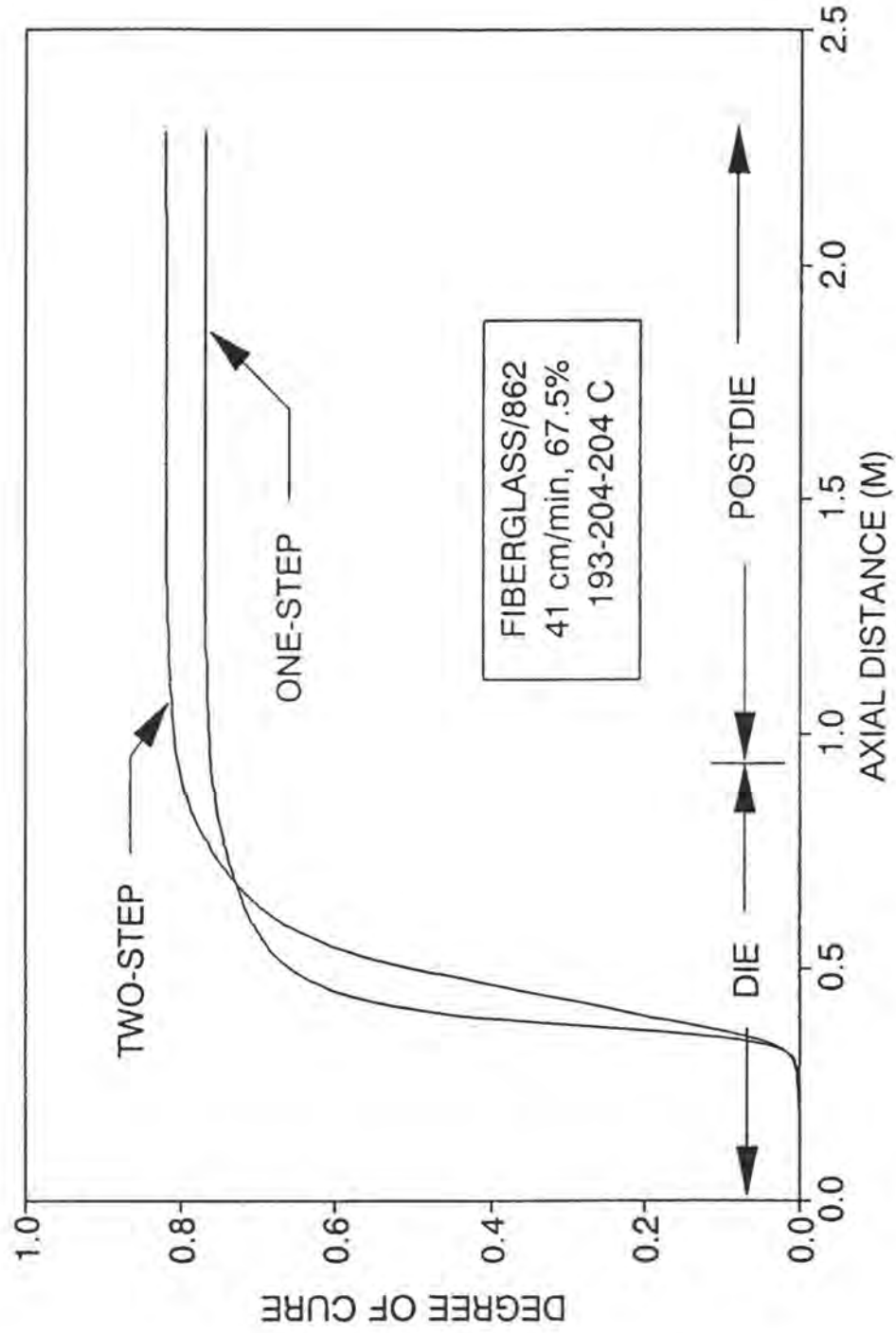

Fig. 12 Comparison of degree of cure profile predicted by the one-step and two-step reaction rate model for case 10 of Table 1.

B9-38

DYNAMIC AND STATIC TORSIONAL CHARACTERIZATION OF PULTRUDED HYBRID CYLINDRICAL COMPOSITE RODS

Sujit S. Kumar
Automated Analysis Corp.
2805 S. Industrial Hwy
Ann Arbor, Michigan 48104

P. Raju Mantena*
Assistant Professor
Dept. of Mechanical Engineering
University, MS 38677

ABSTRACT

The objective of this paper is to demonstrate the effects of hybridization on the static and dynamic behavior of pultruded composite rods subjected to a torsional mode of deformation. Candidate materials that were tested include cylindrical composites made from unidirectional glass and graphite fibers, and hybrids of glass-graphite/epoxy in various shell-core type configurations, fabricated by the pultrusion manufacturing process. The dynamic torsional stiffness and damping were evaluated by the FFT based impulse-frequency response vibration technique. The static shear modulus was obtained using a conventional low torque torsion tester and the initial tangent modulus method. This study has shown that for a given fiber volume fraction glass/epoxy exhibits higher shear modulus than graphite/epoxy; and hybridization of these two material systems results in better dynamic performance by placing glass fibers in the outer shell region.

KEY WORDS

Pultruded composites, dynamic shear modulus, hybrids, impulse-frequency response technique, shear loss factor, static shear modulus.

* Author for all correspondence. Ph: (601) 232 5990

SYMBOLS

f_n natural frequency of vibration

G static shear modulus of the specimen

G' dynamic shear modulus of the specimen

I_p polar area moment of inertia of the specimen

J polar mass moment of inertia of end mass

L length of the specimen (between grips)

λ_n eigenvalue of the nth mode

ω angular frequency of vibration

ϕ angle of twist at the end of the specimen

ρ mass density of the specimen

T torque

INTRODUCTION

The need to develop and optimize pultruded composite materials is recognized by a broad spectrum of governmental and industrial agencies. For many advanced applications, pultruded composites offer inherent advantages such as structural strength, improved physical properties and reduced cost along with increased life, when compared to the other composite manufacturing processes. Cost-competitive advantages are expected to enable pultruded composites to become traditional materials along side steel, wood and aluminum before the end of the 20th century [1]. By focusing research on the effects of process variables on the thermal, static and dynamic characteristics of pultruded polymeric composite products, innovative material systems can be developed. These new material systems will be important to industry in their goal of providing high quality products and services to customers at the lowest possible cost.

For a number of years, commercial pultruders have used continuous glass reinforcing fibers with a thermosetting resin matrix. Processing of more advanced high-performance material systems such as graphite/epoxy is relatively new and the processing details are not as well understood. In the past few years considerable progress has been made in the Composite Materials Research Laboratory at the University of Mississippi on characterizing the effects of pultrusion process variables on the structural, dynamic and thermal properties of a mono-fiber type graphite/epoxy composite material system [2,3,4]. Innovative developments have also been made on pultruding 'hybrids,' i.e., both glass and graphite fibers in a common epoxy binder. The static, dynamic mechanical properties and the failure mechanisms of these hybrids were compared with mono-fiber type pure glass/epoxy and pure graphite/epoxy pultruded composites. Dynamic characterization is important because these pultruded products (which are usually long and slender) are proposed to be used as structural members in aircraft, helicopter rotor blades, transmission and distribution towers, skis etc. The improved characteristics of these hybrids demonstrate the potential for designing stiff, light and well damped composite structures having a number of practical applications. With the proper design of such hybrid systems it is also possible to obtain materials with high impact resistance, as well as, strength and stiffness.

Among various kinds of fibers, fiberglass and graphite fibers are the most widely used due to certain inherent properties and advantages over others. Glass fibers possess high tensile strength, high chemical resistance, excellent insulating properties with the added advantage of low cost. The disadvantages are low tensile modulus, high specific gravity, sensitivity to abrasion with handling, relatively low fatigue resistance and high hardness. Among the advantages of graphite fibers are their exceptionally high tensile strength-weight ratios and tensile modulus-weight ratios, along with a very low coefficient of linear thermal expansion providing high dimensional stability. However, low impact resistance, high electrical conductivity in certain applications and high cost are the disadvantages. The high cost can be compensated with the high specific weight factor. It has been recognized that 'hybridization' of glass and graphite fibers in a single epoxy matrix could enhance the product performance by achieving a balance between the properties of the mono-fiber type

pure-glass and pure-graphite/epoxy properties. The pultrusion process proved to be very useful and economical for manufacturing such glass-graphite/epoxy hybrids.

With hybrids the location of a particular type of fiber from the neutral axis is very important in determining the structures response to flexural, extensional and torsional loading. It has been recognized, and experimentally verified, that locating the stiffer graphite fibers at regions furthest away from the neutral axis would benefit the flexural rigidity. This does not hold good, however, for torsional loads and as demonstrated in this paper, locating glass fibers in the outer shell region results in higher torsional rigidity along with higher damping.

SPECIMEN FABRICATION

There are basically two ways in which two or more types of fibers can be combined to formulate a hybrid composite: either by laminating layers of each type of fiber or intermingling the fibers in a common matrix. With specially designed pre-form plates and dies, hybrid pultruded composites were produced for this research by intermingling glass and graphite fibers in a common epoxy matrix. The pultrusion process is commonly employed for manufacturing products such as solid rods, flats, hollow tubes and various types of structural sections like angles, channels, hat- sections, I-beams and wide-flanged beams. The major constituents of a pultruded composite are continuous fibers and the binder matrix. During pultrusion raw fibrous reinforcements from a creel are pulled through a resin (usually a thermoset) impregnation bath, through a series of preform plates, and into a heated steel die having the profile and dimensions of the final desired product. The preform plates distribute the fibers evenly, squeeze out the excess resin and bring the material into its final configuration before it actually enters the final die. Final shaping, compaction and curing take place in the die wherein the entrance section is usually water cooled to prevent premature gelation and the rest of the die is heated to promote complete curing of the resin before the pultruded product exits the die.

For the purpose of this investigation various combinations of shell-core type round sections with graphite/glass or glass/graphite fiber arrangements were pultruded in a single pass of the pultrusion manufacturing process. The layup of the hybrid sections was designed to be symmetric with respect to the neutral axis. This symmetry about the neutral axis avoids the effects of temperature changes during the manufacturing process leading to undesirable warping, bending and twisting in the final product. After proper selection of the fiber material, fiber volume and placement combinations, the pultrusion process was prepared to produce the desired hybrid composite sections. A set of special 'preform' and post-die' plates were designed to tailor and maintain the fiber placements as required for each desired combination. In order to minimize the effects of the other pultrusion process variables a set of constant process conditions (die temperatures and pull speed) was maintained during the manufacture of all these combinations.

The objective of this research was to study the general trends in static and dynamic property behavior with respect to hybridization. With the overall fiber content of the 0.95 cm (3/8 inch) diameter pultruded rods fixed at 60% (rest 40% epoxy), a few mixed glass and graphite shell-core type hybrid combinations were produced for comparison with the mono fiber type pure-glass and pure-graphite/epoxy specimens. The feasibility of the pultrusion production process in tailoring and controlling the fiber placement was one of the limiting factors in designing these fiber placement combinations. The desired variations were about 10, 20 and 30% of glass and/or graphite fibers in the shell-core regions. The finally pultruded shell-core type products, three with graphite fibers constituting the shell (around glass core) and the other three with glass fibers in the shell (around a graphite core), are listed below and shown schematically in Figure 1.

1) 60% graphite and 40% epoxy (referred to as pure-graphite)

2) 60% glass and 40% epoxy (referred to as pure-glass)

3) 48% glass, 12% graphite and 40% epoxy

4) 37% glass, 23% graphite and 40% epoxy

5) 30% glass, 30% graphite and 40% epoxy

For combinations 1 and 2, the fibers are uniformly distributed throughout the epoxy matrix. For 3, 4 and 5,

the following shell-core configurations were produced:

a) Glass fibers concentrated on the outer shell and graphite fibers concentrated in the inner core

b) Graphite fibers concentrated on the outer shell and glass fibers concentrated in the inner core

The glass fibers used are E-glass (PPG 2001#112), the graphite fibers are AS4W- 12K (Fiberite) and the resin used in all the runs is Shell EPON-862/W.

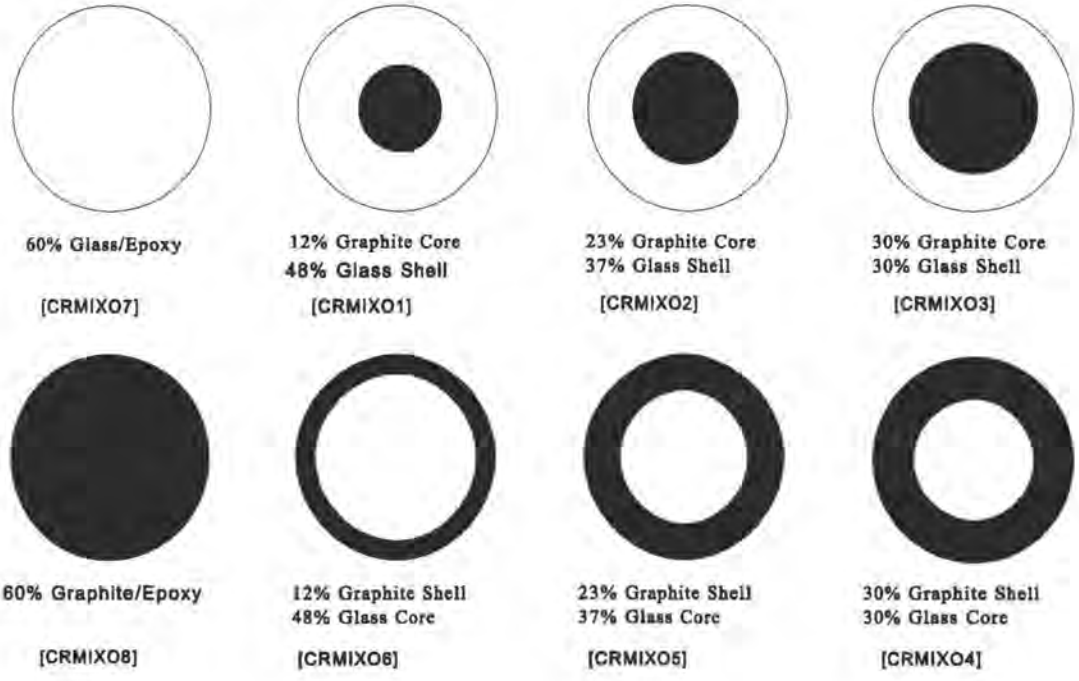

Figure 1. Cross-sections of the pultruded hybrid combinations.

The percent numerical values listed under each of the combinations in Figure 1 represent the actual cross-sectional areas of the glass and graphite fiber tows used in forming the core and annular shell regions of the pultruded product. For example, 101 tows of AS4W-12K graphite fibers were needed for pultruding the 60% pure graphite/epoxy composite and the 60% pure glass/epoxy composite required 28 tows of PPG 2001#112 glass fibers. The other hybrid combinations were manufactured accordingly and the final product was verified for consistency by comparing with the analytical rule of mixtures (ASTM D 792 for estimating composite density). Since it was neither feasible nor economical to produce every possible variation in fiber

content, the above combinations serve a useful purpose for the validation of experimental data with numerical and or finite element models.

EXPERIMENTAL TECHNIQUE

The impulse-frequency response vibration technique has been used for dynamic testing of the pultruded cylindrical specimens. The frequency response was obtained on a HP 35665A spectrum analyzer and the analysis carried out with the help of a HP 9000 series computer. The dynamic shear modulus and damping were calculated from the frequency response spectrum and the half-power bandwidth relationship. The static shear modulus for the plain and hybrid specimens were obtained from a conventional low torque (1000 N-m) Tinius-Olsen torsion tester and the initial tangent modulus method. At least three specimens from each combination were tested to ascertain the scatter in experimental data.

DYNAMIC TORSION TESTS

The dynamic measurements were conducted in a specially designed test fixture (Figure 2) by subjecting the pultruded rods to a torsional mode of vibration [5,6,7]. In this type of testing, the vertically mounted specimen (fixed at the top of an L-plate) was excited by using an impulse hammer with a piezo-electric force transducer in its tip. A small lathe chuck with two projecting 'ears' at diametrically opposite ends was clamped to the lower end of each specimen. One 'ear' of the lathe chuck was impacted with the impulse hammer and the specimen response was picked up by a non-contacting eddy current proximity transducer located at the other 'ear'. During calibration tests, varying lengths of pultruded product were mounted in the torsional set-up and subjected to such off-axis impacts. Under such an excitation the cylindrical specimen undergoes both bending and torsional modes of vibration simultaneously, which are clearly recognizable by sharp peaks on the spectrum analyzer.

A sample length of three inches was found to be too short and rigid for exciting the torsional mode (peak not discernible on analyzer) whereas sample lengths over six inches resulted in the bending mode being dominant. Sample lengths between four to five inches were found to be "optimum" in the sense that torsional

peaks were smooth and distinct, which is crucial for the accurate computation of dynamic shear modulus and damping. If the torsional peaks are not sharp and distinct we have no confidence in the data reduction, especially since loss factor appears to be highly sensitive to any and every extraneous factor. The challenge is to be able to find the test conditions (by performing calibration tests on isotropic material samples) which result in the lowest loss factor (inherent material damping) value and maintain the same conditions for all the pultruded samples. Improper clamping of the specimen (frictional losses), aerodynamic effects, inappropriate curve-fitting routines and/or resolution limits of the spectrum analyzer etc., have been found to result in high values of apparent loss factor [8].

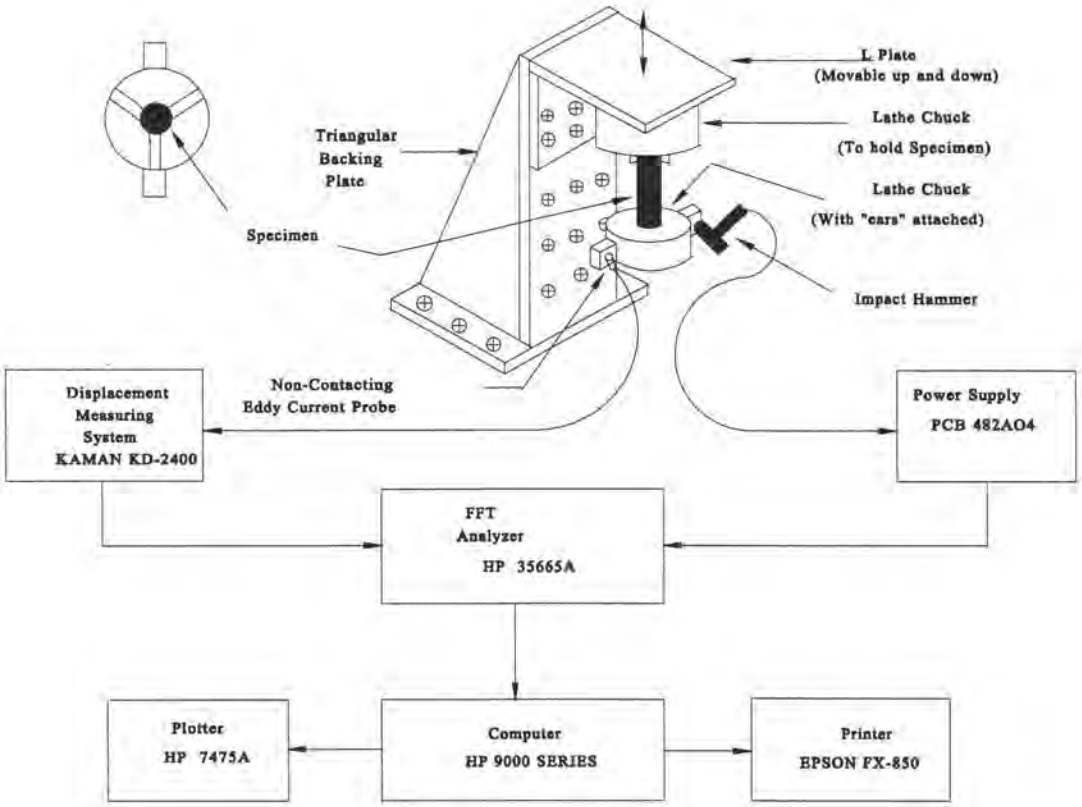

Figure 2. Experimental setup for torsional vibration testing.

The loss factor (a measure of damping) was computed using the half-power bandwidth method on a 'zoomed' narrow band (about 15 Hz span) frequency response function displayed on the screen of a HP35665 spectrum analyzer. As mentioned earlier, when the cylindrical specimens were subjected to off-axis impacts two peaks always dominated the first 100 Hz span on the analyzer. The first peak (around 20 Hz) was identified as the bending mode and the second one (around 35 Hz) was the torsional mode of interest for computing the dynamic shear modulus. Of course, these two peaks moved around depending on the length and type of composite product being tested. The test structure resonances were found to be above 150 Hz and did not interfere with any samples' fundamental torsional peaks/modes.

From the Fourier transformed frequency response function, the dynamic shear modulii of the pultruded rods were computed from the fundamental torsional mode and the loss factors were obtained using the half-power bandwidth relationship. The following characteristic equation for torsional vibration [6] was used in the analysis:

$$\cot \lambda_n = \frac{J \lambda_n}{\rho I_n L} \tag{1}$$

with the corresponding torsional frequency given by,

$$f_n = \left(\frac{\lambda_n}{2\pi L}\right) * \sqrt{\left(\frac{G'}{\rho}\right)} \tag{2}$$

Using the fundamental torsional frequency, mode number, density, and polar mass moment of inertia of the attached mass, Equations (1) and (2) can be solved for the dynamic shear modulus G'. The shear loss factor was calculated by the half-power bandwidth relationship:

$$\eta_G = \frac{\Delta f}{f_n} \tag{3}$$

Calibration tests showed that a 'zoomed' 15 Hz narrow band analysis performed around a sharp resonant peak gave consistent and repeatable loss factor data with the 800 line resolution HP35665 spectrum analyzer and the curve-fit routines used for half-power bandwidth analysis [7].

STATIC TORSION TESTS

The static shear modulus of the cylindrical specimens was obtained from a conventional (1000 N-m) Tinius-Olsen torsion tester using the standard ASTM E 111-82 testing procedure [9,10]. The static shear modulus, G, was calculated from the torque versus angle of twist data obtained from the torsion tester. The torsion tester was interfaced to a computer and the data from the tester was directly recorded on the computer. A program written in QuickBasic served the purpose of data acquisition and analysis from the torsion tester. This gave greater accuracy and higher confidence in the results obtained. From the initial slope of the torque/displacement curve, the shear modulus was obtained according to the following equations:

$$\frac{T}{\Phi} = \frac{G\, I_p}{L} \tag{4}$$

Thus,

$$G = \left(\frac{T}{\Phi}\right) \frac{L}{I_p} \tag{5}$$

The data obtained from static torsion tests also served a very useful purpose in checking the shear modulus computed from dynamic tests. As mentioned earlier, off-axis impact of the end mass attached to the base of the pultruded rods results in the simultaneous excitation of both the bending and torsional modes of vibration. These are portrayed as two closely spaced sharp peaks within the first 100 Hz frequency span of the spectrum analyzer. It is extremely important that the correct (torsional) peak is analyzed and incorporated into Equations 1 and 2 for computing the dynamic shear modulus. Incorporation of the redundant bending peak into this characteristic equation will give erroneous data, which becomes obvious when verified with the static shear modulus computed using the conventional torsion test data along with Equations 4 and 5. The close agreement between these two techniques gave further confidence in the test data.

RESULTS AND DISCUSSION

All the cylindrical samples that were investigated for this research (i.e., pure glass, pure graphite, and the hybrids of glass and graphite) had a common 40% matrix content of EPON 862/W resin. Due to the viscoelastic nature of this matrix it was necessary to determine the effects of frequency (if any, within a 25 Hz range) on the dynamic properties of these pultruded products. With the specially designed torsion test fixture, the effects of frequency on the dynamic shear modulus and damping could be determined by varying either or both the size of the attached lump mass and specimen length, within reasonable levels. Figure 3 shows the dynamic shear modulus and damping data obtained for the pure glass/epoxy and pure graphite/epoxy specimens over a range of frequencies. It is clear from Figure 3 that, for the same fiber volume fraction, pure glass/epoxy exhibits higher dynamic shear modulus than pure graphite/epoxy. The change in frequency is not very large and as seen in this figure the value of dynamic shear modulus does not change significantly as a function of frequency within this test range. However, the damping values change and at a certain frequency glass/epoxy shows higher damping than graphite/epoxy. This can be attributed to the sensitivity of damping to changing pre-loads as a result of adding different structural masses to the bottom of the pultruded samples. Such varying pre-loads have been found to effect both the natural frequency and damping [11], with damping being more sensitive than frequency.

After convincing ourselves that frequency did not have a major effect on these properties and loss factor exhibiting sensitivity to preload variations, only a single 2.2 Kg (4.85 lb.) mass and a fixed specimen length of 12.7 cms (5 inches) were used for further characterization of the pure and hybrid pultruded products. A comparison of the dynamic shear properties of all the combinations is shown in Figures 4 and 5. The different hybrids are represented symbolically on these graphs, signifying the type, volume fraction and location of fibers. Also, the lower X-axis (increasing from left to right) represents the graphite fiber content in each sample, while the upper X-axis (increasing from right to left) represents the glass fiber content; with the remaining 40% consisting of epoxy matrix.

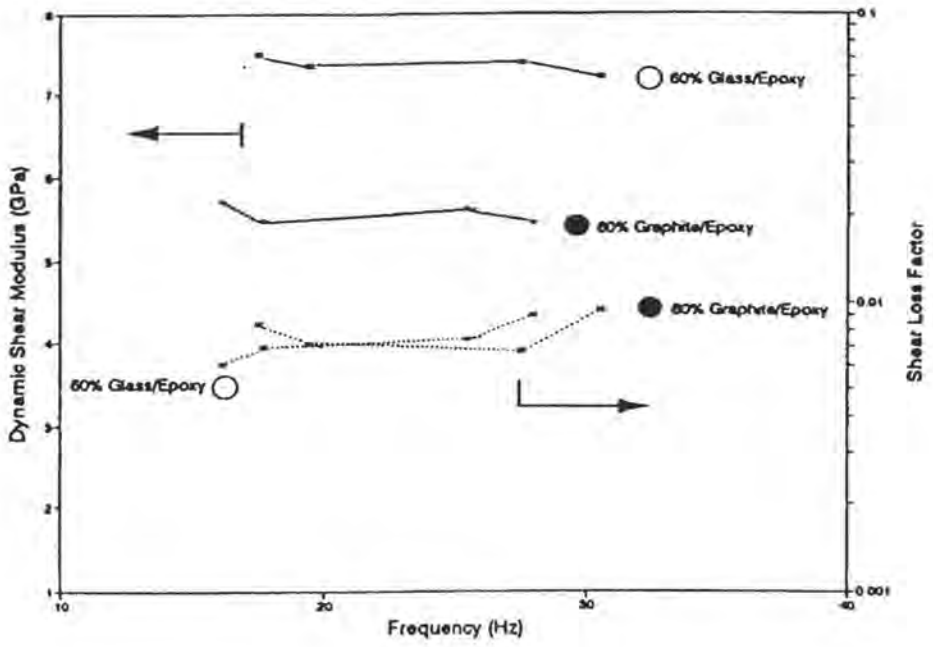

Figure 3. Dynamic shear properties of 60% glass/epoxy and 60% graphite/epoxy specimens as a function of frequency.

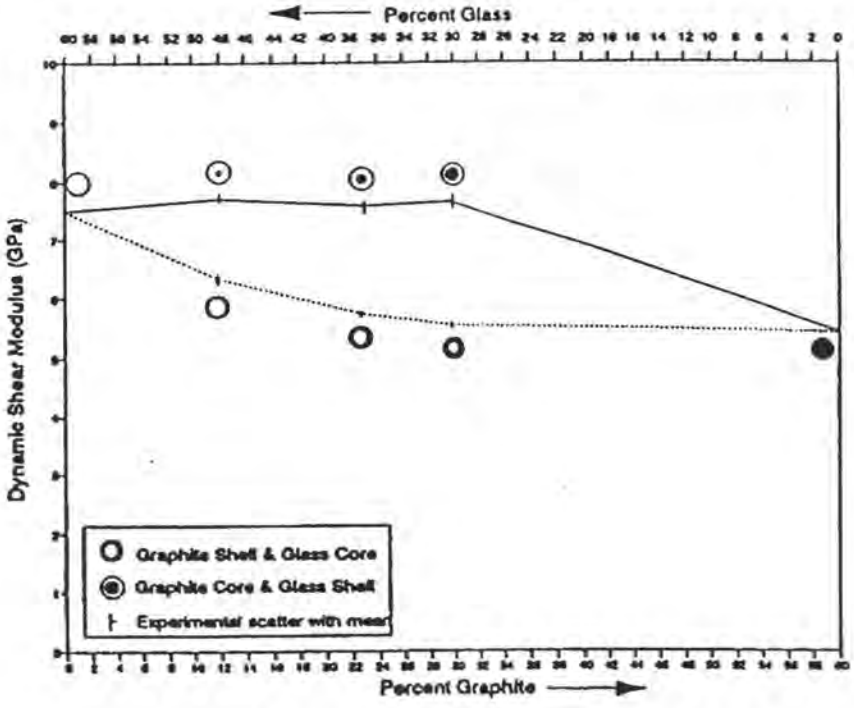

Figure 4. Variation of dynamic shear modulus for all the hybrid combinations.

Figure 4 shows the variation of dynamic shear modulus for all the combinations. As shown in this

figure (and consistent with Figure 3), 60% pure glass/epoxy has a higher shear modulus than 60% pure graphite/epoxy. There is a difference of about 2 GPa between the shear modulii for these two composites. This can be attributed to the fact that glass fibers in addition to being purely isotropic have a higher shear modulus when compared to graphite fibers (which are anisotropic). With a change in fiber type and location from the neutral axis, the modulus changes accordingly. Since glass fibers are stiffer than graphite in shear, locating them in the outer shell region resulted in higher shear modulus compared to locating them in the inner core. This is clearly demonstrated by the upper and lower curves in Figure 4. The curve exhibiting higher shear modulus represents hybrid samples with glass on the outer shell and graphite in the inner core. Also, the hybrid having 48% glass fibers in the outer shell and 12 % graphite in the inner core exhibited marginally higher shear modulus than pure glass/epoxy, suggesting a synergistic effect. The shear modulus is lower and decreases more rapidly with the incorporation of graphite in the outer shell region, and is a minimum for the pure graphite/epoxy among all the combinations. Also shown in the figure is the scatter in experimental data (for three samples tested from each hybrid type) which was found to be minimal.

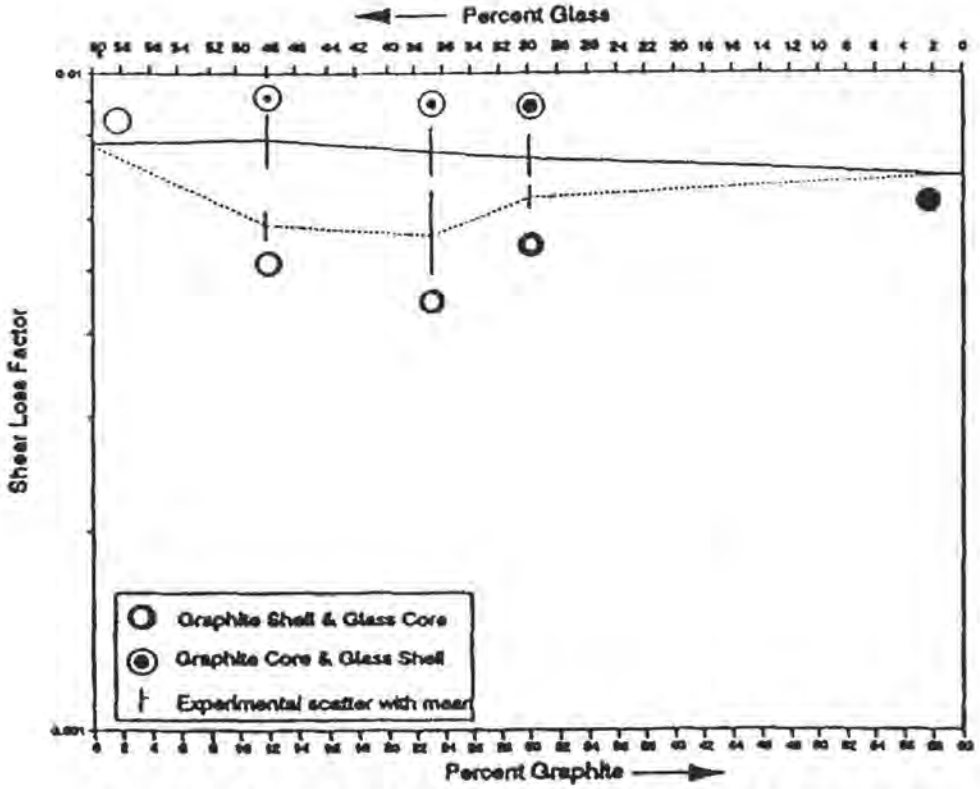

Figure 5. Variation of shear loss factor for all the hybrid combinations.

Figure 5 shows the variation in shear loss factor for these hybrids. As mentioned earlier damping contributions can come from a number of sources such as the shear strain energy stored and dissipated at resonance, bonding between the fibers and matrix, boundary conditions of the test specimen, resolution of the spectrum analyzer, operator carelessness, aerodynamic conditions, etc. In the present investigation, every effort was made through calibration tests to keep all other parameters constant and vary only the constitutive materials in each pultruded product. Among all the combinations, 60% glass/epoxy and their hybrids with the glass fibers located in the outer shell region showed the highest damping values. Considering the larger scatter in experimental data, it appears that there is not a significant variation in the damping properties amongst these combinations, i.e. varying volume fractions of glass fibers in the outer shell region.

It should be noted, however, that although there is not much of a variation in shear loss factor amongst the combinations with glass fibers located in the shell, these hybrids do exhibit higher damping when compared to specimens with similar fiber content but a reversed layup, i.e., graphite fibers in the annular shell and glass fibers in the core. Since all these pultruded products had the same 40% matrix content it was difficult to conclude whether this was a purely matrix dominant response. Complex interactions in terms of the shear strain energy stored and dissipated at a particular location (along with material distribution) under resonant conditions appears to be dictating the dynamic response. It is also possible that, inspite of the precautionary steps taken during experimentation, some of the structural losses attributable to stress concentrations at the specimen clamping interface region is manifested in this damping data. Nevertheless, this experimental data provides qualitative information on the energy dissipative characteristics of these pultruded products with respect to hybridization. The static shear modulus was computed for the pure and hybrid specimens with a standard low torque torsion tester, as outlined earlier. Figure 6 shows the static shear modulus for all the combinations along with the experimental scatter for three samples. A comparison plot of dynamic and static shear modulii is also shown in Figure 7, which is simply an overlay of Figures 4 and 6. It is clear from this figure that there is close agreement between the static and dynamic values of shear modulus (which gives confidence in the test techniques) and that the difference is almost a

constant for all the combinations. The difference between the two values ranged from about 3 to 6 %, which could be attributed to the Viscoelastic nature of the polymeric matrix used for pultruding these specimens.

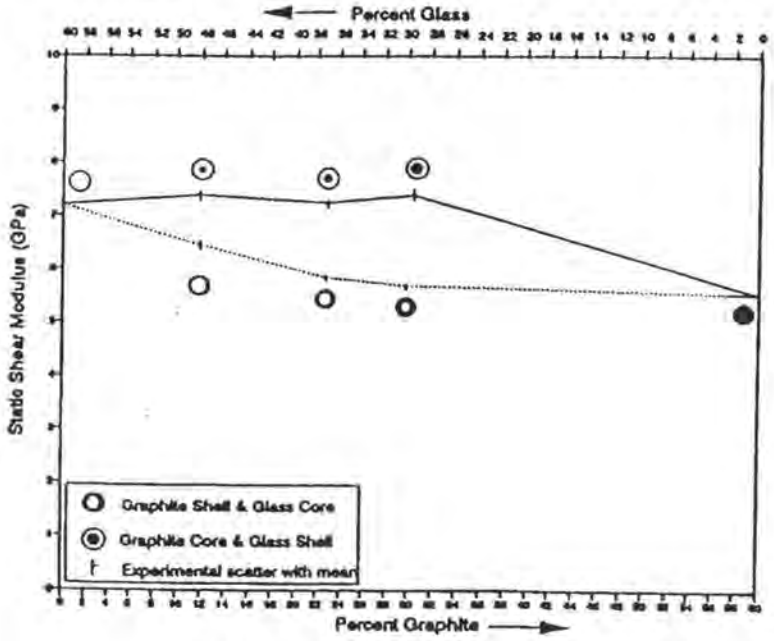

Figure 6. Variation of static shear modulus for all the hybrid combinations.

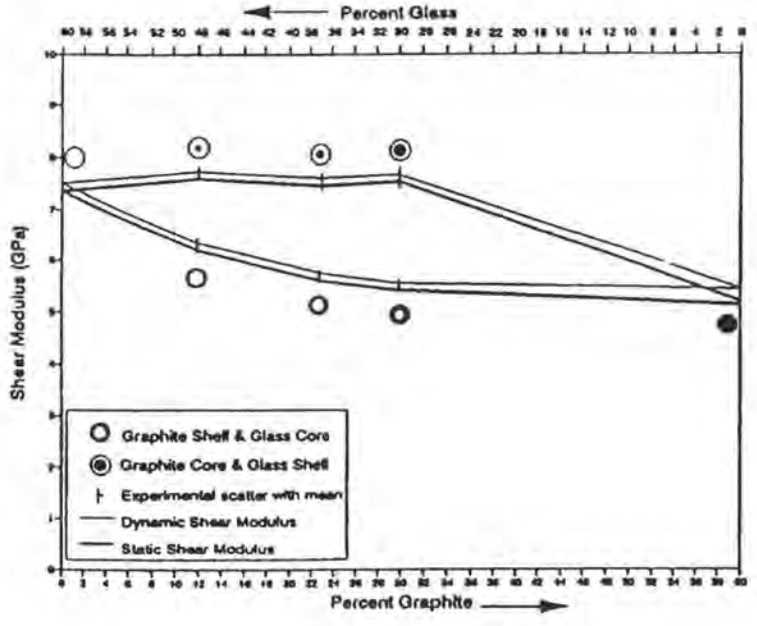

Figure 7. Comparison of the dynamic and static shear modulii obtained for all hybrids.

CONCLUSIONS

The dynamic and static mechanical properties of pultruded hybrid composite rods made of glass and graphite/epoxy have been characterized in the torsional mode of vibration and under static shear loading. It was observed that for the same fiber volume fraction glass/epoxy exhibited higher shear modulus than graphite/epoxy. It was also determined that hybridization of these two materials results in a stiff, light and well damped composite structure having a number of practical applications. The hybrid of 12% graphite and 48% glass, with glass fibers in the outer shell and graphite fibers in the inner core, was found to have better shear properties compared to the pure glass/epoxy and pure graphite/epoxy pultruded products. The impulse-frequency response torsional vibration technique provided an efficient means for the nondestructive evaluation of pultruded cylindrical composite rods.

ACKNOWLEDGEMENTS

Financial support for this research was provided by the National Science Foundation / Electric Power Research Institute (Grant # DDM-9101643), NSF/EPSCOR (Grant # OSR-9108767), the University of Mississippi and the State of Mississippi. The authors also appreciate the help of Mr. Nori Chandrasekhar in the preparation of this paper.

REFERENCES

[1] J.E. Sumerak, 1987, "Understanding Pultrusion Variables for the First Time," *40th Annual Conference, Reinforced Plastics/Composites Institute;* Society of the Plastics Industry, Atlanta, GA.

[2] J.G. Vaughan, P.R. Mantena, R.P. Donti, E. Lackey, Y. Chachad, J.A. Roux, K. Balasubramaniam, and D. Ladnier, 1992, "Material Properties Related to the Pultrusion of Graphite/Epoxy Composite Materials," *Advanced Composites: Design, Materials and Processing Technologies - Proceedings of the 8th Annual Advanced Composite Conference*, 333-342, Chicago, IL.

[3] Murthy Kowsika and P. Raju Mantena, 1993, "Optimal Pultrusion Process Conditions for Improving the Dynamic Properties of Graphite-Epoxy Composite Beams," *Proceedings of NOISE-CON 93, The 1993 National Conference on Noise Control Engineering*, Williamsburg, Virginia, pp. 435-440.

[4] R. Gorthala, J.A. Roux, and J.G. Vaughan, "Resin Flow, Cure and Heat Transfer Analysis for Pultrusion Process," *Journal of Composite Materials*, Vol. 28, No. 6, pp. 486 -506, 1994

[5] T. S. Srivatsan, P.R. Mantena, R. F. Gibson, T. A. Place and T. S. Sudershan, 1989, "Damping Capacity Measurements to Detect Damage in Adhesively Bonded Joints", *Materials Evaluation*, Vol. 47, Number 5, pp. 564-570.

[6] P. Raju Mantena, R. F. Gibson and T. Alan Place, 1990, "A Torsional Impulse-Frequency Response Technique for Evaluating the Dynamic Mechanical Properties of Structural Materials", *Proceedings of the Sixth Annual ASM/ESD Advanced Composites Conference*, Detroit, MI, pp. 477-485.

[7] Sujit S. Kumar, 1994, "Characterization of Dynamic Mechanical Properties of Pultruded Hybrid Cylindrical Composite Rods in the Torsional and Flexural Modes of Vibration", M. S. Thesis, University of Mississippi.

[8] P. Raju Mantena, 1991, "NDE Applications of Damping Measurements" *Proceedings of NOISE-CON 91*, Tarry Town, New York, pp. 361-366

[9] Outwater, J. W, 1989, "The Torsional Failure and Fracture Energy in Shear of a Pultruded Rod", Test Methods for Design Pureowables of Fibrous Composites: 2nd Volume, ASTM STP 1003, C. C. Chamis, Ed., American Society of Testing Materials, Philadelphia, pp. 224-230.

[10] "Standard Test Method for Young's Modulus, Tangent Modulus and Chord Modulus", ASTM E 111 - 82

[11] V.S. Rao, B.V. Sankar, C.T.Sun, R.F. Gibson and P.R.Mantena, 1994, "Analytical and Experimental Investigations of Prestressed laminated Composite Beams with Constrained Viscoelastic Damping Layer" *Journal of Reinforced Plastics and Composites*, Vol. 13, pp. 1023-1042

BIOGRAPHIES OF AUTHORS

Sujit S. Kumar received a BS in Mechanical Engineering from Osmania University, India in 1991 and MS in Mechanical Engineering from the University of Mississippi in 1994. His areas of interest are Computational and Experimental Mechanics, Automobile and Occupant Crash Simulation, Finite Elements, Composite Materials and Structural Dynamics. Sujit is a member of ASME, AIAA, ASCE and is currently doing contract work for the General Motors Company's, Safety and Crashworthiness Group in Troy, MI.

P. Raju Mantena received a BS in Mechanical Engineering from Andhra University in 1973 and a Post-Graduate diploma in Design Engineering from Indian Institute of Technology, Delhi, in 1975. He worked for eight years as a development engineer in Bharat Heavy Electricals Ltd., Hyderabad, India. Dr. Mantena received his MS (1985) and PhD (1989) in Mechanical Engineering from the University of Idaho, after which he was employed as a post-doctoral research associate at Wayne State University in Detroit, Michigan. Beginning Fall 1990, he is an Assistant Professor in the Department of Mechanical Engineering at the University of Mississippi teaching courses in design, vibrations, mechanics of composite materials and experimental stress analysis. His specialization is in optimizing dynamic properties of advanced composite materials and non-destructive evaluation. He has published extensively in these areas, reviewed for journals, organized / chaired technical sessions at conferences and member of ASM, ASME and SAMPE.

OPTIMAL PULTRUSION PROCESS CONDITIONS FOR IMPROVING THE DYNAMIC PROPERTIES OF GRAPHITE-EPOXY COMPOSITE BEAMS

Murthy V. S. L. N. Kowsika and P. Raju Mantena
Department of Mechanical Engineering
The University of Mississippi
University, MS 38677

ABSTRACT

The manufacturing process variables significantly influence the mechanical properties of pultruded composites. In this study, a statistical Central Composite Design (CCD) test pattern has been used to manufacture unidirectional graphite-epoxy pultruded composite beams under carefully controlled process conditions. The influence of significant pultrusion process variables and their effects/interactions on the dynamic mechanical properties were investigated. The pultruded specimens were subjected to free vibration decay tests to determine nondestructively the dynamic flexural modulus and loss factor (a measure of internal damping). Mathematical models were derived based on the observed values of the dynamic properties using regression analysis procedures. These models were used to determine the optimal pultrusion process conditions for improving the dynamic mechanical properties of the finished product. A theoretical model postulating varying distribution of fiber content through the thickness of the pultruded composite is also presented. Static flexural tests and microscopic evaluation were employed to validate the assumption that a thin distinct layer of matrix material is formed on the outer surface of these pultruded products.

---

e-mail: meprm@vm.cc.olemiss.edu

voice: (601) 232-5990

KEY WORDS :

composites, graphite-epoxy, pultrusion, nondestructive testing, regression analysis, vibration analysis, flexural modulus, loss factor, damping

INTRODUCTION

Composite materials/products of constant cross-sectional shape of any desired length can be manufactured with higher productivity using the pultrusion process. Pultruded composites have good surface finish, close dimensional tolerances and improved physical properties when compared with composite products made from other manufacturing processes, indicating a significant market potential.

In the pultrusion process, fibers impregnated with resin are pulled through a heated die allowing sufficient time for the product to cure by setting the pull speed and the die zone temperatures at the desired operating conditions. A schematic of the pultrusion process is shown in Figure 1. Fibers from the creel are pulled through the resin bath, pre-form plate and the heated die by two synchronously operating pullers. The fibers are thoroughly wetted in the resin bath and the pre-form plate is used for removing any extra resin by shaping the uncured composite to the appropriate cross-section of the finished product. The cured product leaving the heated die is cut to the desired length with a cut-off saw at the end of the process line.

The process appears simple but the quality of the pultruded product depends on several process variables and their interactions. The die temperature significantly influences the curing characteristics of the pultruded composite. The process of curing is an exothermic chemical reaction. Initially the uncured composite receives heat from the die until the curing temperature is reached. Then curing initiates on the top surface by liberating heat and progressively moves towards the center portion of the product. After a certain portion of the composite is cured, a reversal of heat flow occurs. For proper curing, a slowly increasing temperature profile along the length of the die is recommended to bring the whole cross-section of the product close to the temperature for initiating gelation (Outwater, 1986). The product pull speed determines the dwell time of the composite in the die and influences the point of gelation, indirectly affecting the curing

characteristics of the composite. High pull speeds increase productivity which is of major interest to manufacturers. Fiber volume fraction influences the stiffness characteristics of the composite. Since, for a particular cross-section the amount of matrix material changes with fiber content, the rate of curing and the degree of cure of the finished product are dependent on the fiber volume fractions (Vaughan et. al., 1992). Apart from the process variables mentioned above, the pull load, viscosity of the resin, filler material, release and curing agents used, and other factors influence the quality of the pultruded product. Since inclusion of all process variables makes this statistical based study cumbersome, only the most significant process variables that affect the mechanical properties of the finished product have been considered (Vaughan et. al., 1990). The process variables included in this investigation are the percent fiber volume, pull speed, die zone 1, zone 2 and zone 3 temperatures (designated, respectively, by the variables X_1, X_2, X_3, X_4 and X_5). A judicious combination of these process variables can be used for manufacturing specimens according to a statistical experimental design such as CCD, to characterize and optimize the pultrusion process (Vaughan, 1988). In previous research, mathematical models were derived for understanding the effects of these process variables on the flexural strength of pultruded graphite-epoxy composite specimens manufactured as per the CCD experimental design. In order to verify the accuracy of the model predictions, samples were once again pultruded according to the recommended factor level settings for obtaining desired values of flexural strength in the finished product. The flexural strength of the finished product was found to be in close agreement with the values predicted by the mathematical model (Lackey, 1993). In the study reported here, the graphite-epoxy specimens manufactured according to the CCD were used to derive mathematical models for optimizing the dynamic mechanical properties, i.e., flexural modulus and loss factor.

Structural components are often subjected to extraneous vibrations which requires characterization of dynamic material properties for modeling real world problems (Mctavish, 1992). Vibration tests provide a rapid and efficient way to determine the dynamic mechanical properties of materials. The impulse-frequency response vibration technique has been effectively used to characterize the dynamic modulus and damping of composite materials (Gibson, et. al., 1987). For the investigations reported here, the time-domain free

vibration decay method which is comparable to the frequency domain impulse technique, has been used for characterizing pultruded materials. Very little research has been conducted to characterize pultruded composite materials under dynamic loading conditions. Conventional materials having good dynamic stiffness usually exhibit low damping and require additional dampers to mitigate extraneous vibration. In polymeric composites, the dampening effect is provided by the viscoelastic matrix, whose properties are in turn dependent on the quantity, type, and degree of cure of the matrix material. Stiffness is provided chiefly by the type and volume fraction of the fibers and the quality of interfacial bond between the fibers and matrix (Mantena et. al., 1991, 1993). Considering the influence of manufacturing process conditions on the dynamic properties of composite materials, an attempt has been made to predict the optimum factor level settings of the pultrusion process variables for obtaining reasonably good stiffness and damping in the finished product.

It has been reported that in the pultrusion manufacturing process a thin sheath of resin surrounds the surface of the uncured composite and that the fibers are pulled towards the center of the die. The role of the interface between the inner die wall and the surface of the composite along with suggestions to manufacture composites with good surface finish have been addressed (Outwater, 1987). Since flexural properties of a composite are influenced by the composition of the surface layers, a theoretical model has been developed postulating uneven distribution of fibers through the thickness of the pultruded beam cross-section. These model predictions were validated with experimental data from static flexural tests and observing the cross-sections using an optical microscope. The possible variation in fiber distribution through the thickness of the pultruded product is substantiated.

EXPERIMENTAL PROCEDURE

Pultruded graphite/epoxy samples were manufactured using an in-house commercial scale pultrusion machine (Pulstar 804). The 92 cm (36 in) long heating die for this model consisted of three heating zones of equal length. Table 1 shows the statistical Central Composite Design (CCD) test pattern utilized for preparing the pultruded samples at various factor level settings and combinations for the five significant

process variables included in this investigation. The processing conditions are coded into five different factor levels (-2, -1, 0, 1, 2) for a total of 32 experimental runs. The manufacturing process conditions for each run are set according to the CCD by making use of the key in Table 1. The raw materials used for manufacturing the composite are graphite fibers (AS4-W-12K) acting as the reinforcing agent and epoxy (EPON® 9310/9360/537) as the matrix. The resin is formulated by using appropriate quantities of accelerator, air release agent, internal release agent, curing agent and filler material (Lackey, 1993). The pultruded composites manufactured according to the experimental design under carefully controlled process conditions resulted in 25.4 by 3.175 mm (1.0 by 0.125 in.) thick rectangular cross-section products. Cantilever beam specimens of length 305 mm (12 in.) were cut-off from the long pultruded product for performing the dynamic free vibration decay and static flexural tests. All samples were kept in vacuum at 10^{-2} torr for at least two days prior to testing for moisture removal and to provide similar environmental history.

A schematic of the experimental setup for performing the free vibration decay flexural tests is shown in Figure 2. Samples are clamped at one end in a vise allowing a cantilever span of 254 mm (10 in.) to facilitate free vibration decay flexural testing. The specimens are subjected to an initial disturbance (by tweaking at the free end) and the stabilized wave form depicting the decaying amplitude-time history for each specimen as displayed on the oscilloscope is digitized and stored on a disk for later analysis. A typical stabilized wave form captured after screening the initial transient disturbance is shown in Figure 3. Each sample was tested twice, with three samples chosen from each run (process condition) to minimize operator and other sources of errors. The digitized data obtained for each wave form is analyzed using a numerical routine to determine the dynamic flexural modulus and loss factor. The average frequency for each wave form is determined and the frequency equation of a cantilever beam in the fundamental mode of vibration is employed for calculating the dynamic flexural modulus. An exponential curve is fitted to the peak amplitude points and the decay of the wave form is used for evaluating the material loss factor. The procedure for acquiring these dynamic properties has been explained in detail elsewhere (Kowsika, 1993, Kowsika and Mantena, 1994).

The experimental value of the static flexural modulus is used as an input to the numerical algorithm for determining the distribution of fibers and matrix through the thickness of the composite. From the CCD design, only the samples manufactured with different fiber volume contents (keeping the other four process variables constant), i.e. test plan number 20, 23 and 28 from Table 1, have been used for this analysis. The static deflection of the beam (δ) is measured with a non-contacting proximity transducer for different dead weights (W) placed in an overhanging pan connected to the free end of the specimen through a wire and pulley arrangement. The loads are applied at a distance 'b' and the deflection of the beam is measured at a distance 'a' from the fixed end. The slope of the linear fit for the observed values of load and deflection ($\Delta W/\Delta\delta$) is substituted in the equation

$$E = \left(\frac{\Delta W}{\Delta \delta}\right)\frac{(3ba^2 - a^3)}{6I} \qquad (1)$$

for computing the static flexural modulus (Beer and Johnston, 1979).

RESULTS AND DISCUSSION

The samples manufactured according to the CCD for various combinations of the process conditions provide considerable information with minimum number of expensive production runs. The influence of the process variables on the response (in this case, the dynamic flexural modulus and loss factor) is not apparent simply by observing the data obtained from different runs. Also, it is difficult to examine the interaction effects of the process variables. Regression analysis procedures are quite effective for understanding the influence of process variables and their interaction effects on the response. Regression analysis was used to fit a second order polynomial for the observed values of the response using SAS software packages (Freund and Littel, 1991). The second order polynomial equation used in this analysis is given by,

$$y = b_0 + b_1 X_1 + \ldots b_{12} X_{12} + \ldots + b_{11} X_1^2 + \ldots \quad (2)$$

Equation 2 consists of fit coefficients such as b_0, crossed terms such as X_{12} (representing process interaction of the variables X_1 and X_2) and quadratic terms such as X_1^2 (square of the variable X_1). The regression output for the entire model (five individual, ten interaction and five quadratic terms) for each response revealed that some of the variables had an insignificant effect on the response. Hence, a reduced model (with fewer parameters) that best estimated the actual experimental values was derived from the full model. This helps to focus attention on the important process parameters and for effective display of the results graphically. These reduced mathematical models were further analyzed using a numerical routine to evaluate the optimum factor level settings that maximizes each response. The predicted optimum factor level settings required for optimizing the dynamic flexural modulus were back substituted into the reduced model for loss factor (to determine the corresponding loss factor), and vice versa. The process conditions that maximizes one response and the corresponding value of the other response as predicted by these regression models are shown in Table 2.

The reduced regression model along with the optimum factor level settings predicted for each response were used to draw response surface plots for the two material properties under consideration, i.e., dynamic modulus and damping (shown in Figures 4-7). Since the three-dimensional response surface plots can accommodate only two variables at a time, Figures 4-7 are drawn by keeping the other process variables, i.e., variables not considered for plotting but appear in the reduced model, at the optimum points (which are also highlighted for each figure). It should be noted that the reduced regression model displayed on top of each figure represents the equation in which the variables take on the values in coded form (-2 to +2), although the axes are shown in actual physical units for easier interpretation of results.

The influence of process variables on the dynamic flexural modulus is shown graphically in Figures 4 and 5. As expected, dynamic flexural modulus increases with percent fiber volume since fibers contribute to the stiffness. This is indicated by the dominant positive coefficient of the variable X_1 in the mathematical model (highlighted on each figure). The influence of the interaction term X_{13} (fiber content and die zone 1

temperature) is evidenced by a decrease in the dynamic flexural modulus with die zone 1 temperature at low fiber volumes and an increase at high fiber volumes. For a particular cross-sectional area, an increase in the fiber content decreases the amount of resin in the composite which in turn reduces the amount of heat liberated due to the exothermic chemical reaction while curing. Additional heat from die zone 1 might be supplementing the required heat for curing. Hence, increasing die zone 1 temperature at high fiber volumes may be influencing the resultant increase in modulus. From Figure 5 it is evident that either high or low die zone 2 temperatures are expected to increase the response (dynamic modulus) if the other process variables are kept at optimum conditions. At low pull speeds, the composite is having adequate time to cure before reaching the intermediate portion of the die, and a lower die zone 2 temperature could prevent over curing (by increasing the heat transfer back to the die). The optimal cure conditions should improve the interfacial bonding between the fibers and matrix, with a resultant increase in the modulus.

Figures 6 and 7 show the response surface plots along with the reduced regression models and optimum process conditions effecting the material damping. It should be noted that the optimum process parameter conditions for maximizing the loss factor are different from the conditions for flexural modulus and caution needs to be exercised when comparing the graphs for these two material properties. It is apparent from Figure 6 that high die zone 1 temperatures result in an increase in loss factor for all the fiber volume fractions, more so for the higher volume fractions. An unequal distribution of cure from the surface to the intermediate layers of the pultruded product is suspected to be causing higher damping under these process conditions. It is interesting that an increase in fiber volume content (contributing to higher stiffness) resulted in an increase in loss factor, a desirable feature for dynamic considerations. It has been reported that the degree of cure marginally drops at high fiber volumes (Vaughan et. al., 1992), consequently increasing the loss factor. It also reiterates that material damping is more sensitive to changes in the degree of cure than the dynamic modulus (Mantena, 1991). Figure 7 indicates that the loss factor also increases with high die zone 2 temperatures and high pull speeds, the reasons for which are not clear.

It is obvious from the above discussion that dynamic properties (flexural modulus and damping) are dependent on several interaction terms, and the inverse relationship between these two material properties may not necessarily hold true for all process conditions. Therefore, it is possible that there might be a combination of process conditions which could yield reasonably good dynamic flexural modulus and loss factor. With this objective, the reduced mathematical models were analyzed further to derive the optimum factor level settings that maximizes both these dynamic properties. Table 3 shows a representative set of pultrusion process manufacturing conditions (derived from the key to the factor level settings given in Table 1) needed for optimizing both these dynamic properties. The general trend of the various possible combinations shown in Table 3 suggests that pultruded composites manufactured with the process conditions set at high fiber content, high pull speed, high die zone 1 and zone 2 temperatures, and a low die zone 3 temperature, are expected to provide the desired levels of damping and stiffness in the final product. It is cautioned that these parameters do not necessarily ensure improvements in other material properties such as tensile, shear strength, etc., for which a set of different processing conditions may be required.

Another objective of this study was to explore the possibility of varying distribution of fibers through the thickness of the composite with a larger concentration of matrix material on the outer surface of the cured pultruded product. As mentioned earlier, considering the nature of the manufacturing process, it has been reported that a sheath of resin encloses the composite and the pressure inside the die reduces at the time of gelation. If the composite is cured under these circumstances, there is a possibility for concentration of matrix material to be formed on the surface of the finished product. The amount of fiber content on the outer most surface of the finished product plays a significant role in influencing its flexural properties.

The basis for this theoretical model is the importance of fiber location with respect to the neutral axis of the beam cross-section, which influences the flexural modulus. For the purpose of theoretical analysis, the beam cross-section was considered to be made up of twelve hypothetical layers with each layer having a 25.5 mm (1 in) by 0.267 mm (0.0105 in) thick rectangular cross-section. The layers were considered to be symmetrically distributed about the neutral axis and the results of the analysis are shown only for the

layers above (or below) the neutral axis (i.e. layers 1 to 6). A numerical routine developed in-house has been used for varying the fiber content in each hypothetical layer and to compute the effective flexural modulus for various possible combinations of fiber distribution through the thickness of each pultruded sample. For this analysis only pultruded samples with three different percent fiber volume (59.7%, 62.1% and 64.4%, with all the other process conditions maintained constant) were considered for theoretical modeling and experimental validation. The experimental static flexural modulus data is needed as an input to the theoretical model. The experimentally obtained values of static flexural modulus for the 59.7%, 62.2% and 64.4% fiber composites were, 118 GPa (17.1 MPsi), 120 GPa (17.4 MPsi), and 125 GPa (18.1 MPsi), respectively. The procedure used for performing the theoretical analysis using the numerical routine is outlined below.

In the theoretical model, for each type of sample, the fiber content of each layer was varied from 0% to 100% to cover all cases of fiber distribution. For each iteration, the modulus of each hypothetical layer is initially computed using the rule of mixtures equation in terms of the fiber and matrix content in that layer. The computed modulus of each hypothetical layer is used for estimating the theoretical static flexural modulus, E_f, of the overall composite using the equation (Blevins, 1979)

$$E_f = \frac{2b}{3I} \sum_{k=0,1,2,..n} E_k(d_{k+1}^3 - d_k^3) \qquad (3)$$

where, n = total number of hypothetical layers

E_k = the modulus of elasticity of layer 'k'

I = area moment of inertia of the beam cross-section

b = width of the beam

d_k = distance from the neutral axis to the bottom of the 'k'th layer, and

d_{k+1} = distance from the neutral axis to the top of the 'k' layer

Since the fiber content in each layer was being varied from 0 to 100%, care was taken to limit the overall fiber volume fractions for each iteration to that of the actually pultruded products being analyzed,

i.e., either 59.7%, 62.2% or 64.4%. Each iteratively computed value of static flexural modulus (E_f, from Equation 3) was compared with the corresponding experimental value (E, from Equation 1), and if they were in close agreement the appropriate percent fiber volume occupied by each hypothetical layer was stored in a separate data file for further analysis. For the next iteration, the fiber content of one of the layers was incremented and the procedure repeated. Numerous iterations performed on each sample resulted in large number of possible combinations that matched the theoretical and experimental values of static flexural modulus. This made it very difficult to derive any conclusions about the nature of fiber distribution through the thickness of the sample. Therefore a frequency distribution numerical routine was adopted to provide more meaningful results.

In this approach, the data file was scanned to determine the number of occurrences for which the percentage fiber content of each layer (i.e. the area occupied by fibers within each hypothetical layer) was within a prescribed range of 0 to 10%. This procedure was repeated by incrementing the limits of the scanning range in steps of 10%, until the maximum limit (100%) was reached. Using the data obtained for each layer, the probability of the number of occurrences (by dividing the number of occurrences obtained for each range with the total number of occurrences) were determined for each range of fiber content. The data of this analysis is shown in Table 4 for the three different fiber volume composite samples. This procedure provided better interpretation of the voluminous data. For example, for the hypothetical layer 1 of the 59.7% fiber content sample, the theoretical model predicts that there is a 45.5% probability that the area occupied by fibers is in the range of 0 to 10%. Similar observations on the 62.2% and 64.4% fiber content samples also show a high probability (71.4% and 95.2%, respectively) that the area occupied by fibers in the outer most layer is less than 10 percent (i.e. about 90% of matrix material). From Table 4 it is interesting to note that even though numerous iterations were performed on each type of sample there is zero percent probability for the fiber content to be greater than 50% for the hypothetical layer 1. The results clearly indicate the possibility of fewer amount of fibers on the outer most layers.

For all the three types of samples, there is a high probability for the cross-sectional area occupied by

layers 2, 3 and 4 to contain more amount of fibers. The region occupied by layers 5 and 6 does not show large variations in the percentage probability over the entire range of fiber distribution. Analysis was also performed considering uniform distribution of fibers through the thickness of the composite. For this distribution, the theoretically computed values of static flexural modulus were 16% higher than the experimental values for all the three different composite samples under investigation. It is evident from this analysis that the distribution of fibers through the thickness of the composite sample is not uniform and that the outer most surface is more likely to contain fewer number of fibers when compared to the rest of the cross section.

Microscopic examination was also performed on few samples having 59.7% fiber content to validate the nature of fiber distribution through the thickness of pultruded products. Sectioned samples mounted using the EPO-KWICK® resin/hardener system were abraded and polished to provide a scratch-free flat surface for microscopic analysis. The samples when viewed under an optical microscope at a magnification of x1350 provided clear distinction between the fiber and matrix phases. The objective of microscopic evaluation was to estimate the percentage fiber volume at various levels through the thickness of the composite sample. Analysis was performed at twelve different locations by incrementing the distance of measurement in steps of 3 mm (through the thickness of the cross-section). This is consistent with the twelve layer model used for theoretical analysis. The microscopic image was projected onto a television screen for determining the volume fractions by the point counting method (ASTM specification E 562). A 7x7 square grid was overlaid on the television screen for counting the number of fibers enclosed in the area of interest. In this method the intersection of a particular phase (either fiber or matrix) with a cross-hair of the grid is usually counted for determining the phase volume fraction. Although this method was adopted for getting a general qualitative idea of the volume fractions in a number of samples, a more rigorous quantitative approach was adopted on a single 59.7% sample. In this procedure the total number of fibers enclosed inside the 7x7 square grid were counted by moving one square at a time. This procedure took more time than the previous one but is believed to yield more reliable results.

Exploratory investigations were initially performed at about 25 locations on the outer layers of the sample cross-section to determine the number of measurement fields required for getting a reasonably good estimate of the fiber content of each hypothetical layer. This procedure is important due to random distribution of the fibers (Voort, 1984). The results indicated that the percentage fiber volume on the outer surface was 42 ‴ 5 percent. Using this data it was determined that in order to obtain 90% relative accuracy in the estimation of results, at least four fields per layer were required. Accordingly, each of the twelve hypothetical layers was analyzed at four different locations across the width. The results of the observed percent fiber content at various locations through the thickness is shown in Figure 8. It is clear from this figure that the percent fiber content is lower at the outer surfaces (0.0 to 0.3 mm, and 3.0 to 3.3 mm) when compared to the central region (1.5 to 2.1 mm). It is also clear that the percent fiber content increases from the outer surface towards the inner region. The scatter in measured data is due to the random distribution of fibers across the width of each layer which is not unusual for this kind of analysis. Typical micrographs obtained at four different locations through the thickness of a graphite-epoxy pultruded composite (59.7% fiber volume) are shown in Figure 9. The micrograph for the outer most region (Figure 9a) clearly shows a distinct layer of matrix material (dark) with the rest occupied by coarsely packed fibers (white). On the other hand, the hypothetical layers closer to the neutral axis are packed densely with fibers (Figure 9d). The other micrographs show characteristics in-between these two extreme cases. It should be noted that only typical micrographs are shown in Figure 9. Other samples showed similar features.

From Figures 8 and 9 it is clear that there is a variation of fiber content through the thickness of the pultruded graphite-epoxy composite products. These figures illustrate this uneven distribution, with fewer fibers (about 45%) present in the outermost regions instead of a desirable uniform distribution (59.7%) in the finished product. The results obtained from the theoretical model for predicting uneven fiber distribution are comparable with experimental results. Both the theoretical and experimental results show that the distribution of fibers through the thickness is not uniform with a concentration of the matrix material at the outer most surfaces. It should also be noted that the theoretical model assumes perfect bonding between the

fibers and matrix, and does not take into account the variation of the fiber content across the width of the sample. This may be the reason for some of the impractical predictions (for the 64.4% sample) given in Table 4, showing extreme cases of 0% or 100% fiber contents in the outer and intermediate regions, respectively.

CONCLUSIONS

This study has shown that pultrusion manufacturing process variables influence the dynamic mechanical properties of a graphite-epoxy composite. A representative set of factor level settings to manufacture pultruded composites having desirable dynamic properties has been presented. The adopted procedure for experimentation and optimization is quite general and can be extended to derive other material properties such as strength, fracture toughness, etc. The theoretical model and the results obtained from microscopic evaluation predict that the distribution of fibers through the thickness of the composite is not uniform. The possibility of a thin layer of matrix material being formed on the outer surface of pultruded composite products has been demonstrated.

ACKNOWLEDGMENTS

The authors would like to acknowledge partial support for this work from the National Science Foundation (Grant # DDM - 9101643); the State of Mississippi / NSF Experimental Program to Stimulate Competitive Research (Grant # R - II - 089 - 02064); and the Electric Power Research Institute (Grant # 8007 - 20).

REFERENCES

Beer, Ferdinard P., Johnston,Russel E. Jr., "*Mechanics of Materials*," McGraw Hill, Inc., 1979.

Blevins, Robert D., "*Formulas for Natural Frequency and Mode Shapes*," Litton Educational Publishing Inc., 1979.

Freund, R.J., and Littel, "*SAS® System for Regression*," 2nd ed., SAS Institute, Inc., Cary, North Carolina, 1991.

Gibson, Ronald F., Vidish S. Rao and Mantena P. Raju, "Vibration Damping Characteristics of Highly Oriented Polyethylene Fiber Reinforced Epoxy Composites," *Proceedings of the 32nd International SAMPE Symposium*, Anaheim, CA, April 6-9, 1987.

Kowsika, Murthy V.S.L.N., "*Optimal Pultrusion Process Variables for Improving the Dynamic Flexural Modulus and Damping in Composite Beams*" M.S. Thesis, University of Mississippi, May 1993.

Kowsika, Murthy V. S. L. N. and Mantena, P. Raju, "Experimental Technique to Determine Dynamic Material Properties Using Time-Domain Vibration Analysis," *Journal of Materials Education*, Vol. 16, no.1, 1994, pp. 73-84.

Lackey, E. and Vaughan, J. G., "Effect of Pultrusion Process Parameters on Flexural Strength," *38th International SAMPE Symposium,* May 10-13, 1993, pp. 461-469.

Mantena P. R., Vangipuram, R., Barpanda, D., "Quality Monitoring of Pultruded Glass-Epoxy Composites with Vibration Damping Measurements," NCA-Vol. 16/AMD-Vol. 172, *Dynamic Characterization of Advanced Materials, ASME Winter Annual Meeting* Nov. 28 - Dec. 3, 1993, pp. 51-57.

Mantena, P.R., "NDE applications of Damping Measurements," *Proceedings of NOISE-CON 91*, Tarrytown, New York, July 14-16, 1991, pp.361-368.

Mctavish, D. J., Hughes, P. C., Soucy, Y and Graham, W. B., "Predicted Measurement of Modal Damping Factors for Viscoelastic Space Structures," *Journal of American Institute of Aeronautics and Astronautics*, Vol. 30, No. 5, May 1992, pp 1392-1399.

Outwater , O. John, "The role of interface in the Pultrusion Process,"*42nd Annual Conference, Composites Institute, The Society of Plastics Industry, Inc*, February 2-6, 1987, Session 12-D / 1-5.

Outwater, O. John, "On the Mechanics of Pultrusions," *41st Annual Conference, Reinforced Plastics/Composites Institute, The Society of Plastics Industry, Inc*, January 27-31, 1986, pp. 6-C/1-4.

Vaughan, James G., et. al., "Material Properties Related to the Pultrusion of Graphite/Epoxy Composite Materials," *Proceedings of the 8th Annual ASM/ESD Advanced Composites Conference*, Chicago, IL, November 2-5, 1992, pp 333-342.

Vaughan, James G., Dillard, Terry W and Seal, Ellis C., "A Characterization of Important Parameters for Graphite/PEEK Pultrusion,"*Journal of Thermoplastic Composite Materials*, Vol. 3, 1990, pp 131-149.

Vaughan, James G., "Use of Statistical Design Experimentation to Characterize and Optimize the Pultrusion Process," *Proceedings of the 43rd Annual Conference, The Society of Plastics Industry, Inc*, 1988, 6D:1-6.

Voort, V. G. F., "*Metallography Principles and Practice*," McGraw-Hill Publishing Inc., 1984, pp. 423-435.

Table 1. The Central Composite Design Test Pattern.

Random plan #	Test plan #	Test variables X1	X2	X3	X4	X5
17	1	-1	-1	-1	-1	-1
1	2	1	-1	-1	-1	-1
11	3	-1	1	-1	-1	-1
5	4	1	1	-1	-1	1
18	5	-1	-1	1	-1	-1
4	6	1	-1	1	-1	1
12	7	-1	1	1	-1	1
19	8	1	1	1	-1	-1
10	9	-1	-1	-1	1	-1
2	10	1	-1	-1	1	1
7	11	-1	1	-1	1	1
9	12	1	1	-1	1	-1
6	13	-1	-1	1	1	1
14	14	1	-1	1	1	-1
16	15	-1	1	1	1	-1
13	16	1	1	1	1	1
3	17	0	0	0	0	0
8	18	0	0	0	0	0
15	19	0	0	0	0	0
22	20	0	0	0	0	0
20	21	0	0	0	0	0
30	22	0	0	0	0	0
24	23	-2	0	0	0	0
27	24	0	-2	0	0	0
23	25	0	0	-2	0	0
31	26	0	0	0	-2	0
29	27	0	0	0	0	-2
21	28	2	0	0	0	0
26	29	0	2	0	0	0
28	30	0	0	2	0	0
25	31	0	0	0	2	0
32	32	0	0	0	0	2

Key to the coded levels of the processing variables

Variable	Type of variable	Coded factor level settings -2	-1	0	1	2
X1	Fiber volume %	59.7	60.9	62.1	63.3	64.4
X2	Pull speed (mm/sec)	3.4	4.2	5.1	5.9	6.8
X3	Zone 1 temp. (C)	160.0	165.5	171.1	176.7	182.2
X4	Zone 2 temp. (C)	176.7	182.2	187.8	193.3	198.9
X5	Zone 3 temp. (C)	176.7	182.2	187.8	193.3	198.9

Table 2. Processing conditions to attain maximum value of one desired property with the corresponding value of the other material property.

Process variables					Dynamic flexural properties	
		Die zone temperatures				
Fiber vol. (%)	Pull speed (mm/sec)	Zone 1 (C)	zone 2 (C)	zone 3 (C)	Modulus (GPa.)	Loss factor
64.4	3.4	182.2	176.7	198.9	150.70	0.0061
59.7	6.8	182.2	198.9	----	113.4	0.0078

Table 3. A representative set of processing conditions to obtain reasonably good dynamic properties.

Process variables					Dynamic flexural properties	
		Die zone temperatures				
Fiber vol. (%)	Pull speed (mm/sec)	Zone 1 (C)	Zone 2 (C)	Zone 3 (C)	Modulus (GPa.)	Loss factor
63.7	6.5	182.2	198.9	176.7	129.7	0.0065
64.0	6.6	181.1	197.8	178.9	129.6	0.0063
64.0	6.6	182.2	196.7	178.9	129.6	0.0062
64.0	6.6	182.2	197.8	180.0	129.5	0.0065
64.0	6.8	178.9	196.7	176.7	129.8	0.0061
64.0	6.8	181.1	195.6	177.8	129.6	0.0061
64.0	6.8	182.2	196.7	180.0	129.5	0.0065
64.2	6.6	178.9	197.8	180.0	129.6	0.0061
64.2	6.6	181.1	196.7	181.1	129.6	0.0060
64.2	6.6	182.2	196.7	182.3	129.6	0.0061
64.2	6.8	175.5	197.8	177.8	129.7	0.0060
64.2	6.8	175.5	198.9	178.9	129.7	0.0063
64.2	6.8	176.7	197.8	178.9	129.6	0.0062
64.2	6.8	176.7	198.9	180.0	129.6	0.0064
64.5	6.5	181.1	198.9	184.5	129.9	0.0062
64.5	6.8	177.8	197.8	182.3	129.8	0.0063
64.5	6.8	182.2	195.6	185.6	129.7	0.0061

Table 4. The percentage probability predicted by the theoretical model for various ranges of fiber content through the thickness of pultruded graphite-epoxy composites.

Sample type	Range of fiber content (%)	Percentage probability obtained for each layer for various ranges of fiber content					
		Layer 1	Layer 2	Layer 3	Layer 4	Layer 5	Layer 6
59.7%	0 - 10	45.5	0.0	0.0	0.0	15.3	6.6
	10 - 20	30.1	0.6	0.0	0.0	14.0	7.5
	20 - 30	16.3	2.2	0.0	0.0	13.0	8.4
	30 - 40	6.6	4.2	0.0	0.0	0.0	9.4
	40 - 50	1.5	6.8	0.0	0.0	11.0	10.4
	50 - 60	0.0	10.4	1.7	0.0	9.8	11.4
	60 - 70	0.0	14.4	8.1	0.9	9.0	12.5
	70 - 80	0.0	19.5	18.1	8.8	8.0	13.5
	80 - 90	0.0	24.1	29.5	29.0	10.4	12.7
	90 - 100	0.0	17.8	42.4	61.2	9.6	7.5
62.2%	0 - 10	71.4	0.0	0.0	0.0	21.3	3.1
	10 - 20	24.5	0.0	0.0	0.0	18.0	4.5
	20 - 30	4.1	0.0	0.0	0.0	16.6	5.5
	30 - 40	0.0	0.0	0.0	0.0	0.0	7.2
	40 - 50	0.0	0.4	0.0	0.0	11.4	9.0
	50 - 60	0.0	3.7	0.0	0.0	9.0	10.8
	60 - 70	0.0	12.2	0.0	0.0	7.1	13.1
	70 - 80	0.0	23.7	7.0	0.0	6.2	15.3
	80 - 90	0.0	36.3	29.7	12.7	4.3	17.6
	90 - 100	0.0	23.7	63.6	87.4	6.2	13.9
64.4%	0 - 10	95.2	0.0	0.0	0.0	32.1	0.0
	10 - 20	4.8	0.0	0.0	0.0	25.0	0.0
	20 - 30	0.0	0.0	0.0	0.0	21.4	2.9
	30 - 40	0.0	0.0	0.0	0.0	0.0	2.9
	40 - 50	0.0	0.0	0.0	0.0	7.1	7.4
	50 - 60	0.0	0.0	0.0	0.0	7.1	7.4
	60 - 70	0.0	0.0	0.0	0.0	3.6	14.7
	70 - 80	0.0	3.3	0.0	0.0	3.6	17.6
	80 - 90	0.0	26.7	0.0	0.0	0.0	22.1
	90 - 100	0.0	70.0	100.0	100.0	0.0	25.0

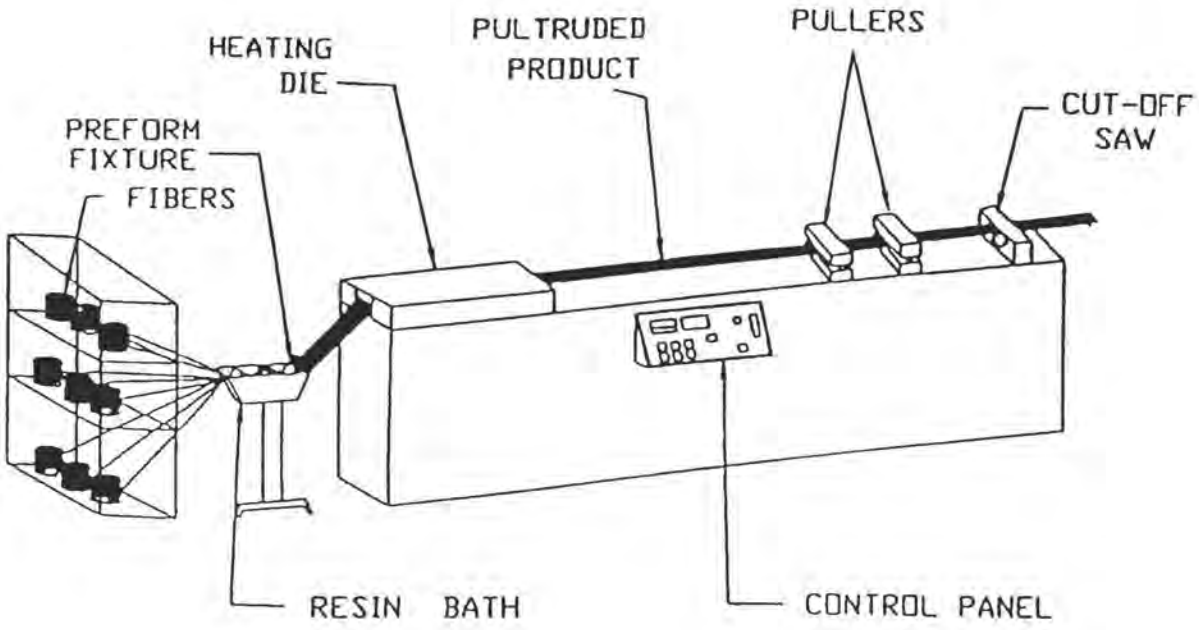

Figure 1. Schematic of the pultrusion process.

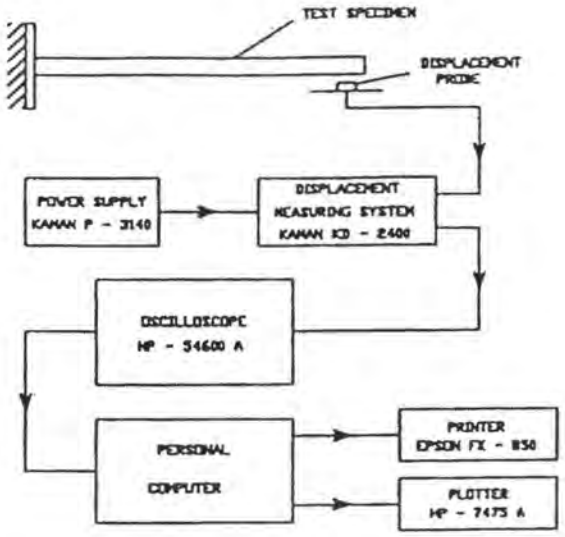

Figure 2. Schematic diagram of flexural free vibration decay test.

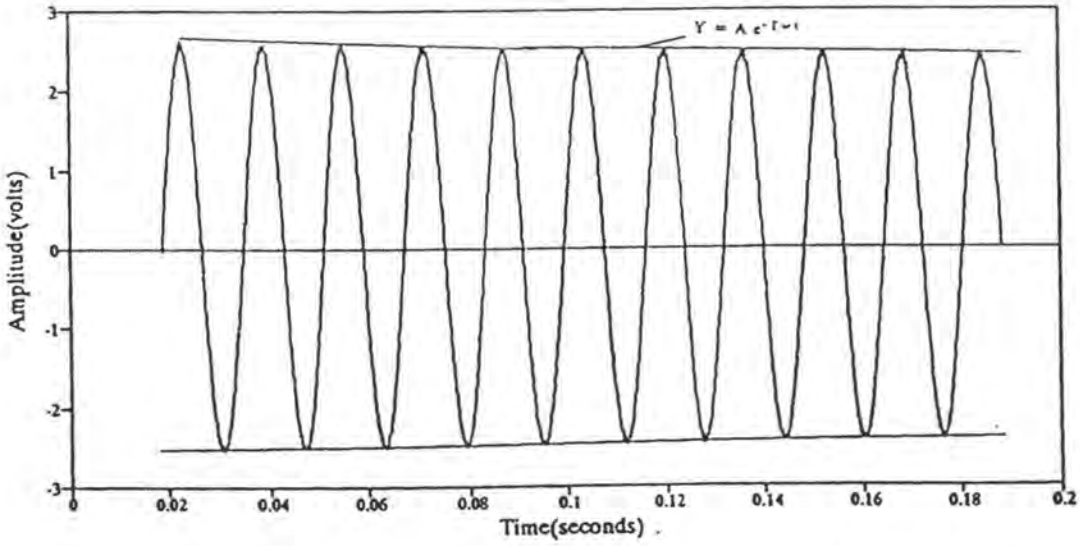

Figure 3. Amplitude-time history of a typical stabilized wave form.

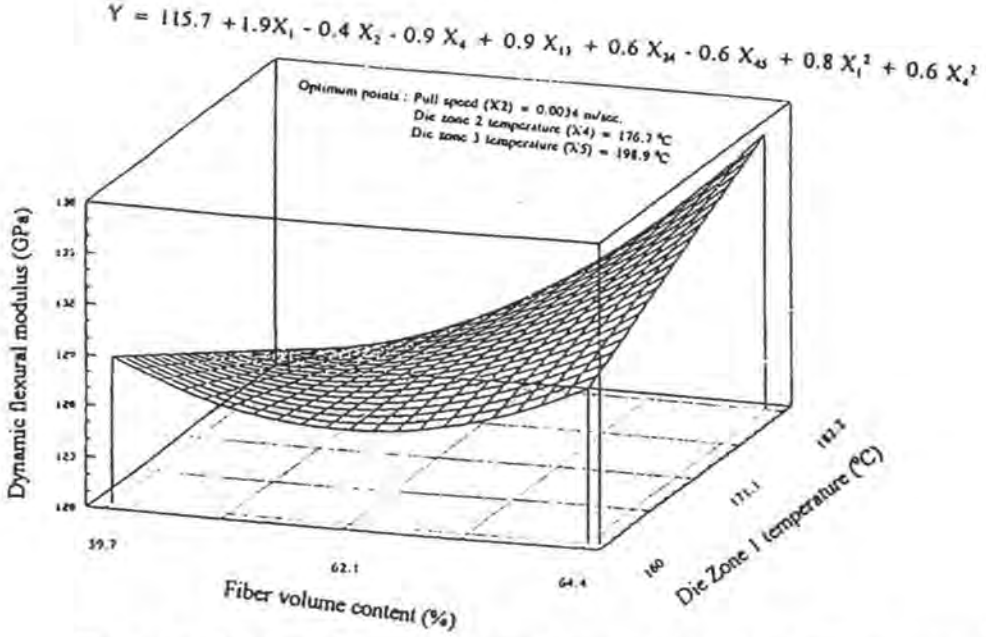

Figure 4. Variation of dynamic flexural modulus with fiber volume content and die zone 1 temperature.

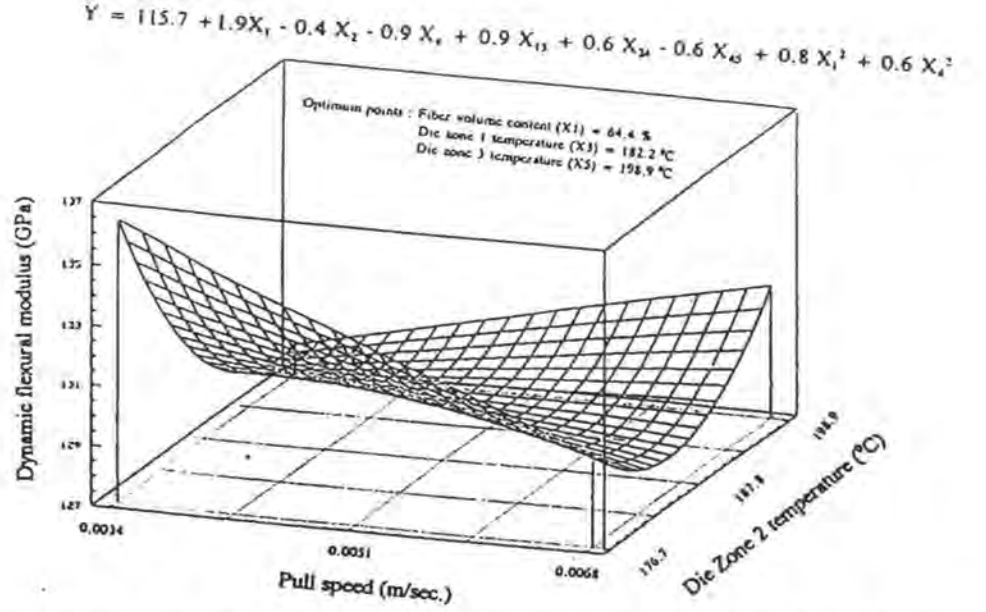

Figure 5. Variation of dynamic flexural modulus with pull speed and die zone 2 temperature.

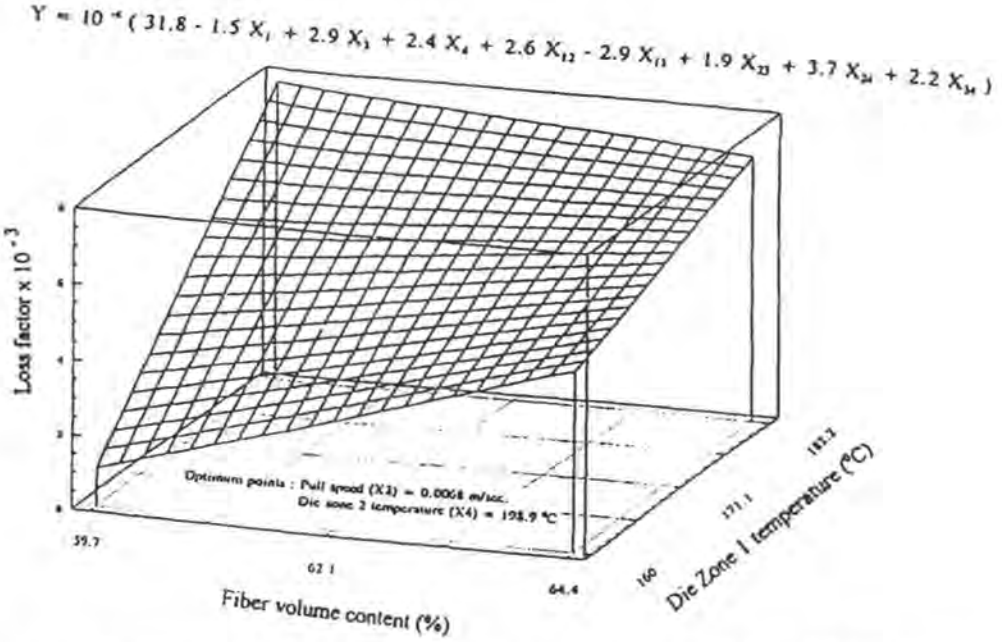

Figure 6. Variation of loss factor with fiber volume content and die zone 1 temperature.

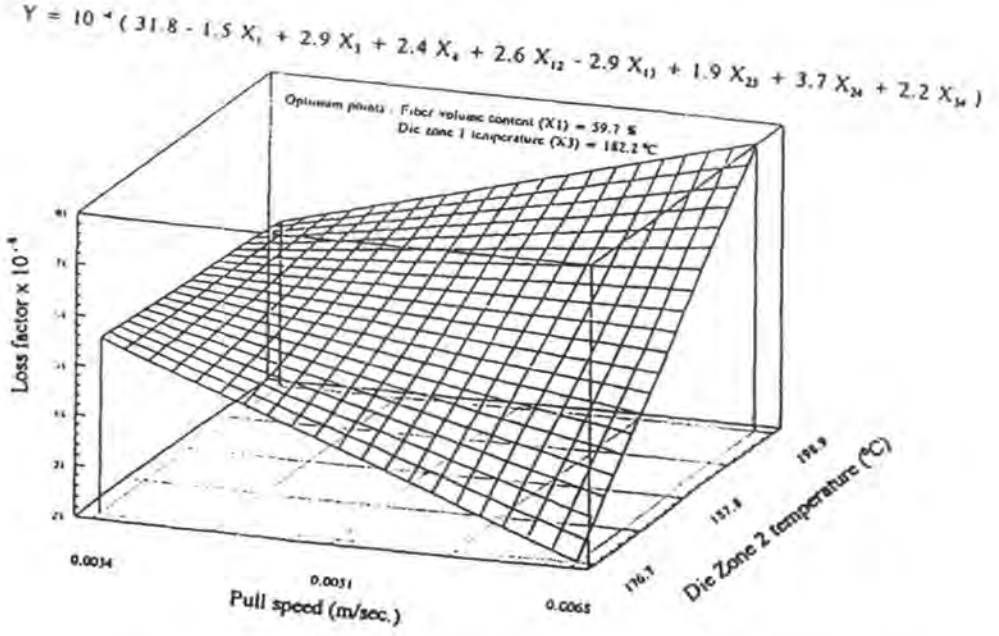

Figure 7. Variation of loss factor with pull speed and die zone 2 temperature.

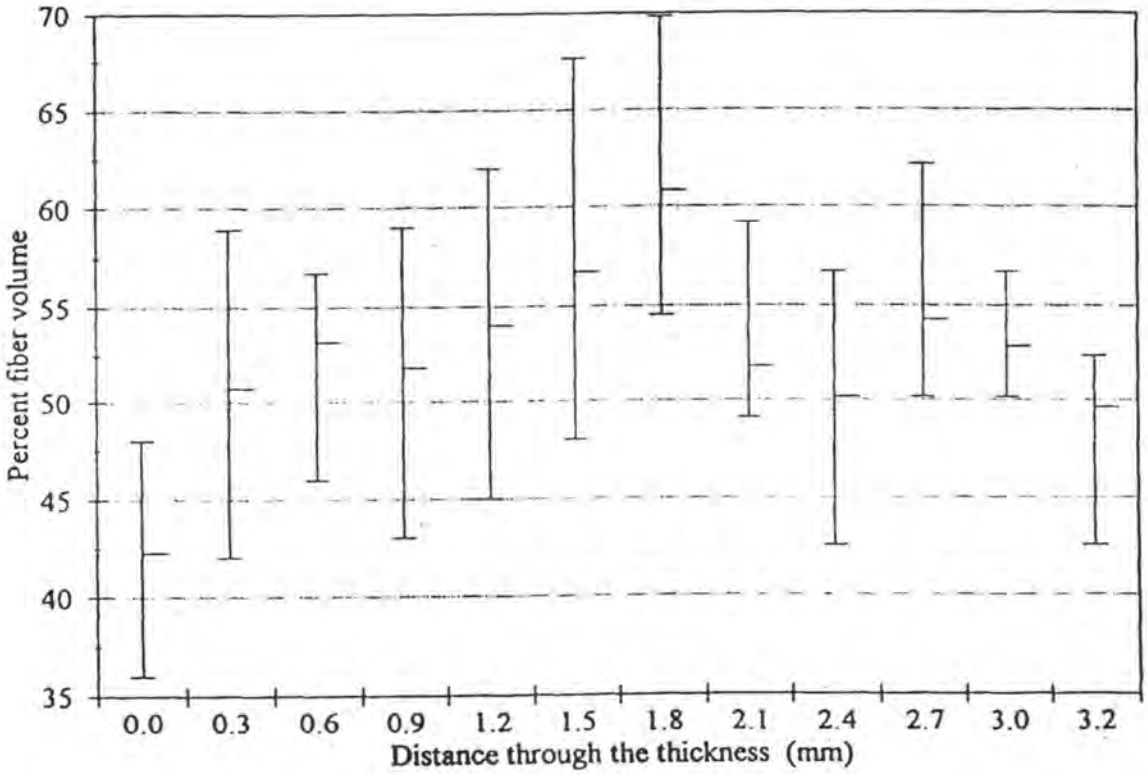

Figure 8. Variation of percent fiber content through the thickness of a typical 59.7% graphite-epoxy pultruded composite.

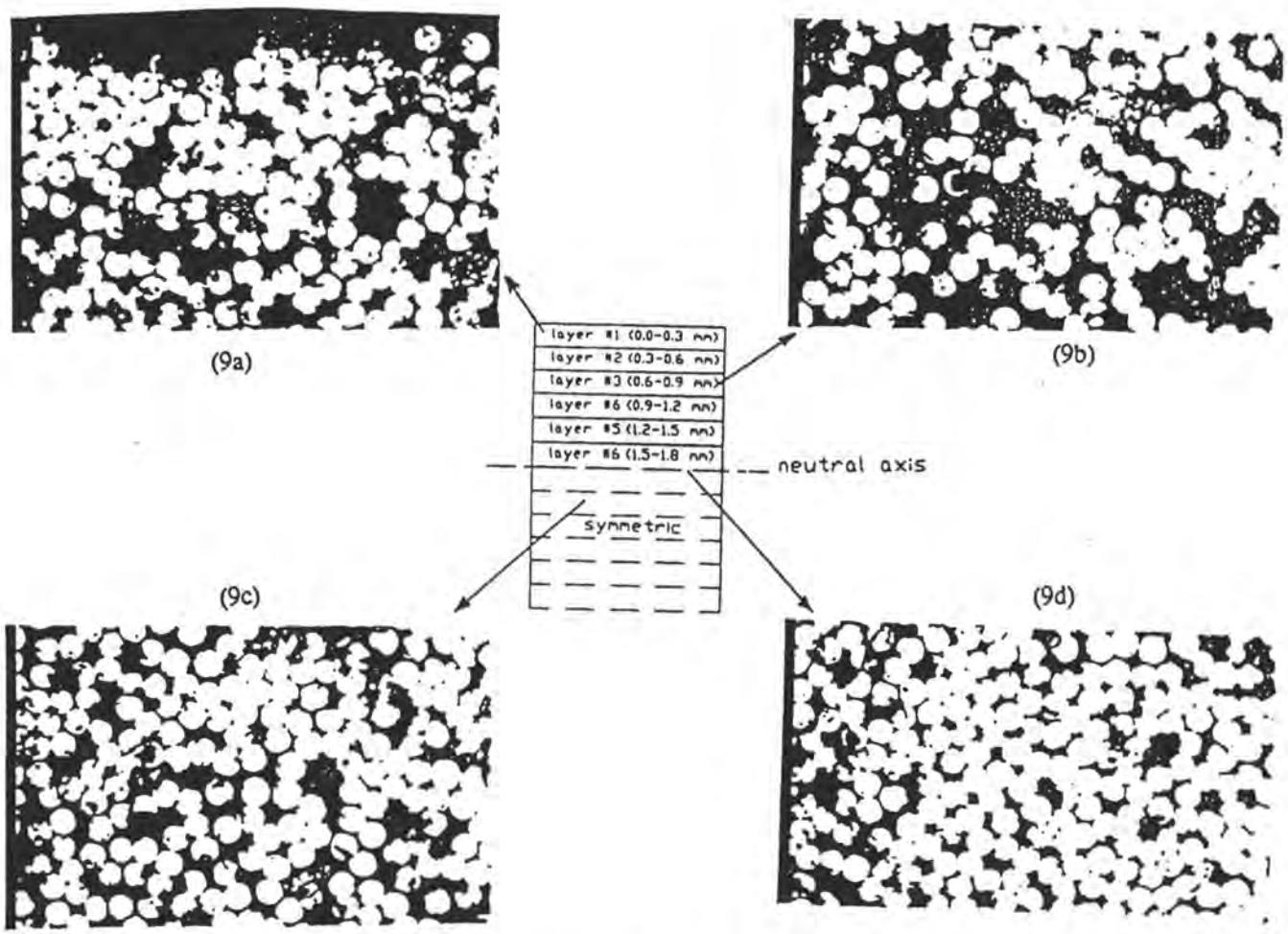

Figure 9. Typical micrographs obtained at various locations through the thickness for the 59.7% fiber content graphite-epoxy pultruded composite (x1350).

BIOGRAPHY OF AUTHORS

Murthy V. S. L. N. Kowsika received a B.Tech. (1990) in Mechanical Engineering from Jawaharlal Nehru Technological University, India and a MS (1993) in Mechanical Engineering from the University of Mississippi. Currently he is a doctoral candidate at the University of Mississippi, working on characterizing and modeling the behavior of pultruded hybrid composite materials subjected to impact loads. Murthy is interested in failure analysis of composites and plans to pursue a research oriented career either in industry or at a university.

P. Raju Mantena received a BE (1973) in Mechanical Engineering from Andhra University and a post-graduate diploma in Design Engineering (1975) from the Indian Institute of Technology, Delhi. He worked for eight years as a Development Engineer in BHEL, Corporate Research and Development Laboratories, Hyderabad, India. Dr. Mantena received his MS (1985) and PhD (1989) in Mechanical Engineering from the University of Idaho, after which he was employed as a research associate in Wayne State University, Detroit. Presently he is an assistant professor in the Department of Mechanical Engineering,the University of Mississippi teaching design, vibrations, mechanics of composite materials, and experimental stress analysis. His research interests are in optimizing the dynamic properties of composites and nondestructive evaluation. He has published extensively in these areas, organized and served as session chair in international conferences, and is an active member of ASM, ASME and SAMPE.

RHEOLOGICAL CHARACTERISTICS AND CURE KINETICS OF EPON 862/W EPOXY USED IN PULTRUSION

R. Shanku, J. G. Vaughan, J. A. Roux
University of Mississippi
University, MS - 38677

ABSTRACT

Differential scanning calorimetry (DSC) was used to measure the kinetic parameters of EPON 862/W (Shell EPON® Resin DPL-862/EPON CURING AGENT® W/EPON CURING AGENT® Accelerator 537) epoxy system. Heat of reaction, degree of cure, pre-exponential constant, and activation energy were determined using dynamic scanning at heating rates of 5, 10, and 20 °C/min. Using a Brookfield DV-III rotational type rheometer, the viscosity was measured isothermally as a function of time at temperatures 23, 35, 45, 55, 65, 80, 90, and 100 °C. Experimental modeling of the rheological characteristics of the resin was conducted using expressions correlating the viscosity data and the degree of cure. Viscosities calculated by the model were in good agreement with data obtained experimentally.

INTRODUCTION

Rheology, or the viscosity history of thermosetting resins, is a critical factor in the processing of thermosetting resins in pultrusion as the viscosity varies with temperature as well as time. The pultrusion process continuously draws a bundle of fibers (rovings or mats) through a resin bath for impregnation, then through a heated die for curing. The initial viscosity of the resin falls rapidly as the die temperatures are experienced, followed by a sharp increase as the cure reaction proceeds. In pultrusion, the knowledge of the resin's rheological behavior is essential in determining the optimum process conditions (pull speed, fiber volume, die zone temperatures, etc.), thus the need for a study of this type. Most analytical models developed require a knowledge of the thermal, chemical, and physical properties of the resin which affect the curing process, which can be a formidable task. In this investigation a suitable method for characterizing the 862/W (Shell EPON® Resin DPL-862/EPON CURING AGENT® W/EPON CURING AGENT® Accelerator 537)

resin system was developed based on previous studies of similar thermoset resins [1-3]. The main parameters used in cure process simulations, heat of reaction, kinetic parameters, degree of cure and the viscosity were investigated.

EXPERIMENTAL PROCEDURE

The first phase of the experimentation involved the monitoring of the time-temperature history of the resin viscosity. The degrees of cure of the resin samples were measured using differential scanning calorimetry (DSC) while viscosity measurements were being recorded. The next phase of the investigation included the analysis and calculations involved in the formulation of the predictive models. The composition of the resin system is given in Table 1 [4].

Degree of Cure and Viscosity Measurements

A TA DuPont 2910 differential scanning calorimeter was used to obtain the reaction kinetics of the resin. The DSC measures the rate of heat generated, (dQ/dt), as a function of temperature or time. The heat of reaction, kinetic parameters and the degree of cure were measured according to the procedures specified by the manufacturer [5]. Resin samples of about 5 mg to 7 mg were taken and tested to obtain the heat of reaction and the kinetic parameters of the resin.

The tests were conducted at three different heating rates (5, 10, and 20°C/min.) to obtain the kinetic parameters (Figure 1). The heats of reaction from the dynamic scans are independent of the heating rate, thus the total heat of reaction of resin at room temperature was considered to be the average value of a number of dynamic scans at 20°C/min. of the resin within 50 minutes of resin mix. The heat of reaction was calculated by

$$H_r = \int_0^t (dQ / dt)\, dt \qquad (1)$$

where H_r is the heat given off by the sample from time zero to time t, until the cure reaction is complete, and dQ/dt is the heat flow rate per unit mass (Figure 1). The experimental degree of cure, α, was obtained from the heat of reaction and is expressed as

$$\alpha = 1 - (H_s / H_r) \qquad (2)$$

where H_s is the heat of reaction of the sample given by the DSC dynamic scans and H_r is the total heat of reaction.

The viscosity measurements were made using a Brookfield DV-III programmable, spindle type rheometer. The rheometer used was of the rotational type which measures the torque required to rotate an immersed element (the spindle) in a fluid. The spindle is driven by a synchronous motor through a calibrated spring. Deflection of the spring is indicated by a digital display which is the viscous drag or resistance to the flow of the fluid. For a given viscosity, the viscous drag is proportional to the spindle's speed of rotation and is related to the spindle's geometry. The higher temperature runs were performed using the Brookfield Thermosel system. The clearance between the spindle periphery and the inner wall of the sample chamber was only 600 microns [6]. Spindle speed selected was 0.2 rpm.

The viscosity (in centipoise) was measured isothermally at 23, 35, 45, 55, 65, 80, 90, and 100 °C (73.4, 95, 113, 131, 149, 176, 194, and 212 °F) as a function of time. The experiment time required ranged from 450 minutes at 23°C to 20 minutes at 100°C minutes. The resin samples were taken from the viscometer chamber at these various temperatures and tested using the DSC to obtain the degree of cure of the resin at various intervals of time.

RESULTS AND ANALYSIS

The data acquired from the viscosity and DSC experiments were analyzed to develop predicted degree of cure and viscosity models. To obtain a model which predicts the degree of cure of a resin at a particular temperature and time, accurate temperature and time measurements are necessary. During the viscosity measurements care was taken to ensure the accurate monitoring of the time-temperature history of the resin system.

Predicted degree of cure model

The total heat of reaction (H_r) was determined to be 341 Joules/gram which was the average value of a number of dynamic scans performed within 50 minutes of resin mix. The heat released by the sample (H_s) after it has been at a certain temperature for a certain period of time was obtained from the DSC scans. As done in a previous study using the EPON 9310 and 9420 epoxy resin systems [3], the present study also assumed an Arrhenius behavior. Since the resin selected for this investigation was an epoxy resin system, the DSC thermal stability kinetics data analysis program was used to analyze data obtained by running samples at different heating rates. The program operates in accordance with ASTM method E-698, "Standard test method for Arrhenius kinetic constants for thermally unstable materials." The basis for the analysis was the species reaction [7]

$$d\alpha/dt = K(1-\alpha)^n, \quad K = K_0 \exp(-E_a/RT) \tag{3}$$

where $d\alpha/dt$ is the rate of degree of cure, K is the reaction rate, α is the degree of cure, n is the reaction order, K_0 is the frequency or pre-exponential factor (1/min), E_a is the activation energy (J/mole), R is the universal gas constant (8.314 J/mole-K) and T is the temperature in Kelvin. The kinetic model used by the DSC thermal stability kinetics data analysis program [8] is the first order form of the general rate law described by Equation (3) and is written as

$$d\alpha/dt = f(\alpha)\ [K_0 \exp(-E_a/RT)] \tag{4}$$

where α is the fraction of the resin reacted, t is the time, $f(\alpha)$ is any function of α not involving temperature. A linear heating rate is assumed thus,

$$T = Bt + A, \qquad dT/dt = B \tag{5}$$

where B is the heating rate, t is the time and T is the temperature. By substituting Equation (5) into (4) and solving, the resulting differential Equation (6) shows a linear relationship between the logarithm of the heating rate versus 1/T, the peak temperature at each heating rate.

$$B\ d\alpha/dT = f(\alpha)\ [K_0 \exp(-E_a/RT)] \tag{6}$$

The heating rates used for this study were 5, 10, and 20 °C/min. The activation energy E_a is obtained from the slope of the linear fit of the logarithm of the heating rate versus 1/T as shown in Figure 2. The pre-exponential constant, K_0, is also calculated for different percentage conversions from the plot shown in Figure 2.

The degree of cure of the resin system at every temperature as a function of time was calculated by Equation (3). The equation was integrated using the trapezoidal rule. The resulting equation is as follows:

$$\alpha_{t+\Delta t} = K_0\ (1-\alpha_t)^n\ (\Delta t)\ \frac{\exp(-\frac{E_a}{RT_t}) + \exp(-\frac{E_a}{RT_{t+\Delta t}})}{2} + \alpha_t \tag{7}$$

Equation (7) shows the degree of cure as a function of temperature and time. The kinetic parameters obtained from the DSC, E_a, K_0, and n, and the time-temperature history of the resin monitored, are substituted into this equation to obtain the predicted degree of cure. The predicted degree of cure was calculated at 23, 35, 45, 55,

65, 80, 90, and 100 °C (73.4, 95, 113, 131, 149, 176, 194, and 212°F).

For lower temperatures, i.e., 23, 35, 45, and 55 °C, the kinetic parameters corresponding to the peak conversion were used to calculate the predicted degree of cure as the rate of degree of cure is much lower than that at higher temperatures. At 23 °C, the degree of cure after 450 minutes of resin mix was 8.5 percent but the resin was 52 percent cured after only 20 minutes at 100 °C. Due to this difference in the rate of degree of cure, the kinetic parameters used to calculate the predicted degree of cure for high temperature experiments were the values at 50 percent conversion level and for lower temperatures the values corresponding to the peak conversion level were used. Table 2 lists all the kinetic parameters at peak, 10, 20, 30, 40, 50, 60, 80, and 99.8 percent conversion. Figures 3a and 3b illustrate the predicted degree of cure and the experimental values at 23, 35, 45, 55, 65, 80, 90, and 100°C.

Predicted Viscosity Model

The measured values of the viscosity as a function of time are given in Figure 4. As the viscosity does not vary linearly with the degree of cure as shown in Figure 5, the correlation used in a previous investigation [1] was modified to a quadratic form

$$\mu = \mu_\infty \exp\left(\frac{U}{RT} + K_1\alpha + K_2\alpha^2\right) \tag{8}$$

where K_1 and K_2 are two constants assumed to be temperature dependent. Equation (8) can also be written as

$$\ln\mu = \ln\mu_\infty + \frac{U}{RT} + K_1\alpha + K_2\alpha^2 \tag{9}$$

If a constant A is taken as

$$A = \ln\mu_\infty + \frac{U}{RT} \tag{10}$$

then a second order fit at each temperature between the logarithm of the viscosity from the rising portion of the viscosity curve and the degree of cure gives constants A, K_1, and K_2. The values obtained are shown in Table 3 and Figures 6a and 6b. From Equation (10), a least squares fit between A and 1/T values for the temperatures considered gives the values of U and μ_∞.

$U_{(23 \text{ to } 55\ C)} = 62515$ Joules, $\quad \mu_{\infty\ (23 \text{ to } 55\ C)} = 1.3E\text{-}7$ Centipoise

$U_{(65 \text{ to } 100\ C)} = 25169$ Joules, $\quad \mu_{\infty\ (65 \text{ to } 100\ C)} = 0.077$ Centipoise

Constants K_1 and K_2 are considered temperature dependent and a second order relationship is assumed to exist between K_1 and K_2 and temperature, T in Kelvin, as shown in Equations (11) and (12).

$$K_1 = X_1 + Y_1 T + Z_1 T^2 \tag{11}$$

$$K_2 = X_2 + Y_2 T + Z_2 T^2 \tag{12}$$

A second order regression fit is done between K_1 and K_2 and temperature, T, to obtain X_1, Y_1, Z_1, X_2, Y_2, and Z_2. The coefficients are shown in Table 4. The predicted values of K_1 and K_2 are shown in Table 3 and Figure 6b. These values are used in the viscosity model as employing the correct values of these constants is vital in developing an accurate predictive model. The constants obtained were substituted into Equation (8) to calculate the predicted viscosity as a function of time and temperature. The predicted viscosity and the measured viscosity versus time characteristics for all the temperatures considered for this study are shown in Figures 7a and 7b. Considering the complex reaction mechanism of epoxy curing the results are considered satisfactory.

The viscosity model developed can be used to predict the viscosity at any temperature tested for any particular percentage of cure. The predicted viscosity at 35, 45, 55, 65, 80, 90 and 100 °C for 1, 5, 15, 25, 35, 45, and 50 percent cure are listed in Table 5. The cure curves are obtained from the viscosity model developed from the experimental data.

Analysis of the Viscosity and Degree of Cure Models

Resin used in pultrusion undergoes a wide range of temperatures inside the die. The viscosity of the resin initially decreases and then rises as the cure process begins. The degree of cure model developed predicts the degree of cure as a function of time and temperature using the method employed in this study. Accurate viscosity measurements and appropriate constants are required to obtain reliable predictive models . The analysis of the predicted degree of cure and viscosity models involved the separate analysis of the data obtained at high and low temperature. The viscosity modeling was done only up to 100°C, but the pultrusion die temperatures are much higher, and the viscosity values at die temperatures could be of more practical importance. The present procedure can be used to predict viscosities at die temperatures, only if the appropriate constants are obtained from the experiments conducted at these temperatures.

The viscosity and degree of cure values determined as a function of time can be used directly in modeling the curing process of the EPON 862/W resin system. The analytically developed expressions for the degree of cure and viscosity can provide useful information in resin flow and heat transfer models.

REFERENCES

1. Springer, G. S., Loos, A. C., and Lee, W. I., "Heat of Reaction, Degree of Cure, and Viscosity of Hercules 3501-6 Resin," *Journal of Composite Materials,* Vol. 16, November 1982, pp. 510-520.

2. Dusi, R., Lee, W. I., Criscioli, P. R., and Springer, G. S., "Cure Kinetics and Viscosity of Fiberite 976 Resin," *Journal of Composite Materials,* Vol. 21, March 1987, pp. 243-261.

3. Bhattacharjee, S. K., "Experimental Modeling of the Rheological Characteristics of Epoxy Resins in Pultrusion," Master's Thesis, University of Mississippi, August 1992.

4. Technical Bulletin, *"EPON® Resin 862/EPON CURING AGENT® W,"* Shell Chemical Company, SC:1183-90.

5. Operator's Manual, "DSC 2910 Differential Scanning Calorimeter," TA Instruments, January 1989.

6. "More Solutions to Sticky Problems : A Guide to Getting More from Your Brookfield Viscometer," Brookfield Engineering Laboratories, Inc.

7. Turi, E., A.,*Thermal Characterization of Polymeric Materials,* Academic Press, 1981.

8. Software Manual, "DSC Thermal Stability Kinetics Data Analysis Program,".Version 4.0, E. I. du Pont de Nemours & Co. (Inc.), 1988.

Table 1. Composition of the Shell EPON 862/W/537 resin system [4].

Material	PHR[1]	Function and Composition
EPON® RESIN DPL-862	100	Base of the matrix. Epoxy Bisphenol F (BPF) Resin.
EPON CURING AGENT® W	26.4	Cures the monomer thermoset to a polymeric chain. Non-MDA, aromatic amine curing agent.
EPON CURING AGENT® ACCELERATOR 537	2	Acts as a catalyst to the epoxy resin curing reaction and decreases gel time. Composed of organic salts.
FILLER - CLAY ASP 400-P	20	Filler clay, aluminum silicate
RELEASE AGENT - AXEL-INT 1846	0.6	Mold release agent. Synthetic resins, glycerides, fatty acids and phosphate esters.

[1] PHR is parts per hundred resin

Table 2. Kinetic parameters obtained from the ASTM kinetics method at various conversion levels.

	Kinetics Parameters at Different Conversion Levels		
% Conversion	Activation Energy kJ/mole	Log(Preexp Factor) 1/min	60 min.½ Life Temp. C
Peak (automatic)	74.5	9.444	68.8
10.0	81.4	10.148	78.8
20.0	79.9	9.923	78.8
30.0	76.3	9.356	79.7
40.0	73.2	8.855	81.3
50.0	70.5	8.391	83.4
60.0	67.8	7.912	86.5
80.0	71.3	7.915	105.1
99.8	84.3	9.028	128.6

Table 3.Calculated values of the constants A, K_1, and K_2 at 23, 35, 45, 55 C, and 65, 80, 90, 100 C (Shown in separate tables as they are analyzed separately).

T in Celsius	A Calculated	A Predicted	K_1 Calculated	K_1 Predicted	K_2 Calculated	K_2 Predicted
23	9.76	9.53	-6.42	-6.62	79.78	79.09
35	8.16	8.55	-2.26	-1.72	46.56	48.86
45	7.7	7.78	1.1	0.34	34.37	31.8
55	7.27	7.06	0.38	0.52	21.27	22.12

T in Celsius	A Calculated	A Predicted	K_1 Calculated	K_1 Predicted	K_2 Calculated	K_2 Predicted
65	6.42	6.39	6.55	6.41	16.73	17.48
80	5.95	6.01	4.47	5.49	13.58	11.49
90	5.77	5.77	7.21	6.18	3.35	6.41
100	5.57	5.55	7.41	7.91	1.19	.46

Table 4. Coefficients obtained from Equations (11) and (12).

Constants	K_1	K_1	Constants	K_2	K_2
	23 to 55 C	65 to 100 C		23 to 55 C	65 to 100 C
X_1	-986.806	649.32285	X_2	4197.102	-366.97641
Y_1	6.09357	-3.6627067	Y_2	-24.8466	2.6079151
Z_1	0.0094	0.005209	Z_2	0.036946	-0.00435

Table 5. Predicted viscosity at various degrees of cure.

T in Celsius	1%	5%	10%	15%	25%	35%	45%
23	12318	12,365	15,055	22,686	97,674	990,000	23,000,000
35	5,895	6,199	8,246	14,048	85,658	1,405,275	62,000,000
45	3,164	3,467	4,500	6,872	26,087	189,666	2,600,000
55	1,649	1,777	2,157	2,928	7,548	30,438	190,000
65	623	839	1,319	2,262	8,647	46,886	360,000
80	428	548	787	1,196	3,281	11,331	49,000
90	346	450	644	950	2,281	6,221	19,289
100	288	396	591	883	1,985	4,505	10,319

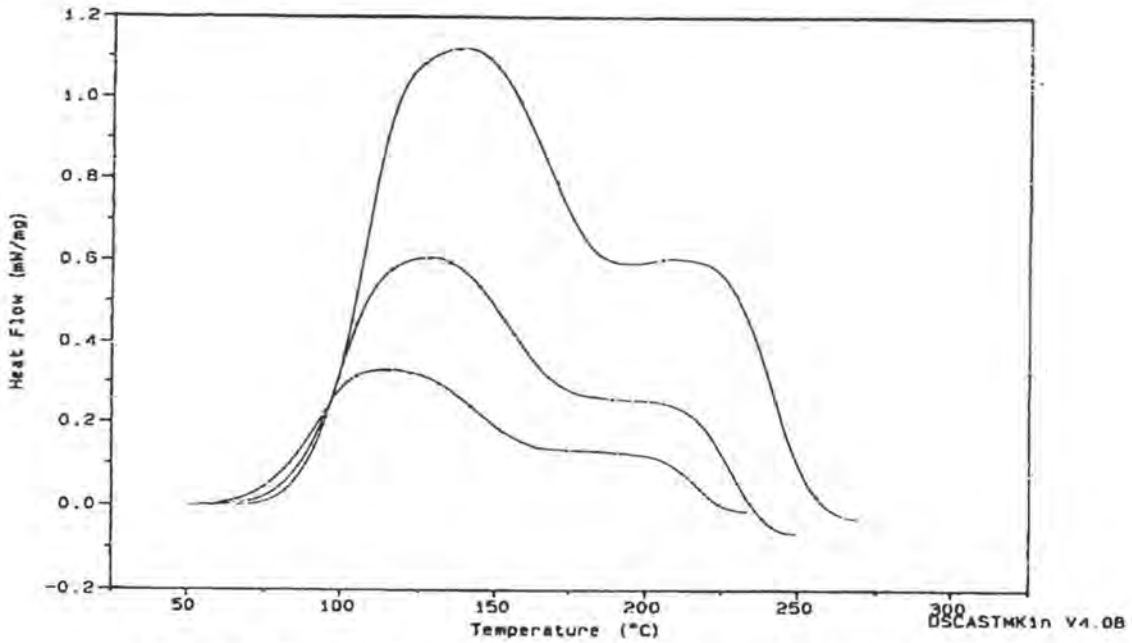

Figure 1 Common thermogram for heating rates 5, 10, and 20°C/min.

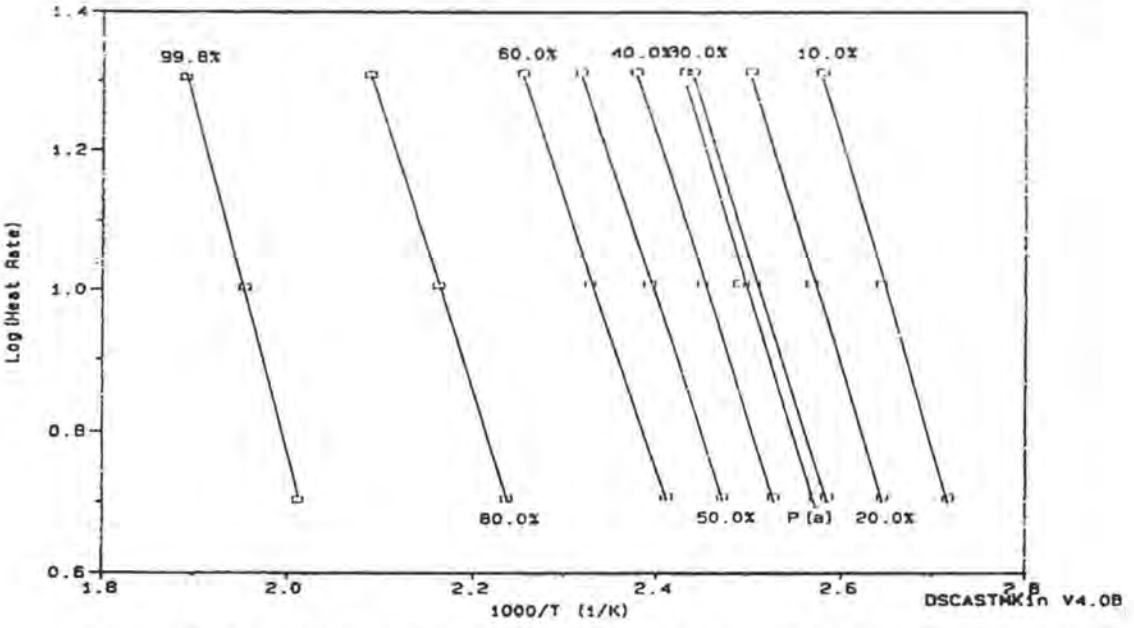

Figure 2. Logarithm of the rate versus 1/T for different degrees of conversion.

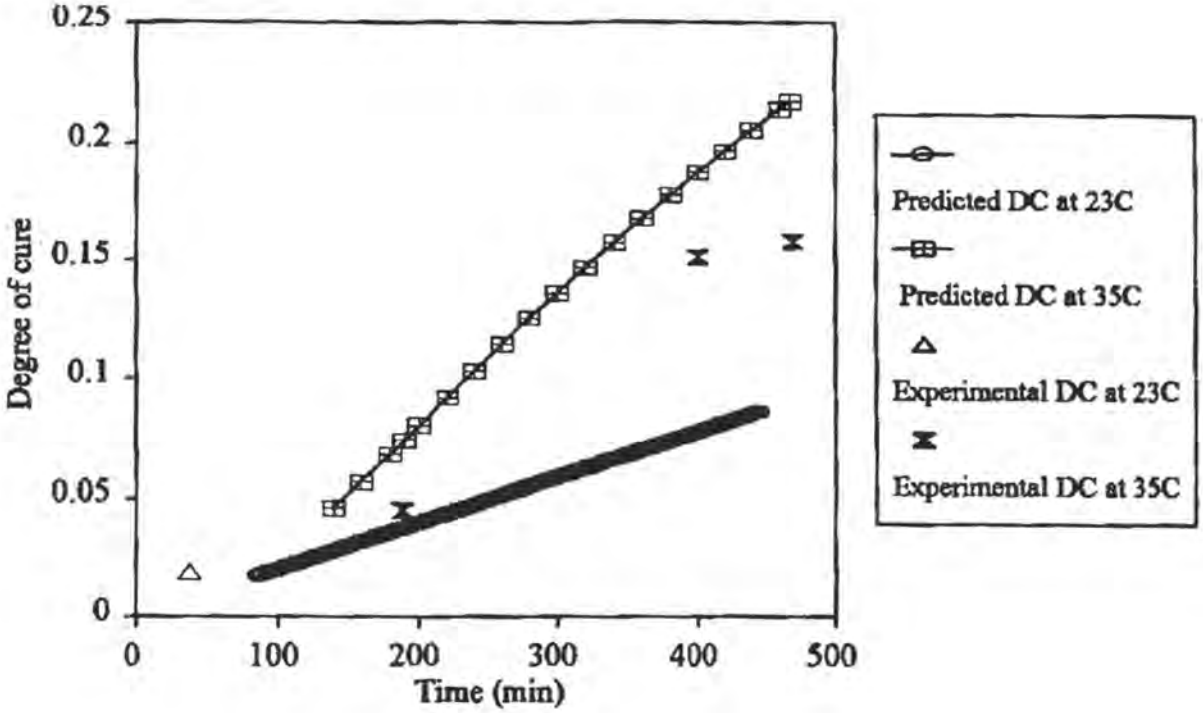

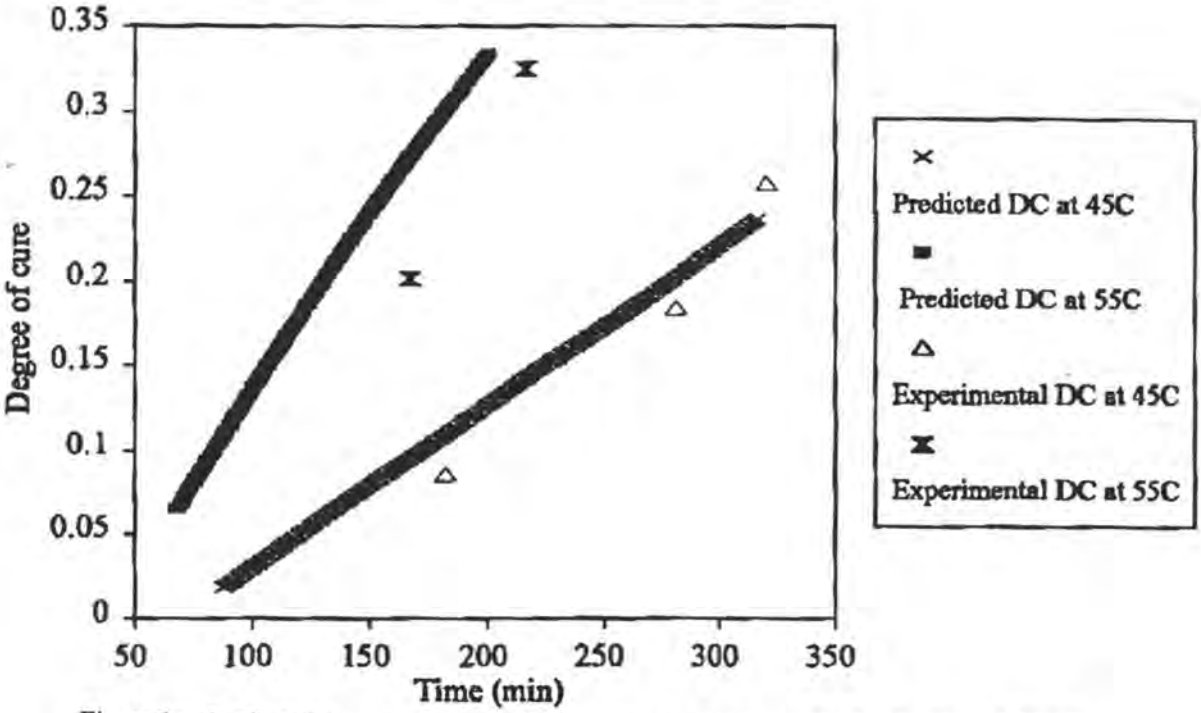

Figure 3a. Predicted degree of cure and the experimental values at 23, 35, 45, and 55 °C.

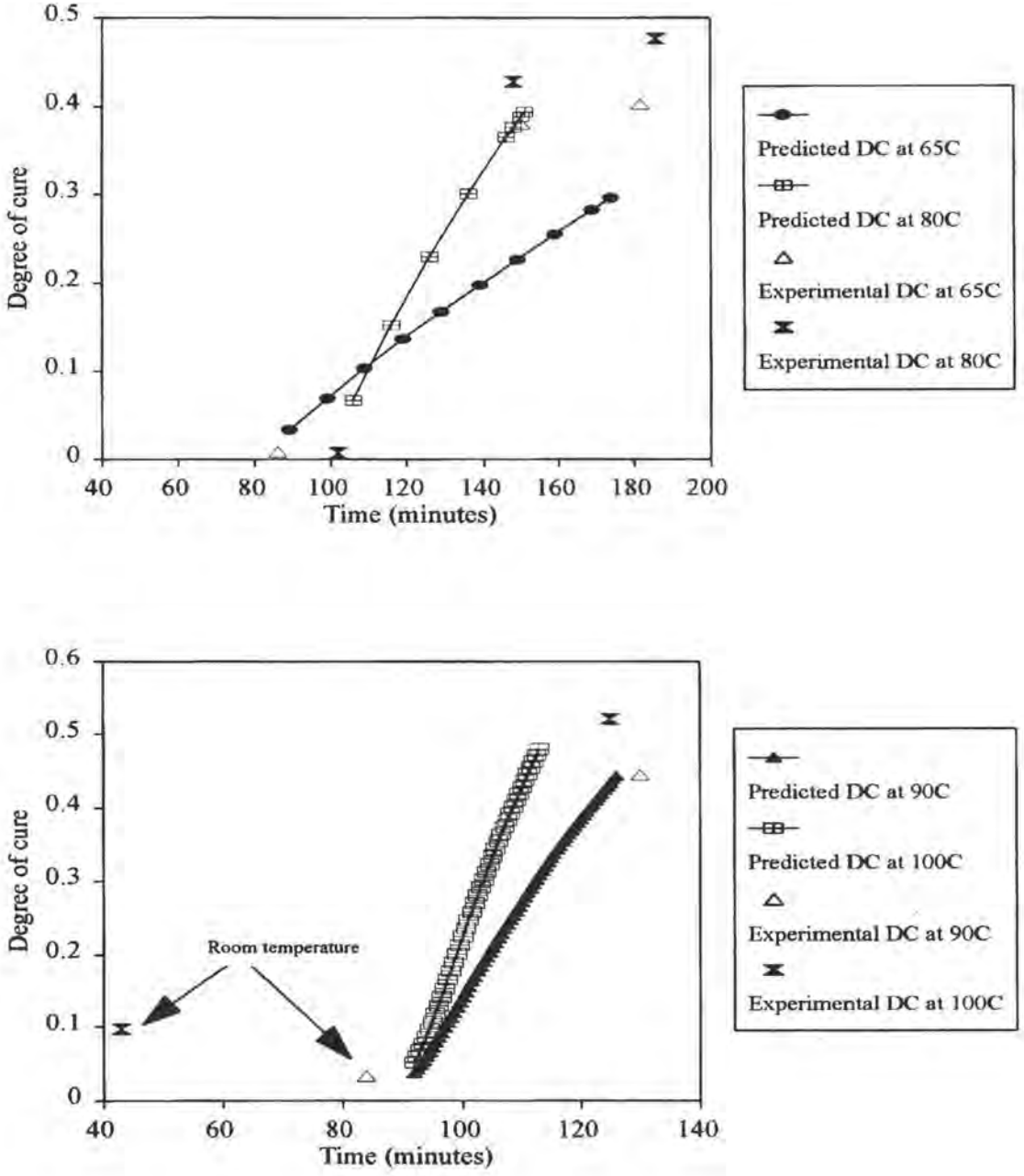

Figure 3b. Predicted degree of cure and the experimental values at 65°, 80°, 90° and 100° C.

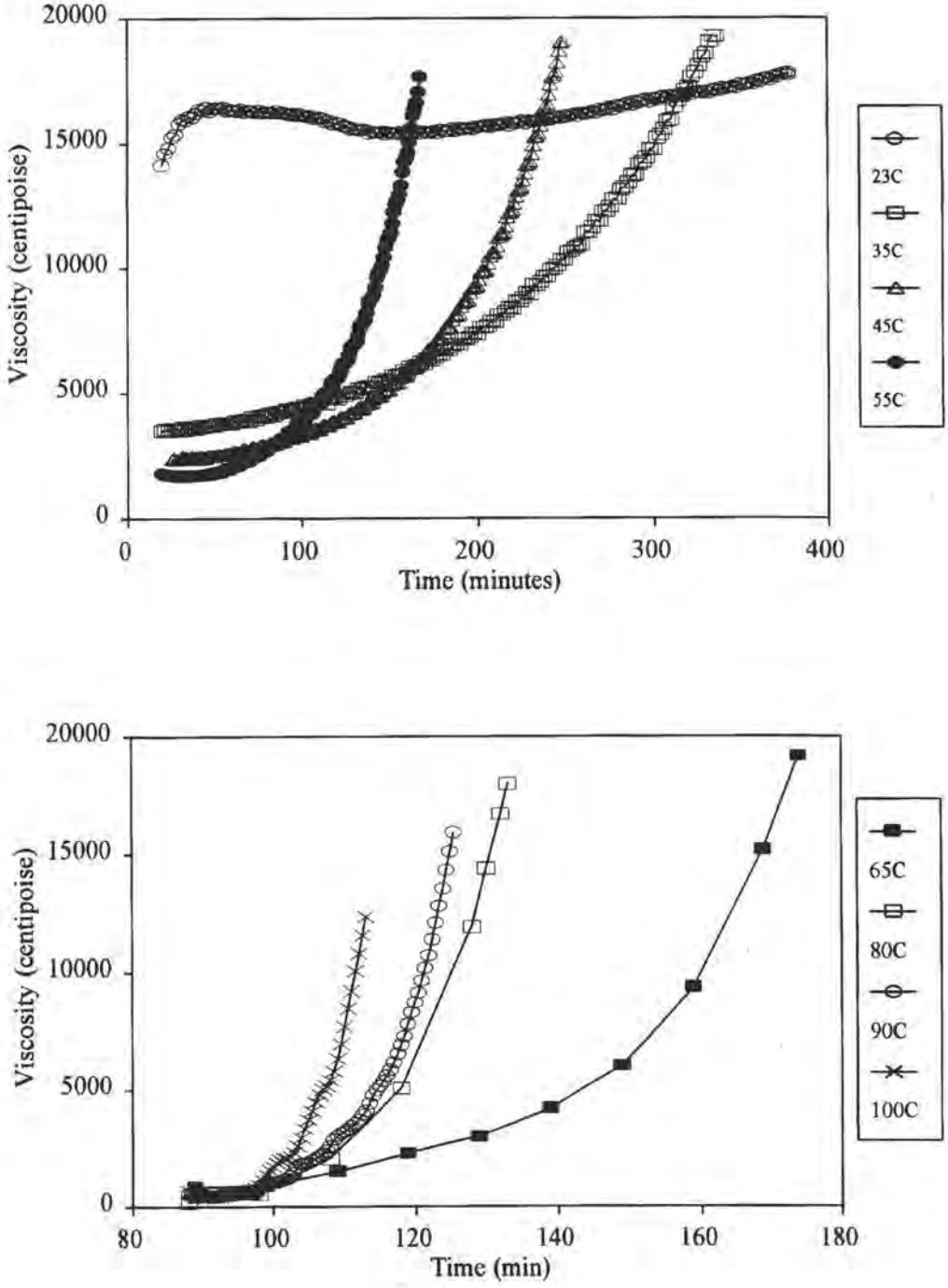

Figure 4 Measured viscosity as a function of time at various temperatures.

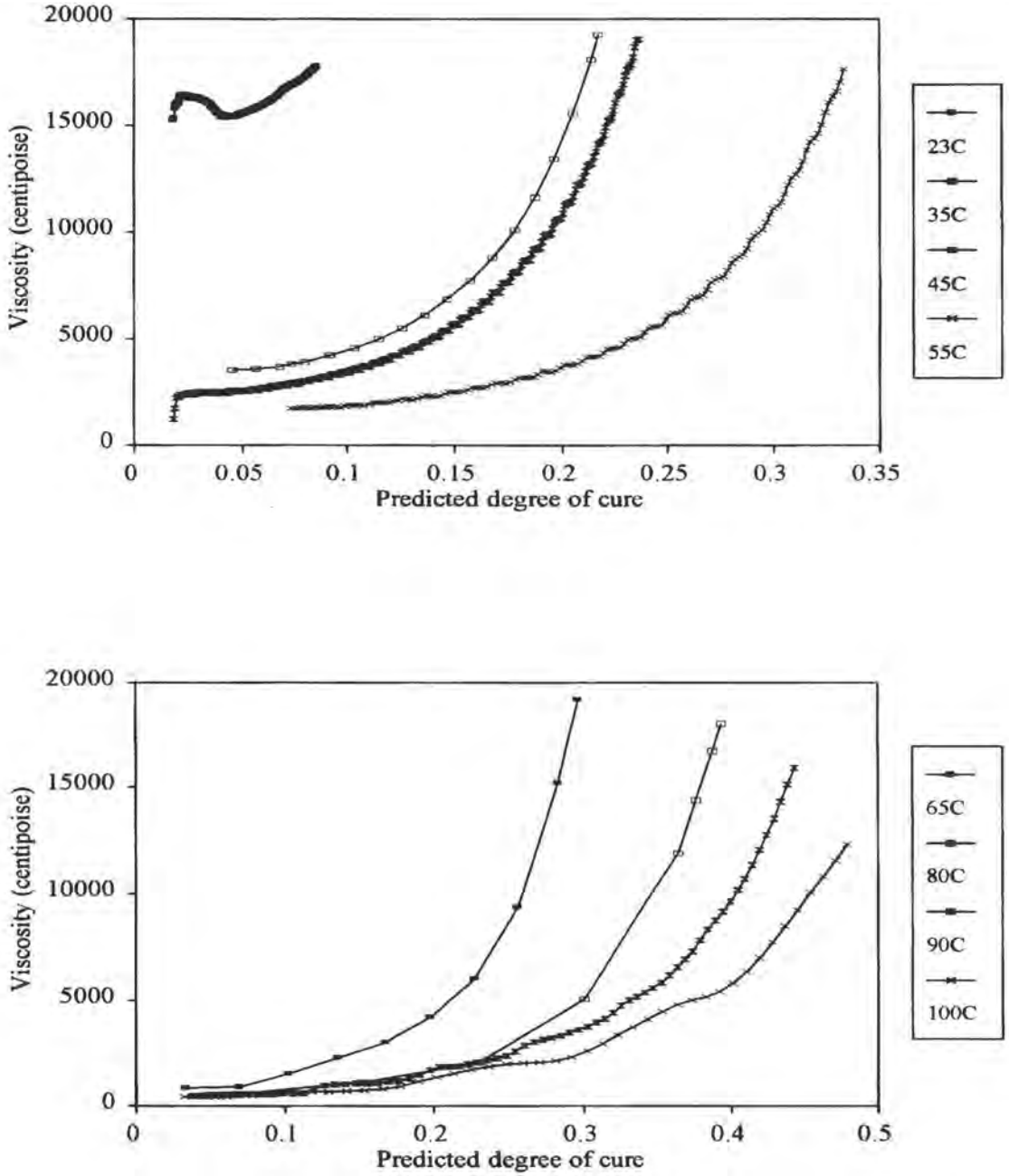

Figure 5. Viscosity versus predicted degree of cure plots.

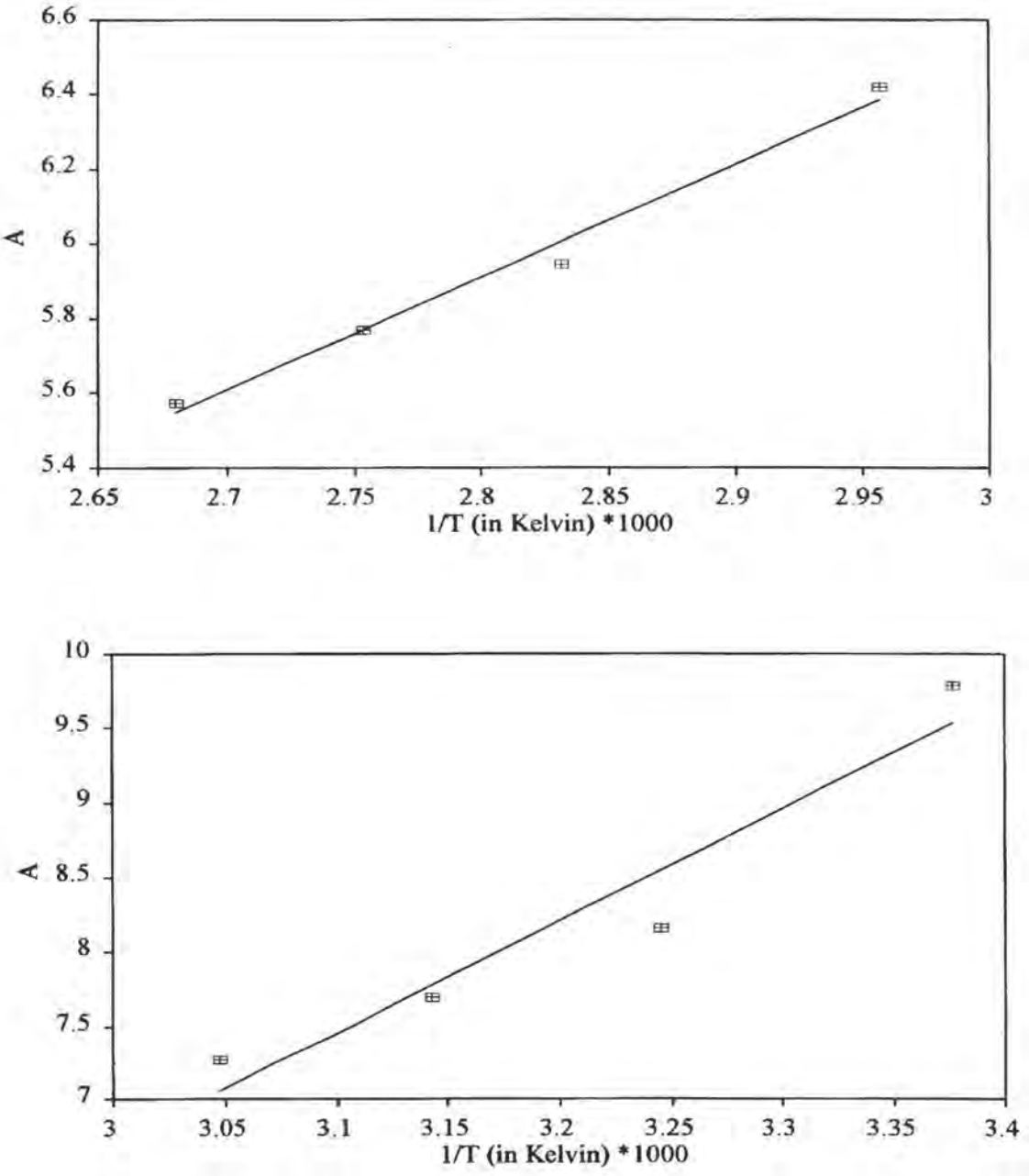

Figure 6a. Calculated and predicted values of constant A for all temperatures.

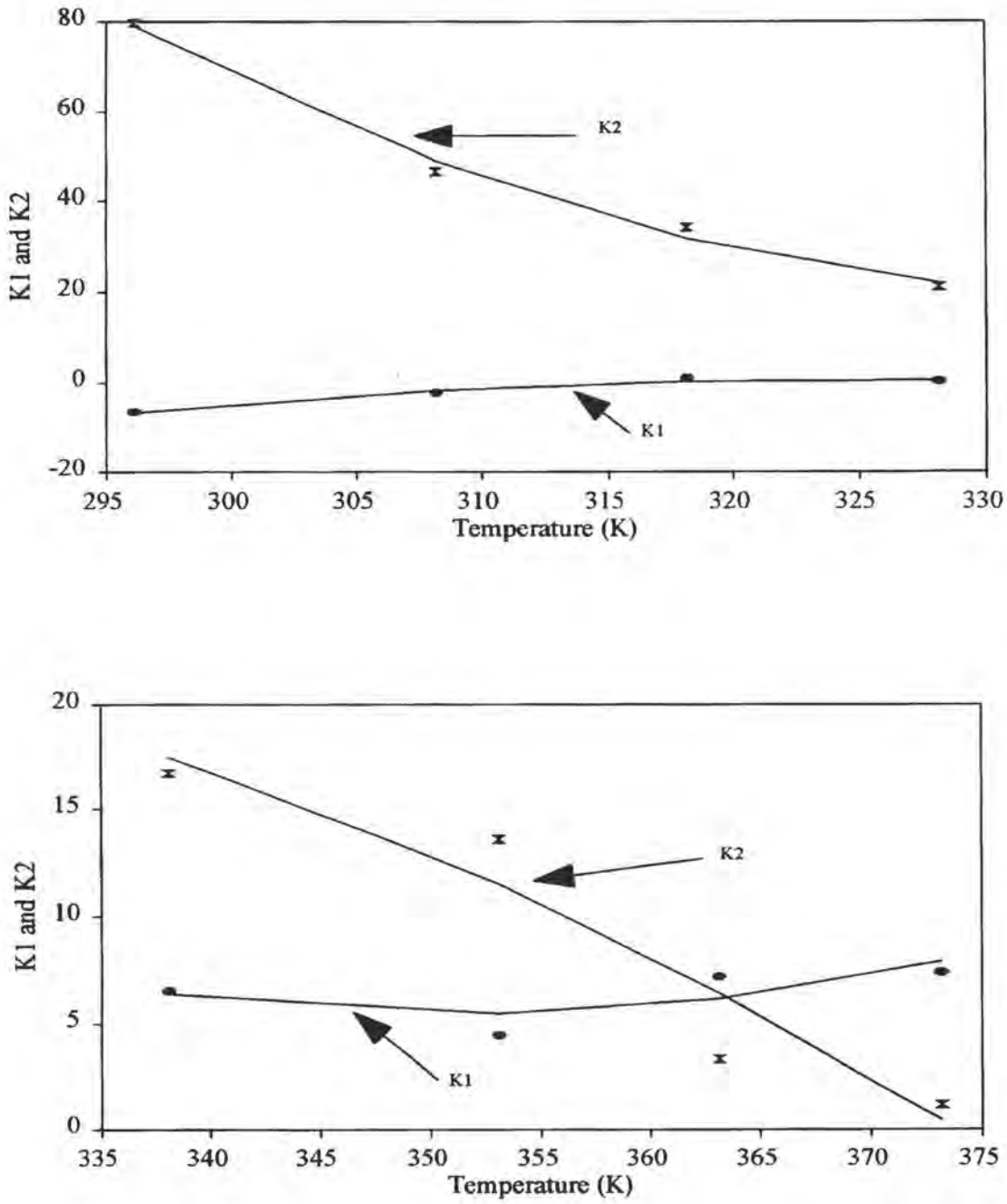

Figure 6b. Calculated and predicted values of constants k_1 and k_2 for all temperatures.

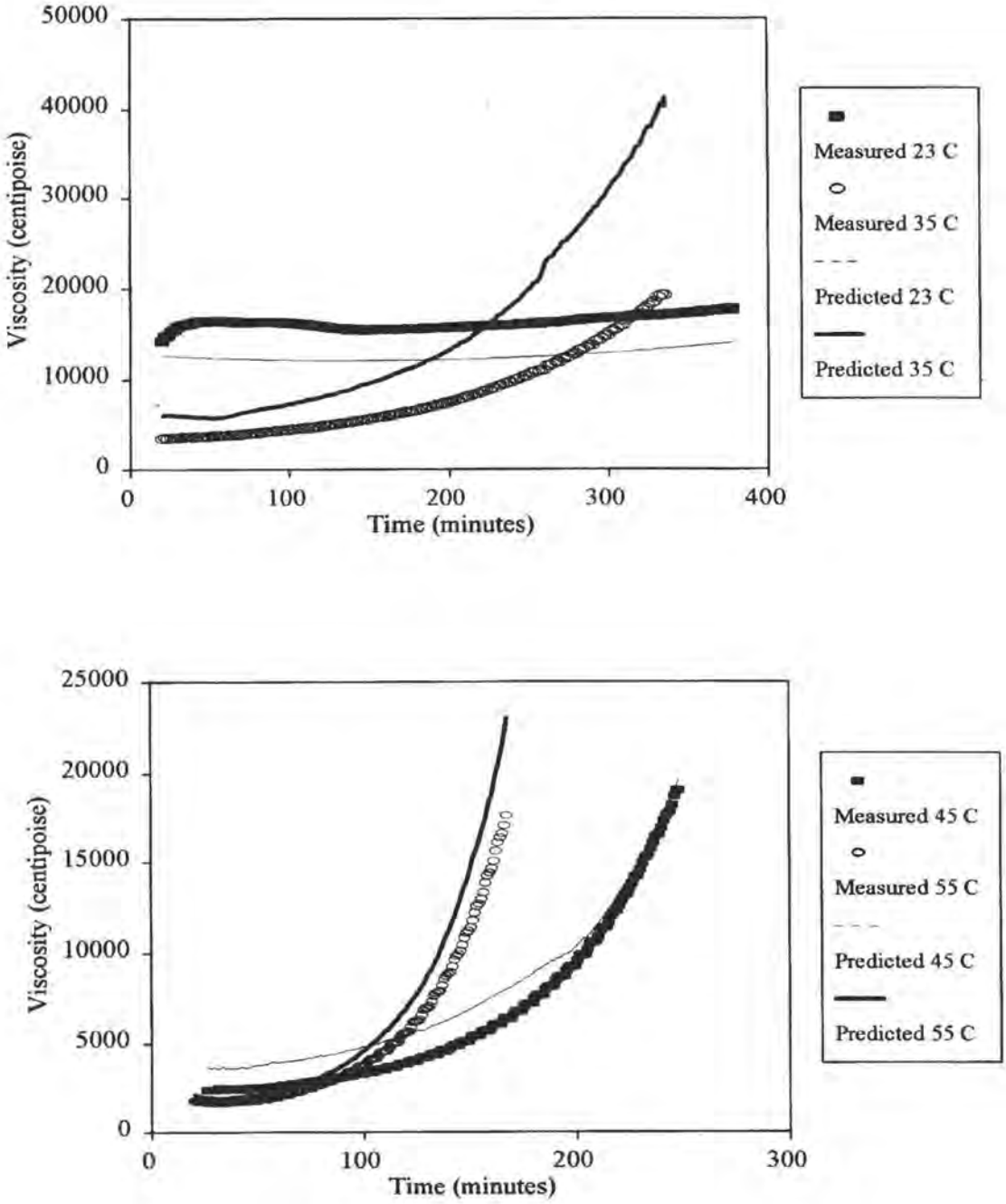

Figure 7a. Measured and predicted viscosity versus time characteristics for temperatures 23°, 35°, 45°, and 55° C.

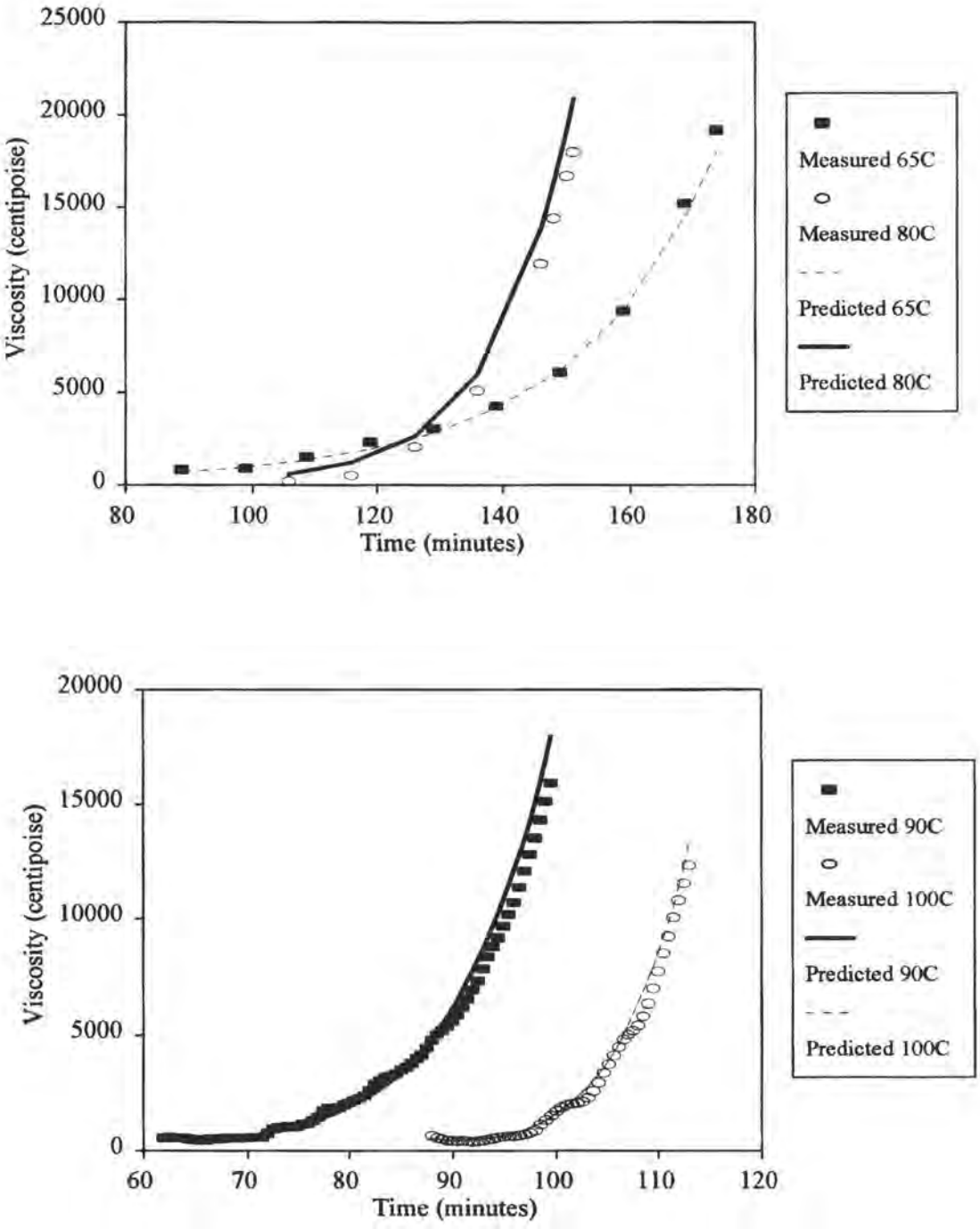

Figure 7b. Measured and predicted viscosity versus time characteristics for temperature 65°, 80°, 90°, and 100°

EFFECT OF PULTRUSION VARIABLES ON THE CURE OF SHELL EPON 862 / W EPOXY / FIBERGLASS SYSTEM

R. Shanku†, J. G. Vaughan*, and J. A. Roux*
University of Mississippi
University, MS 38677

ABSTRACT

This study employs statistical analysis to investigate the effects of the pultrusion process parameters on the degree of cure for a pultruded composite. The five process variables taken into consideration are fiber volume, pull speed, die zone 1, 2, and 3 temperatures of the die. Experiments were conducted according to a five factor, half-factorial, central composite design which used 32 experiments to establish the parameter settings for composite production. Samples were taken from the finished composite product and tested using a differential scanning calorimeter (DSC) to determine the degree of cure. The matrix material was EPON 862/W (Shell EPON® Resin DPL-862/EPON CURING AGENT® W/EPON CURING AGENT® Accelerator 537) epoxy resin system and PPG Hybon 2001 # 112 yield E-glass was used as reinforcement. The heat of reaction of the resin system contained in the composite was measured to obtain the degree of cure. Regression analysis was performed on the data to study the influence of processing parameters on degree of cure for the composite system. Surface plots were used to discern the effects of significant variables. Results indicate that pull speed has the most significant effect - lower pull speeds producing higher degrees of cure - followed by the die exit zone temperature.

† Graduate Assistant * Professor

INTRODUCTION

Pultrusion is one of the least expensive methods for fabricating composite parts due to its simplicity and efficiency. The pultrusion process continuously draws a bundle of fibers (rovings or mats) through a resin bath for impregnation, then through preform plates for shaping, and a heated die for curing. The preform plates are attached to the pultrusion die to ensure proper alignment of the formed materials within the die cavity, to strip the excess resin and to compact the fibers. The finished product can then be cut to required lengths using a cutoff saw. In 1988, a statistical experimental design conducted by Vaughan et al [1] to optimize various physical and mechanical properties of a graphite epoxy system indicated that fiber volume, pull speed, and the three die zone temperatures were the most important process variables. In the past, the effect of these pultrusion parameters on flexural strength and pull force have been addressed [2,3]. The present study investigates the influence of the five process variables on the degree of cure of the composite. As numerous process variables and their interactions exist, it is necessary that an experimental test plan be developed to aid in better understanding of the process. The central composite design procedure provides the necessary information needed for analysis using fewer experimental runs.

EXPERIMENTAL PROCEDURE

The Shell EPON 862/W/537 resin system was used as the matrix material ; the composition of the resin system is shown in Table 1 [4]. PPG Hybon 2001 # 112 yield E-glass was used as reinforcement. The pultrusion runs were conducted on a Pulstar 804 pultruder located in the Composite Materials Laboratory at the University of Mississippi which has a pull load capacity of approximately 44.82 kiloNewtons (10,000 pounds) in the continuous mode and a maximum pull speed of 1.52 m/min (60 in/min). Pultrusion process data including static die wall temperatures, pull speed, pull load, clamp pressure, and system pressure were recorded every five seconds using a PC-based data acquisition unit. The pull speed was recorded by an encoder wheel which detects the speed while rolling over the pultruded composite. The thermostat temperatures were set at test condition levels within each of the three heating zones of the 91.44 cm (36 inch) long die in accordance with Table 2.

Statistical experimental design is a scientific approach which allows the researcher to better understand the process and to determine how the inputs (processing conditions which are controlled for the experiment) affect the response (the quantity measured). Improved performance characteristics result from the identification of the critical factor levels that optimize the mean response and minimize response variability. When designing an experiment, the critical factors to be considered and the range of values of these factors must be determined. Among the wide variety of design types and analysis strategies available, the CCD (central composite design) technique was used to conduct the experiments for this study.

Central composite designs developed by Box and Wilson are a very flexible and efficient second order modeling design for quantitative factors [5]. The design is a full (2^k) or fractional factorial design with central and axial points symmetric to the design region intended for study. The basic central composite design for 'k' variables consists of a 2^k factorial design with each factor at coded factor levels: - , -1, 0, +1, + . The value of (radius of the axial points) is chosen by the experimenter to achieve required design properties. The CCD is used to fit the second-order model

$$Y = \beta_0 + \sum \beta_i X_i + \sum \beta_{ii} X_i^2 + \sum \sum \beta_{ij} X_i X_j + \epsilon \qquad (1)$$

A graphical representation of a three factor CCD is shown in Figure 1. The two-way interactions, linear, and quadratic terms can be estimated by using central composite designs. The linear terms are the process variables and the squared terms are the square of the linear terms which account for nonlinear effects. The interaction terms are the products of each of the combinations of process variables to allow study of coupled effects of the variables.

It was determined that a five factor, half-factorial design was appropriate for this experiment and that 32 experiments were required to collect the necessary data. The factor level, , is usually set at $(n_F)^{1/4}$ where n_F is the number of runs in the factorial portion of the design to produce ratability. Ratability implies that the predicted response is capable of being estimated with equal variance regardless of the direction from the center of the design space. For this test the number of factorial runs, n_F

was 16. The number of axial points, 2k, where k is the five variables considered was 10, and the center points account for 6 runs (Figure 1 and Table 2). The factor level, , was thus taken as 2. The central composite design matrix along with the coded variables are given in Table 2. The 32 experiments were conducted with the parameters set at required levels also shown in Table 2.

Regression techniques were used to obtain least-squares estimates of the coefficients of Equation (1). P-values (Prob > T) and the magnitudes of the parameter estimates were then examined to obtain a reduced set model with the most significant regression coefficients.

The composite product produced was of uniform cross-section with dimensions of 3.18 mm by 25.4 mm (1/8 inch by 1 inch). Samples of 4.5 x 4.5 x 1 mm were cut from these pultruded products and tested using a DSC to determine the degree of cure of the composite. At least 15.24 m (50 feet) of product were pultruded for each experimental case. The product from each experiment was cut into pieces of five feet (1.524 m) each and numbered one through ten. Two samples from each odd numbered piece were tested i.e., pieces numbered 1, 3, 5, 7, and 9, thus in all about 320 samples were tested, ten from each experimental run.

A typical DSC plot for the 320 samples is shown in Figure 2. A DuPont 2910 DSC was used to obtain the reaction kinetics of the resin. The necessary calibration procedures were performed according to manufacturer specifications [6]. The samples were enclosed in a nonhermetic aluminum pan and heated from ambient to 300 C (572 F) at a scan rate of 20 C/minute. The exothermic reaction occurred within this temperature range. The sample was weighed before testing and the weight of the glass fibers was removed from the total weight while calculating the heat of reaction of the sample using the composite sample weight method ; thus, the heat of reaction was based on a per resin mass basis. Weight of the resin in milligrams is given by

$$W_r = (1 - VF) * V * \rho_R \qquad (2)$$

where

$$W_S = (VF * V * \rho_F) + ((1 - VF) * V * \rho_R) \qquad (3)$$

$$V = W_S / [(VF * \rho_F) + ((1 - VF) * \rho_F)] \quad (4)$$

W_S : weight of solid composite sample

VF : fiber volume fraction for experimental run

V : volume of sample (to be determined from the equation)

$_F$: density of glass fiber - 2.5 g/cm^3

$_R$: density of resin being tested - 1.2 g/cm^3

The heats of reaction from the DSC scans were essentially independent of the heating rate, thus the total heat of reaction of resin at room temperature was considered to be the average value of a number of dynamic scans at 20 C/min. of the uncured resin within 50 minutes of resin mix. The heat of reaction was calculated by

$$H_r = \int_0^t (dQ/dt) \quad (5)$$

where H_r is the heat given off by the sample from time zero to time t, when the cure reaction is complete, and dQ/dt is the heat flow rate per unit mass (Figure 2). The experimental degree of cure, , was obtained from the heat of reaction and is expressed as

$$\alpha = 1 - (H_s/H_r) \quad (6)$$

where H_s is the heat of reaction of the composite sample given by the DSC dynamic scans and H_r is the total heat of reaction of the resin. The total heat of reaction, H_r, was obtained from DSC tests performed on the liquid resin system samples taken within 50 minutes from the time of mix (when curing agent is added to the resin). The degree of cure for all the 320 samples was measured. The average degree of cure for each of the 32 experimental runs is listed in Table 3.

Regression analysis was performed on the degree of cure data and the effects of the process variables on the data were analyzed using response surface techniques. The regression analysis was conducted on all 320 observations and also on the 32 average degrees of cure data separately and then compared to obtain a model that best fit the data.

ANALYSIS AND RESULTS

The maximum, minimum, and the average degree of cure observations for the 32 runs are shown in Figure 3 and listed in Table 3. The measured degree of cure was a maximum for Test plan # 27 (fiber volume 68.2%, pull speed 30.48 cm/min (12 in/min.), and the die zone temperatures of 193.33, 204.44, and 193.33 C (380, 400, and 380 F)) and a minimum for Test plan # 11 (fiber volume 66%, pull speed 35.56 cm/min (14 in/min), and the die zone temperatures of 187.78, 210, and 210 C (370, 410, and 410 F)).

Regression analysis was conducted to develop a statistical model to predict the degree of cure for the composite system by isolating the most significant terms influencing the degree of cure. The multiple regression model is of the form

$$\begin{aligned} y = {} & 91.88 + 0.64X1 - 0.41X2 + 0.44X3 - 0.43X4 - 0.14X5 - 0.41X1X2 + 0.02X1X3 + 0.33X1X4 \\ & + 0.45X1X5 - 0.19X2X3 - 0.52X2X4 - 0.47X2X5 + 0.21X3X4 + 0.39X3X5 + 0.05X4X5 \\ & + 0.01X1X1 + 0.13X2X2 + 0.11X3X3 + 0.03X4X4 + 0.42X5X5 \end{aligned} \quad (7)$$

where y is the degree of cure, the numbers are the regression coefficients, and XI and XJ are the independent pultrusion variables as defined in the lower portion of Table 2. The analysis was performed on all 320 observations and also on the 32 average degree of cure data separately to identify influential variables. Reduced set models were developed by examining the output of the regression analysis, parameter estimates and P-values. The reduced set model with 11 variables (instead of the full 21 shown in Eq (7)) after elimination of insignificant variables is shown in Table 4 and is given by the following equation

$$\begin{aligned} y = {} & 92.11 + 0.63X1 - 0.42X2 + 0.44X3 - 0.44X4 - 0.14X5 + 0.40X55 \\ & - 0.41X12 + 0.45X15 - 0.52X24 - 0.47X25 + 0.39X35 \end{aligned} \quad (8)$$

The analysis of 320 observations revealed that the probability that coefficients of the 11 variables were

equal to zero was very low, but when the average degrees of cure data were considered, the coefficient of variable X5 had a high probability of being zero (P = 0.54). Figure 4 illustrates the maximum, minimum and the average degree of cure values obtained experimentally and from the reduced set model (Eq. (8)). The regression coefficients are shown in Table 5. The model indicates that 6 interaction terms are significant. The interaction terms involving the die zone temperatures were particularly important.

From the regression analysis the linear term of the fiber volume (X1) appears to have a high positive influence (coefficient = 0.63), which implies that an increase in the fiber volume would result in high degrees of cure. This is an unusual behavior as it would be expected that the degree of cure would decrease as fiber volume is increased. However, all terms involving the fiber volume must be examined to really understand the influence of fiber volume on the degree of cure. A fiber volume interaction term, X12, (fiber volume and pull speed interaction term) shows a high negative coefficient equal to -0.41, which implies that fiber volume and pull speed interact to affect the degree of cure. From Figure 5 the influence of the linear fiber volume term, pull speed and their interactions on the degree of cure can be observed clearly. The variables X3, X4, and X5 (the three die zone temperatures) are kept constant at coded level 0 and the effects of the terms involving the fiber volume and pull speed are observed. It can be concluded that changes in fiber volume do not have a major effect on degree of cure from this plot compared to the effect due to pull speed. The degree of cure appears to increase sharply with decrease in pull speed, but the change in degree of cure with fiber volume is not strong. The interaction of the terms indicates that a high fiber volume and a high pull speed will decrease the degree of cure.

Since the zone 3 die temperature (X5) emerged as a significant variable from the regression analysis of the 320 observations, it was included in the predictive model. The interaction terms involving the zone 3 die temperature were X55, X15, X25, and X35. The relatively high parameter estimate of X55, which is the squared term of the zone 3 die temperature, indicates that it significantly influences the degree of cure. Figure 6 illustrates the influence of terms involving zone 3 die temperature and pull speed on the degree of cure. The other variables are held constant at coded level 0 since the fiber volume did not have a significant effect. It is evident from the plot that the degree of cure increases with zone 3 die temperature and as the pull speed decreases. High degrees of cure at conditions of low pull speeds are expected as the

residence time of the composite in the die is greater than that at higher pull speeds. High die zone temperatures accelerate the curing reaction of the epoxy. However, die exit temperatures cannot be set at very high levels since thermal cracking due to thermal shock of the product can be a serious problem. Also from this analysis it is clear that a high die entrance temperature is required to obtain a high degree of cure.

CONCLUSIONS

Results show that designed experiments allow the influence of pultrusion variables to be identified. Interaction terms are important and must be considered while analyzing the effect of the variables on the degree of cure. A statistical model relating the degree of cure to the process variables and their interactions was developed. The model indicates that the linear fiber volume term (X1) has a high positive effect on degree of cure. However, the interaction term (X12) between the fiber volume and the pull speed has a high negative influence. Plots show that the overall effect of fiber volume is not significant and that the degree of cure is influenced more by pull speed (X2). Data show that increased levels of pull speeds have a negative effect which agrees with the assumption that degree of cure decreases with increasing pull speeds. Response plots also indicate that the degree of cure increases with increasing zone 3 die temperatures and low pull speeds. Zone 3 die temperature and pull speed terms emerge as significant variables.

ACKNOWLEDGMENT

The authors want to gratefully acknowledge the National Science Foundation, Division of Design and Manufacturing Systems, grant DDM-9101643, and the Electric Power Research Institute, contract RP 8007 20, for their support and the opportunity to conduct this research.

REFERENCES

1. Seal, E., Mills, J. P., Vaughan, J. G., and Gordon G., "Characterization of the Pultrusion Process for Graphite Epoxy," Technical paper, SME, 1988, pp. 1-17.
2. Lackey, E., and Vaughan, J. G., "Effect of Pultrusion Process Parameters on Flexural Strength," *Proceedings of the 38th International SAMPE Symposium,* May 10-13, 1993, pp.461-470.
3. Lackey, E., and Vaughan, J. G., "An Analysis of Factors Affecting Pull Force for the Pultrusion of Graphite/Epoxy Composites," *48th Annual Conference, Composites Institute,* The Society of the Plastics Industry, Inc., Feb 8-11, 1993, pp. 1-5.
4. Technical Bulletin, "EPON® Resin 862/EPON CURING AGENT® W," Shell Chemical Company, SC:1183-90.
5. Schmidt, S. R., and Launsby, R. G., *Understanding Industrial Designed Experiments,* 3rd Edition, Air Academy Press, Colorado Springs, CO, 1991.
6. Operator's Manual, "DSC 2910 Differential Scanning Calorimeter," TA Instruments, January 1989.

Table 1. Composition of the Shell EPON 862/W/537 resin system [4].

Material	PHR[1]	Function and Composition
EPON® RESIN DPL-862	100	Base of the matrix. Epoxy Bisphenol F (BPF) Resin.
EPON CURING AGENT® W	26.4	Cures the monomer thermoset to a polymeric chain. Non-MDA, aromatic amine curing agent.
EPON CURING AGENT® ACCELERATOR 537	2	Acts as a catalyst to the epoxy resin curing reaction and decreases gel time. Composed of organic salts.
FILLER - CLAY ASP 400-P	20	Filler clay, aluminum silicate
RELEASE AGENT - AXEL-INT 1846	0.6	Mold release agent. Synthetic resins, glycerides, fatty acids and phosphate esters.

[1] PHR is parts per hundred resin

Table 2. Test plan for experiments.

Randomized Test Plan Number	***Test Plan Number***	***Test Variables***				
		X1	***X2***	***X3***	***X4***	***X5***
16	1	-1	-1	-1	-1	1
1	2	1	-1	-1	-1	-1
11	3	-1	1	-1	-1	-1
17	4	1	1	-1	-1	1
5	5	-1	-1	1	-1	-1
10	6	1	-1	1	-1	1
12	7	-1	1	1	-1	1
18	8	1	1	1	-1	-1
8	9	-1	-1	-1	1	-1
2	10	1	-1	-1	1	1
7	11	-1	1	-1	1	1
9	12	1	1	-1	1	-1
6	13	-1	-1	1	1	1
14	14	1	-1	1	1	-1
15	15	-1	1	1	1	-1
13	16	1	1	1	1	1
3	17	0	0	0	0	0
4	18	0	0	0	0	0
19	19	0	0	0	0	0
22	20	0	0	0	0	0
20	21	0	0	0	0	0
30	22	0	0	0	0	0
24	23	-2	0	0	0	0
27	24	0	-2	0	0	0
23	25	0	0	-2	0	0
31	26	0	0	0	-2	0
29	27	0	0	0	0	-2
21	28	2	0	0	0	0
26	29	0	2	0	0	0
28	30	0	0	2	0	0
25	31	0	0	0	2	0
32	32	0	0	0	0	2

	-2	-1	0	1	2
X1: Glass ends	30	31	32	33	34
Fiber vol. (%)	63.9	66	68.2	70.3	72.4
X2: Pull speed (in/min), (cm/min)	8 (20.32)	10 (25.40)	12 (30.48)	14 (35.56)	16 (40.64)
X3: Zone 1 temp F (C)	360 (182)	370 (187)	380 (193)	390 (198)	400 (204)
X4: Zone 2 temp F (C)	380 (193)	390 (198)	400 (204)	410 (210)	420 (215)
X5: Zone 3 temp F (C)	380 (193)	390 (198)	400 (204)	410 (210)	420 (215)

Table 3. Degree of cure data for samples from the 32 CCD experiments.

Test Plan #	Minimum DC %	Maximum DC %	Average DC %	St. Dev. %
1	87.59	94.14	90.51	2.30
2	89.32	95.00	92.18	1.66
3	93.31	94.94	93.91	0.42
4	90.69	93.82	92.34	1.01
5	89.29	92.41	91.43	0.97
6	93.62	96.60	95.03	0.84
7	90.28	93.37	92.23	0.84
8	91.84	93.11	92.66	0.47
9	89.71	91.32	90.56	0.49
10	92.87	94.99	94.04	0.53
11	88.14	89.22	88.71	0.41
12	90.26	92.71	91.70	0.65
13	90.82	93.75	92.56	0.75
14	93.30	95.27	93.85	0.55
15	90.66	91.80	91.34	0.38
16	92.21	93.99	92.96	0.52
17	89.52	91.90	90.90	0.58
18	88.57	91.91	90.32	0.80
19	90.51	93.13	91.74	0.94
20	88.97	93.03	90.84	1.25
21	91.71	93.92	92.90	0.62
22	92.40	94.19	93.26	0.51
23	91.53	92.89	92.19	0.40
24	93.40	95.39	94.54	0.50
25	90.59	94.02	92.42	0.94
26	93.34	95.45	94.14	0.59
27	93.71	97.22	95.25	1.11
28	91.99	93.57	93.03	0.46
29	90.49	93.85	91.63	0.86
30	93.22	94.22	93.59	0.27
31	90.57	92.22	91.18	0.60
32	91.78	95.82	93.22	1.00

Table 4. Regression output for the degree of cure (reduced set with 11 variables.

Regression Statistics

Multiple R	0.70
R Square	0.49
Adjusted R Square	0.47
Standard Error	1.24
Observations	320.00

Analysis of Variance

	df	Sum of Squares	Mean Square	F	Significance F
Regression	11.00	446.62	40.60	26.46	0.00
Residual	308.00	472.61	1.53		
Total	319.00	919.22			

Variables	Coefficients	Standard Error	t Statistic	P-value
Intercept	92.11	0.09	1051.54	0.00
X1	0.63	0.08	7.91	0.00
X2	-0.42	0.08	-5.29	0.00
X3	0.44	0.08	5.53	0.00
X4	-0.44	0.08	-5.46	0.00
X5	-0.14	0.08	-1.73	0.08
X55	0.40	0.07	5.63	0.00
X12	-0.41	0.10	-4.19	0.00
X15	0.45	0.10	4.60	0.00
X24	-0.52	0.10	-5.30	0.00
X25	-0.47	0.10	-4.76	0.00
X35	0.39	0.10	4.00	0.00

Table 5. Regression coefficients of the reduced set model.

Intercept	92.11
Fiber Volume	0.63
Pull Speed	-0.42
Zone 1 Temperature	0.44
Zone 2 Temperature	-0.44
Zone 3 Temperature	-0.14
Zone 3 Temp. * Zone 3 Temp.	0.40
Fiber Volume * Pull Speed	-0.41
Fiber Volume * Zone 3 Temp.	0.45
Pull Speed * Zone 2 Temp.	-0.52
Pull Speed * Zone 3 Temp.	-0.47
Zone 1 Temp. * Zone 3 Temp.	0.39

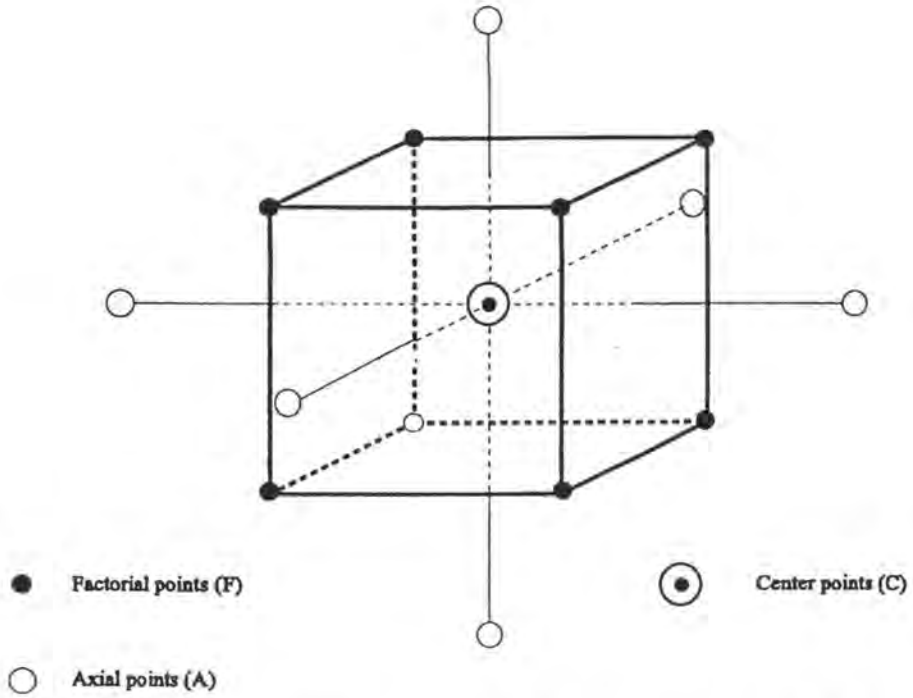

Figure 1. Configuration of points in a three-factor central composite design.

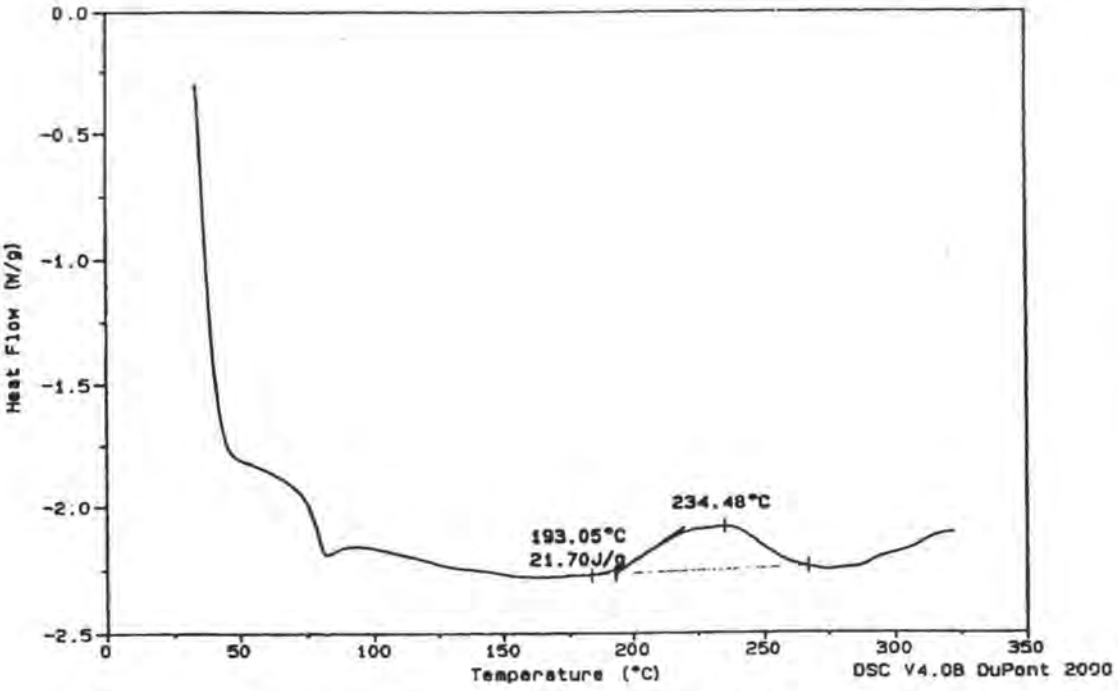

Figure 2. A typical DSC thermogram.

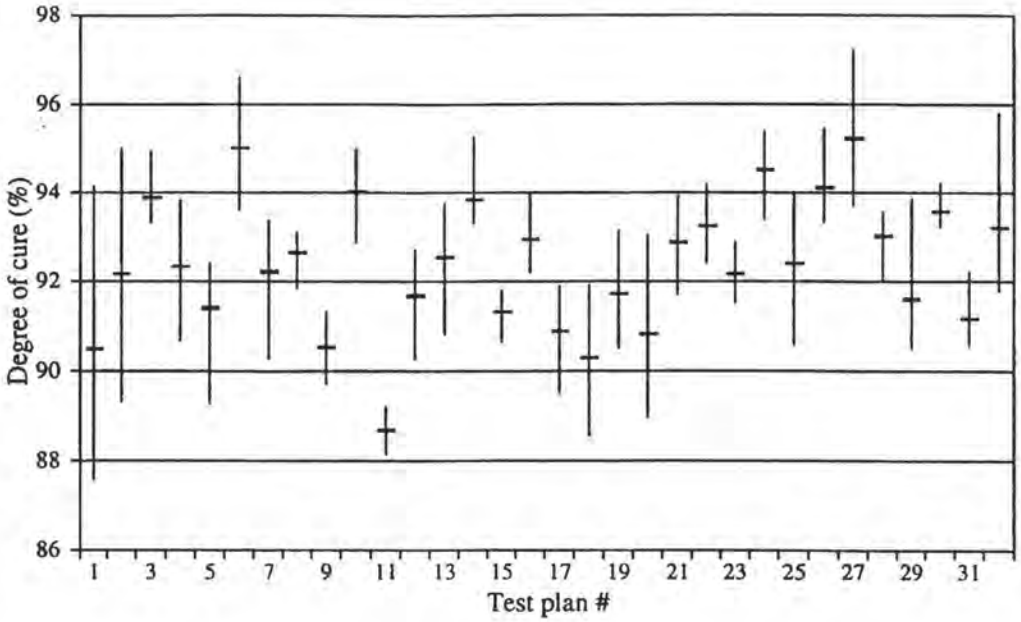

Figure 3. Maximum, minimum, and average degree of cure data.

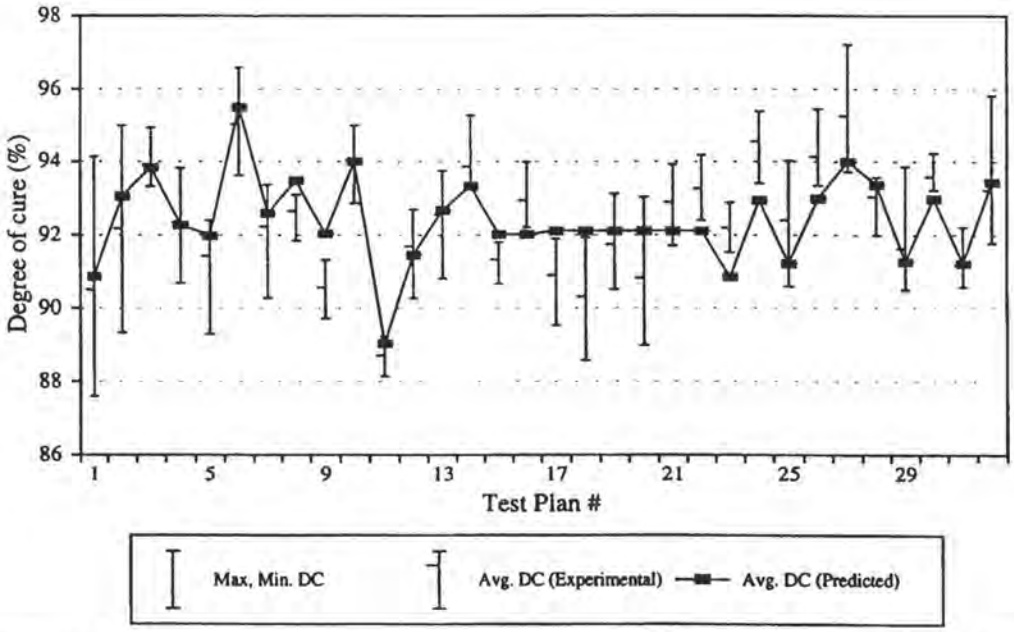

Figure 4. Comparison of the experimental and predicted degree of cure (DC) obtained from the reduced model.

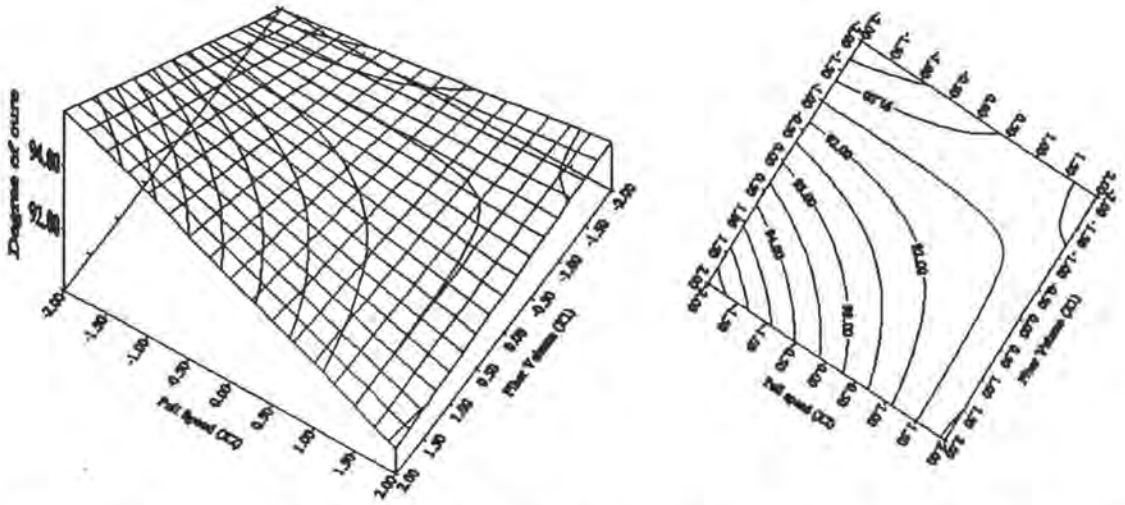

Figure 5. Contour plot showing the effect of fiber volume (X1) and pull speed (X2) on the degree of cure.

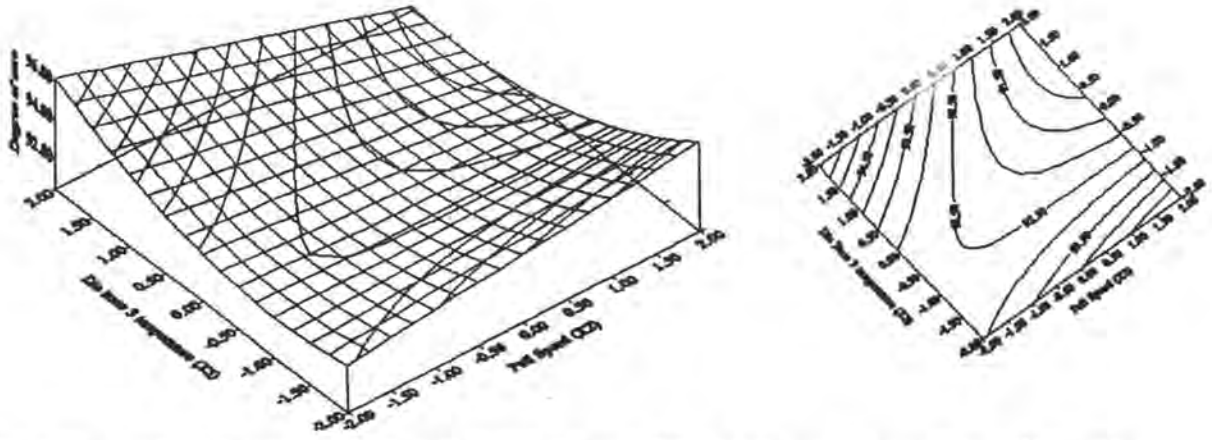

Figure 6 Surface plot illustrating the effect of pull speed (X2) and die zone 3 temperature (X5) on the degree of cure.

ABOUT EPRI

Electricity is increasingly recognized as a key to societal progress throughout the world, driving economic prosperity and improving the quality of life. The Electronic Power Research Institute delivers the science and technology to make the generation, delivery, and use of electricity affordable, efficient, and environmentally sound.

Created by the nation's electric utilities in 1973, EPRI is one of America's oldest and largest research consortia, with some 700 members and an annual budget of about $500 million. Linked to global network of technical specialists, EPRI scientists and engineers develop innovative solutions to the world's toughest energy problems while expanding opportunities for a dynamic industry.

EPRI—*Powering Progress*

Printed on recycled paper (50% recycled fiber, including 10% postconsumer waste) in the United States of America.